# 海峽兩岸學術研討會“亞洲大陸增生與造山作用”
# Symposium on Continental Growth and Orogeny in Asia

**時間**：2006 年 3 月 19 日至 26 日
**地點**：中央研究院地球科學研究所二樓演講廳
**主持人**：江博明(中央研究院地球科學研究所)
鍾孫霖(國立臺灣大學地質學系)

**贊助單位**：

中央研究院地球科學研究所
國立臺灣大學地質科學學系
行政院國家科學委員會
經濟部中央地質調查所

**會議主題**：(3 月 20-21 日)

（1） 增生造山帶與碰撞造山帶的形成機制
（2） 增生造山帶與碰撞造山帶的地殼組成與結構
（3） 大陸地殼生長的時空範圍和生長量
（4） 侵入岩及火山岩的年代學、物源示蹤及與地殼生長的關係
（5） 大陸地殼演化與成礦作用關係
（6） 青藏、新疆、內蒙和東北地區研究成果

**地質考察**：東台灣大南澳雜岩及現代增生造山帶野外地質行程 （3/22-26）

| | |
|---|---|
| 3/22（週三） | 東澳粉鳥林角閃片岩<br>南澳源頭山花崗岩<br>和平開南岡片麻岩<br>宿花蓮 |
| 3/23（週四） | 溪畔花崗岩<br>天祥變質混雜岩、大理岩、綠色片岩、黑色片岩、變質混雜岩<br>宿花蓮 |
| 3/24（週五） | 海岸山脈嶺頂都巒山火山碎屑岩<br>橄子樹八里灣濁流岩<br>石梯坪都巒山火山碎屑岩及上升海蝕平台<br>穿越海岸山脈：奇美斷層、秀姑巒溪曲流及濁岩、奇美火成雜岩<br>宿台東 |
| 3/25（週六） | 台東利吉混雜岩<br>小野柳外來岩塊<br>太麻里中央山脈南端地質構造<br>宿台南市 |
| 3/26（週日） | 成功大學地球科學系<br>集集大地震地表破裂－阜豐橋、石岡水壩<br>宿台北 |

# 會議議程

## 3/20 (週一)

| 時間 | 演講者/題目 | 頁 |
|---|---|---|
| 9:00 | 江博明 / Opening Remarks | |
| *Session 1* | 主持人：鍾孫霖 | |
| 9:30 | 陸松年、李懷坤、陳志宏、相振群 / 中亞南部大陸的早期增生 | 73 |
| 9:50 | 肖文交、韓春明、秦克章、袁超、孫敏、陳漢林、李繼亮、孫樞 /新疆北部古生代複式增生造山作用與中亞大陸側向生長 | 127 |
| 10:10 | 高俊, R. klemd, Q. Qian, L. Long and X. Xiong / The South Tianshan in northwestern China: a Late Paleozoic or a Triassic collisional orogenic belt between the Tarim and Yili blocks? | 13 |
| 10:30 | *Break* | |
| *Session 2* | 主持人：王濤 | |
| 10:50 | 姜枚、李海鷗、王亞軍、張立樹 / 新疆境內天山山脈的地殼上地幔結構 | 54 |
| 11:10 | 胡靄琴、韋剛健 / 新疆北部阿勒泰和天山造山帶基底時代研究中的新進展 | 40 |
| 11:30 | 夏林圻, Zu-Chun Xia, Xue-Yi Xu, Xiang-Min Li, Zhong-Pin Ma, Li-She Wang / the Tianshan Carboniferous-Permian rift-related volcanism and mantle plume | 119 |
| 11:50 | 魏春景, Wei Tian, Lin Qiu / Kyanite- and andalusite- type metamorphic zones from the Altai orogen, Xinjiang, China | 111 |
| 12:10 | *Lunch* | |
| *Session 3* | 主持人：李正祥 | |
| 14:00 | 孫敏, Chao Yuan, Wenjiao Xiao, Xiaoping Long, Xiaoping Xia, Chunming Han, Shoufa Lin / Zircon U-Pb ages of granitic gneisses and intrusions in the Central Terrane of the Chinese Altai Orogen and tectonic implications | 99 |
| 14:20 | 王濤, V. P. Kovach, Ying Tong, Bor-Ming Jahn, Da-Wei Hong, Bao-Fu Han / Sr-Nd isotopic mapping for intrusions from the Altai orogen, NW China: implications for magma origin, accretionary orogeny and continental growth | 107 |
| 14:40 | 趙振華、王強、熊小林、張海祥、牛賀才、許繼峰、白正華、喬玉樓 / 新疆北部晚古生代地殼增生方式的多樣性-來自艾達克岩及富堿火成岩的證據 | 143 |
| 15:00 | 舒良樹、朱文斌、王博、J. Charvet、M Faure / 新疆柏格達地區早二疊世後碰撞期陸內裂谷和水下垮塌構造的幾何學、地球化學與年代學制約 | 92 |

| | | |
|---|---|---|
| 15:20 | 徐新、何國琦、李華芹 / 準噶爾盆地西北緣古生代陸殼側向與垂向增生事件的 SHRIMP 年齡資訊 | 131 |
| 15:40 | 王京彬、王玉往、王麗娟 / 準噶爾初生陸殼省及其成礦作用 | 109 |
| 16:00 | *Break* | |
| *Session 4* | 主持人：李獻華 | |
| 16:20 | 陸松年、李懷坤、王惠初、陳志宏、相振群 /秦–祁–昆造山帶中前寒武紀地塊的類型及主要地質特徵 | 75 |
| 16:40 | 高銳、馬永生、朱鉉、李秋生、王海燕、白金 / 松潘地塊-西秦嶺造山帶岩石圈結構深地震反射剖面探測 | 16 |
| 17:00 | 聶鳳軍、胡朋、江思宏、劉妍 / 北山北部古生代兩類花崗岩及有關礦床的鈫同位素特徵 | 85 |
| 17:20 | 趙越, B. Song , S.H. Zhang / The Central Mongolian Microcontinent: its Yangtze affinity and tectonic implications | 137 |
| 17:40 | 李錦軼 /中國北方及鄰區地殼構造格架及其形成過程的初步探討 | 62 |
| 18:00 | 李昭興, C.L. Su and C.H. Hu / Continental Rifting of the South China Sea | 56 |

**3/21 (週二)**

| 時間 | 演講者/題目 | 頁 |
|---|---|---|
| *Session 1* | 主持人：孫敏 | |
| 9:00 | 趙越, Gang Xu, Shuanhong Zhang., Biao Song, Zhenyu Yang, Jianmin Hu, Yinsheng Ma / Timing of Major Mesozoic Deformational Episodes of the Yanshan Fold and Thrust Belt, northern North China: Their Tectonic Implications | 139 |
| 9:20 | 陳斌, M.G. Zhai, W. Tian / Origin of the Mesozoic magmatism in the north China craton: constraints from petrological and geochemical data | 1 |
| 9:40 | 楊進輝, Fu-Yuan Wu, Simon A. Wilde / Multiple sources and magma mixing for the origin of Early Cretaceous I- and A-type granites in the eastern North China Craton | 133 |
| 10:00 | 吳福元, De-You Sun, Wen-Chun Ge, Yan-Bin Zhang, Simon A. Wilde, Bor-Ming Jahn / Geochronological Framework of the Immense Granites in Northeastern China | 115 |
| 10:20 | 李正祥, X.H. Li / Mesozoic Indosinian Orogeny and Jurassic- Cretaceous Post-orogenic Magmatism in South China Revisited | 67 |

| | | |
|---|---|---|
| 10:40 | 李獻華, Zheng-Xiang Li, Wu-xian Li, Yuejun Wang / A Permian magmatic arc on the Hainan Island: implications for initiation of the Indosinian Orogeny in South China | 66 |
| 11:00 | *Break* | |
| *Session 2* | 主持人：戚務正 | |
| 11:20 | 吳大銘, G.C. Huang, A.F. Sheehan, Roecker, S., H.B. Liu, R. Gao / Is Himalaya Unique Among the Collision Mountain Ranges? Results of HIMNT experiment | 116 |
| 11:40 | 高銳, Zhanwu Lu, Qiusheng Li, Ye Guan, Jisheng Zhang, Rizheng He, Liyan Huang / Deep Geophysical Probing and geodynamic study for Lithospheric Structure in the Tibetan Plateau | 19 |
| 12:00 | 陳望平, M. Martin, T.L. Tseng, Z. Yang, M. Jiang, J. Nabelek, B.S. Huang, the Hi-CLIMB Seismic Team / Mantle lithosphere beneath the Tibetan Plateau, Part I: Constraints from Shear-Wave Splitting with Special Reference to New Results from the Hi-CLIMB Seismic Array, part II: A synthesis | 78,3 |
| 12:30 | *Lunch* | |
| *Session 3* | 主持人：吳福元 | |
| 14:00 | 曾泰琳, W.P. Chen / Small 660-km seismic discontinuity beneath Tibet: Implies resting ground for detached lithosphere | 105 |
| 14:20 | 許繼峰、王強、董彥輝、陳建林、王寶弟 / 青藏高原新生代下地殼岩漿活動及其成因：年代學和地球化學證據 | 128 |
| 14:40 | 莫宣學、董國臣、周肅、趙志丹 /西藏南部林子宗火山岩系：印度－亞洲碰撞時限及大陸生長的記錄 | 81 |
| 15:00 | 潘桂棠, XuanXue Mo, ZengQian Hou, DiCheng Zhu, LiQuan Wang, GuangMing Li, ZhiDan Zhao, QuanRu Geng, ZhongLi Liao / Spatial-Temporal Framework of the Gangdese Orogenic Belt and Its Evolution | 91 |
| 15:20 | 鍾孫霖, D. Liu, J. Ji , Q. Zhang, B. Song, Q. Qian, D.J. Wen, M.F. Chu, T.Y. Lee, C.H. Lo / Magmatic Evidence for the Evolution from Accretionary to Collisional Orogeny in Southern Tibet | 9 |
| 15:40 | 朱弟成, GuiTang Pan, XuanXue Mo, LiQuan Wang, ZhongLi Liao, ZhiDan Zhao, GuoChen Dong, ChangYong Zhou / Late Jurassic – Early Cretaceous geodynamic setting in middle – northern Gangdese: new insights from volcanic rocks | 153 |
| 16:00 | *Break* | |

海報

Symposium on Continental Growth and Orogeny in Asia
海峽兩岸學術研討會“亞洲大陸增生與造山作用”
論文摘要集

目錄

# Origin of the Mesozoic magmatism in the north China craton: Constraints from petrological and geochemical data

B. CHEN (1), M.G. ZHAI (2), W. TIAN (1)

(1) School of Earth and Space Sciences, Peking University, Beijing 100871, China
(e-mail: binchen@pku.edu.cn)
(2) Institute of Geology and Geophysics, Chinese Academy of Sciences, Beijing 100029, China

The north China craton (NCC) is one of the oldest continental nuclei (Archean in age) in the world. The craton was stabilized in the early Proterozoic, and much of it remained stable up to Triassic time. However, the eastern part of the NCC has been tectonically active since the early Mesozoic, symbolized by the development of large sedimentary basins, high heat flow and widespread magmatism (and related metallogeny). Many published data indicate that the chemical and isotopic signature of the subcontinental lithospheric mantle (SCLM) beneath the eastern NCC changed significantly after the Mesozoic tectono-thermal event. Because the occurrence of diamonds in *Paleozoic* kimberlites implies the presence of a thick (150-220 km), old and refractory lithospheric keel underlying the craton in *pre-Mesozoic* time, while mantle xenoliths in *Cenozoic* basalts suggest a thin (60-120 km), young and fertile oceanic-type lithosphere in the Cenozoic (*post-Mesozoic*). Such a change of lithospheric nature implies a significant erosion of the old SCLM during the Mesozoic, and distinguishes the NCC from most other old cratons on Earth. What is the origin and cause of the sudden surge of Mesozoic magmatism, and in what kind of geodynamic setting? What is the relationship between the Mesozoic magmstism and lithosphere evolution/thinning? These issues have been subjects of extensive research of both domestic and international workers in recent years.

The Mesozoic magmatism in NCC is characterized by intrusion of voluminous intermediate to felsic rocks (mainly *monzonitic to locally syenitic* in composition) and subordinate mafic rocks, as well as eruption of contemporaneous volcanics including basaltic andesites, trachyandesites and rhyolites. Syn-plutonic mafic enclaves are frequently seen within the Mesozoic plutons; zircon grains from the mafic enclaves yield U-Pb ages identical to these from monzonitic host plutons. Geochemically, the Mesozoic magmatism show high-K calc-alkaline to shoshonitic affinity, highly fractionated REE patterns, high Sr/Y ratios and high Sr-Ba and LREE, and highly enriched Sr-Nd isotopic signatures with $\varepsilon_{Nd}(t)$ ranging from －8 to －20 and $I_{Sr}$ from 0.7053 to 0710. Zircon SHRIMP dating reveals these Mesozoic rocks formed over a time period of 180 Ma to 120 Ma, but dominantly confined to a narrow range 138-126 Ma. The sudden surge of Mesozoic magmatism was genetically linked to the upwelling of asthenospheric mantle material in an extensional regime that was developed probably as a result of subduction of the paleo-Pacific plate beneath eastern NCC. Upwelling of hot asthenospheric mantle material triggered partial melting of the enriched SCLM, generating voluminous alkali-rich mafic magmas. The mafic magmas subsequently underplated in the lower crust and sparked melting of the latter, producing granitic melts. We suggest the Mesozoic rocks in NCC likely originated from mixing/mingling between the coeval mafic and granitic melts, followed by fractionation of ferromagnesian phases and subordinate plagioclase, rather than from partial melting of mafic lower crust as previously suggested by many others.

## Mantle Lithosphere beneath the Tibetan Plateau, Part II: A Synthesis

Wang-Ping Chen[1], Michael Martin[1], Tai-Lin (Ellen) Tseng[1], Zhaohui Yang[1], Mei Jiang[2], John Nabelek[3], Bor-Shouh Huang[4], and the Hi-CLIMB Seismic Team[5]

[1] Department of Geology, University of Illinois at Urbana-Champaign Urbana, IL 61801 USA
[2] Chinese Academy of Geological Sciences, Beijing, People's Rep. of China
[3] College of Oceanography, Oregon State University, Corvallis, OR USA
[4] Institute of Earth Sciences, Academia Sinica, Taiwan, R. O. C.
[5] Other Principal Scientists: Heping Su[2], Youxue Wang[2]; M. R. Pandey, S. Sapkota, and B. Kafle, Department of Mines and Geology, Kathmandu, Nepal;
and John Chen, Institute of Geophysics, Peking University, People's Rep. of China

We carried out a synthesis regarding the configuration of mantle lithosphere beneath the Himalayan-Tibetan collision zone based on a combination of 1) new results of seismic anisotropy, primarily birefringence of *SKS* and *SKKS* phases recorded by the Hi-CLIMB seismic array (An Integrated Study of the Himalayan-Tibetan Continental Lithosphere during Mountain Building), 2) close re-examination of similar datasets that are in the public domain, and 3) latest findings regarding detached mantle lithosphere resting in the mantle transition zone, and 4) other independent constraints such as previous results from modelling of gravity data.

The main arm of the Hi-CLIMB seismic array is distributed along a north-south trending corridor between meridians of 84° and 85°E. Along the southern portion of the corridor, no resolvable birefringence is observed for near-vertically incident shear-waves (split-time, $\delta t$, is less than 0.3 s). Significant birefringence, with approximately east-west trends of polarization for the fast-travelling component and $\delta t$ on the order of 1 s, begins about 80 km north of the IYS and continues northward beyond the BNS. This pattern is consistent with observations along the Yadong-Gulmod profile, about 1,000 km farther to the east (see data and references compiled in *Chen and Ozalaybey* [1998]).

Based on an unusual observation that the Indian shield is characterized by null shear-wave birefringence and a correlation between amplitudes of birefringence and Bouguer gravity anomalies in Tibet, *Chen and Ozalaybey* [1998] interpreted the onset of birefringence north of the IYS to mark the southernmost limit of Eurasian lithosphere (the mantle suture, MS), or equivalently the minimal extent of intact Greater Indian lithosphere that is thrusting beneath Tibetan crust. Furthermore, along the Yadong-Gulmod profile, a second jump in $\delta t$

and a corresponding low in Bouguer gravity anomaly occur in the central Qiangtang Terrane north of the BNS, interpreted to mark the northernmost extent of Greater India lithosphere or the Indian mantle front (IMF) [*Chen and Ozalaybey*, 1998; *Jin et al.*, 1996].

At the moment, the only piece of the puzzle that does not seem to fit this broad pattern is the report of *Huang et al.* [2000] who contended that along the intervening INDEPTH-III profile, the onset of birefringence did not occur until just south of the BNS, at a location where we found no corresponding feature in gravity data. Moreover, the sudden jump from null birefringence to an unusually large $\delta t$ of 2 s as reported by *Huang et al.* [2000] is inconsistent with a mantle source of anisotropy yet the amount of anisotropy is about an order of magnitude too large to be accounted for by a crustal source alone. In order to clarify this potential inconsistency, we are re-examining all relevant *SKS* and *SKKS* data in the public domain using most recent tools of analysis.

Meanwhile, independent work based on triplicate, broadband seismic waveforms indicate that a detached piece of mantle lithosphere, probably convectively removed quite recently (about 15 Ma or so ago) from thickened Eurasian lithospheric mantle of the Qiangtang Terrane [*Chung et al.*, 2005], is resting directly above the 660-km discontinuity beneath the Qiangtang Terrane [*Tseng and Chen*, 2006]. The detached lithosphere is at least 300 km in length when measured along the Hi-CLIMB profile. Based on seismic constraints, gravity, geodetic data, and spatio-temporal distribution of recent volcanics, a preliminary palinspatic reconstruction suggests that at the onset of the last episode of lithosphere detachment, both the IMF and the BNS were near the current position of the MS. Thus we can now account for at least one half of thickened Eurasian mantle lithosphere which apparently sank en masse.

**Acknowledgements.** This work is supported by the US National Science Foundation under Grant No. EAR9909362. Any opinions, findings and conclusions or recommendations expressed in this material are those of the authors and do not necessarily reflect those of the National Science Foundation.

**References**

Chen, W.-P. and Özalaybey, Correlation between seismic anisotropy and Bouguer gravity anomalies in Tibet and its implications for lithospheric structures, *Geophys J. Int.*, **135**, 93-101, 1998.

Chung, S.-L., M.-F. Chu, Y. Zhang, Y. Xie, C.-H. Lo, T.-Y. Lee, C.-Y. Lan, X. Li, Q. Zhang, and Y. Wang, Tibetan tectonic evolution inferred from spatial and temporal variations in post-collisional magmatism, *Earth Sci. Rev.*, **68**, 173–196, 2005.

Huang, W.-C., Ni, J.F., Tilmann, F., Nelson, D., Guo, J., Zhao, W., Mechie, J., Kind, R., Saul, J., Rapine, R. and Hearn, T.H., Seismic polarization anisotropy beneath the central Tibetan Plateau, *J. Geophys. Res.*, **105**, 27979-27989, 2000.

Jin, Y., M. K. McNutt, and Y.-S. Zhu, Mapping the descent of Indian and Eurasian plates beneath the Tibetan Plateau from gravity anomalies, J. Geophys. Res., **101**, 11275–11290, 1996.

Tseng, T.-L., and W.-P. Chen, Small 660-km seismic discontinuity beneath Tibet implies resting ground for detached lithosphere (Extended Abstract), **This volume**, 2006.

# Crustal Thermal Evolution from Subduction to Collision: An Example from Taiwan

Wu-Cheng Chi (戚務正)
Institute of Earth Sciences, Academia Sinica, Taipei, Taiwan, ROC

Many mountain belts around the world are results of collision preceded by subduction. At the same time, some geologic and geophysical processes are affected by thermal structures of the crust, e.g. metamorphism, crustal rheology, and seismicity. Currently, there is little observational study on how the thermal structures of the crust evolve from subduction to collision. Taiwan is located along a convergent boundary with subduction to the south and arc-continent collision to the north. Thus by studying the thermal structures across several transects, it is possible to derive an example of how thermal structures evolve from subduction to collision. In the collision zone on land, there is an extensive heat flow dataset from exploration and geothermal wells. However, regional-scale geothermal gradient and heat flow in the offshore region in the initial collision zone and subduction zone have yet been studied systematically. We used a bottom simulating reflector (BSR) offshore southern Taiwan to derive more than 1000 geothermal gradients in the accretionary prism in the subduction zone and initial collision zone. The BSR represents the base of the hydrate stability field underneath seafloor. As a result, we can apply hydrostatic pressure to the hydrate phase diagram to derive the temperature at the BSR, which then was combined with the temperature at seafloor and the BSR sub-bottom depth to derive the geothermal gradient. We use published thermal conductively of the sediments in this region to convert the geothermal gradient to heat flow. The BSR-based heat flows in the subduction zone range mostly within 35 to 55 $mW/m^2$, and decrease toward the ridge of the accretionary prism. We interpreted this pattern as a result of intensive dewatering at the toe, sediment blanketing effect, topographic effect, and the cooling from the subducting plate. The heat flow reduction from blanketing effect can be up to 50% due to the fast sedimentation rate in this region. We perform a 2D finite element thermal modeling showing that bathymetry can strongly influence the geothermal gradient pattern in the subduction zone. The heat flows in the collision zone are very high, mostly ranging from 100 to 250 $mW/m^2$, and increase, instead of decrease, toward the ridge. Previous studies suggest that this is caused by exhumation, erosion, and topographic-induced ground water circulation. The results from this study have several geodynamic and seismologic implications. For example, the high heat flow in collision zone correlates with shallower seismicity zone. While the lower heat flow in the subduction zone implies the seismogenic zone might be wider and capable of reaching greater depth.

# Zircon U-Pb and Hf Isotope Constraints on the Crustal Evolution and Mesozoic Tectonics of Southern Tibet

朱美妃[1], 鍾孫霖[1], 劉敦一[2], 宋彪[2], Suzanne Y. O’Reilly[3], Norman J. Pearson[3],
季建清[4], 溫大任[1], 錢青[5]

1. 台灣大學地質科學系，台北10699
2. 中國地質科學院地質所北京離子探針中心，北京100037
3. GEMOC, Macquarie University, NSW 2109, Australia
4. 北京大學地球與空間學院，北京100037
5. 中國科學院地質與地球物理研究所，北京100037

As part of our study of the Transhimalayan magmatism, this paper reports the first set of in situ U-Pb dating and Hf isotope analyses of zircon separates from three granites in the Lhasa Terrane by using the sensitive high resolution ion microprobe (SHRIMP) and laser ablation microprobe-multiple collector-inductively coupled plasma mass spectrometry (LAM-MC-ICPMS), respectively. 34 grains of igneous zircons from a granite within the Gangdese batholith show a weighted mean of $^{206}Pb/^{238}U$ ages of 188.1 ± 1.4 Ma and $\varepsilon_{Hf}(T)$ values between +10.4 and +16.8, suggesting an early Jurassic intrusive activity marked with dominant contribution by a juvenile mantle source. 23 out of 40 inherited zircons from two neighboring Cretaceous S-type granites in the Nyainqentanglha belt delineate a slightly older $^{206}Pb/^{238}U$ age cluster between 188 and 210 Ma. These zircons have $\varepsilon_{Hf}(T)$ values from –3.9 to –13.7, which yield Hf “crustal” model ages from ca. 1.4 to 2.1 Ga suggesting a major episode of crustal growth during Proterozoic time and remelting of this crust in the early Jurassic. Combining our geochemical data and literature geologic information, we interpret the newly identified “Jurassic Gangdese” magmatism as product of the early phase of the Neo-Tethyan northward subduction, which started soon after the breakup of the Lhasa Terrane from Gondwanaland and played a longer-lasting role than have been thought in the tectonic evolution of southern Tibet.

# Magmatic Evidence for the Evolution from Accretionary to Collisional Orogeny in Southern Tibet

Sun-Lin Chung [a], Dunyi Liu [b], Jianqing Ji [c], Qi Zhang [d], Biao Song [b], Qing Qian [d], Da-Jen Wen [a], Mei-Fei Chu [a], Tung-Yi Lee [e], Ching-Hua Lo [a]

[a] Department of Geosciences, National Taiwan University, Taipei, Taiwan
[b] Institute of Geology, Chinese Academy of Geological Sciences, Beijing, China
[c] School of Earth and Space Sciences, Peking University, Beijing, China
[d] Institute of Geology and Geophysics, Chinese Academy of Sciences, Beijing, China
[e] Department of Earth Sciences, National Taiwan Normal University, Taipei, Taiwan

The Tibetan plateau, which is generally regarded as the archetype of collisional orogens, is also an outstanding natural laboratory for investigating accretionary orogeny because it was located in an Andean-style convergent margin related to the northward subduction of the Neotethyan oceanic lithosphere before India started colliding with Asia along the Indus-Yarlung suture. Knowledge about the pre-collisional geologic processes, however, remains limited because most of investigations in this region have been focused on post-collisional geology. The Trans-Himalayan magmatism, which occurred extensively within the Lhasa terrane of southern Tibet related to the Neotethyan subduction, has long been documented but thus remains poorly studied. Here we report new SHRIMP zircon U-Pb age results for the Gangdese Batholith that represents the largest Trans-Himalayan plutonic complex. These data indicate two episodes of plutonism in the Late Cretaceous (ca. 103-80 Ma) and early Paleogene (ca. 65-46 Ma), respectively. Our results, together with literature information and petrochemical constraints, suggest that the older episode ended up with a combined magmatic and tectonic thickening of the crust while the younger episode resulted in little crustal thickening despite significant melt additions from the juvenile mantle. We attribute the former to a flattening of the Neotethyan northward subduction and the latter to rollback of the subducting slab, which caused tectonic switching from a contractional to extensional setting marked with southward migration and intensification of the magmatism that enhanced thermal softening of the Lhasa lithosphere. Therefore, subsequent India-Asia collision gave rise to distributed lithospheric thickening in southern Tibet where the orogeny eventually evolved from accretionary to collisional with a transitional stage of extension in between.

# Trace element mobilization in subducting oceanic slabs: constraints from dehydration and transport veins in the western Tianshan HP-LT metamorphic belt, NWChina*

J. Gao[1] , T. John[2], R. Klemd[3], C. Garbe-Schönberg[2] , W. Su[1], X. Xiong[1], D. Huang[4]

[1] Key Laboratory of Mineral Resources, Institute of Geology and Geophysics, Chinese Academy of Sciences, P.O. 9825, Beijing 100029, China (gaojun@mail.igcas.ac.cn)
[2]Institut für Geowissenschaften and SFB 574, Universität Kiel, Olshausenstr. 40, 24098 Kiel, Germany (tj@min.uni-kiel.de; dgs@gpi.uni-kiel.de)
[3]Mineralogisches Institut, Universität Würzburg, Am Hubland, 97074 Würzburg, Germany (reiner.klemd@mail.uni-wuerzburg.de)
[4]College of Resources, Central South University, Changsha, 410083, China

The aqueous fluids released by dehydration of subducted oceanic crust have been introduced into the overlying mantle wedge and have caused the metasomatism and partial melting of the overlying mantle wedge and the genesis of arc magma[1-3]. And, high-pressure veins were regarded as the mineral precipitates from fluids formed by dehydration of host eclogites and consequently monitor the major and trace element composition of the fluids[4]. The trace element composition of the fluids could be approximately constrained by the detailed studies on the chemical compositions of the high-presure veins and related host eclogites[4]. Here, we investigate the representative high-pressure veins which are cutting through host blueschists and eclogites from the western Tianshan subduction complex in northwestern China in order to discuss the trace element mobilization of fluids released by dedydration during subduction of oceanic crusts.

Eclogites in Tianshan are intercalated with blueschist layers as pods, boudins, thin layers or large massive blocks. High or ultrahigh-pressure conditions have been suggested for the peak metamorphism of the eclogites during Paleozoic time [5-12]. The presence of abundant centimetre-wide veins filled with coarse-grained omphacite, garnet, quartz and late carbonate in massive omphacite-bearing blueschists and eclogites indicates that a free fluid phase had been present during eclogite-facies conditions [13]. In fact the largest eclogite block in Tianshan is not only composed of true eclogite (garnet + omphacite >70%), but also of omphacitite, epidosite and omphacite-bearing blueschist which are crosscut by eclogite-facies veins.

* This study is financially supported the 'State Key Project for Basic Research of China' (No.2001CB409803) and National Natural Science Foundation of China (40421202)

The vein-network consists of the dehydration veins- derived by dehydration of the immediate eclogite hosts- and transport veins which cross the blueschist host foliation and display sharp interfaces towards theirs wall rocks. They provide unique insights into fluid-rock interaction and trace element mobilization during dehydration and long-distance fluid flow respectively during the major releasing of subducting oceanic crusts.

For dehydration veins, we have tried to calculate the trace element concentrations in the fluids, which have been equilibrated with the veins during dehydration, on the basis of the mineral-mineral and fluid-mineral partition coefficients summarized by Becker et al.[4], experimentally determined fluid-mineral partition coefficients and mineral-mineral partition coefficients obtained from the concentration of minerals in eclogites. The calculation method is taken after Becker et al.[4]. The enrichment of fluid-mobile elements (Li, Be, Cs, Rb, Ba and Pb) in the modeled original fluids from which the veins were precipitated resembles the enrichments in island arc lavas, whereas high-field strength elements (Nb, Ta, Zr), rare earth elements (except for La) and Y in both original fluids and in veins are depleted with respect to N-MORB and arc lavas. The Sr concentrations in the original fluids and the veins show slightly depletion or non enrichment relative to N-MORB, indicating that contributions from subducted oceanic crusts cannot explain the Sr enrichment in arc lave, in agreement with the previous studies. The positive fractionation of La and Be in the veins compared to their neighbouring elements may indicate that both of them are mobile during dehydration. In general, low atomic mass elements (Be and Li), LIL elements, La and Pb- rich and HFS and REE elements– depleted fluids were released by dehydration of subducting oceanic slabs.

For transport vein, the almost twice as high Li-concentration of the vein and the blueschist alteration zone in comparison to the blueschist host supports the assumption of an external origin of the fluids [14]. The low in trace element vein-forming fluid caused a strong mobilization of all trace elements in those parts of the host the passing fluid reacted with. 40-80 % of the trace elements were scavenged which coincided with a loss of the large-ion-lithophile- and light – rare –earth – elements (LILE and LREE), almost double the loss of the heavy-rare-earth and high - field-strength-elements (HREE and HFSE). Around 75% of the total carbon was released as $CO_2$ into the reactive fluid. The main difference between the blueschist host and the blueschist alteration zone is the replacement of glaucophane, dolomite and titanite by omphacite, garnet and minor rutile respectively, while garnet, epidote, rutile and phengite occur in both zones of the rock. Therefore, the fluid-flow regime rather than the mineral assemblages and equilibrium partition coefficients controls the trace element mobility. The mobilized trace elements coincide with those needed to create the slab signature of arc magmas.

**References**


[1] J.B. Gill, Springer-Verlag, New York, 1981, 390pp.

[2] Y. Tatsumi, J. Geophys. Res. 94 (1989) 4697-4707.

[3] S.M. Peacock, Science 248 (1990) 329-337.

[4] H. Becker, et al., Chem. Geol. 160 (1999) 291-308.

[5] J. Gao, et al., J. Metamorph. Geol. 17 (1999) 621-636.

[6] L. Zhang, et al., Sci. China (Series D) 44 (2001) 86-96.

[7] R. Klemd, et al., J. Metamorph. Geol. 20 (2002) 239-254.

[8] L. Zhang, et al., Am. Mineral. 87 (2002) 853-860.

[9] C.J. Wei, et al., J. Metamorph. Geol. 21 (2003) 163-179.

[10] L. Zhang, et al., J. Metamorph. Geol. 21 (2003) 523-529.

[11] J. Gao & R. Klemd, Lithos 66 (2003) 1-22.

[12] R. Klemd et al., J. Geol. 113 (2005) 157-168.

[13] J. Gao & R. Klemd, Contrib. Mineral. Petrol.142 (2001) 1-14.

[14] T. John et al., Lithos (in press, 2006).

# The South Tianshan in northwestern China: a Late Paleozoic or a Triassic collisional orogenic belt between the Tarim and Yili blocks? *

J. Gao[1], R. klemd[2], Q. Qian[1], L. Long[1] and X. Xiong[1]

[1]Key Laboratory of Mineral Resources, Institute of Geology and Geophysics, Chinese Academy of Sciences, P.O. 9825, Beijing 100029, China (gaojun@mail.igcas.ac.cn)
[2]Mineralogisches Institut, Universität Würzburg, Am Hubland 97074, Würzburg, Germany (reiner.klemd @mail.uni-wuerzburg.de)

The 'Altaid orogenic collage' or the 'Central-Asia Orogenic belt'was as resulted from the growth of voluminous subduction-accretionary complexes along a single magmatic arc system and the duplication along large-scale strike-slip fault, and was the world's largest site of juvenile crustal formation in the Phanerozoic eon (Sengor et al., 1993; Jahn, 2004). The growth may be produced by both the lateral accretion of arc complexes before Late Carboniferous and the vertical accretion of post-collisional underplated material of mantle derivation since Late Carboniferous in the North Xinjiang and adjacent Central-Asia region (e.g. Han et al., 1997; Gao et al., 2002; Jahn, 2004). The South Tianshan orogenic belt in northwestern China is located between the Tarim and Yili basins and represents the the last oceanic consumption of the Turkestan Ocean in the west segment of the 'Alaids'. It is traditionally regarded as a Late Paleozoic collisional orogenic belt during last decades (Colemen, 1989; Windley et al, 1990; Allen et al., 1992; Xiao et al., 1992; Gao et al., 1998; Chen et al., 1999). However, recent discovery of suspective Late Permian Radiolaria fossils (Li et al., 2002) and SHRIMP age data obtained from the rim of zircons of the South Tianshan eclogites (220-230Ma; Zhang et al., 2005) may suggest that it is a Triassic collisional orogenic belt between the Tarim and Yili blocks. Thus, new constraints on the collisional orogenic time of the South Tianshan is very important for us to understand the tectonic evolution and continental growth of the 'Central-Asia Orogenic Belt'. Here, we present new age data obtained from ophiolites, blueschists-eclogites and granites for discussion on the collisional orogenic time.

An age of 425 Ma was obtained for zircons from the basalts of the Kulehu ophiolite by SHRIMP method (Long et al., 2006). The age of 569–436 Ma obtained from the core of

* This study is financially supported the 'State Key Project for Basic Research of China' (No.2001CB409803) and National Natural Science Foundation of China (40421202)

zircons from the granulites of the Youshugou ophiolite has been suggested as the age of oceanic crust, and the age of 390–384 Ma obtained from the rim of zircons represents the metamorphic age for the granulite-facies (Zhou et al., 1999). Additionally, an age of 494 Ma was obtained for zircons from the gabbro of the Kanggurtage ophiolites by the SHRIMP method (Li et al., 2006). Additionally, Early Carboniferous Radiolarian Fauna have also been found in the chert which is exposed within the ophiolitic mélange in the South Tianshan (Liu et al., 2001). Although suspective Late Permian Radiolaria fossils have been reported by Li et al. (2002), Late Devonian Conodonts (*Palmatolepis, Polygnathus, Palmatolepis delicatula*) had also been flound from the same Aiketik Group at the same locality (Wang, 1997). Combined with the previous age data obtained from the ophiolites in the South Tianshan (Gao et al., 1998), we suggest that the oceanic crusts have not disappeared until the end of Early Carboniferous.

Sm-Nd isochron dating of 343 $\pm$ 44 Ma (Omp-Gln-Grt-WR) and an age of 346 $\pm$ 3 Ma (Grt-Gln) were determined using an eclogite boudin within blueschists of the Tianshan low-temperature/high-pressure metamorphic belt (Gao and Klemd, 2003). A well-defined $^{40}Ar/^{39}Ar$ plateau age of 344 Ma was obtained for crossite from an omphacite-phengite-bearing blueschist and is concordant with the Sm-Nd isochron age for the eclogite, suggesting that neither argon loss nor excess argon affected the crossite. A well-defined $^{40}Ar/^{39}Ar$ plateau age of 331 Ma was determined for phengite from the same sample. Rb-Sr isochron ages of mica - whole rocks and mica – epidote – glaucophane of blueschists range between 313 and 302 Ma (Klemd et al., 2005). Therefore. we infer that the HP rocks were formed by the B-type subduction of a Paleozoic ‘South Tianshan Ocean’ about 344 Ma ago. They were, however, exhumed to higher crustal levels during the collision of the Tarim and Yili-central Tianshan plates about 331-310 Ma ago. The age of 299 Ma for granulie-facies metamorphism of gneisses and two-pyroxene granulites (Li et al., 2004) and a age of 291 Ma for rodingitization of rodingites associated with eclogites (Li et al.,2005) may also suggest that a post-collisional tectonic event in the South Tianshan, in according with the retrograde and exhumation process of the HP rocks.

New age data have been obtained for granitic or dioritic intrusions exposed in the South Tianshan orogenic belt by the SHRIMP or LA-ICP-MS U-Pb methods recently. The oldest age of 896 Ma was obtained for the gneissic granite at Laerdundaban, similar to the previous results (Chen et al., 1999). The ages of 357- 320 Ma were also obtained for the granites exposed at Laerdundaban. The ages of 478-402 Ma were obtained for the granites exposed along the Akeyazi river. The ages of 433-277 Ma were obtained for the granites exposed along the Kekesu river. The ages of 430-325 Ma were obtained for the granites exposed along the Qiongkushitai river. The ages of 411 and 285 Ma were obtained for the granites exposed in the Heiyingshan area. An age of 420Ma was obtained for the granites in Huolashan. Furthmore, an age of 416 Ma was reported for a dioritic-granitic pluton in north of Baluntai area (Yang et al., 2006). Additionally, the SHRIMP zircon ages of 354 and 313 Ma were also reported for the island-arc type volcanics in the Nalatishan Mountains (Zhu et al, 2005).

On the basis of the data presented here, we conclude that the collision of the Tarim and Yili blocks in the South Tianshan may start at the end of Early Carboniferous, and end at the beginning of Early Permian. In an another word, the South Tianshan is a Late Paleozoic, not a Triassic, collisional orogenic belt. This is further supported by the foreland basin was developed along the northern margin of the Tarim in Later Permian (Chen et al., 1999; Yang et al., 1996) and Early Permian post-collisional granites in the South Tianshan, Kyrgystan (Solomovich et al., 2002).

# 松潘地块-西秦岭造山带岩石圈结构深地震反射剖面探测

高锐[1]　马永生[2]　朱铉[2]　李秋生[1]　王海燕[1]　白金[1]

1 中国地质科学院地质所，北京，100037；
2 中石化股份有限公司南方勘探开发分公司，昆明，650021

松潘地块位于青藏高原东北缘，平均海拔为 3500m 以上，夹持于金沙江缝合带、西秦岭造山带和龙门山造山带之间，其地表广泛地覆盖着三叠纪复理石沉积建造，主体形态酷似一个倒三角形。区域地球物理与地球化学研究显示西秦岭造山带基底构造可能归属于松潘地块。

松潘地块是资源开发的宝地，特别是随着全球石油的紧缺，石油地质界加快了新区勘探，松潘地块被列为油气勘探评价值得重视和重新认识的重要新区之一。虽然目前已经开始了前期勘探与研究，但关于其内部状态及其与西秦岭关系的深部探测研究尚未开展，揭示它们的内部结构、构造属性及其变化，尽快摸清中生代、古生代沉积地层厚度，变质与变形程度，已是急需且为紧迫的任务。深地震反射剖面探测研究将为该区油气资源潜力评价提供重要依据。

由于松潘地块特殊的大地构造环境和雪山、草地、沼泽等恶劣的自然环境，使得研究地壳基底及其盖层存在很大的困难。它的内部结构、构造性质及在大陆演化中所扮演的角色被披上神密的色彩，吸引着许多中内外学者竞相研究。

黄汲清（1962）和任纪舜等（1980）推测它的基底是一个古老地块。Sengör（1984）认为松潘地块可能缺失大陆基底，其上的复理石建造可能直接沉积在俯冲带的洋壳上。Burchfield 等（1995）提出松潘基底是华南陆块的一部分，三叠系地层覆盖于华南古生代浅海层序的顶部。尹安（2000）支持 Burchfield 的松潘基底属陆相的观点，并指出松潘是座落于华南陆盆基底上的残留洋盆。总之，仅从地表零星出露的地质体研究很难确定松潘地块基底的构造属性。

2004 年秋季至冬季，在中国国家自然科学基金和中国国土资源部油气战略中心、中国石油化工集团公司联合资助下，我们完成了一条横过松潘地块北缘和西秦岭造山带的深地震反射剖面。该剖面从北到南全长 254 km，北起西秦岭造山带北边界的甘肃省合作市，向南跨越西秦岭造山带，进入若尔盖盆地，止于盆地南缘四川省的唐克乡。简称合作－唐克（HT）剖面。

合作-唐克剖面是一条深地震共中心点反射剖面，野外采集采用爆破震源，使用 SN388 多道 24 位有限遥测地震仪，480 道接收，道间距 50 m，记录长度 30 s，采样间

隔为 2 ms。为了获得高分辨率地下信息，在施工中采用了小炮、中炮和大炮三种爆炸震源，药量分别为 16 kg、40 kg 和 200 kg。小炮采用单井激发，激发井深 20 m，炮间距 100 m，120 次覆盖；中炮采用两井组合激发，单井井深为 20 m，炮间距为 400 m，30 次覆盖。上述两种爆炸震源采取中间放炮，480 道接收，道间距 50 m，最小偏移距为 175 m。大炮采用单井激发或 3 井组合激发，单井井深为 50 m，5 km 炮间距，最大偏移距为 29175 m。在野外数据采集中采用 GRISYS 和 PROMAX 两套数据处理系统来进行监控工作。通过回放记录来监控信噪比。对每天采集的数据进行初步处理，根据得到初叠剖面来检查每天的数据采集工作质量，调整安排下一天采集工作。这样可以确保野外采集能够获得高质量的数据。

使用 CGG\GRISYS\FUCOS\PROMAX 等先进软件进行数据常规处理, 初步得到的深地震反射时间剖面揭示了松潘地块及西秦岭造山带岩石圈结构, 地壳内部和上地幔构造的反射特征。初步解释取得的以下若干发现：

1. 地壳整体反射特征。地壳变形并非是连续变形，上地壳整体呈现出弱反射，整条测线都在 6-7s 左右开始下地壳出现强反射，推测 7s 左右为上地壳和下地壳的分界线，并呈现弱反射的上地壳、强反射的下地壳全球造山带特有的反射特征。弱反射的上地壳反映了盖层沉积的面貌，强反射下地壳的顶部反映出结晶基底特征。
2. Moho 反射特征。Moho 南北清晰，对应下地壳强反射的底部，呈近似平的略向北倾的层状多组强反射。Moho 大约在 16.50 s－18.00 s 之间(双程走时)，用平均速度 6.00km/s 折合计算, 深度大约在 49.50-54.00 km。最浅 Moho 在剖面南端,约 16.50 s( 约 49.50 km ）,是青藏高原最浅的反射 Moho。
3. 若尔盖盆地构造变形特征与基底性质。若尔盖盆地可能发育双重基底：3 s 左右的中生代地层基底与 6.5-7.0sd 显示微隆起的反射特征，盆地基底之上南侧发育强烈的向北逆冲推覆构造，说明在盆地中存在一个地块，受到两侧的挤压作用形成微隆起，其内部还保留有推覆构造前硬性的的地块反射形迹。盆地基底之上（7s 附近）发育双重逆冲构造面，越靠近盆地南部逆冲构造越强烈，且盆地浅层地层反射高角度南倾。
4. 新生代盆山耦合关系。若尔盖盆地北部地壳向北倾斜，插入到西秦岭下地壳底部，西秦岭造山带由北向南逆冲推覆到若尔盖盆地上。对应其浅层，发育一个深度约 5 km 的山前凹陷（黑河凹陷？)。
5. 西秦岭造山带构造变形特征与基底性质。发现西秦岭造山带浅部（2-3s）构造层受深部控制，与基底构造（7s）同步起伏。推测西秦岭造山带存在双重的基底，(2-3s）构造层是中生界的底，(7s）构造层反映了古老的基底。下地壳向北连续大规模北倾

的强反射说明西秦岭造山带地壳向北多次俯冲,下地壳呈现出指向南的叠瓦状多组逆冲构造，表现出地壳是挤压逆冲缩短加厚。西秦岭造山带地壳与若尔盖盆地一样呈现出弱反射的上地壳、强反射的下地壳特征,（7s）强反射将地壳明显分为上下两部分，说明西秦岭造山带基底性质与若尔盖盆地类同。

6. 重磁场多尺度分析支持西秦岭造山带与若尔盖盆地基底性质同属统一稳定的基底。弱磁性区覆盖了西秦岭造山带与若尔盖盆地, 显示西秦岭造山带与若尔盖盆地基底性质同属统一稳定的松潘地块，环境有利于油气发育。
7. 三叠系沉积厚度。深反射剖面反射特征和区域重磁场多尺度分析一致发现，三叠系沉积巨厚，山区厚度一般大约在（2-3s），盆地内情况不明。由于浅层反射需要进一步的精细与特殊处理，更详细的情况待解释。

**参考文献**


An Yin and T. Mark Harrison, *Annu. Rev. Earth Planet. Sci.,* 2000, 28, 211-80.

Burchfiel, BC, Chen Zhiliang, Liu Yuping Royden LH, *Int. Geol. Re*v., 1995,37, 661-735.

Molnar P, Lyon-Caen H, *Geophys. J. In*t., 1989,99,123-153.

Sengor AMC, *Geol. Soc. Am. Spedcial Paper* 195, 1984, 1-82.

# Deep Geophysical Probing and geodynamic study for Lithospheric Structure in the Tibetan Plateau

Rui Gao, Zhanwu Lu, Qiusheng Li, Ye Guan, Jisheng Zhang, Rizheng He, and Liyan Huang

Lithosphere Research Centre, Institute of Geology, CAGS, Beijing, 100037, China. E-mail: gaorui@cags.net.cn

## Introduction

In the process of continental evolution, continent-continent collision substantially affects the earth's structure. As a typical example, the Tibetan Plateau Plateau, the highest, biggest and youngest orogen in the world, was brought about by collision of the Indian plate with the Eurasian plate, as well as continuous northward movement of the former. Continent-continent collision is still going on. The plateau is considered an optimal place for studying the basic problems of continental dynamics such as continent-continent collision, convergence and subduction of plates, and formation of the plateau. Probing into the structure of the crust and upper mantle of the Tibetan Plateau Plateau is a key to explaining continent-continent collision, and a necessary approach to understanding the forming and uplifting mechanism and geodynamic process of the plateau. Chinese geophysicists have carried out deep seismic reflection research in the Qaidam Basin in this region since the 1950s, and have acquired a wealth of scientific data. This paper summarizes the deep geophysical probing of the crust and upper mantle on the Tibetan Plateau conducted chiefly by Chinese geophysicists, and presents a series of summary diagrams for different methods to illustrate the results. The longitudinal and latitudinal ranges discussed in this paper are 76°–106°E and 26°–40°N respectively, and the tectonic settings in the diagrams refer to Yin et al. (2001). On this basis, primary research results with regard to the crustal structure, electrical properties of the lithosphere, and the uplifting mechanism and geodynamical model of the plateau are reviewed. The authors hope this paper may provide valuable references for the further study of the Tibetan Plateau.

## Status of deep geophysical survey and research

In 1958, the Institute of Geophysics of the Chinese Academy of Science (CAS) and the Ministry of Petroleum Industry jointly detected the deep foundation bed with low-frequency seismographs, and studied the deep crustal structure in the Qaidam Basin (Zeng et al., 1961), which was the prelude of the geophysical survey of the crust and upper mantle on the Tibetan

Plateau Plateau.

**Deep seismic sounding (DSS)**

In 1977, CAS carried out a 460 km-long N-S-stretching profile along the Yadong-Damxung line, and acquired information on the crustal and upper-mantle structure and velocity distribution (Institute of Geology, 1981). Since 1980, Chinese and French scientists have cooperated in conducting DSS along some sections in northern and southern Tibet and obtained abundant valuable data, which has brought about a high tide of DSS application in this region. The Ministry of Land and Resources (formerly Ministry of Geology and Mineral Resources), CAS, and the State Seismological Bureau increased their input into the DSS work. The cumulative length of DSS profiles conducted before 2004 on the Tibetan Plateau Plateau was about 12,000 km, and the profiles are deployed over the major part of the plateau.

**Nearly-vertical seismic reflection (Deep seismic reflection)**

Deep seismic reflection is the most effective method for studying the fine structure of the lithosphere. In 1958, Zeng and his group carried out a seismic reflection test in the Qaidam Basin, but techniques including multiple coverage and migration were not employed at that time due to the poor technical conditions (Zeng et al., 1961). The nearly-vertical seismic reflection method with multiple coverage was used for the first time by Project INDEPTH in the study of the Tibetan Plateau Plateau. The deep seismic reflection profiles finished in this project showed fine crustal structure on both sides of the Indus-Yalu suture (IYS), which has exerted a far-reaching influence on the world. Several deep seismic reflection profiles crossing the mountain-basin junction on the northern margin of the plateau were carried out by geophysicists with the Chinese Academy of Geological Science (CAGS), which afforded an effective basis for studying the deep deformation process resulting from collision. The profiles in this plateau, however, were not intensively studied, due to high cost, and the total length of them was just 1,300 km, about 10 per cent of that of the DSS.

**Broadband seismic observation (BB)**

In 1991, Zeng and Wu (Zengetal.,1992) deployed 11 broadband seismographs along the Golmud-Xigazê line to observe crustal and upper-mantle structure for the first time in China. Since then, Chinese scientists have acquired a host of observation findings by means of international or regional cooperation. At the present time, this method has covered all the main sutures in this region. Triggered seismographs were first applied along the Tibetan Plateauan Highway in the Sino-French Project in June, 1992, and improved single-component seismographs were used in 1993, which ensured high equality of data (Jiang et al., 1994). Subsequent work in the period 1995–1998 disclosed the lithospherical characteristics of the northern part of the plateau (Xu et al., 2001). Broadband seismic observation in the INDEPTH crossed the Bangong-Nujiang suture (BNS) and entered the Qiangtang block, so as to deepen the research on the deformation mechanism of the interior structure of the plateau. During the period 1997–1998, the CAGS and the Institute of Earth Sciences, Academia Sinica based in Taiwan jointly studied the deep structure of the Tarim and western Kunlun region with the TEFTEK-72 digital acquisition system, STS-II broadband receiver and GPS equipment. This program detected hundreds of effective seismic events and acquired dozens of gigabytes of data (Kao et al., 2001).

**Magnetotelluric sounding (MT)**

Magnetotelluric sounding is a natural-source electromagnetic method, which takes surface electromagnetic waves as the field source, and traces underground records by observing quadrature electromagnetic components. The MT has proved successful in studying continental dynamic problems. During the period 1980–1981, a Sino-French team applied this method for the first time to the study of the Tibetan Plateau Plateau (Yuan et al., 1990). Two MT sections, the Yadong-Golmud and Golmud-Ejin Qi global geological transects (GGTs), traversed the whole plateau and revealed its electrical structure (Guo et al., 1990; Zhu et al., 1995). The INDEPTH-MT research team, composed of Chinese and American geophysicists, observed long-period and broadband magnetotelluric fields as a whole by means of 21 long-period observation instruments, LIMS (period of signal acquisition: 10~300,000 s) and a broadband instrument (period of signal acquisition: 1/320–2,000 s) (Wei et al., 2001). Appropriate observation methods and high-precision equipment greatly enhanced the quality of the acquired data. The MT profiles accomplished thus far run through the Tibetan Plateau Plateau from north to south, and have laid a solid foundation for studying the electrical structure of the whole plateau. By 2004, the cumulative length of MT profiles was more than 10,000 km.

**Deep gravity and Deep magnetic surveys**

Deep gravity and magnetic surveys are very important approaches to examining the crustal structure and uplifting mechanism of the Tibetan Plateau Plateau. Both of these surveys were conducted during the study of the Yadong–Golmud and Golmud–Ejin Qi GGTs. The total lengths of deep gravity and magnetic sections completed from 1982 to 2004 were more than 8,300 km and 5,800 km respectively.

**Heat flow observation**

Discussion and study of the deep thermal regime of terranes, thermal structure of the crust and mantle and formation of the Tibetan Plateau Plateau are the key to disclosing the uplifting mechanism of the plateau. In this regard, the heat flow observation serves as an indispensable geophysical approach, having been employed in the survey of the Yadong–Golmud and Golmud–Ejin Qi GGTs (Shen et al., 1990; 1995). This work revealed the heat flow distribution, deep geothermal regime, thermal structure of the crust and mantle, and lateral heterogeneity and formation mechanism of the plateau).

**Major achievements of geophysical surveys of crust and upper mantle in the Tibetan Plateau**

**Crustal structure**

Deep geophysical surveys have covered the main structure units of the Tibetan Plateau Plateau since 1958. They cross the Himalayas, west Kunlun-Altyn-Qilian Mountains and Longmen Mountains. The profiles have a total length of about 45,000 km, and have disclosed the 3D structure and structural frame of the crust and upper mantle of the plateau.

***Moho depth and its changes***

The Moho depth is a significant indicator of crustal structure. The great thickness of the Tibetan Plateau Plateau is unique in the world. So far, seismic methods have been used to explore the Moho depth, among which DSS is the most effective one. We usually use Pm and Pn wave phases to ascertain the Moho depth, and the P wave velocity at the top of the upper mantle. The Pn wave phase, however, is not easily observed in the interior of the plateau. Geophysical researches throughout the world show that strong response to the Moho can be obtained in terms of deep seismic reflections.

The lower crust often appears as a compressional reflection layer beneath an orogenic zone, while the bottom of the layer corresponds with the refraction Moho. The broadband seismic observation has been developing rapidly and made great progress on the Tibetan Plateau Plateau. P wave conversion (e.g. P-S conversion) while passing the Moho can be recorded by broadband seismic stations. The Moho depth and configuration are imaged with the receiver function method. Detailed changes of the Moho can be detected by deep seismic reflection, the resolution of which is higher than that of the DSS. Researches conducted extensively worldwide show that the results of these two methods can be correlated in general. Resolution of the broadband seismic observation is lower than those of the deep seismic reflection and DSS. However, the receiver function method and the reflection method have a similar theory. Converted waves from teleseismic events are fairly sensitive to the location of the Moho surface. Research findings reported both in China and abroad show that the broadband seismic method and the DSS present almost consistent images of the Moho along the section from Lhasa to Golmud. Our discussion on the Moho depth and its changes are right based on this understanding.

**a. The deepest and shallowest Moho**

The latest broadband seismic observation reveals that the deepest Moho in the Tibetan Plateau Plateau is located at the west Kunlun structural knot (90±2 km in thickness) beneath the southern branch of the Altyn fault (Wittlinger et al., 2004). Gao et al. (2005) accomplished a deep seismic reflection profile crossing the west Qinling orogen and the Zoigê basin, and discovered a strong reflection of the Moho at 16.50 s TWT (two-way travel time), corresponding to a depth of approximately 49.50 km, which may be considered the shallowest Moho in this region.

**b. Variation of the Moho across the plateau from north to south**

Scientists have paid great attention to the changes of the Moho from north to south across the Tibetan Plateau Plateau. Xiong et al. (1985) and Hirn et al. (1984) studied such changes by using the data obtained by the Sino-French research project (1981–1982). Afterwards, some new probe sections were finished in northern Tibet. To summarize, the Moho is shallow on the northern and southern margins of the plateau, and deep in the central part. Besides, offsets can be observed on both sides of the main sutures.

To date, no completed active-source seismic profile has been done for the purpose of investigating crustal thickness, so the Moho depth and its changes beneath the Himalayas are still unclear. The Sino-French team suggested a depth of 55–53 km for the Moho beneath the high Himalayan organic belt, with a gentle rise in its northern part. They gave this estimate based on the records along a profile with the shotpoint in Tibet and the receiver in Nepal (Xiong et al., 1985). The INDEPTH-I seismic reflection profile gave a Moho depth of 75 km. With its southern end at Pagri, this profile crosses the high peak region of the Himalayas, so 75 km may indicate the largest depth of the Moho under the Himalayas (Zhao et al., 1993). However, there exist high-Himalayan crystalline rocks on the southern slope of the Himalayas, and therefore some geophysicists think that the depth of 75 km is consistent with the value of 75–78 km obtained by the Sino-French Project along the Paikü Co–Puma Yumgco profile (Teng et al., 1983; Xiong et al., 1985). Pelkum et al. (2005) considered that the Moho depth is ~45 km from Nepal to the southern high Himalayas and reaches ~75 km beneath the Tethyan Himalayas.

The Moho is offset beneath the IYS suture. Hirn et al. (1984) proposed a larger offset (~20 km), while Xiong et al. (1985) suggested a smaller offset (~10 km).

The Moho depth under the Lhasa block has been a disputable question for a long time. Some have concluded that the average Moho depth of the Lhasa block is 55 km (Hirn et al., 1984), but others estimated the value at 70 km (Xiong et al., 1985). After reinterpreting the Siling Co–Y'angamdo wide-angle seismic profile, Zhang et al. (2001) hypothesised a downwarping form of the Moho in northern Tibet, and thought the depth to be at least 80 km. To the south of BNS, the Moho is reportedly as deep as 80–84 km (Zeng et al., 1994). Unfortunately, the INDEPTH-II seismic reflection profile was not able to detect the Moho under the Lhasa block..

The Moho is also offset as crossing the BNS, and becomes shallower upon entering the Qiangtang block. Wideband seismic observation revealed a Moho offset of ~ 10 km (Zeng et al., 1994), but the INDEPTH-III presented a value of only 5 km (Ross et al., 2004). Despite the disagreement, it should be commonly accepted that the Moho becomes shallower when it crosses the BNS.

Beneath the northern Qiangtang block along the TuotuoheGolmud wide-angle seismic profile, the Moho has a depth of 68–70 km (Lu et al., 1990) and a small offset, 60 km, under the Jinshajiang suture (Li et al., 2004a). From the eastern Kunlun Mountains to the Qaidam Basin, the Moho depth undulates in a range from 60 km to 52±2 km (Lu et al., 1990). The Moho offset does not exceed 10 km, which is close to the finding by Wu Q.J. et al. (1998), but obviously different from the value of 15–20 km estimated by Zhu et al. (1998). The difference is aroused by the disagreement with respect to the Moho depth in the Qaidam block. Blasting seismic profiles across the Qaidam Basin present an average Moho depth of 55–60 km (Xu et al., 1993; Cui et al., 1995; Zhao et al., 2001), but merely 40 km was the Moho depth in the model proposed by Zhu et al. (1998). The Golmud–Ejin Qi transect (1990–1995) revealed a Moho depth of 60–70 km under the Qilian Mountains, 57 km on the northern margin of the Qilian Mountains and 48–52 km in the Hexi Corridor basin (Cui et al., 1995).

**c. Variation of Moho in the nearly east-west direction**

Though there is a limited number of east-west deep seismic survey sections in the Tibetan Plateau Plateau, we can still qualitatively describe the east-west changes of the Moho depth in this area. The existing data suggest that the Moho is deeper in the west and shallower in the east. This is probably related to the eastward flow of the matter out of the plateau.

**Depth and characteristics of low-velocity and highconductivity layers in the crust**

Low-velocity and high-conductivity layers occur extensively but discontinuously in the Tibetan crust, with a depth of 20±5 km, a velocity of 5.6–5.8 km/s and a thickness of 5–10 km. Though not exactly coincident with each other, they have a similar variation trend in depth and thickness (Gao et al., 1995).

There are different opinions on the formation of the layer. Nelson et al. (1996) concluded that a partial-melting layer existed broadly in the middle crust beneath southern Tibet. Notably, where low-velocity zones are recognised, partial melting is manifest. Kind et al. (1996) agreed with this viewpoint. Wang et al. (1990) hold that the mid-crustal low-velocity layer beneath southern Tibet may be a brashy zone composed of partially-melting matter, which formed a detachment surface in the mid-crust where most surficial faults are terminated. Spratt et al. (2005) considered that the high-conductivity layer originated from partially-melting matter in northern Tibet, whereas Wei et al. (2001) reported that this layer is probably due to both partial melting and fluids in southern Tibet.

*Characteristics and types of velocity structure in the lower crust*

Thickening of the lower crust in the Tibetan Plateau Plateau is influenced by heterogeneity of the crust. We can divide the lower crust into several types, as below, in terms of velocity structure and reflection characteristics obtained with DSS and deep seismic reflection profiles.

**a. Lower crust with reverse velocity structure.** The Yadong-Golmud GGT depicts a reverse velocity structure, which is characteristic of the lower crust under the Tethyan Himalayan orogen, where seismic waves are reversed extensively (Wu et al., 1991). Such a lower crust is 38–78 km in depth, with a thickness of 40 km;

**b. Lowercrustwithgradedvelocitystructure.** Wangetal.(1990) reported lower crust with graded structure of velocity in northern Tibet. The gradient belt he estimated is 20–30 km thick and 55–82 km deep in the lower crust, with an average velocity of 7.40 km/s. There is a great dispute on whether the Moho depth is 50~56 km or 70~75 km, because of the disagreement on the velocity gradient belt of 7.4 km/s. The belt with this velocity was classified as the lower crust, based on the correlation between reflection and refraction waves in the study of the Yadong-Golmud GGT (Wu et al., 1991). A similar phenomenon can be seen in the Kunlun structural belt (Lu et al., 1990);

**c. Lower crust with multilayer close reflections.** Lower crust with close reflection has been widely discovered beneath orogens throughout the world. Strong reflectivity was found at 10 s– 20 s on the Bangoin deep seismic reflection profile studied in the third phase of the INDEPTH (INDEPTH-III), which resembles the typical reflectivity in the lower crust along the BIRPS WAM line in Western Europe (Ross et al., 2004). Gao et al. (2005) interpreted the strong reflection layer at 7 s on the Songpanwestern Qinling reflection profile as the lower crust.

**d. Thinning lower crust.** A number of facts have been noticed, such as the shallowing of the Moho (65–58 km) when crossing the BNS, low velocity of Pn waves in the Qiangtang block (McNamara et al., 1995), great attenuation of Sn waves and large-scale high-conductivity zones. All these imply that the lower crust is structurally thinning, and a mass of heat flows are existing in the region (Wei et al., 2001); e. Steady platform lower crust. Based on the study in the eastern Qaidam Basin, Teng et al. (1974) discovered a steady high-velocity layer near the Moho, and he considered it to be steady basic matter in the lower crust under the Qaidam Basin.

### Uncertainty of lithosphere thickness

Seismic methods serve as the principal means for geophysical investigations, but they need super-long profiles, usually over 1,000 km, to study the lithosphere. Up to now, active-source seismicmethods have not yielded helpful information on lithospheric thickness in the Tibetan Plateau Plateau, due to complexity of the crustal structure. At present, natural earthquake data are used as primary information in this respect. Song et al. (1985) assumed that the thickness of the Tibet plateau was 120 km, the same finding was obtained by Zhuang et al. (1992). Chen et al. (1985) reported 100 km by means of the surface wave dispersion of frequency, and Wu J.P. et al. (1998) gave a thickness of 110 km based on body wave inversion. The difference among these findings is brought about by different seismic wave traces, different data and different operation methods. However, natural earthquake records probably suggest that the lithospheric mantle is not quite thick, in spite of the extreme thickness of the crust.

Geophysicists usually infer lithospheric thickness based on the thickness and variation of high-conductivity layers in the upper mantle acquired by the MT, which has been employed to study the depth and undulation of the upper mantle under the Tibetan Plateau Plateau. Discussions and descriptions of the lithospheric thickness were made during the Sino-French Project and in the study of the YadongGolmud GGT (Guo et al., 1990). However, the reliability of the information about the deep structure is somewhat weakened due to lack of measuring points, large spacing of the points and narrow frequency band of the MT. Nevertheless, the above study can still be regarded as successful under the poor working conditions of that time.

The broadband magnetotelluric system (MT24) and the superlong-period MT system (LIMS) were used together to collect superlong-period magnetotelluric signals. The electrical structure of the crust and mantle beneath the plateau was described with modern MT data-processing and inversion techniques (Chen et al., 1996; Wei et al., 2003; Tan et al, 2004; Spratt et al., 2005). The INDEPTH-MT team did not find high-conductivity layers in the upper mantle. The low-resistivity layer in the upper mantle lies at a great depth in the

Himalayan orogen in southern Tibet, while the low-resisitivity layer in the asthenosphere is upwarped beneath the Gangdisê structural belt in Central Tibet, which implies fine regional conductivity. Presently, none of the published INDEPTH-MT findings has specified the exact thickness of the lithosphere in the Tibetan Plateau Plateau.

It can thus be seen that seismic methods as well as the MT sounding method cannot accurately decide the lithospheric thickness of the Tibetan Plateau Plateau, suggesting that the lithospheric thickness of the plateau is uncertain.

## Uplift mechanism and geodynamic process of the Tibetan Plateau

The formation and uplift mechanism of the Tibetan Plateau Plateau is a complex question. Despite a considerable body of research, there are still diverse opinions (Gao, 1997; Pan, 1999).

### *Amalgamation of terranes and uplift of the plateau*

Chinese geologists discussed the forming process of the Tibetan Plateau Plateau at a fairly early date. Chang et al. (1982) argued that the plateau was not a uniform body, but came into being as an assemblage of terranes of diverse periods. This viewpoint was supported by geophysical surveys (e.g. Wu et al., 1991; Gao et al., 1995).

Wu et al. (1991) pointed out that the plateau kept uplifting in the course of terrane amalgamation, which underwent a process of "ocean-crust underthrusting→ continent-continent collision→intracontinent underthrusting". Ocean-crust underthrusting induced thickening of continental crust, and continent-continent collision gave rise to thrusting and overlapping of slabs, thus thickening the crust. The intracontinent underthrusting taking place after continentcontinent collision was perhaps due to gravitational sinking of oceanic lithospheric plates or continental inserting along crustal weak zones. It was assumed that inhomogeneous uplift occurred as early as when terranes were assembled to form the Tibetan Plateau Plateau, which was actually confirmed by a subsequent research (Murphy et al., 1997). After the plateau was formed, the crust slid along terrane boundaries under persistent bidirectional extrusion of the Indian and Asian plates. North-south shortening and east-west extension of the crust were absorbed by active old sutures and NE- and NW-stretching strike-slip faults developing in the terranes.

Li (1995) summarised the uplift mechanism of the plateau as "intracontinental converging→layering thickening of crust→gravitational isostatic adjustment". Northward continuous move of the Indian plate and obstruction of the surrounding rigid blocks brought about violent intracontinental convergence. Affected by strong compressing stress, intracontinental underthrusting took place along old sutures between structural belts; on the other hand, there took place multiple detachment in the crust. The upper, middle and lower crust became either thicker or shorter in different ways. The plateau uplifted slowly, and the upper mantle subsided greatly, thus forming a "mountain root". During the Pliocene and Middle Pleistocene, especially the latter, the plateau drifted more slowly on the whole, and the differences in drift velocity of different blocks became less significant. As a result, stress was relaxed and press reduced. Strong isostatic readjustment was then reached under the influence of the mountain root. In this case, the whole plateau was uplifted considerably and quickly, eventuating on the huge Tibetan Plateau Plateau.

Zhong et al. (1996) considered the uplift of the plateau a multistage, speed-variable and inhomogeneous process. At least two mechanisms are responsible for the entire uplift and local rapid rise of the plateau since the Late Pliocene.

According to the 3D velocity structure of the Rayleigh wave and the result of the DSS, Teng et al. (1999) put forward a model of two-layer "wedge plates", that is, the crust and upper mantle of the Indian plate was blocked by various tectonic bodies while moving northwards and finally terminated at different positions. The first "wedge plate" is the middle and upper crust, where the matter above the Moho moves northwards and is obstructed by steep faults around the Yarlung Zangbo River. The second "wedge plate" is at the bottom of the low-velocity layer above the Moho, and the top of the mantle low-velocity layer as its upper and lower detachment surfaces. Pushed by a strong collisional and compressional system, it moved northwards, breaking through the Yarlung Zangbo fault, and stopped at the southern margin of the Tarim-Qaidam terrane when obstructed by the northern continental core.

Based on four seismic tomographic profiles across the QinghaiTibet Plateau, 3D travel-time data and transformed waves, Xu et al. (2004) obtained seismic wave anisotropy, seismic velocity layers and velocity images of layers from surface down to a depth of 400 km, which demonstrate the structural and physical characteristics of the mantle. Furthermore, a new collisional model for the Tibetan Plateau Plateau was proposed, which involved the following geological events: ultradeep intracontinental subduction of the Indian lithosptheric slab in the southern plateau, deep subduction of the craton on the northern margin, deep mantle plume in the interior, and "dextral uplift" and eastward extrusion of material beyond the lithosphere.

***Lithospheric detachment and slab abruption***

Bird (1978) put forward a detachment mode on the basis of heat sources of collision and orogeny, and discussed the granite magmatism, metamorphism and uplift mechanism of the Himalayan orogen. Detachment caused descending of the lithospheric mantle and ascending of asthenosphere, followed by material exchanges between the lower crust, lithospheric mantle and asthenosphere, and consequently magmatism, uplift of mountains, and extension and collapse took place. Geophysical surveys can be an effective approach to yielding information on lithospheric detachment on the plateau.

Based on seismic tomographic images, Kosarev et al., (1999) held that the north-plunging Indian lithospheric mantle began to detach from the crust 50 km north of the Indus-Yalu suture. The lithospheric mantle kept undertrusting northwards, met with the Asian lithospheric mantle 50–100 km north of the BNS at depths of 200–250 km, and then subsided beneath the mantle. Mass transfer might have occurred at the boundary of the irregular 410-km discontinuity beneath northern Tibet. Kind et al. (2002), in terms of the same technique, proved the underthrust of the south-dipping Asian lithospheric mantle toward the Qiangtang block. Tilmann et al. (2003) reported that the front of the Indian lithospheric mantle was detached 100 km below the Qiangtang block, where a mass of asthenospheric matter ascended and was exchanged with the lithosphere.

Zeng et al. (2000) observed multiple crustal subductions in the Himalayas and southern Tibet. The subducting Indian crust must have split apart from its upper mantle, and the Indian lithospheric mantle subducted continuously in the upper mantle, which can be showed by geophysical evidence (Wu et al., 2004). Xu et al. (2004) reported that the Indian lithospheric slap subducted gently 400 km north of the IYS, beneath the Tanggula mountains. A large highvelocity anomalous zone was split into separate high-velocity anomalous bodies, which may be considered as geophysical evidence for abruption brought about by Indian lithospheric mantle subduction.

## Conclusions

Thanks to the efforts made over the past fifty years, geophysicists have carried out numerous projects on the Tibetan Plateau Plateau, studying the crust and upper mantle. The total length of the accomplished survey profiles has already amounted to more than 45,000 km. These projects have provided convincing geophysical evidence for the study of many interesting questions about the plateau such as the formation process, lithosphere structure and uplift mechanism.

(1) In general, the crust of the Tibetan Plateau Plateau is thinner in its southern, northern and eastern parts, but thicker in the western part, with asymmetrical thickening revealed in the central part. The thickest crust is found in the Tethyan Himalayan structure belt, while the thinnest is located in the Zoigê block in northeastern Tibet. The Moho is offset more or less when crossing all the main sutures. There are distributed nonuniform low-velocity and high-conductivity layers or structural detachment layers in the crust of all the terranes. It is hard to ascertain the thickness of the lithosphere for the time being. Although the crust is extremely thick, no evidence has been found for the thickening of the lithospheric mantle.

(2) The lower crust of the Tibetan Plateau Plateau is characterised by inhomogeneous structure, exhibited in different forms: reverse velocity structure in southern Tibet, graded velocity structure in northern Tibet, and lower crust with multi-layer close reflections, thinning lower crust and steady platform lower crust. Different types of structure are related to different behaviours of crustal activity.

(3) The Tibetan Plateau Plateau is a nonuniform body composed of terranes possessing diverse development processes. Actually, inhomogeneous uplift already occurred in the course of terrane amalgamation. Bi-directional convergence and compression of the Indian plate and the Eurasian plate was the major driving force behind the plateau uplift, whereas lithospheric detachment and slab abruption brought about quick uplift and subsequent extension of the plateau.

Geoscientists have done much in the study of the Tibetan Plateau Plateau based on geophysical exploration, however, no thorough understanding has been gained. There are still disagreements with respect to many significant scientific issues. The plateau is so huge and complex that much more research needs to be done before we can get a clear geological picture.

**Acknowledgements**

We wish to thank Wang Chunyong, Zhang Zhongjie, Chen Zhiliang and Fang Shengming for their assistance and advice. Thanks are also due to Teng Jiwen, who provided us with data and study findings he obtained in 1958. We sincerely thank Liu Xinzhu, Wang Huaxiao and Zhang Zhaoyuan for their careful revision of the English. This paper was financed by the National Natural Science Foundation of China (No. 40334035) and the Ministry of Land and Resources of China (No. 200010101).

**References**

Bird, P., 1978, Initiation of intracontinental subduction in the Himalayas: J. Geophys. Res., 83: pp.4975~4987.

Chang, C.F., Pan, Y.S., Zheng, X.L. and Zhang, X.M.,1982, The geological tectonics of Qinghai-Xizang (Tibet) Plateau, China Science Press.

Chen, L.S., Booker, J.R., Jones, A.G., Wu, N., Unsworth, M.J., Wei, W.B. and Tan, H.D., 1996, Electrically conductive crust in southern Tibet from INDEPTH magnetotelluric surveying: Science, 274, pp.1694~1696.

Chen, G.Y. and Zeng, R.S., 1985, The difference of lithospheric structure between Himalayan mountain and Tibetan plateau from surface wave dispersion: Acta Geophysica Sinica (in Chinese), 28 (Suppl.), pp.161~173.

Cui, Z.Z., Li, Q.S., Wu, Ch.D., Yin, Z.X. and Liu, H.B., 1995, The crustal and deep tectonics in Golmud-Ejin Qi GGT: Chinese Journal of Geophysics (in Chinese), 38 (Suppl. Ⅱ), pp.15~28.

Gao, R. and Wu, G.J., 1995, Geophysical model and geodynamic process of Yadong-Golmud geoscience transect on Tibetan Plateau plateau: Journal of Changchun University of Earth Sciences (in Chinese), 25(3), pp.241~250.

Gao, R., 1997, Thirty problems of the lithospheric structure and geodynamics on the Qinghai-Xizang plateau: Geological Review (in Chinese), 43(5), pp.460~464.

Gao, R., Huang, D.D., Lu, D.Y., Qian, G.H., Li, Y.K., Kuang, C.Y., Li, Q.S., Li, P.W. Feng, R.J. and Guan, Y. 2000, Deep seismic reflection profile across the contact zone of the West Kunlun orogenic belt and the Tarim Basin: Chinese Science Bulletin (in Chinese), 45(17), pp.1874~1879.

Gao, R., Li, P. W., Li, Q. S., Guan, Y., Shi, D.N., Kong, X.R. and Liu, H.B., 2001, Deep process of the collision and deformation in northern Tibetan Plateau-implications from deep seismic sounding results. Science in China (Series D) (in Chinese), 31(suppl.), pp. 66~71.

Gao, R., Ma, Y.S., and Zhu, X., 2005, The Lithospheric structures of the Songpan block in the northeastern Tibetan plateau—revelation from investigation of the deep seismic profile: GEOLOGIE ALPINE, 20th Himalayan- Karakoruam-Tibet Workshop Special extended abstracts, Aussois France, pp. 44,.

Guo, B., Liu, Q.Y., Chen, J.H., Zhao, D.P., Li, S.C.and Lai, Y.G., 2004, Seismic tomographic imaging of the crust and upper mantle beneath the Northeastern edge of the Qinghai-Xizang plateau and the Ordos area: Chinese Journal of Geophysics (in Chinese) , 47(5), 790~797.

Guo, X.F., Zhang, Y.C., Cheng, Q.Y., Gao, R. and Pan, Y., 1990, Magnetotelluric studies along Yadong-Golmud geosciences transect on Qinghai-Xizang plateau: Bulletin of The Chinese Academy of Geological Sciences (in Chinese), 21, pp. 191~202.

Hirn, A., Lepine, J.C., Jobert, T.G., Sapin, M., Wittlinger, G., Xu, Z.X., Gao, E.Y., Wang, X.J., Teng, J.W., Xiong, S.B., Pandey, M.R. and Talte, J.M., 1984, Crust structure and variability of the Himalayan border of Tibet. Nature, 307(5946), pp.23~25.

Institute of Geophysics, Academic Sinica, 1981, Explosion seismic study for velocity distribution and structure of the crust and upper mantle from Damxung to Yadong of Xizang plateau. Acta Geophysica Sinica (in Chinese), 24(2), pp.155~170.

Jiang, M., Lu, Q.T., and Xue, G.Q., 1994, Research on crustal structure of the Tibetan Plateau using seismic experiment jointly by Chinese and French geophysicists: Chinese Journal of Geophysics (in Chinese), 37(3), pp. 412~413.

Jiang, M., Lu, Q.T., and Shi, D.N., 1996, The study on the structure of crustal and upper mantle with natural earthquakes on central Tibetan Plateau: Chinese Journal of Geophysics (in Chinese), 39(4), pp. 470~482.

Kao, H., Gao, R., Rau, R,J., Chen., R.Y, Shi, D.N., Chen, W.P., and Wu, F.T., 2001, Seismic image of the Tarim basin and its collision with Tibet: Geology, 29(7), pp.575~578.

Kosarev, G., Kind, R., Sobolev, S.V., Yuan, X., Hanka, W. and Oreshin, S., 1999, Seismic evidence for a detached Indian lithospheric mantle beneath Tibet: Science, 283, pp.1306~1309.

Kind, R., Ni, J., Zhao, W.J. Wu, J.X., Yuan, X.H., Zhao, L.H., Sandvol, E., Reese, C., Nabelek, J. and Hearn, T., 1996, Evidence from earthquake data for a partially molten crustal layer in Southern Tibet: Science, 274, pp.1692~1694.

Kind, R., Yuan, X., Saul, J., Nelson, D., Sobolev, S.V., Mechie, J., Zhao, W., Kosarev, G., Ni, J., Achauer, U. and Jiang, M. 2002, Seismic images of crust and upper mantle beneath Tibet: evidence for Eurasian plate subduction: Science, 298, pp. 1219~1221.

Li, Q.S., Lu, D.Y., Gao, R., Zhang, Z.Y., Liu, W., Li, Y.K., Li, J.W., Fan, J.Y. and Xiong, S.M., 2001, An integrated study of deep seismic sounding profile along Xinjiang Global Geoscience Transect (Quanshuigou-Dushanzi): Acta Geoscientia Sinica (in Chinese ), 22(6), pp.534~540.

Li, Q.S., Peng, S.P., and Gao, R., 2004a, A review on the Moho discontinuity beneath the

Tibetan plateau. Geological Review (in Chinese), 50(6), pp. 598~612.

Li, Q.S., Peng, S.P., Gao, R., Guan, Y. and Fan, J.Y., 2004b, Deep tectonic background of the 8.1 Ms earthquake in the east Kunlun: Acta Geoscientica Sinica (in Chinese), 25(1), pp.11~16.

Li, S.L., Zhang, X.K., and Zhang, C.K., 2002, A preliminary study on the crustal velocity structure of Maqin-Lanzhou-Jingbian by means of deep seismic sounding profile: Chinese Journal of Geophysics (in Chinese), 45(2), pp.210–217.

Li, T.D., 1995, The uplifting process and mechanism of the Tibetan Plateau plateau: Acta Geoscientia Sinica (in Chinese), (1), pp.1–9.

Lithosphere Research Center of CAGS, 1996, Lithospheric structure and tectonics in Tibet and its formation and evolution. In: Geological Special, China : Geological Publishing House.,.20,pp.83~93

Liu, H.B., Kong, X.R., Ma, X.B., Wang, Q.S., Yan, Y.L., Yan, Y.F. and Yang, Z.Q., 2001, Crustal structure characteristics of southeastern Tibet: Science in China (Series D) (in Chinese), 31(Suppl.), pp.61–71.

Lu, D.Y., Huang, L.Y., Chen, J.P., Li, X.P., Hu, A.B., Wang, Y.Z., Wang, Z.C. Liu, W.T. and Zhang, Z.Y., 1990, Structural model and velocity dispersion characteristics of the crust and upper mantle in Tuotuohe-Golmud region of north Qinghai-Xizang plateau, in Geophysical Memoir on Xizang-Qinghai Plateau, China Geological Publishing House, pp.51–62.

Lü, Q.T., Jiang, M., and Ma, K.Y., 1996, 3-D travel time tomography inversion and the deep structure of southern Tibet: Acta Seismologica Sinica (in Chinese), 18(4), pp.451–459.

Ma, X.B., Kong, X.R. and Yu, S., 1997, Magnetotelluric sounding in western Tibet. Chinese Science Bulletin (in Chinese) , 42(11) : 1185–1187.

Ma, X.B., Kong, X.R., Liu, H.B., and Yan, Y.L., 2001, Magnetotelluric sounding results in eastern Tibetan Plateau: Science in China (Series D) (in Chinese), 31 (Suppl.), pp.72–76.

McNamara, D.E., Owens, T.J., and Walter, W.R., 1995, Observations of the regional phase propagation across the Tibetan Plateau: Journal of Geophysical Research, 100(22), pp.22215–22229.

Meng, L.S., Shen, J.S., Qi, L., Zhang, F.H., Zhang, L., Wu, L.G., Meulebrouck, J. and Tarits, P., 1984, The preliminary interpretation of the gravity profile of well Yang No.8, Nielamu, Tibet: Geophysical Prospecting for Petroleum (in Chinese), 23(2), pp.1–21.

Meng, L.S., Gao, R., Zhou, F.X., Li, L. and Wang, H.X., 1990a, Intepretation of the crustal structure in Yadong-Golmud area using gravity anomalies: Bulletin of The Chinese Academy of Geological Sciences (in Chinese), 21, pp.149–161.

Meng, L.S., Jiang, X.R., Zhang, F.H. and Xian, E.D., 1990b, Gravity profile and the crustal structure of Yecheng-Shiquanhe: Acta Geophysica Sinica (in Chinese), 33(6), pp.670~677.

Meng, L.S., Guan, Y., Qi, L. and Gao, R., 1995, Gravity field and deep crustal structure in

Golmud-Ejin Qi geoscience transect and nearby area: Chinese Journal of Geophysics (in Chinese), 38 (Suppl.a), pp.36–45.

Meng, L.S., Qi, L., Gao, R., and Chen, Y.M., 1998, Gravity survey and isostatic message along the profile of Aergan (in Xinjiang)–Laomangya (in Qinghai): Journal of Changchun University of Science and Technology (in Chinese), 28(3), pp.345~350.

Murphy, M.A., Yin, A., Harrison, T.M., Dürr, S.B., Chen, Z., Ryerson, F.J., Kidd, W., Wang, X. and Zhou, X., 1997, Did the Indo-Asian collision alone create the Tibetan plateau: Geology, 25(8), pp. 719–722.

Nelson, K.D., Zhao, W.J., Brown, L.D., Kuo, J., Che, J.K., Liu, X.W., Klemperer, S.L., Marovsky, Y., Meissner, R., Mechie, J., Kind, R., Wenzel, F., Ni, J., Nabelek, J., Chen, L.S., Tan, H.D., Wei, W.B., Jones, A.G., Booker, J., Unsworth, M., Kidd, W., Hauck, M., Alsdorf, D., Ross, A., Cogan, M.,Wu, C.D., Sandvol, E. and Edwards, M., 1996, Partially molten middle crust beneath Southern Tibet: Synthesis of project INDEPTH results: Science, 274, pp.1684–1688.

Pan, Y.S., 1999, Formation and uplifting of the Tibetan Plateau plateau: Earth Science Frontiers (in Chinese), 6(3), pp.153–163.

Pelkum, S., Monsalve, G., Sheehan, A., Pandey, M.R., Sapkota, S., Bilham, R. and Wu, F. 2005, Imaging the Indian subcontinent beneath the Himalaya: Nature, 435, pp.1222–1225.

Qian, H., Jiang, M., Xue, G.Q. and Su, H.P., 2001, Crustal structure of eastern Tibet inferred from natural earthquake receiver function analysis: Acta Seismological Sinica (in Chinese), 23(1), pp.103–108.

Qin, G.Q., Chen, J.H., Liu, D.J., Gu, Q. and Xiong, Y.W., 1994, The characteristics of the electrical structure of the crust and upper mantle in the region of the Kunlun and Karakorum mountains: Acta Geophysica Sinica (in Chinese), 37(2), pp.193–199.

Ross, A., Brown, L., Passakorn, P., Nelson, K.D., Klemperer, S., Haines, S., Zhao, W.J. and Guo, J.R., 2004, Deep reflection surveying in central Tibet: lower-crustal layering and crustal flow: Geophysical Journal International, 156, pp.115–128.

Shen, X.J., Zhang W R., Yang, S.Z., Guan, Y. and Jin, X., 1990, Heat flow evidence for the differentiated crust-mantle thermal structures of the Qinghai-Xizang plateau: Bulletin of the Chinese Academy of Geological Sciences (in Chinese), 21, pp.203–214.

Shen, X.J., Yang, S.Z. and Shen, J.Y., 1995, Heat flow study and analysis along the Golmud-Ejin Qi geotransect: Acta Geophysica Sinica (in Chinese), 38 (Suppl.a), pp. 86–97.

Shi, D.N., Jiang, M., Ma, K.Y., Xue, G.Q., Dong, Y.J., Poupinet, G., Wittlinger, G. and Herquel, G., 1999, Crust and upper mantle tomographic structure across the Altyn fault zone using teleseismic p-waves. Chinese Journal of Geophysics (in Chinese), 42(3), pp. 341–350.

Song, Z.H., An, C.Q., Wang, C.Y., Chou, Z.R. and Zhang, L.J., 1985, The P-wave velocity of upper mantle beneath Tibetan Plateau plateau and north-south seismic zone: Acta Geophysica Sinica (in Chinese), 28(Suppl.), pp. 148–160.

Spratt, J.E., Jones A.G., Nelson, K.D., Unsworth, M.J. and INDEPTH-MT Team., 2005, Crustal structure of the India-Asia collision zone, southern Tibet, from INDEPTH MT investigations: Physics of the Earth and Planetary Interiors, pp.1–11.

Sun, J., Jin, G.W., Bai, D.H. and Wang, L.F., 2003, Electrical structure of the crust and upper mantle and tectonics sense on the edge of the East Tibet. Science in China(Series D) (in Chinese), 33(Suppl.) , PP.173–180

Tan, H.D., Wei, W.B., Unsworth, M. Deng, M., Jin, S., Booker, J. and Jones, A., 2004, Crustal electrical conductivity structure beneath the Yarlung Zangbo suture in the southern Xizang plateau, Chinese Journal of Geophysics (in Chinese), 47( 4), pp. 685–690.

Teng, J.W., 1974, Deep reflected waves and the structure of the earth crust of the eastern part of Qaidam basin: Acta Geophysica Sinica (in Chinese), 17(2), pp. 121–134.

Teng, J.W., Xiong, S.B., Yin, Z.X., Xu, Z.X., Wang, X.T. and Lu, D.Y., 1983, Structure of the crust and upper mantle pattern and velocity distributional characteristics in the Northern Himalayan mountain region: Acta Geophysica Sinica (in Chinese), 26(6), pp. 525–540.

Teng, J.W., Yin, Z.X., and Xiong, S.B., 1985, Crustal structure and velocity distribution beneath Selin Co–Peng Co–Na Qu–Suo County region in northern Xizang plateau: Acta Geophysica Sinica (in Chinese), 28(Suppl.), pp. 28–42.

Teng, J.W., Zhang, Z.J., Wang, G.J., Liu, H.B., Hu, J.F., Zhang, B.M., Chen, Y. and Zhang, H., 1999, The deep internal dynamical processes and new model of continent-continent collision in Himalayan collision orogenic zone: Chinese Journal of Geophysics (in Chinese), 42(4), pp. 481–494.

Tilmann, F., Ni, J., and INDEPTH Seismic Team, 2003, Seismic imaging of the down-welling Indian lithosphere beneath central Tibet, Science, 300, pp. 1424–1427.

Wang, C.Y., Wu, J.P., and Lou, H., 2003a, Crustal P-wave velocity structure in western Sichuan and eastern Tibet: Science in China (Series D) (in Chinese), 33(Suppl.), pp. 181–189.

Wang, C.Y., Han, W.B., Wu, J.P., Lou, H. and Bai, Z.M., 2003b, Crustal structure beneath the Songpan-Garze orogenic belt: Acta Seimologica Sinica, 16(3), pp. 237–250.

Wang, Q.S., Wu, C.Z., and Wang, W.W., 1997, Gravity field and crustal structure of Jilong-Lugu region in western Tibet: Chinese Science Bulletin (in Chinese), 42(8), pp. 858–862.

Wang, Q.S. and An, Y.L., 2001, Gravity field and deep structure of Madoi-Shama region in eastern Qinghai-Xizang(Tibetan) plateau: Process in Geophysics (in Chinese), 16(4), pp. 4–10.

Wang, S., Lu, D.Y., Huang, L.Y., Li, X.P. and Hirn, A., 1990, Velocity distribution characteristics and N-S variation of the depth of the earth's crust in the Xizang (Tibet) plateau: Geophysical Memoir on Xizang-Qinghai plateau (in Chinese), China Geological Publishing House, pp. 38–47.

Wang, Y.X. and Qian, H. 2000, Study of crustal velocity structure in the east Qinghai. Earth Science Fronties(in Chinese), 7(4) : 568–579.

Wei, W.B., Unsworth, M., Jones, A., Booker, J., Tan. H.D, Nelson, D., Chen, L.S., Li, S.H., Solon, K. and Bedrosian, P., 2001, Detection of widespread fluids in the Tibetan crust by magnetotelluric studies: Science, 292, pp. 716–718.

Wittlinger, G., Vergne, J., Tapponnier, P., Farra, V., Poupinet, G., Jiang, M., Su, H., Herquel, G. and Paul, A., 2004, Teleseismic imaging of subducting lithosphere and Moho offsets beneath western Tibet: Earth and Planetary Science Letter, 221, pp. 117–130.

Wu, G.J., Gao, R., Yu, Q.F. Cheng, Q.Y., Meng, L.S., Dong, X.B., Cui, Z.Z., Yin, Z.X., Shen, X.J. and Zhou., Y.X., 1991, Intergrated investigations of the Tibetan Plateau plateau along the Yadong-Golmud geoscience transect: Acta Geophysica Sinica (in Chinese), 34(5), pp. 552–562.

Wu, J.P., Ming, Y.H., Ye, T.L., and Zeng, R.S., 1998, Upper mantle velocity structure in the Qinghai-Xizang Plateau from inversion of body waveforms: Acta Geophysica Sinica (in Chinese), 41(Suppl.), pp. 15–25.

Wu, Q.J. and Zeng, R.S., 1998, The crustal stucture of Qinghai-Xizang plateau inferred from broadband teleseismic waveform: Acta Geophysica Sinica (in Chinese), 41(5), pp. 669–679.

Wu, Q.J., Zeng, R.S., and Zhao, W.J., 2004, Dipping structure of upper mantle and continent-continent collision in Himalayas–Tibet Plateau: Science in China (Series D) (in Chinese), 34(10), pp. 919–925.

Wu, X.Z., Wu, C.L., Lu, J. and Wu, J. 1995, Research on the fine crustal structure of the northern Qilian-Hexi Corridor by deep seismic reflection: Chinese Journal of Geophysics (in Chinese), 38(Suppl.a), pp. 29–35.

Xiong, S.B., Teng, J.W., and Yin, Z.X., 1985, The thickness of the crust and undulation of discontinuity in Xizang (Tibet) plateau: Acta Geophysica Sinica (in Chinese), 28(Suppl.), pp. 16–27.

Xiong, S.B. and Liu, H.B., 1997, Crustal structure in the western Tibetan plateau: Chinese Science Bulletin (in Chinese), 42(12), pp. 1309–1312.

Xu, X. Z., Qi, X. F., Yang, C. L. and Dang, S.J, Results of man-made explosion seismic sounding from Huashixia (in Qinghai) to Aksay (in Gansu) . Annual of the Chinese Geophysical Society. China: Seismological Press. 1993,pp.80.

Xu, Z.Q., Yang, J.S., and Jiang, M., 2001, Collision-orogeny of the northern Tibetan Plateau plateau and its deep dynamics: Acta Geoscientia Sinica (in Chinese), 22(1), pp. 5–10.

Xu, Z.Q., Jiang, M., Yang, J.S., Xue, G.Q., Su, H.P., Li, H.B., Cui, J.W., Wu, C.L. and Liang, F.H., 2004, Mantle structure of Qinghai–Tibet plateau: Mantle plume, mantle shear zone and delamination of lithospheric slab, Earth Science Frontiers (in Chinese ), 11(4), pp. 329–343.

Xue, G.Q., Jiang, M. and Su, H.P., 2004, A study on deep structure of Yecheng-Shiquanhe region on Tibetan plateau by tomographic imaging: Science in China (Series D) (in Chinese ), 34 (4), pp. 329–334.

Yin, A., 2001, Geologic evolution of the Himalayan-Tibtan orogen—Phanerozoic growth of Aisa continetal: Acta Geoscientia Sinica (in Chinese), 22(3), pp. 193–230.

Yu, Q.F., Sun, Y.S., Lou, H., Li, Q.X. and Lü, Q.T., 1990, The magnetic structure of geoscience transect from Yadong to Golmud: Bulletin of The Chinese Academy of Geological Sciences (in Chinese), 21, pp. 183–190.

Yu, Q.F., Lou, H., Hu, Z.D., 1995, Magnetic data interpretation of the crustal structure of the geoscience transect from Golmud to Ejin Qi: Chinese Journal of Geophysics (in Chinese), 38 (Suppl.a), pp. 58–70.

Yuan, X.C., Li, L., Jin, G.Y., Feng, Y.P., Zhu, J.H., Lu, G., Phan, V.N., Boyer, D., Therme, P. and Miel, J.L., 1990, Magnetotelluric investigations in Lhozang-Sangxung area, Tibet, in Geophysical Memoir on Xizang-Qinghai Plateau, China Geological Publishing House, pp.63–71.

Zeng, R.S. and Gan, R.J. Reflected waves from crustal interface in western Qaidam Basin: Acta Geophysica Sinica (in Chinese), 1961, 10(1), pp.120–125.

Zeng, R.S., Ding, Z.F. and Wu, Q.J. 1994, A review of the lithospheric structures in Tibetan plateau and constraints for dynamics: Acta Geophysica Sinica (in Chinese), 37 (suppl.), pp. 99–116.

Zeng, R.S., Ding, Z.F., and Wu, Q.J., 1998, The crustal structure from Himalaya to Qilian and its implications for continent-continent collision process. Chinese Journal of Geophysics (in Chinese), 41(1), pp. 49–60.

Zeng, R.S., Ding, Z.F., Wu, Q.J. and Wu, J.P., 2000, Seismological evidence for the multiple income crustal subductions in Himalayas and southern Tibet. Chinese Journal of Geophysics (in Chinese), 43(6), 780–797.

Zhang, Z.J., Teng, J.W., Li, Y.K., Klemperer, S. and Yang, L.Q., 2002, Crustal velocity structure and eastward escaping of crustal material in the southern Tibet. Science in China (Ser. D) (in Chinese), 32(10), pp. 793–798.

Zhang, Z.J., Li, Y.K., Wang, G.J., Teng, J.W., Klemplerer, S., Li, J.W., Fan, J.Y. and Chen, Y., 2001, E-W Crustal stucture under the northern Tibet and 'down-bowing' Moho under the northern Tibet revealed by wideangle seismic profile. Science in China (Series D) (in Chinese), 31(11), pp. 881–888.

Zhao, J.M. , Zhang, X.K., Wang, S.X., Lu, B., Zhang, J. and Lu, M.A., 2001, The lithospheric structure and dynamic process of the Junggar Basin, the Tianshan Orogenic Belt, the Tarim Basin, the Altun Orogenic Belt, the Qaidam Basin, and the Kunlun Orogenic Belt (northern margin), in Chinese Geophysical Society, ed, Annual of the Chinese Geophysical Society, pp. 13.

Zhao, J.M., Zhang, X.K., Deng, H.Z. and Zhang, J., 2003, Q value structure of the upper crust along the profile from Baicheng to Da Qaidam: Chinese Journal of Geophysics (in Chinese): 46(4), pp. 503–509.

Zhao, W.J., Nelson, K.D., and Project INDEPTH Team, 1993, Deep seismic reflection evidence for continental underthrusting beneath southern Tibet, Nature, 366(9), pp. 557–559.

Zhao, W.J., Nelson, K.D. and Meissner, R.,1997, Advances of INDEPTH—A deep profiling study in Tibet and the Himalayas: Episodes, 20(4), pp. 266–272.

Zhao, W.J., Mechie, J., Brown, L.D., Guo, J., Haines, S., Hearn, T., Klemperer, S.L., Ma, Y. S., Meissner, R., Nelson, K.D., Ni, J.F., Pananont, P., Rapine, R., Ross, A. and Saul, J. 2001, Crustal structure of central Tibet as derived from INDEPTH wide-angle seismic data: Geophysical Journal International, 145. pp. 486–498.

Zhao, W.J., Xue G.Q., Zhao, X., Wu, Z.H., Shi, D.N. Liu, K., Jiang, W., Xiong, J.Y. and INDEPTH Team, 2004, Seismic imaging of the subducting Indian lithosphere beneath northern Tibet: Acta Geoscientia Sinica (in Chinese), 25(1), pp.1–10.

Zhong, D. L. and Ding L., 1996, Research on the uplift process and mechanism of the Tibetan plateau: Science in China (Series D) (in Chinese), 26(4), pp. 289–295.

Zhu, L.P., and Helmberger, D.V., 1998, Moho offset across the northern margin of the Tibetan plateau: Science, 281,1170–1172.

Zhu R.X. and Hu X.Y., 1995, Study on the resistivity structure of the lithosphere along the Golmud–Ejin Qi geoscience transect: Chinese Journal of Geophysics (in Chinese), 38(Suppl.a), pp.46–57.

Zhuang, Z., Fu, Z.W., Lu, Z.L., Hu, J.F., Song, Z.H., Chen, G..Y., An, C.Q. and Chen, L.H., 1992, 3-D shear velocity model of crust and upper mantle beneath the Tibetan plateau and its adjacent regions: Acta Geophysica Sinica (in Chinese), 35(6), pp.694–709.

# 新疆北部阿尔泰和天山造山带基底时代研究中的新进展

胡霭琴　　韦刚健

中国科学院广州地球化学研究所同位素年代学和地球化学重点实验室，广州 510640

新疆北部造山带包括阿尔泰、准噶尔和天山造山带，它们是中亚造山带的组成部分，其造山带基底时代和特征对古生代增生地壳的成分有明显的制约性。可靠的同位素年代学研究结果可以为建立造山带演化模式提供重要的基础资料，但是就目前对地层、岩浆活动的同位素定年研究还存在不少问题，在国内外构造演化研究中，有时得不到可靠数据的支持，或是从文献中得到的年龄数据并不可靠等。值此两岸学术交流的机会，报导一些近期获得的可靠年龄结果，以提供研究者使用，同时对一些用不正确的"年龄"使用中的问题提出看法供交流和讨论，为后人研究中亚造山带借鉴。

## 一、　阿尔泰地区青河县城西南变质岩的 SHRIMP 锆石 U-Pb 年龄以及其地质意义（胡霭琴等，2006a）

有关阿尔泰造山带中变质岩形成时代问题，目前仍有争议。特别是中国—哈萨克斯坦联合地质科学考察队将阿尔泰地区绝大部份变质岩均划为古—中元古代地层后，近年的一些文章、专著中较多的引用了这一结果（陈毓川等，1996；王京彬等，1998；李天德等，2001）。图 1 示出按李天德等（1996）划分出的前寒武纪地层或地质体出露的范围。

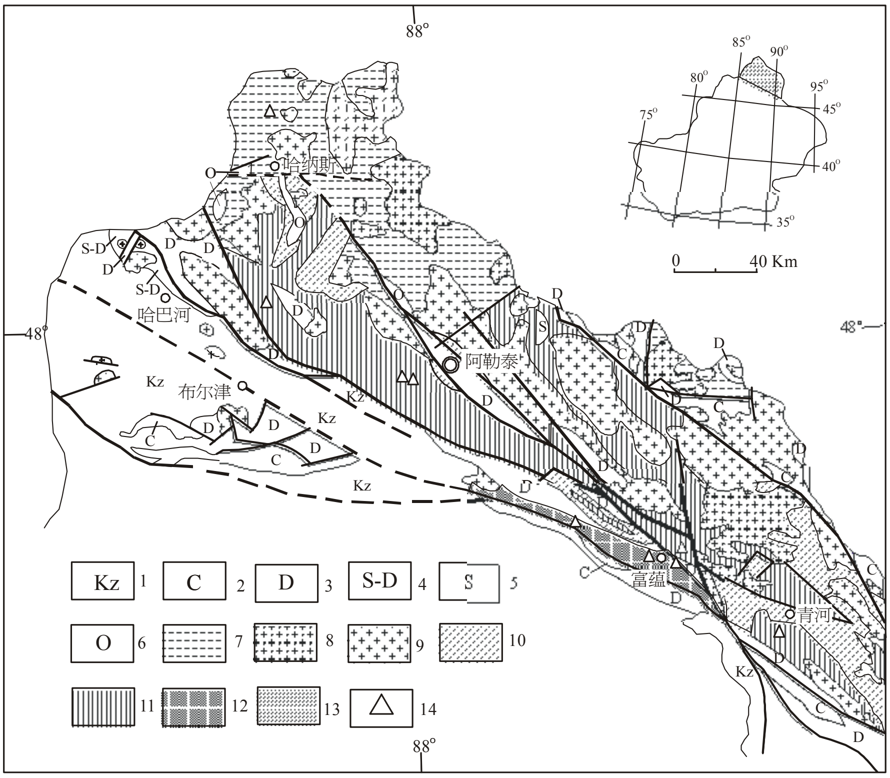


图 1 阿尔泰地区地质略图，图中示出的前寒武纪部分，据李天德等（1996）的划分
（胡霭琴等，2002）
其中：划为前寒武纪地层和地质体的部分：10.新元古界富蕴群；11.古-中元古界克木齐群；12.克木齐群+富蕴群；13.研究区位置；14.主要样品采集范围

青河片麻岩出露在青河县西南地区，在构造上处于额尔齐斯剪切带。是阿尔泰地区的变质岩中唯一根据锆石 U-Pb 上交点年龄（1375 ± 24 Ma）（李天德等，1996）划为古—中元古代克木齐群的地区。但是，这个数据是有问题的确，因为在谐和图中数据点均分布在近下交点的位置，实际上该上交点年龄并确切的地质年龄意义。为此我们作了重新采样和定年研究。样品采集范围为 $46^{o}$35'06.2"，$90^{o}$14'41.9"至 $46^{o}$41'47.9"，$90^{o}$21'56.4"。

1. 青河片麻岩的元素地球化学和 Nd-Sr 同位素组成特征表明其原岩形成于岛弧构造环境

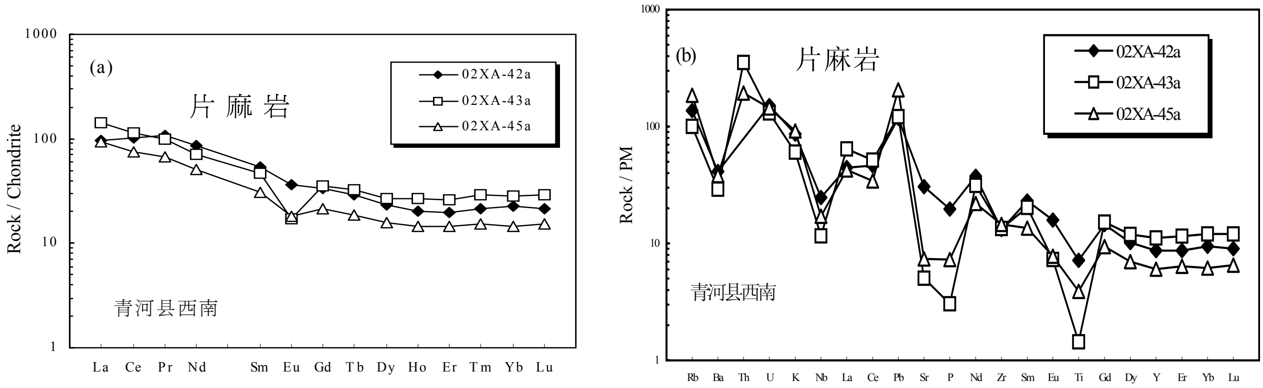


图 2 青河片麻岩类岩石的（a）球粒陨石标准化 REE 分布曲线和

（b）原始地幔标准化微量元素蛛网图

主量元素研究显示青河县西南地区出露的变质岩有正变质岩，也有副变质岩。正变质岩的成分相当于安山岩、英安岩至流纹岩（或闪长岩质、花岗闪长岩质至花岗岩）质岩石，副变质岩为泥质粉砂质沉积岩。三个片麻岩的 REE 总含量在 155~234ppm，具有中等程度的 LREE 富集，$(La/Sm)_N = 1.8\sim3$，构成向右倾斜的 REE 分布曲线，均具有弱至中等程度的 Eu 负亏损（Eu/Eu*=0.87~0.42）（图 2a）。在微量元素蛛网图中元素 Nb，Ti，Ba，P，Sr 均相对亏损，并有明显的负异常（图 2b）。以上特征表明片麻岩的原岩形成于岛弧构造环境。

青河片麻岩的 $f_{Sm/Nd}$ 比值在-0.35 ~ -0.38 之间，$\varepsilon_{Nd}(T)$和 Isr 值均有较大的变化范围，鴲$_{Nd}$(T)变化于+3.49 至-1.86 之间，Isr 值在 0.7045~0.7110 范围内，若将它们放在 $\varepsilon_{Nd}(T)$—$^{87}Sr/^{86}Sr$ 相关图中，譤个片麻岩分布在二端元组份的混合的曲线上（略），Nd 模式年龄（$T_{DM}$）分别为 0.78、 1.07 和 1.23 Ma，这些特征表明其原组份受到不同程度大陆地壳的亏染。

2. 青河片麻岩的 SHRIMP 锆石 U-Pb 定年结果和地质意义

应用精确的 SHRIMP 锆石 U-Pb 定年，获得该变质岩系中英安质片麻岩中锆石的年龄为 281±3 (2σ) Ma，代表其片麻岩的形成年龄。研究中未发现有任何前寒武纪古老锆石或相关的年龄信息，因此研究结果不支持该区变质岩为"前寒武纪"的观点。结合片麻岩中锆石阴极发光图像特征，说明该地区的变质作用和岩浆作用的时间范围在 293±6 Ma ~ 271±5 Ma 期间。因此，该项研究结果确定了阿尔泰造山带发生在二叠纪早期一次重要地质热事件的可靠时限。额尔齐斯构造

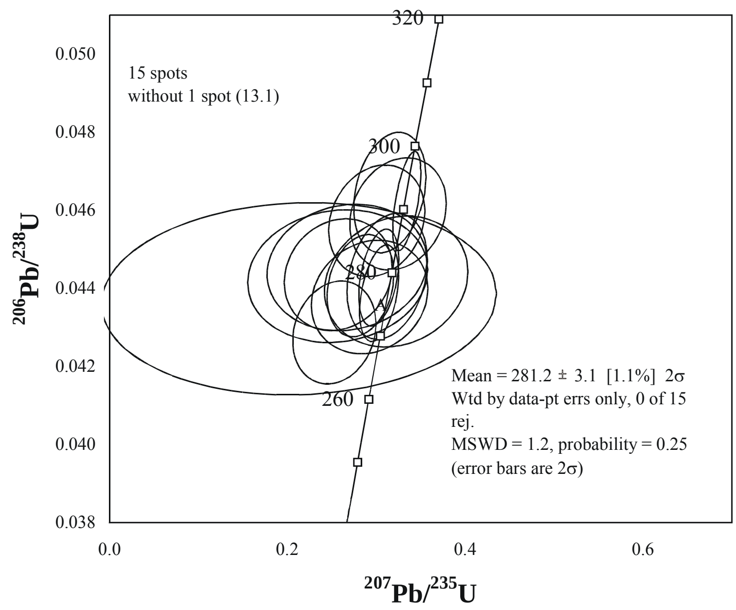


图 3 片麻岩中锆石 U-P**b** 谐和图

剪切带中青河片麻岩的锆石 U-Pb 年龄，以及各种变质岩中角闪石和黑云母的 $^{40}Ar/^{39}Ar$ 年龄（胡霭琴等，1997；Laurent-Charvet et al., 2003; Melnikov et al. 1998; Xiao et al., 2004），记录了阿尔泰造山带晚古生代时期一次重要的构造、变质作用、快速隆升的动力学过程，为研究晚古生代古亚洲洋的闭合或大陆的回返时限提供了初步的证据。

二、 天山东段基底变质岩浆岩的 SHRIMP 锆石 U-Pb 年龄及其地质意义（胡霭琴等，2006b）

在全球范围内 1.4Ga 的岩浆岩在北美大陆和欧洲广泛分布，至今仍是研究的热点问题之一，特别是对 1.4Ga 岩浆岩的成因和形成的构造环境，以及探讨中元古代时期，Rodinia 超大陆之前的地壳活动特征等研究正在深入之中（Dickin et al., 1992; Alleinikoff et al., 1993; Nyman et al., 1994; Åhäll et al., 1998; Anderson et al., 1999; Frost et al., 1999; Persson et al., 1999; Corrigan et al., 2000; Barnes et al., 2002; Blein et al., 2003; Vigneresse et al., 2005）。

天山最东段星星峡地区出露的片麻岩 、混合岩和斜长角闪岩等，一般看作天山最老的地层星星峡群，实际上是前寒武纪变质的岩浆杂岩体（图 4 为星星峡地区地质简图)。胡霭琴等（1986）曾由星星峡群的片麻岩和混合岩中 15 个组份锆石，获得了 U-Pb 上交点年龄为 1400Ma。此后，新疆地质志中将该年龄结果作为将星星峡群划为中元古代地层的依据（新疆维吾尔自治区地质矿产局，1993)。此后，应用单颗粒锆石 TIMS 方法重新测定了片麻岩的时代，得到了大致相同的锆石 U-Pb 上交点年龄(1404 ± 18Ma，胡霭琴等，2006c)。然而，多年来在东、西天山造山带的其它地段再也没有发现有 1.4Ga 的岩浆岩（陈义兵等，1999，2000；修群业等，2002；刘树文等，2004)，在中国大陆上，除了报导过海南岛抱扳地区的花岗闪长岩中获得了 1.4Ga 锆石 U-Pb 年龄外（俞受鋆等，1992；Li et al., 2002)，其它地区均未发现有该时期的岩浆活动。考虑到单颗粒锆石 TIMS 方法获得的星星峡片麻岩中锆石的 U-Pb 年龄均为具有不同程度 Pb 丢失的年龄，其上交点年龄的地质含义并不十分确定，为此我们重新研究了天山东段前寒武纪变质岩的地质特征，并应用 SHRIMP 锆石 U-Pb 定年，进一步确证星星峡最古老的变质岩浆岩的形成时代的确为 1.4Ga。这一个可靠的年龄结果，对研究天山基底在中国大陆地壳演化中的特征，以及在全球大陆演化的对比研究中，将具有非常特殊的意义。

## 1・星星峡变质岩浆杂岩的岩石和元素地球化学特征

星星峡变质岩浆杂岩由中细粒灰色片麻岩、各种混合岩，以及斜长角闪岩等组成。斜长角闪岩为深灰至近黑色的变质基性岩，它们以包体或残留脉体的形式存在于片麻岩或混合岩之间，也有的呈互相包裹或穿插关系。斜长角闪岩 $SiO_2$ 含量为 48.4～54.1%，$TiO_2$ 在 0.95～1.31%之间，MgO 为 6～11.7%。

星星峡中酸性变质岩浆岩主要为片麻岩和混合岩。灰色片麻岩主要由更长石、石英、黑云母及少量角闪石和微斜长石组成，随着混合岩化程度的增高，微斜长石的含量明显增加。灰色片麻岩多数具有花岗闪长岩成分，个别为石英二长质片麻岩，均具有过铝质的特征，其铝饱和指数 ASI 在 1.1～1.2 之间，多数片麻岩的 $Na_2O \geq K_2O$。混合岩类岩石的 $SiO_2$ 含量相对偏高 $Na_2O/K_2O$＜1， ASI 变化范围大（0.9～1.2)，岩石成分变化于花岗闪长岩至花岗岩类岩石范围，但是多数具有花岗岩的化学成分。

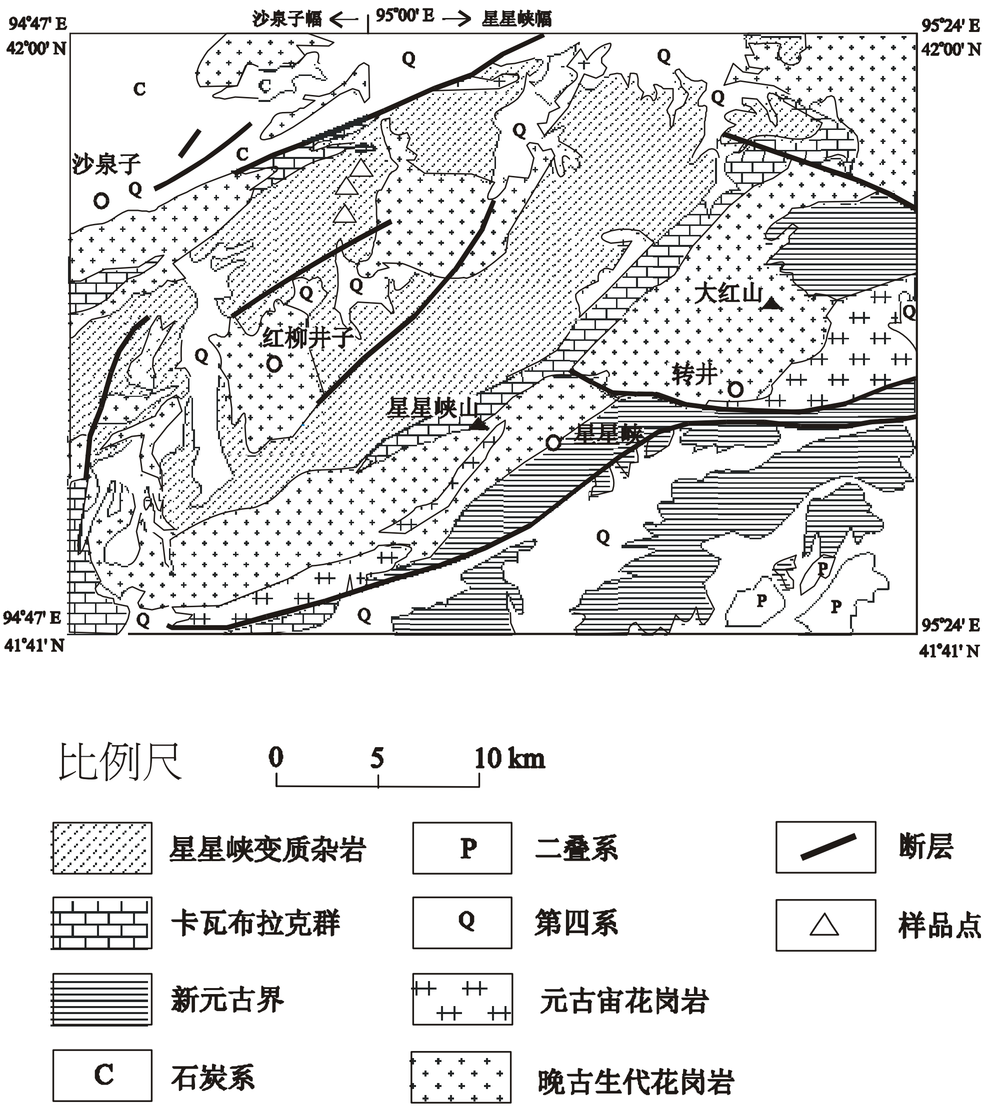


图4　天山东段星星峡地区地质简图

星星峡变质岩浆杂岩中各类岩石的 REE 球粒陨石标准化曲线有明显的区别（图 5a）。5 个灰色片麻岩（图中用白色菱形表示）的 REE 含量中等（164 ~ 207ppm），轻稀土富集（$La_N/Sm_N$=6.0~7.8），重稀土部分曲线较为平坦， Eu 负异常均不明显（Eu/Eu*=0.80~0.90），形成一组向右倾斜度较大的曲线，$(La/Yb)_N$ 比值在 14.6 ~ 29.6 之间，个别高达 40.1。混合岩类（图中用白色园形表示）REE 含量较高（374 ~672ppm），也有较为明显的 LREE 富集（$La_N/Sm_N$ = 3.8~6.0），与灰色片麻岩不同的是各种混合岩类均具有明显的 Eu 负异常（Eu/Eu*在 0.33 ~ 0.50 之间），组成 HREE 部分亦比较平坦的向右倾斜的一组曲线，$(La/Yb)_N$ 在 12.3~16.2。星星峡片麻岩和混合岩在原始地幔标准化的微量元素蛛网图中均显示了富集元素 Rb、K、Th、Pb，而元素 Ba、Nb、Sr、Ti 、P 形

成明显的负异常（图 5b），具有岛弧岩浆岩的特征。灰色片麻岩和混合岩之间的差别表现在混合岩比片麻岩更富含 Rb。3 个斜长角闪岩的 REE 含量低（86~93ppm），Eu 异常不明显（Eu/Eu*在 0.96~1.2 之间），构成大致平坦的 REE 分布曲线（图 5a）。在原始地幔标准化微量元素蛛网图中同样显示出富集 Rb、Th、U、Pb，相对贫元素 Nb、Sr、Zr、Ti，并形成明显的负异常（图 5b），显示岛弧玄武岩的特征。

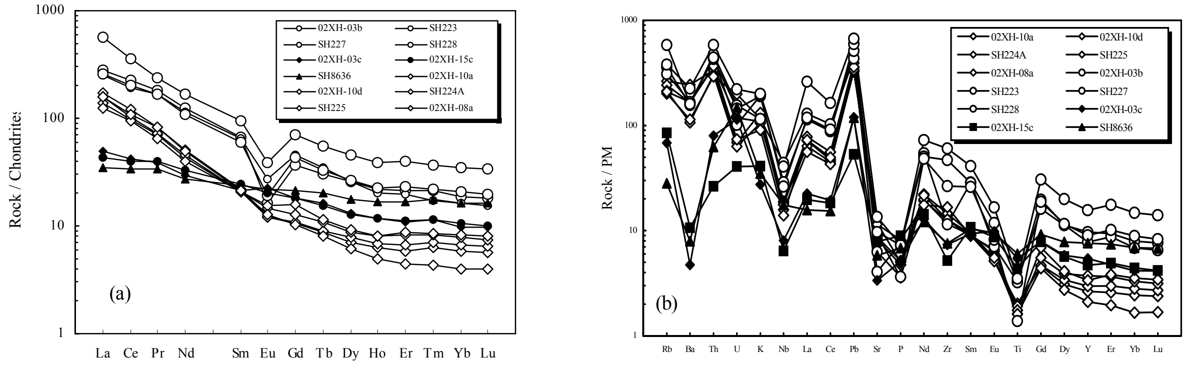


图 5　星星峡变质岩的 REE 分布图（a）和微量元素蛛网图（b）

2．星星峡片麻岩的锆石SHRIMP U-Pb定年结果

应用 SHRIMP 锆石 U-Pb 定年分析了星星峡花岗闪长质片麻岩中 19 颗锆石，由其中谐和性较好的 14 个锆石的分析结果得到 $^{206}Pb/^{238}U$ 和 $^{207}Pb/^{206}Pb$ 加权平均年龄分别为 1436 ± 13 (2瓏) Ma（MSWD = 1.14）和 1405.2 ± 7.8 (2瓏) Ma（MSWD = 0.94），为天山东段星星峡花岗闪长岩的形成年龄，从而确定了天山造山带中元古代基底岩浆岩形成的时间（图 6）。

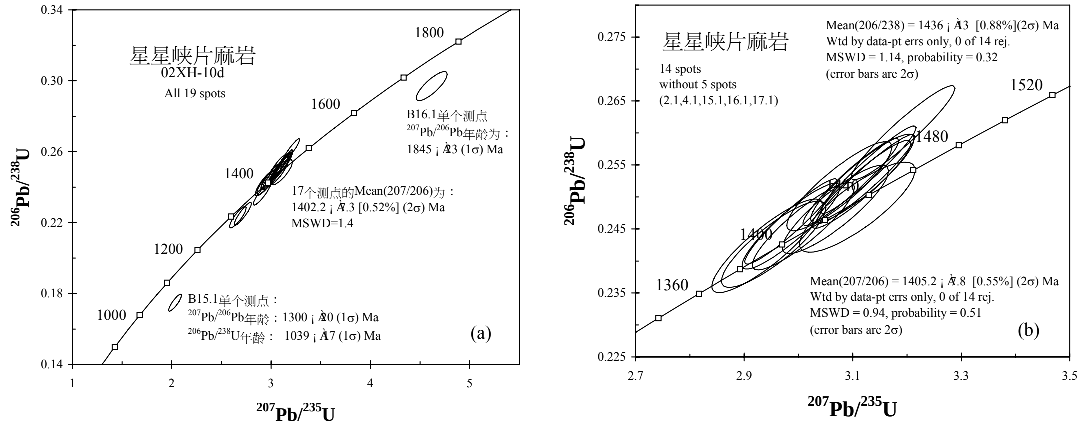


图 6　东天山星星峡片麻岩锆石 U-Pb 谐和图（a-19 个锆石测定点，b-14 个锆石测定点）

3·关于天山东段前寒武纪岩浆岩时代问题的讨论

1） 天山东段星星峡花岗闪长岩的形成与全球范围内中元古代 1.4Ga 岩浆活动具有同时性

天山东段 1.4Ga 星星峡花岗闪长质片麻岩环绕在塔里木北缘太古宙地体（Hu et al., 2000；胡霭琴等，2006d）的北部外侧边缘地带分布，与全球范围内的中元古代 1.4Ga 岩浆活动不但具有同时性，其分布特征也有可比性（Nyman et al., 1994）。但是，星星峡 1.4Ga 花岗闪长质片麻岩具有岛弧岩浆岩的地球化学特征，与北美中部大陆和欧洲大陆中元古代非造山作用形成的岩浆岩（Frost et al., 1999; Barnes et al., 2002; Vigneresse et al., 2005）有所不同。星星峡花岗闪长质片麻岩普遍受到了新元古代的岩浆活动的影响，形成的一些混合岩或是混合岩化的片麻岩中锆石的 U-Pb 年龄为 0.95 ~ 1.10 Ga，与该区内的新元古代片麻状花岗岩的侵位年龄均在同一个时间范围内，这一点与全球 1.4Ga 岩浆岩带有类似之处。明显不同的是，在北美大陆和欧洲波罗地 1.4Ga 造山带中，除了中酸性岩浆岩还存在大量同时代的基性岩浆活动，而在天山东段至今尚不能确定哪些变质的基性岩是与 1.4Ga 岩浆活动有关的玄武岩？一些研究者曾报导过一些基性变质岩的岩石化学组成，并讨论了其构造意义（郭召杰等，1991），但是均没有得到年代学研究结果的证实。作者曾在天山东段研究过一些与花岗质片麻岩出露在同一地区的基性变质岩的 Sm-Nd 同位素组成，其研究结果说明天山东段的基性岩可能是在不同时期形成的（胡霭琴等，1997），只有一部分基性变质岩与片麻岩或混合岩的地壳存留时间上有可比性，尚无可靠的年代学证据说明它们与中-酸性岩浆活动是同期的，这正是今后继续研究的重要课题之一。

本文应用 SHRIMP 锆石 U-Pb 定年研究不但精确地确定了星星峡片麻岩的形成时代，而且揭示了天山造山带存在有可与全球中元古代 1.4Ga 时期对比的岩浆活动，这一研究结果对进一步探讨天山造山带中古老大陆地块在元古宙时期的演化是非常有意义的。尽管目前在天山以及中亚造山带中 1.4Ga 的岩浆岩体并不多见，但是在新元古代的岩浆岩中时常残留有 1.4Ga 的锆石，比如，作者新获得的星星山片麻状花岗岩的 SHRIMP 锆石 U-Pb 年龄数据中发现有 1.4Ga 的锆石存在（另文发表）；修群业等（2002）报导的卡瓦布拉克群花岗闪长岩锆石 U-Pb 分析数据中也有 2 粒锆石的 $^{207}Pb/^{206}Pb$ 年龄为 1400 Ma 和 1444Ma。因此，今后的研究中更应注意在天山造山带内进一步发现该时代的岩浆岩。目前国内关于 1.4Ga（锆石 U-Pb 年龄）岩浆活动的报导并不多见。自胡霭琴等（1986）[1]发表了天山东段星星峡片麻岩中锆石 U-Pb 年龄后，仅在我国海南岛抱扳地区的花岗闪长岩中获得了 1.4Ga 锆石 U-Pb 年龄（俞受鋆等，1992；Li et al., 2002）。不但相距甚

远的两个地区花岗闪长岩的 SHRIMP 锆石 U-Pb 定年结果一致，而且在海南抱扳地区片麻状花岗闪长岩中，也发现了一个大约 1770 Ma 的锆石继承核（Li et al., 2002），即两地的岩体中均有古元古代大约 1.8Ga 时形成的残留锆石。这些研究结果使我们进一步思考天山造山带基底和海南抱扳地区的 1.4Ga 岩浆活动在全球超大陆中元古代的聚合—裂解演化中的位置具有重要的意义。

这里必须指出，塔里木北缘地区有一些关于 1.3~1.5 Ga 的 Rb-Sr 全岩等时线年龄的报导（冯本智等，1995；高振家等，1993），其年龄结果的可靠程度以及地质意义应作进一步的复查研究。可以说，至今在塔里木北缘地体尚未发现有 1.4Ga 时期的岩浆活动。因此，在中元古代 1.4Ga 时期，天山造山带中天山东段的基底大陆地块与塔里木北缘有不同构造和岩浆活动特征。

2）星星峡 1.4Ga 片麻岩经受了新元古代时期的岩浆活动和变质作用的改造

星星峡片麻岩分布区域内也出露有各种混合岩化花岗片麻岩和混合岩类岩石，与灰色片麻岩为侵入接触关系。混合岩类岩石中微斜长石含量增加，出现长石变斑晶，具肠状构造等，两者岩石化学特征也有明显的区别。花岗片麻岩和混合岩中锆石的 U-Pb 年龄在 950~1100Ma 之间（胡霭琴等，1986），明显比灰色片麻岩年轻，反映了混合岩化作用的时间。最近得到了天山东段星星山片麻状花岗岩的 SHRIMP 锆石 U-Pb 年龄（另文发表），与转井山片麻状花岗岩的锆石 $t_{7/6}$ 年龄相一致（946~963Ma）（胡霭琴等，1986），说明天山东段新元古代的变质和岩浆活动时间在 0.9 ~ 1.1 Ga 范围内。该星星峡灰色片麻岩中有的锆石具有新的生长边，并给出年轻化和较大的不一致年龄（B15.1 锆石测点 $^{206}Pb/^{238}U$ 和 $^{207}Pb/^{235}U$ 比值年龄分别为 1039 Ma 和 1127 Ma，见胡霭琴等，2006b），也反映受该期岩浆活动的影响。研究中未发现晚古生代时期岩浆活动的记录，与过去用单颗粒锆石 TIMS 方法的研究结果截然不同。另外，星星峡变质岩浆杂岩，包括片麻岩、片麻状花岗岩，以及各种混合岩等均具有十分一致的 Nd 模式年龄（$T_{DM}$ 值在 1.6 ~ 2.0Ga 范围内）（Hu et al., 2000），说明它们都具有更古老的地壳物质成分。

近来报导的东天山尾亚地区（刘树文等，2004）和卡瓦布拉克群（修群业等，2004）的花岗闪长岩中单颗粒锆石 U-Pb 年龄结果也反映了新元古代岩浆活动的时间。但是，东天山尾亚地区的副变质围岩（夕线石黑云母片）中 5 个锆石的 U-Pb 数据中，只有一个锆石的年龄数据反映了新元古代年龄（$t_{7/6}$=1076Ma），而其它 4 颗锆石均给出古生代的年龄值。因此，刘树文等（2004）将其上交点年龄 1216 ± 74 Ma 看作“早期变质年龄”的观点是值得商榷的。

3）天山东段是否有 1.8Ga 或更古老的岩浆岩？

星星峡变质浆杂岩中的片麻岩和各种类型混合岩的 Nd 模式年龄均在 1.6~2.0 Ga(峰值为 1.8 Ga)（Hu et al., 2000），至今在天山造山带尚未发现有这个时期形成的岩浆岩体存在。但是，在一些变质岩中有时存在大致 1.8 Ga 的锆石 U-Pb 年龄信息。比如，本研究中星星峡灰色片麻岩的 19 个锆石测定点中出现了一个测点(B16.1)的 $t_{7/6}$ 为 1845 ± 24 (1䶮) Ma（图 6a），以及天山东段天湖群二云母石英片岩中锆石的 $t_{7/6}$ 为 1933Ma（胡霭琴等，1986）等，均反映了在岩浆形成或是地层沉积过程中捕获了更古老的继承锆石，其年龄只代表继承锆石寄主岩石形成的时间，不能代表该地质体的形成年龄，这些古老锆石 U-Pb 年龄与星星峡变质杂岩 Nd 模式年龄的一致性，可能反映了天山基底岩石形成的时代。

需要指出的是，胡霭琴等（1995）[1]曾报导过东天山尾亚麻粒岩中 7 个组份锆石给出的二组 U-Pb 的上交点年龄分别为~1.8Ga 和~2.4Ga，西天山独—库公路黑云母斜长片麻岩中 4 个组份锆石的上交点年龄~2.4Ga 等[1]，由于数据点在 U-Pb 谐和图中非常靠近下交点，其上交点年龄不但不可靠，而且也不具有地质实体年龄意义，是否具有源区年龄意义，也存在太多的疑义。修群业等（2002）研究的卡瓦布拉克群花岗闪长岩中 4 个锆石组成不一致的上交点年龄 1832 ± 48 Ma 也存在同样的问题[8]，因为所有锆石的 $t_{7/6}$ 值并未反映出有近 1.8Ga 的年龄信息，所以其上交点年龄可能有很大的误差。

**参考文献**

陈义兵、胡霭琴、张国新、张前锋，2000. 西南天山前寒武纪基底时代和特征：锆石 U-Pb 年龄和 Nd-Sr 同位素组成，岩石学报，16（1）: 91-98.

陈义兵、胡霭琴、张国新、张前锋. 西天山前寒武纪天窗花岗片麻岩的锆石 U-Pb 年龄及 Nd-Sr 同位素特征. 地球化学, 1999, 28（6）: 515 ~ 520 (in Chinese with English abstract).

陈毓川，叶庆同等. 1996. 阿舍勒铜锌成矿带成矿条件和成矿预测. 北京：地质出版社，5 – 17

冯本智，周裕文，迟仕福，杨天奇，钟崇学，叶松青，彭齐鸣，刘正宏，姜琦刚，邢立新. 新疆库鲁克塔格地区前震旦纪地质与贵重、有色金属矿床. 北京: 地质出版社，1995, 107 ~ 214.

[1] 胡霭琴，张国新，张前锋，陈义兵. 新疆北部造山带前寒武纪基底特征及其成矿前景研究. 1995，新疆维吾尔自治区人民政府国家三0五项目办公室（研究报告）

高振家，陈晋镰，陆松年，彭昌文，秦正永.新疆北部前寒武系. 见前寒武纪地质, 地质矿产部《前寒武纪地质》编辑委员会编，第 6 号. 北京：地质出版社，1993, 1 ~ 83.

胡霭琴, 王中刚, 涂光炽等.1997. 新疆北部地质演化及其成岩成矿规律. 北京：科学出版社, 9–105.

胡霭琴, 张积斌, 章振根, 赵殿甲, 刘菊英, 杨升祖, 彭建华, 周位. 天山东段中天山隆起带前寒武纪变质岩系时代及演化—据 U-Pb 年代学研究. 地球化学，1986, (1): 23 ~ 35.

胡霭琴，韦刚健，邓文峰，陈林丽.2006a. 阿尔泰地区青河县城西南变质岩的 SHRIMP 锆石 U-Pb 年龄以及其地质意义.岩石学报，22（1）(出版中).

胡霭琴，韦刚健，邓文峰，张积斌，陈林丽.2006b.天山东段基底变质岩浆岩的 SHRIMP 锆石 U-Pb 年龄及其地质意义. 地球化学（待刊）.

胡霭琴，韦刚健. 2006d. 塔里木盆地北缘新太古代辛格尔灰色片麻岩形成时代问题. 地质学报（出版中）.

胡霭琴，张国新，张前锋，李天德，张积斌. 2002. 阿尔泰造山带变质岩系时代问题的讨论. 地质科学, 37（2）：129 – 142.

胡霭琴，张国新等. 2006c. 新疆地壳演化主要地质事件年代学和地球化学.北京：地质出版社（出版中）.

李天德，B.H. 波里扬斯基. 2001. 中国和哈萨克斯坦阿尔泰大地构造及地壳演化. 新疆地质，19（1）：27–32

李天德，祁志明，吴柏青，肖世禄，赵昌龙，XA 别斯帕耶夫，HB 波利扬斯基，БA 季亚契科夫，ГД 甘任科，HП 叶夫图申科，OП 叶夫图申科. 1996. 中国和哈萨克斯坦阿尔泰地质及成矿研究的新进展. 见：中国地质学会编，献给三十届国际地质大会"八五"地质科技重要成果学术交流会议论文选集. 北京：冶金工业出版社, 256 – 259

刘树文，郭召杰，张志诚，李秋根，郑海飞. 中天山东段前寒武纪变质地块的性质：地质年代学和钕同位素地球化学的约束. 中国科学，2004, 34（5）：395~403.

王京彬, 秦克章, 吴志亮等. 1998. 阿尔泰山南缘火山喷流沉积型铅锌矿床. 北京:地质出版社，1 – 5

新疆维吾尔自治区地质矿产局. 1993. 新疆维吾尔自治区区域地质志. 北京：地质出版社, 6 ~ 206.

修群业，于海峰，李铨. 卡瓦布拉克群花岗闪长岩单颗粒锆石 U-Pb 年龄. 新疆地质，2002, 20（4）：335 ~ 337.

俞受鋆，夏萍，邓铁殷，李强，陈毓蔚. 1992. 海南抱板地区中元古代花岗岩副矿物锆石的特征及U-Pb同位素年龄测定. 地球化学，(3)：214 ~ 220.

Åhäll K.-I., Connelly J. Intermittent 1.53–1.13 Ga magmatism in western Baltica; age constraints and correlations within a postulated supercontinent. Precambrian Research, 1998, 92: 1 ~ 20.

Alleinikoff, J.N., Jr Reed, J.C., DeWitt, ED. The mount Evans batholith in the Colorado front range: revision of its age and reinterpretation of its structure. Geological Society of America Bulletin, 1993, 105: 797 ~ 806.

Anderson, J.L., Cullers, R.L. Paleo- and Mesoproterozoic granite plutonism of Colorado and Wyoming. Rocky Mountain Geol, 1999, 34 (2), 149 ~ 164.

Barnes M. A., Anthony, E.Y., Williams, I., Asquith, G.B. Architecture of a 1.38-/1.34 Ga granite-/rhyolite complex as revealed by geochronology and isotopic and elemental geochemistry of subsurface samples from west Texas, USA. Precam. Research, 2002, 119: 9~43.

Blein O., LaFle`che M.R., Corriveau L. Geochemistry of the granulitic Bondy gneiss complex: a 1.4 Ga arc in the Central Metasedimentary Belt, Grenville Province, Canada. Precambrian Research, 2003, 120: 193 ~ 217.

Corrigan D., G. Dunning T. R.U–Pb constraints for the plutonic and tectonometamorphic evolution of Lake Melville terrane, Labrador and implications for basement reworking in the northeastern Grenville Province. Precambrian Research, 2000, 99: 65 ~ 90.

Dickin, A.P., Higgins, M.D. Sm/Nd evidence for a major 1.5 Ga crust-forming event in the central Grenville province. Geology , 1992, 20: 137 ~ 140.

Frost, C.D., Frost, B. R., Chamberlain, K.R., and Edwards, B.R. Petrogenesis of the 1.43 Ga Sherman batholith, SE Wyoming, USA: a reduced, rapkivi-type anorogenic granite. Journal of Petrology, 1999, 40(12): 1771 ~ 1802.

Hu, A. Q., Zhang, G. X., Zhang Q. F. and Chen, Y.B., 1998. Constrains on the age of basement and crustal growth in the Tianshan Orogen by Nd isotopic composition. Science in China (Series D), 41(6): 648 ~ 657.

Laurent-Charvet, S., Charvet, J., Monié, P. & Shu, L. 2003. Late Paleozoic strike-slip shear zones in eastern central Asia (NW China): new structural and geochronological data. Tectonics, 22, doi 10.1029/2001TC901047.

Li, Zheng-Xiang, Li, Xian-hua, Zhou, Hanwen, Kinny, Peter D. Grenvillian continental collision in south China: New SHRIMP U-Pb zircon results and implications for the configuration of Rodinia. Geology, 2002, 30 (2): 163 ~ 166.

Melnikov, A., A. Travin, A. Plotnikov, L. Smirnova, and K. Theunissen. 1998. Kinematics and Ar/Ar geochronology of the Irtysh Shear zone in the NE Kazakhstan, in IGCP 420, edited by B. M. Jahn and D. W. Hong, Int. Union of Geol. Sci., Ottawa, Ont., Canada, 60

Nyman, M. W., Karlstrom, K. E., Kirby, E. and Graubard, C. M. Mesoproterozoic contractional orogeny in western North America: Evidence from ca. 1.4 Ga plutons. Geology, 1994, 22 (10): 901 ~ 904.

Persson A.I. Absolute (U–Pb) and relative age determinations of intrusive rocks in the Ragunda rapakivi complex, central Sweden. Precambrian Research, 1999, 95: 109 ~ 127.

Vigneresse, J.L. The specific case of the Mid-Proterozoic rapakivi granites and associated suite within the context of the Columbia supercontinent. Precambrian Research, 2005, 137 : 1 ~ 34.

Xiao, W.J., Windley, B.F., Badarch, G., Sun, S., Li, J., Qin, K.Z., & Wang, Z.H. 2004. Palaeozoic accretionary and convergent tectonics of the southern Altaids: implications for the lateral growth of Central Asia. Journal of the Geological Society, London, 161, 339–342.

# The Lichi Mélange: a tectonic collision complex originated form sheared forearc in Coastal Range, eastern Taiwan

Chi-Yue Huang and Chih- Wei Jien

Department of Earth Sciences, National Cheng Kung University, Tainan, Taiwan

The Lichi Mélange in the Coastal Range is well-known for a young chaotic and sheared block-in-matrix sequence (late Pliocene) in the accreted Luzon arc-forearc of eastern Taiwan. However, proposed models for its origin are still controversial. Independent lines of evidence, including field survey, microfossil, clay mineral composition and fission track analyses on sandstone blocks, are used in this study to constrain the origin and formation mechanism of the Lichi Mélange.

Planktic foraminifers in Lichi Mélange are dated as late Pliocene in age (~3.5 to 3.0 Ma), compatible with the juxtaposed lower forearc strata. This is much younger than the last subduction event of the South China Sea oceanic crust (end of Miocene) along the Manila Trench, suggesting that the Lichi Mélange was not a subduction complex. The subduction origin model also conflicts with regional marine geology off southern Taiwan. The benthic foraminiferal fauna are similar in samples with different grades of shearing, and are comparable to the fauna in the juxtaposed non-sheared coherent forearc turbidites (Taiyuan basin) to the east, suggesting the Lichi Mélange was deposited in the North Luzon Trough forearc basin before shearing. Although the Lichi Mélange was deposited in forearc basin, clay mineral composition in the mélange differs significantly from the coherent forearc sequences by bearing of kaolinite. This implies that the arc-origin kaolinites are unlikely being derived into the Lichi Mélange by the eastward sedimentary slumping process from the exposed accretionary prism. Instead, the arc-origin kaolinite could have been derived from the hydrothermal altered volcanic arc materials beneath the forearc basin via fluid flows along faults and sheared fractures when the whole Luzon arc/forearc were thrust westward and accreted on to the exhumed Eurasian continent during the advanced arc-continent collision in the last 1 Ma. By such an arc thrusting, part of the volcanic rocks is exposed between the Lichi Mélange and the remnant forearc basin in the southern Coastal Range.

In addition, zircon grains separated from the coherent forearc turbidites (Taiyuan basin) and the Lichi Mélange show contrast fission track patterns. This further infers that the allochothonous sedimentary sandstone blocks in the Lichi Mélange was not emplaced into the mélange by sedimentary slumping process. Instead, they could be tectonically transferred from the accretionary prism into the Lichi Mélange by the eastward thrusting during the initial arc-continent collision at ~ 3 Ma, a scenario similar to the formation of the modern deformed forearc Huatung Ridge off SE Coastal Range.

The above lines of new evidence suggest that the Lichi Mélange represents a collision complex originated from the sheared forearc strata by a two-stage tectonic process: an early eastward thrusting to develop a deformed forearc unit like the modern Huatung Ridge during the initial arc-continent collision stage (~ 3 Ma), followed by westward thrusting and shearing during the advanced stage of the collision when the whole Luzon arc-forearc were accreted westward onto the exhumed underthrust Eurasian continent in eastern Taiwan in the last 1 Ma.

# 新疆境内天山山脉的地壳上地幔结构

姜枚　李海鸥　王亚军　张立树

中国地质科学院地质研究所

穿越新疆境内天山山脉的东段和西段的克拉玛依—库车、富蕴—库尔勒两条剖面进行了宽频地震探测，依据地震层析和接收函数的结果使我们获得了天山山脉东段和西段的深部构造的速度图像，从而探讨了印度洋板块向北推进和青藏高原隆升对天山山脉造山作用的影响以及天山山脉不同地段的地壳上地幔构造的差异。

在天山山脉西段由克拉玛依—库车剖面上清楚地展示出天山是由高速和低速的地体拼合而成的结构形态。来自塔里木的高速体向北俯冲到天山深部，达 200km 以下的深度，而来自准噶尔盆地的高速体则没有明显地向南的推进，说明由南向北的推进是很强的，它是造成天山山脉继续隆升的主要动力，而北部准噶尔盆地的高速体则是被动挤推地造就了天山山脉。在 Moho 面以上的部分可以看到天山山脉由北天山和中天山南缘的两个低速体夹着中天山南缘附近的一高速体，拼合成天山山脉，其南北宽度超过 350km，山根深度越过 200km。

在天山山脉东段 Moho 面以上的地壳部分，塔里木盆地和准噶尔盆地均为高速体的范围，南部高速体有向北推进和俯冲的特征，但不明显。夹在两盆地之间的天山主要为低速体，仅在乌鲁木齐和北天山山前断裂以南有残留的高速体，深度不超过 30km，这表明天山地体是速度不同的地质体挤压而成的。天山延伸到乌鲁木齐以东，山势比西部在为降低，其深部天山山根延伸也仅仅到 100km 上下。塔里木盆地的高速物质向北推进，可能在南天山有不强的下插进入南天山。虽然天山南北缘均为逆冲断裂，但与西部天山的情况有明显差异。

在富蕴—库尔勒部剖面上塔里木板块向北的推进相对于西部有所减弱，该地区处于塔里木盆地东北部。在西部剖面上表现出强烈的造山作用，向东逐步减缓，到达本剖面涉及的地段，虽然天山深部的构造活动仍然在继续进行，地震活动频繁，可是，活动区域集中在天山底部不过 100km 上下。说明山根的范围比西部减少了近一半。

岩石圈物质的流向因南北盆地的推压使天山隆升而部分物质向东移，这与东部的阿尔金山走滑断裂也不无关系。同时，东南部物质运转方向发生变化，部分向东推移，这都导致了天山隆升作用的降低，从而造成新疆境内天山西东段的深部构造和地表山势都出现了明显的差异。

本文同时介绍了中国西部自 1991 年以来宽频地震探测工作的进展。

# Crustral Evoluction of Continental Taiwan – Revised

Ching-Ying Lan[1], Bor-ming Jahn[1], Chun-Sun Lee[2], Tzen-Fu Yui[1], Hao-Tsu Chu[3]

[1.] Institute of Earth Sciences, Academia Sinica, Nankang, Taipei, Taiwan, ROC
[2.] Department of Earth Sciences, National Taiwan Normal University, Taipei, Taiwan, ROC
[3.] Central Geological Survey, Minister of Economic Affair, Taipei, Taiwan, ROC

The crustal evolution of the western continental unit of Taiwan is summarized. Paleoproterozoic era is the most important period in terms of crustal formation and the continental crust thus formed became a major protolith incorporated in the generation of younger Taiwan rocks. The crustal evolution history began in the late Paleozoic (250±20 Ma). Five episodes of mantle inputs since then can be delineated: (1) the early Mesozoic event (200-175 Ma) registered in the marble and metapelites of the Tananao metamorphic basement complex; (2) the middle Mesozoic event (~153 Ma) registered in the granitoid of the Tananao metamorphic basement complex of southern Taiwan; (3) the late Mesozoic event (97-77 Ma) registered in the rocks of the Tananao metamorphic basement complex and offshore of northern Taiwan; (4) The Cenozoic of pre-Pliocene event (episodic from 56 to 8 Ma) registered in the dikes in the Central Range and the intraplate basalts of mainland Taiwan and offshore northern Taiwan; (5) the ongoing event (since 3 Ma) registered in the recent volcanics of onshore and offshore of northern Taiwan. The first two events is believed to have been a consequence of Yanshanian thermal activity, while the third event could have been affiliated with the subduction of a paleo-Pacific plate. The fourth event is resulted from the extension in the continental margin of SE China. Rather than directly related to the magmatism of Ryukyu subduction zone, the last event is attributed to the late Pliocene extensional collapse of the northern Taiwan mountain belt in response to the oblique collision of the northern Luzon arc with Asia continent.

# Continental Rifting of the South China Sea

Chao-Shing Lee, Chin-Li Su and Chung-Han Hu

Institute of Applied Geoscience, National Taiwan Ocean University, Keelung, Taiwan

The continental rifting of the South China Sea Probably happened in Mesozoic; the seafloor spreading was started in Oligocene and stopped in Miocene (Fig.1). There are many differences between the north and south continental shelf of the South China Sea. The north shelf is covered by thick sediments, where the south is numerous coral reef islands (i.e., the Spratly Islands, and Dangerous Grounds; they are covered by 2-3 km thick of carbonates). Based on the industrial seismic profiles, the north side shows a series of normal faults, and the south side is a mixture of normal and thrust faults with different slip directions. It is interpreted that the early continental rifting of the South China Sea is the passive Atlantic type shear processes. Because of territory dispute among 6 countries over the Spratly Islands, it is not so easy to conduct any large scale exploration in the south continental shelf. In 2005, we managed to run a 45-day survey on one of Taiwan-owned Taiping Island (the largest reef in the Spratly) and its surround lagoon. It is suggested that the 1500-m isobaths have the steep side in the NW of the atolls and more smooth in the SE, as resemble to the trend of normal faulting (Fig. 2). From the age-depth curve (Fig. 3), the continental rifting (~145-65 mabp) was in a very slow process of 1.6m/ma and the seafloor spreading (~65-16 mabp) move up to the rates of 33.8-47.7 m/ma. Since 16 mabp, the subduction and collision in the South China Sea have quickened the tectonic processes (126.3 m/ma).

**Reference**

1. Briais, A., Patriat, P. & Tapponnier, P. Updated interpretation of magnetic anomalies and seafloor spreading stages in the South China Sea: Implications for the tertiary tectonics of Southeast Asia. J. Geophys. Res. 98, 6299-6328 (1993).

2. Clift, P. D., Lin, J. and ODP Leg 184 Scientific Party. Patterns of extension and magmatism along the continentocean boundary, South China margin, in: Wilson, et al. R. C. (ed.) Non-Volcanic Rifting of Continental Margins: a Comparison of Evidence from Land and Sea. Geological Society, London 187, 489-510 (2001).

3. Gong, S. Y. et al. Dry climate near the Western Pacific Warm Pool: Pleistocene caliches of the Nansha Islands, South China Sea. PALAEO 226, 205-213 (2005).

4. Hsu, S. K., Yeh, Y. C., Doo, W. B. & Tsai, C. H. New bathymetry and magnetic lineations identifications in the northernmost South China Sea and their tectonic implications.

Marine Geophysical Researches 25, 29-44 (2004).

5. Lee, T. Y. & Lawver, L. A. Cenozoic plate reconstruction of Southeast Asia. Tectonophysics 251, 85-138 (1995).

6. Pautot, G. et al. Spreading direction in the central South China Sea. Nature 321, 150-154 (1986).

7. Su, D., White, N. & Mckenzie, D. Extension and subsidence of the Pearl River Mouth Basin, northern South China Sea. Basin Research 2, 205-222 (1989).

8. Tsai, C.-H., Hsu, S.-K., Yeh, Y.-C., Lee, C.-S. & Xia, K. Crustal thinning of the northern continental margin of the South China Sea. Marine Geophysical Researches 25, 63-78 (2004).

9. Yan, P. & Liu, H. Tectonic-stratigraphic division and blind fold structures in Nansha Waters, South China Sea. Journal of Asian Earth Sciences 24, 337-348 (2004).

10. Yan, P., Zhou, D. & Liu, Z. A crustal structure profile across the northern continental margin of the South China Sea. Tectonophysics 338, 1-21 (2001)

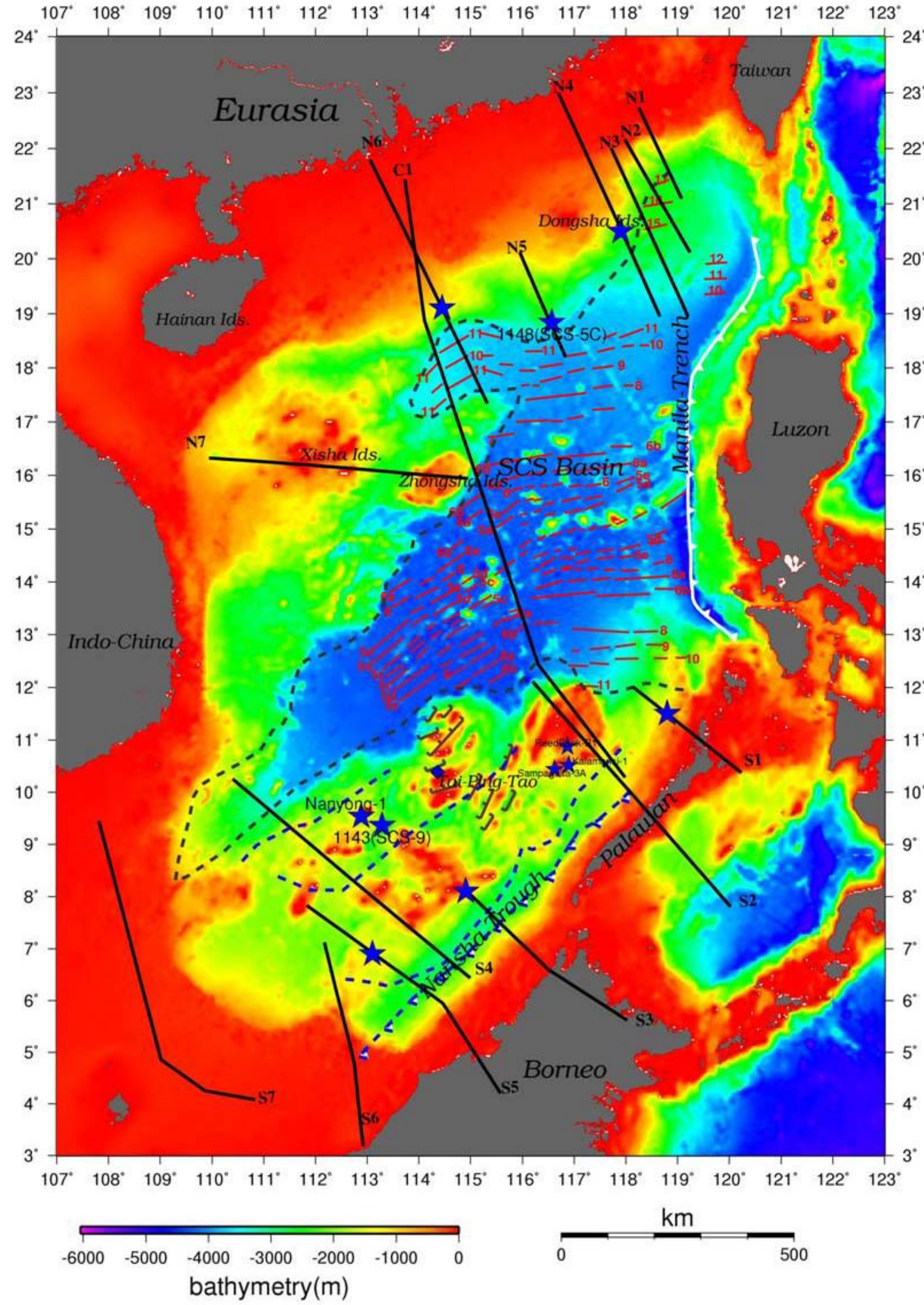


Fig 1. Structural map and seismic/drilling data in the South China Sea.

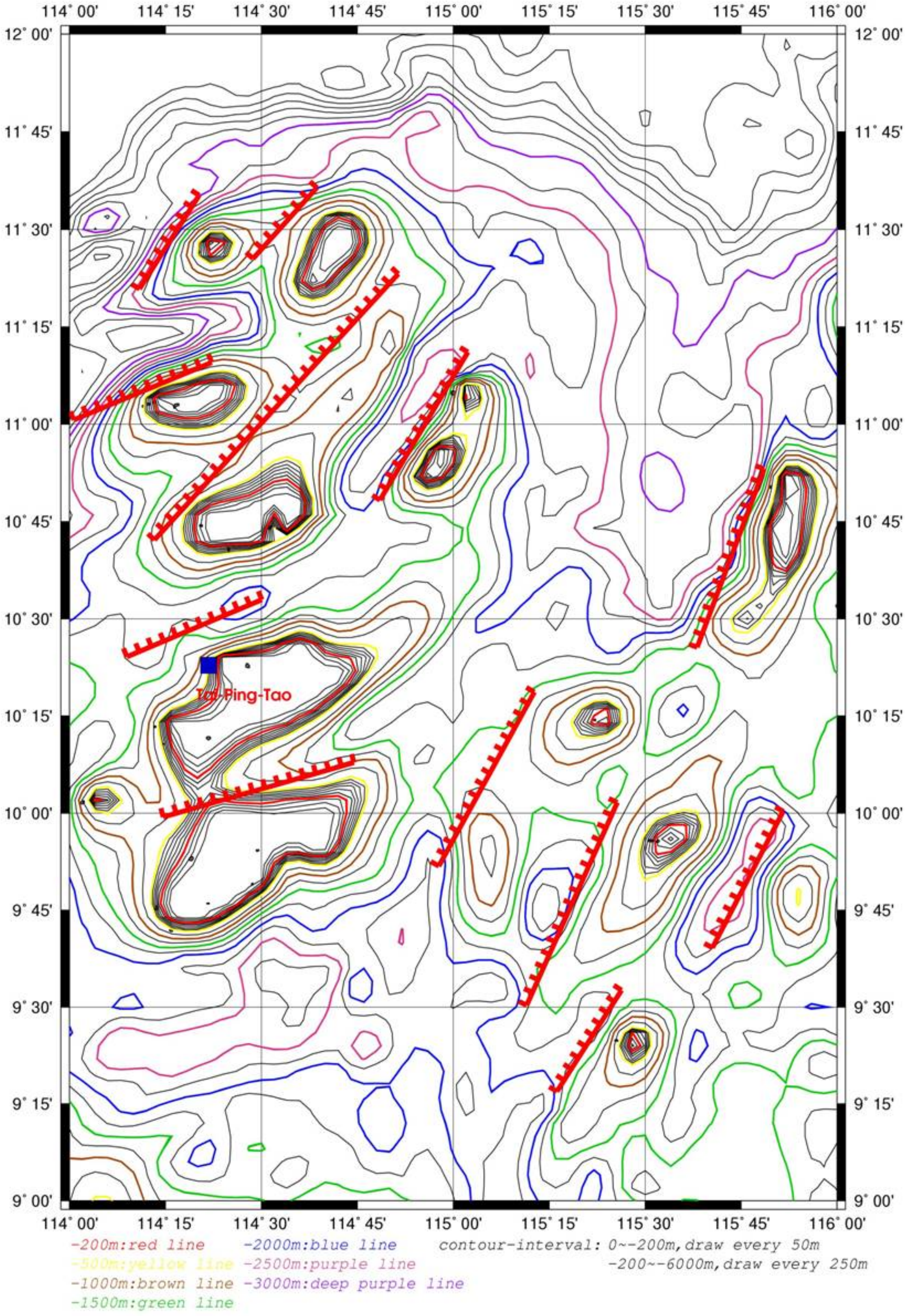


Fig 2. Interpreted fault pattern in the Spratly atolls.

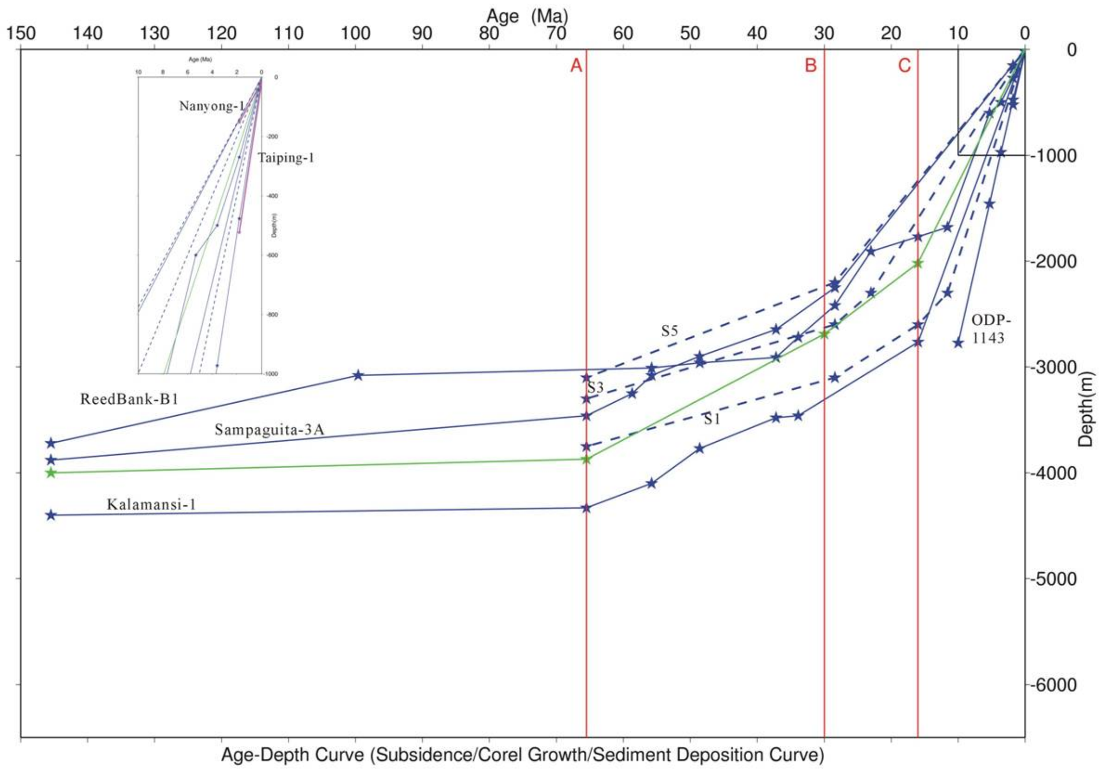


Fig. 3 The age-depth curve of the South China Sea drilling and seismic data.

# On the age, geochemical characteristics and geodynamic significance of the Linzizong volcanic successions, southern Tibet


李皓揚[1], 鍾孫霖[1], 季建清[2], 羅清華[1], 李通藝[3], 錢青[4], 溫大任[1]

1. 台灣大學地質科學系，台北
2. 北京大學地球與空間科學學院，北京
3. 台灣師範大學地球科學系，台北
4. 中國科學院地質與地球物理研究所，北京



The Linzizong volcanic successions emplaced in the Lhasa terrane, southern Tibet are generally considered as products of northward subduction of the Neo-Tethyan oceanic slab beneath South Asia that resulted in an Andean-type convergent margin before the India-Asia collision. Here we report new $^{40}Ar/^{39}Ar$ dating and geochemical results to constrain the tempo-spatial distribution and petrogenesis of the Linzizong volcanism. Our results show two major episodes of eruptions, namely, a Cretaceous episode that occurred widely over the Lhasa terrane from ~110 to 70 Ma and a Paleogene episode that occurred only in the southern part of the Lhasa terrane from ~60 to 45 Ma. We therefore re-define the younger episode of rocks to represent the Linzizong volcanic successions. Moreover, our results suggest a southward migration and intensification of the volcanism marked with a period of magmatic "flare-ups" in the southern Lhasa terrane at ~50-45 Ma. Whereas the Paleogene volcanics in general show calc-alkaline geochemical characteristics, rocks produced by the magmatic flare-ups in the ending phase of the volcanism are more heterogeneous, with compositions ranging from low-K tholeiitic to high-K calc-alkaline accompanied by a shoshonitic suite in the Linzhou area, ~50 km north of the Lhasa city. These lead us to propose a rollback and then breakoff of the subducting Neo-Tethyan slab during the early stage of the India-Asia collision. The slab breakoff, as exemplified in the Mediterranean-Carpathian orogenic system, may have brought up the hot asthenosphere and thus caused compositionally heterogeneous magmatism via partial melting of the ascended asthenospheric mantle and different levels in the continental lithosphere.

# 中国北方及邻区地壳构造格架及其形成过程的初步探讨

李锦轶

中国地质科学院地质研究所，北京 100037，中国

中国北方及邻区系指中朝地台和塔里木地台以北、西伯利亚地台以南、日本海以西、乌拉尔山脉以东的广大地区。该区地表出露的地质体主要是在中元古代以来形成的，太古代和古元古代地质体只在局部地区零星散布。这些不同时代的地质体，从形成构造背景看，分别归属于古陆基底结晶岩系、古洋岩石圈残片、活动陆缘杂岩、被动陆缘沉积岩系、裂谷型火山沉积岩系、同碰撞—后碰撞岩浆杂岩和沉积岩系、陆内火山岩和碎屑沉积岩系等。因此，研究该区地壳构造格架及其形成过程，对于揭示亚洲大陆形成过程和大陆地壳形成演化的动力学机制，具有重要的意义。迄今为止，相关研究或者侧重于某一时段，或者侧重于某一区域，或者侧重于某一方面。本文基于作者近 20 年来对其中部分地区的持续研究，试图通过对现有资料的综合，探讨该区地壳构造格架及其形成的全过程。

## 1 地壳构造格架

该区地壳表层构造格架的突出特征是没有贯穿全区的线性造山带。在文献中，多数中国学者将其归入古亚洲构造域，进一步划分为不同时代的（褶皱）造山区、（褶皱）造山系和（褶皱）造山带（任纪舜等，1999），Sengor 等（1993）将其划分为贝加尔、阿尔泰和满洲等构造拼合体，反映出该区地壳构成的块带镶嵌的特点。该区地壳构造格架的另一个特征是不同时代不同构造背景形成的地质体在一个地区构造叠覆，几乎每一个构造单元都是由在至少两个不同动力学背景形成的地质体组成的，并且从西到东，从南到北，不同地区都有比较明显的差别，反映出该区地壳形成演化涉及不同的动力学体制，具有明显的阶段性。考虑到上述特征，该区地壳构造格架在侧向上大体可以划分为三个区域，每个区域在纵向上具有不同的组成特征。

中亚—蒙古区：系指塔里木地台和北山—索伦山—黑河一线以北，蒙古湖区—中蒙古断裂以南的区域。该区地壳主体由前震旦纪地块与震旦纪至石炭纪洋岩石圈残片及陆缘岩系镶嵌组成，进一步划分为阿尔泰帚状构造、斋桑线性构造、巴尔喀什弧形构造、天山—中亚帚状构造、南天山线性构造、东准噶尔—南蒙古线性构造带等构造单元，在中国西北及毗邻的中亚地区，其上叠加了石炭纪晚期至二叠纪后碰撞岩浆杂岩及沉积岩系、三叠纪至第四纪陆内火山沉积岩系及盆地堆积物，在新生代晚期经历了陆内造山作

用的改造；在蒙古东部和中国东北北部，其上叠加了与古太平洋演化相关的中生代火山沉积岩系，被同时期的中酸性侵入岩侵入，以及白垩纪断陷盆地堆积物和新生代幔源玄武岩及陆内断陷盆地堆积物。

蒙古—鄂霍茨克区：为蒙古湖区—中蒙古断裂和西伯利亚地台之间的地区。该区地壳主体由早前寒武纪地块结晶岩系、中元古代至石炭纪洋岩石圈残片及中元古代至侏罗纪的活动陆缘杂岩组成，进一步划分为中蒙古—萨彦岭弧形构造、外贝加尔镶嵌构造、中蒙古—额尔古纳镶嵌构造和杭盖—肯特线性构造及上黑龙江—鄂霍茨克线性构造等构造单元，其上叠加了白垩纪火山沉积建造及新生代幔源玄武岩—碎屑沉积岩系组成的上叠断陷盆地构造。

北山—内蒙古—中国东北—远东区：为位于中朝地台与北山—索伦山—黑河一线之间的地区，由早前寒武纪地块结晶岩系、中元古代至侏罗纪洋岩石圈残片及中元古代至白垩纪活动陆缘杂岩等组成，包括大兴安岭线性构造、北山—内蒙线性构造、布列亚—佳木斯镶嵌构造、中朝地台北缘线性构造和远东南部线性构造等构造单元，其上叠加新生代幔源岩浆岩及陆相沉积岩等组成的上叠断陷盆地构造。

## 2 地壳构造格架形成过程

根据地质记录中的不整合界面以及沉积环境的差别，研究区上述地壳构造格架的形成，可以划分为太古代—古元古代、中元古代—新元古代早期、新元古代晚期—新生代等三个构造阶段，大体分别对应于全球超大陆形成演化的三个裂解—聚合阶段。其中中元古代以来两个大陆裂解—聚合阶段是该区现今地壳构造格架形成的时期，第一个阶段形成的地质体都呈古陆地壳碎块产出。

### 2·1 太古代—古元古代大陆裂解—聚合阶段

这一时期形成的地壳见于塔里木盆地北缘的库鲁克塔格地区，中亚地区的穆云库姆、克孜尔库姆和楚—伊犁地区，蒙古中部的巴彦洪戈尔以西，俄罗斯的萨彦岭及其以北、外贝加尔以及远东南部等地区。包括 TTG 岩系和绿岩带，类似于中元古代以来的活动陆缘杂岩。这些块体之间的相互关系，目前还不清楚。推测为古元古代聚合的超大陆的组成部分。它们其中是否有更古老的超大陆的碎块以及它们的形成是否始于该超大陆的裂解，目前还不清楚。但是根据区域地质背景资料推测，这些古陆碎块可能是在古元古代晚期聚合形成的超大陆的组成部分。

### 2·2 中元古代—新元古代早期超大陆裂解—聚合阶段

中元古代大陆裂解的证据主要见于中朝地台和西伯利亚地台内部。在研究区内出露的中元古代和新元古代早期地质体主要为活动陆缘杂岩，相对零星的出露在天山、中

亚、蒙古和俄罗斯境内西伯利亚地台周缘地区。东南萨彦岭1020Ma蛇绿岩是研究区最古老的蛇绿岩，具有SSZ型蛇绿岩的特征，揭示出它们形成时古洋盆在收缩而不是在扩张，所以Khain等（2002）关于其代表古亚洲洋打开的认识是值得商榷的。

塔里木盆地西北缘阿克苏地区出露的蓝片岩（肖序常等，1990）是迄今为止发现的最古老的蓝片岩，指示新元古代早期古洋岩石圈板块俯冲乃至中亚地区的一些前震旦纪地质体聚合成一个新的超大陆。而现今西伯利亚地台南缘当时可能持续发育古岛链，中朝地台北缘也面临正在收缩的古大洋。

2·3 新元古代晚期－新生代大陆裂解－聚合阶段

新元古代中－晚期，中亚地区在新元古代早期聚合的超大陆发生裂解，古亚洲洋形成。同时，西伯利亚与中朝地台面临的大洋在持续收缩，这一构造格局可能持续到了奥陶纪初期。

奥陶纪期间，额尔古纳、中蒙古和图瓦地区的古岛弧聚合在一起并与西伯利亚地台连接在一起，把蒙古－鄂霍茨克造山带前身的洋盆（古太平洋）与古亚洲洋分开；同时，布列亚－佳木斯一带的古岛屿也聚合在一起，构成古太平洋中的复合地体或古板块；中国西北及毗邻地区的古亚洲洋开始收缩，新的俯冲带形成；中朝地台北缘的古俯冲带继续发展。

泥盆纪期间，中亚地区的构造格局持续发展，而古亚洲洋西伯利亚地台一侧的边缘，可能由于古洋扩张脊俯冲到大陆之下而发生裂解作用，形成陆缘洋盆或弧后盆地，其地质记录保存在东准噶尔、南蒙古和大兴安岭中部等地区，中朝地台北缘因古俯冲带停止活动而演变为被动边缘。

石炭纪晚期，持续的洋岩石圈板块俯冲作用，导致中亚地区的古亚洲洋关闭，塔里木地台与西伯利亚地台的增生边缘连接，组成同一的大陆板块；中朝地台北缘因新的古洋岩石圈板块俯冲带形成，演变为安第斯型活动大陆边缘，并持续发展到二叠纪晚期，古生代的欧亚板块形成。

中生代初期，古俯冲带分别发生在中朝地台和塔里木地台以南地区，以及蒙古鄂霍茨克造山带前身洋盆的边缘。前者在三叠纪中期随着扬子－羌塘微大陆与古生代晚期形成的欧亚板块碰撞而停止活动，后者则持续到侏罗纪晚期。中国北方及邻区的大部分地区，都受到了后者的影响。随着蒙古－鄂霍茨克造山带前身洋盆的关闭，一个与青藏高原类似的晚侏罗世高原出现在中国东北及毗邻地区，并在白垩纪初期大规模岩浆喷发之后继之为大型陆内热塌陷盆地的形成（李锦轶，1998）。在这一过程中，中国西北及邻区因蒙古－鄂霍茨克造山带前身洋盆关闭过程中的南侧大陆的逆时针旋转，有整体向南

的运动。

白垩纪期间，中国东北及邻区的活动陆缘只发育在中国东北东部及俄罗斯的远东地区，并在白垩纪晚期随着库拉－太平洋的关闭而结束。

新生代初期，中国东北及邻区幔源基性岩浆喷发强烈，Windley 和 Allen（1993）将其解释为蒙古地幔柱，但是在中国东北地区，可能与大陆边缘裂解或弧后扩张关系更为密切。随着日本海等弧后盆地的形成，现今所见构造格局形成。新生代晚期，印度板块与欧亚板块的碰撞，导致中亚地区陆内造山作用的发育，以及该区地壳的向北迁移，到达现今位置。

在上述中国北方及邻区地壳形成演化过程中，所涉及的古洋盆有两个，分别是古太平洋和古亚洲洋。前者在中元古代大陆裂解形成，直到中生代晚期才关闭；后者在新元古代中期大陆裂解形成，二叠纪晚期才最后关闭。在这两个洋盆关闭以后，研究区的地壳构造演化，主要受周边古洋岩石圈板块俯冲及大陆碰撞的影响和软流圈地幔与上覆岩石圈相互作用的制约。

**主要参考文献**


李锦轶. 1998. 中国东北及邻区若干地质构造问题的新认识. 地质论评, 44(4): 339~347

任纪舜, 王作勋, 陈炳蔚, 姜春发, 牛宝贵, 李锦轶, 谢广连, 和政军,刘志刚. 1999. 从全球看中国大地构造——中国及邻区大地构造图简要说明. 北京: 地质出版社, 1~50.

肖序常,格雷厄姆 S.A,卡罗尔 A.R,朱锦志,亨德里克斯 M.S.,梁云海,刘忠光,丸山茂德,麦克奈特 M. L.,汤耀庆, 王小民, 王作勋, 赵民,朱宝清. 1990.中国西部元古代蓝片岩带-世界最老的前寒武纪蓝片岩,新疆地质,8(1): 12~21.

Khain E V, Bibikova E V, Kröner A, Zhuravlev D Z, Sklyarov E V, Fedotova A A, Kravchenko- Berezhnoy I R. 2002. The most ancient ophiolite of the Central Asian fold belt: U~Pb and Pb~Pb zircon ages for the Dunzhugur Complex, Eastern Sayan, Siberia, and geodynamic implications. Earth and Planetary Science Letter, 199: 311~325.

Sengor A M C, Natal’in B A, Burtman V S. 1993. Evolution of the Altaid tectonic collage and Paleozoic crustal growth in Eurasia. Nature, 364: 299~307.

Windley B F, Allen M B. 1993. Mongolian plateau: evidence for a late Cenozoic mantle plume under central Asia. Geology, 21: 295~298.

# A Permian magmatic arc on the Hainan Island: implications for initiation of the Indosinian Orogeny in South China

Xian-hua Li[1], Zheng-Xiang Li[2], Wu-xian Li[1], Yuejun Wang[1]

[1] Guangzhou Institute of Geochemistry, Chinese Academy of Sciences
[2] Tectonics Special Research Centre, The University of Western Australia

It has been widely accepted that an active continental margin existed along the Southeast China during the Mesozoic time that produced extensive magmatism in the region. However, there is little constraint as to when was this active margin first initiated. Here we present new SHRIMP U-Pb zircon ages, and geochemical and Sr-Nd isotopic data for syn-tectonic granites in the Hainan Island. Our data demonstrate that these rocks, dated at 267-262 Ma, are typical of calc-alkaline I-type granites formed in continental arc environments. The age of this magmatic arc coincides with a sudden change in sedimentary environments in South China during the Permian time, suggesting that the South China Indosinian Orogeny was likely contemporaneous with the onset of continental arc magmatsim.

# Mesozoic Indosinian Orogeny and Jurassic-Cretaceous Post-orogenic Magmatism in South China Revisited

Z.X. Li [a] and X.H. Li [b]

[a] Tectonics Special Research Centre, School of Earth and Geographical Sciences, The University of Western Australia, Crawley, WA 6009, Australia
[b] Guangzhou Institute of Geochemistry, Chinese Academy of Sciences, PO Box 1131, Guangzhou, China

The current South China topography was largely inherited from Mesozoic tectonics. Whereas the Qinling-Dabie Orogen to the north and the Longmenshan ranges to the northwest are due to either continental collision or terrane accretion, the ca. 1300km-wide orogen that affected at least the southeastern half of the continent can not readily be explained. Equally hard to explain is the widespread post-orogenic (often rift-related) magmatism in this part of the continent. An early archipelago models by Hsü and co-workers (e.g., Hsu, 1994) contradicts many geological observations such as facies continuity between coastal South China (or Cathaysia) and its interior (Yangtze Craton) since at least Devonian (e.g., Liu and Xu, 1994). The far-field stress model related to the North China-South China collision by Li (1998) failed to explain the extraordinary width and intraplate nature of the orogen.

Here we present a flat-slab model for the broad Indosinian intracontinental orogen, and a model involving slab delamination/fundering and plate-capture for the Jurassic-Cretaceous anorogenic magmatism and basin-and-range development.

*Flat-slab subduction and Indosinian intro-continental orogeny:* Apart from its enormous width, other key features of the Indosinian Orogeny in South China include (1) the orogeny started from the southeastern coastal region in as early as mid-Permian, and migrated inland toward the northwest until the Late Triassic/Early Juraasic (Li, 1998); (2) accompanying the northwest-ward migration of the orogeny was a similar migration of (but rare) arc-type magmatism at the front of the orogen; and (3) the development of shallow-marine basins tailing the NW-migrating orogen. We thus propose that like the Cretaceous to early Paleogene Lamaride Orogeny in the Cordillera and section of the Andes during the Cenozoic, the Indosinian Orogeny in southeastern South China was also due to a phase of flat-slab subduction. This model explains the migration of orogenesis and arc-magmatism, and the over 1300km width of the orogen. The development of topographic down-warping at the tail of the orogen was possibly due to the gravitational pull of the flat-subducted oceanic lithosphere as it went through phase changes, plus the downward push of the normal oceanic slab from behind the subducted flat-slab.

*Post-orogenic slab delamination/foundering and widespread anorogenic magmatism:* Previous models typically involve a continental arc (e.g., John et al., 1990; Zhou and Li, 2000) for explaining the widespread Jurasic-Cretaceous anorogenic magmatism in the region. The difficulties with those models are that (1) those magmatism are not typically of arc-type; rather, they are bimodal and many are intraplate alkalic rocks (Li et al., 2003; Li et al., 2004; Wang et al., 2005); (2) there was also a basin-and-range province developed in southeastern South China at that time (Gilder et al., 1991); (3) the magmatic province stretched to ca. 1000 km from the continental margin, not just along the coastal region; and (4) the temporal-spatial distribution of the magmatism was not a simple coast-ward migration as the model by Zhou and Li (2000) requires. We propose here that this wide anorogenic magmatic province was partly due to the delamination and foundering of the subducted flat-slab, partly due to the coupling of the coastal region with the oceanic plate during the Late Jurassic-Cretaceous. We envisage that phase-changes of the flat-slab after subduction first led to the slab foundering at the central part of the flat-slab, causing the intrusion of the ca. 190 Ma granites and ca. 175 -170 Ma alkaline mafic and felsic volcanic and plutonic rocks in southern Hunan to southern Jiangxi Province. This was followed by the further delamination and foundering of slab in regions to the west-southwest, as shown by the intrusion of the 165-155 Ma granites (including A- and I-type granites) and minor syenites.

During the Late Jurassic (ca. 150 Ma) and the Cretaceous, a basin-and-range province was developed in the coastal region (Gilder et al., 1991), with extensive intrusions/extrusions of bimodal magmatism (including A-type granite, syenite, dabbro, diorite/granodiorite, and gabbro) which display a general coast-ward migration trend (Zhou and Li, 2000). We believe that two mechanisms were at play during that time. First, the sea-ward retrograde steepening of the remaining subducted flat-slab explains the sea-ward migration of the magmatism and some extension. Second, the arrival of the Pacific-Izanagi ridge during the Late Jurassic may have led to the coupling of the Isanagi Plate (oceanic) with the coastal region of East Asia, causing the development of a basin-and-range province and widespread left-lateral faults.

**References**

Gilder, S.A., Keller, G.R., Luo, M., and Goodell, P.C., 1991, Timing and spatial distribution of rifting in China: Tectonophysics, v. 197, p. 225-243.

Hsu, K.J., 1994, Tectonic facies in an archipelago model of intra-plate orogenesis: GSA Today, v. 4, p. 289-293.

Jahn, B.M., Zhou, X.H., and Li, J.L., 1990, Formation and tectonic evolution of Southeastern

China and Taiwan: Isotopic and geochemical contraints: Tectonophysics, v. 183, p. 145-160.

Li, X.H., Chen, Z., Liu, D.Y., and Li, W.X., 2003, Jurassic gabbro-granite-syenite suites from Southern Jiangxi province, SE China: Age, origin, and tectonic significance: International Geology Review, v. 45, p. 898-921.

Li, X.H., Chung, S.L., Zhou, H.W., Lo, C.H., Liu, Y., and Chen, C.H., 2004, Jurassic intraplate magmatism in southern Hunan-eastern Guangxi: 40Ar/39Ar dating, geochemistry, Sr-Nd isotopes and implications for tectonic evolution of SE China, *in* Malpas, J., Fletcher, C.J., Aitchison, J.C., and Ali, J., eds., Aspects of the Tectonic Evolution of China. Geological Society, London, Special Publications, Volume 226, Geological Society, London, Special Publications, p. 193-216.

Li, Z.X., 1998, Tectonic history of the major East Asian lithospheric blocks since the mid-Proterozoic -- a synthesis, *in* Flower, M.J., Chung, S.-L., Lo, C.-H., and Lee, T.-Y., eds., Mantle dynamics and plate interactions in East Asia., Volume 27: Geodynamics Series: Washington, DC, United States, American Geophysical Union, p. 221-243.

Liu, B., and Xu, X., 1994, Atlas of Lithofacies and Paleogeography of South China: Beijing, Science Press, 188 p.

Wang, Q., Li, J.W., Jian, P., Zhao, Z.H., Xiong, X.L., Bao, Z.W., Xu, J.F., Li, C.F., and Ma, J.L., 2005, Alkaline syenites in eastern Cathaysia (South China): link to Permian-Triassic transtension: Earth and Planetary Science Letters, v. 230, p. 339-354.

Zhou, X.M., and Li, W.X., 2000, Origin of Late Mesozoic igneous rocks in Southeastern China: implications for lithosphere subduction and underplating of mafic magmas: Tectonophysics, v. 326, p. 269-287.

# Detrital zircon study along the Yarlung-Tsangpo River, SE Tibet

梁育瑄 [1], 鍾孫霖 [1], 劉敦一 [2], Suzanne Y. O'Reilly [3],
朱美妃 [1], 季建清 [4], 宋彪 [2], Norman J. Pearson [3]

[1] 臺灣大學地質科學系，台北 10699
[2] 中國地質科學院地質所北京離子探針中心，北京 100037
[3] GEMOC, Macquarie University, Sydney, NSW2109, Australia
[4] 北京大學地球與空間學院，北京 100037

The interactions among tectonic uplift, river erosion and alluvial deposition are fundamental processes that shape the landscape of the Himalayan-Tibetan orogen since its creation from early Cenozoic time. To understand these processes around the eastern Himalayan Syntaxis and southeastern Tibet, we conducted a study of riverbank sediments along the Yarlung-Tsangpo River. Detrital zircons separated from the sediments were subjected to *in-situ* U-Pb dating using SHRIMP II at the Beijing SHRIMP Center and Hf isotope measurements using LAM-MC-ICPMS at GEMOC. These results, together with the U-Pb ages and Hf isotope data that we have recently obtained for the Transhimalayan plutonic and surrounding basement rocks, allow a more quantitative examination of the provenance or "protosource" areas for the riverbank sediments. From the upper reaches of the River in the west to the Namche Barwa Syntaxis in the east, our results indicate that the percentage inputs from the major source provenances vary significantly, e.g., those of detrital zircons from the Gangdese batholith increase from ~18% to ~50% and those from the Tethyan Himalayan sequences decrease from ~80% to <50%. Before the River flows into the Big Bend gorge, the percentage of Gangdese-derived zircons lowers to ~35%, but it arises back to ~50% in the Muotuo area. Moreover, in each part of the River, these Gangdese-derived zircons show characteristic εHf(T) values that could be correlated to the neighboring batholithic values and thus interpreted as reflecting the River's power on "focused erosion". Comparing with the sediment budget estimated for the downstream Brahmaputra River, the strongest erosional processes are suspected to have been taking place in the eastern Himalayan Syntaxis that, in turn, implies the Yarlung-Tsangpo and Brahmaputra River system to be one of the most dynamic mountain rivers on modern Earth. Its piracy relation with the Irrawaddy River may be explored by using literature information and our preliminary data from Myanmar that appear to signal Gangdese-derived zircons in the riverbank sediments.

# Interactions between tectonics and surface processes in Taiwan: Insights from sandbox experiments

Chia-Yu Lu[1], Jacques Malavieille[2], Kuo-Jen Chang[3], Yuchang Chan[3]

[1]Department of Geosciences, National Taiwan University
[2] Laboratoire Dynamique de la Lithosphere, UMR 5573, Universite Montpellier 2, place E. Bataillon, 34095 Montpellier Cedex 5, France
[3]Institute of Earth Sciences, Academia Sinica, P.O. Box 1-55, Nankang, Taipei

In recent years attention has been paid on the major role of surface processes in numerous studies dealing with the evolution of orogens at different time scales. For example, the roles of erosion and sedimentation on exhumation and deformation history of accretionary orogens are widely studied through experimental and geological methods. In Taiwan today, the subduction of the Chinese continental margin under the Luzon arc results in the progressive growth of an active orogenic wedge. It is one of the best places to study the complex relationships that occurs between the tectonic processes controlling deformation (plate rheology and kinematics, metamorphism and magmatism) and surface processes (erosion and sedimentation).

In the Central Range of Taiwan, foliation and lineation traces outline the shape of both, the foreland structure and relative backstop of the orogenic wedge. The foliation dip and the strain ellipsoids distribution show the fan shape of a large pop-up structure characterizing the effects of plate convergence. On the eastern flank, regionally developed penetrative cleavage dips gently toward the east. Stretching lineations defined by phyllosilicates lie approximately parallel to the axes of regional folds with varying trends from northeast to east. Geometry of strain shadows indicates that (a) extension directions changed from along-strike toward down-dip and (b) top-to-the southwest or west shearing occurred in the direction of along-strike. The orogen-parallel shearing determined in the hinterland side, which is different from the orogen-perpendicular thrusting observed in the western flank of the Central Range (the foreland side), has to be related with strain partitioning induced by the oblique plate-convergence.

In order to study the kinematics of the present day convergence of Philippine Sea plate to the Asian continent around Taiwan, we perform 2D and 3D sandbox modeling and we analyzed the models with PIV (Particle Image Velocimetry) software. In 2D experiments, a model Coulomb wedge is submitted to erosion and sedimentation under topography and flux steady state conditions. The 3D experiments are mainly used to study the escape tectonics occurring in the middle west and southwest Taiwan. A wedge shaped indenter and a basement relief were used to simulate the mechanical plate boundary between Philippine Sea plate and Eurasia plate and the basement topography to the west of Taiwan respectively. We examine the exhumation patterns, the mode of fault propagation and displacement patterns by strain partitioning of vertical vs. horizontal displacement and convergent parallel vs. orogen parallel components.

The preliminary conclusions are: 1. The interactions between tectonics, erosion and sedimentation control geometry and kinematics of the doubly vergent transpressional orogen. 2. Exhumation processes are controlled by the balance between erosion, frontal accretion and underplating in different structural domains of the wedge. 3. Retrowedge erosion favorites backfolding and backthrusting, induces flower structures and fan shaped cleavage distribution. 4. Sedimentation promotes underplating and out-of sequences thrusting. 5. Structural heritage (normal faults or topographic relief) controls inversion of sedimentary basins during wedge growth.

# 中亚南部大陆的早期增生

陆松年、李怀坤、陈志宏、相振群

天津地质矿产研究所

亚洲大陆的形成经历了整个显生宙地质历史过程，在罗迪尼亚超大陆中，组成现代亚洲大陆的几个主要陆台分散在超大陆西缘(如塔里木和华南)、东或东北缘(西伯利亚和华北)，或远离罗迪尼亚超大陆（印度）。始于新元古代中期的超大陆裂解为新的洋–陆转换和亚洲大陆的诞生创造了条件。在罗迪尼亚超大陆形过成程中，亚洲的主要陆台有各自独立的演化历史，而只有超大陆裂解并经历了显生宙地质演化以后，组成亚洲大陆的几个主要陆台在经历了几期重大演变以后，于新生代亚洲大陆才最终形成，所以就一个大陆最终完成统一而言，亚洲是一个年轻的大陆。但是，亚洲大陆的雏形从新元古代末至古生代早期就已经开始形成，突出表现在中亚南部，在经历了早古生代造山作用以后，塔里木和华北陆台，及与其相邻的祁连–全吉地块、柴达木地块、中阿尔金地块和北秦岭地块等实现了统一，该陆块群构成北部古亚洲洋和南部古特提斯洋之间的大陆屏障，成为亚洲大陆的中轴。统一的中亚南部陆块群早期地质历史可概述如下：

1. ～820Ma 基性岩墙群和基性–超基性杂岩的发育（如塔里木北缘且干布拉克基性–超基性杂岩的侵入时代为 817±11Ma，龙首山金昌超基性杂岩为 827±8Ma，全吉地块鹰峰辉绿岩墙群为 821±11Ma，扬子陆台三防基性岩墙群 824±4Ma，汉南杂岩基性–超基性杂岩斜锆石 U–Pb 年龄为 825.3±2.6Ma，南澳大利亚 Garidner 基性岩墙群为 827±6Ma 等）(除斜锆石为 TIMS/U–Pb 年龄外，余均为 SHRIMP/U–Pb 年龄)，指示罗迪尼亚超大陆西缘塔里木–扬子–澳大利亚陆块群所发生的第一幕大陆破裂，造成了该陆块群与劳伦大陆之间的逐步分离，但尚无证据表明塔里木–扬子–澳大利亚陆块群从～820Ma 即开始瓦解，彼此之间发生了漂移。新元古代第一和第二冰碛层在组成陆块群的各陆台上的发育(澳大利亚的斯图特冰碛层和马临诺冰碛层、扬子陆台的古城冰碛层和南沱冰碛层、塔里木陆台的贝义西冰碛层和特瑞爱肯冰碛层)，说明塔里木–扬子–澳大利亚陆块群至少在 635Ma(第二冰碛层的结束时间)前仍然存在；

2. 635Ma 以后，塔里木与扬子逐步分离，华北向塔里木漂移，形成具有区域特色和层位可对比的震旦纪顶部冰碛层（新元古代第三冰碛层），如塔里木陆台北缘的汉格尔乔克组、祁连–全吉地块上的红铁沟组、华北陆台西缘正目观组和南缘的罗圈组等，而在扬子陆台上未见第三冰碛层的发育；

3. 新元古代晚期，西伯利亚与塔里木、华北陆台之间的古亚洲洋形成，中亚北部进人"中亚造山带"的演化过程。与此同时，塔里木、华北陆台的南缘步入"中央造山带"的演化历程；

4. "中央造山带"中早古生代的泛华夏造山作用对中亚南部陆块群的形成起了至关重要的作用。在"中央造山带"保留了多条缝合带，现在仍可鉴别的早古生代缝合带有库地、红柳沟–肃北、北祁连、索尔库里–滩间山、昆中、朱阳关–夏馆和商丹等 7 条缝合带。通过它们的焊接，塔里木和华北陆台及祁连–全吉、柴达木、中阿尔金、北秦岭等地块之间实现了汇聚，形成环冈瓦纳大陆的中亚南部陆块群。中亚陆块群的形成是中国和亚洲大陆一次十分关键的早期生长过程。

5·"中央造山带"中泛华夏造山作用的证据来自保留的蛇绿岩–弧火山岩残片、高压–超高压变质作用、深熔作用、同造山火山–沉积地层组合和同造山深成侵入体等。它们的同位素时代指示这一期造山作用主要发生于寒武纪至奥陶纪。例如，库地蛇绿岩中伟晶辉长岩和石英辉长岩分别为 526±3Ma 和 510±10Ma、北祁连玉石沟蛇绿岩中辉长岩为 550±17Ma、昆中蛇绿混杂岩中的辉长岩为 522.3±4.1Ma、丹凤弧火山岩年龄为 499.8±4Ma、二郎坪弧火山岩为 469.7±7Ma；鱼卡河–沙柳河榴辉岩变质时代分别为 499.6±5Ma、 484±3Ma、 473±4Ma 和 466.7±1.2Ma 等；秦岭岩群和金水口岩群的深熔时代分别为 499.3±4.3Ma 和 430.7±9.1Ma，而同造山花岗岩的时代多集中在 500Ma～430Ma 之间，少数后碰撞花岗岩可延至 400Ma 左右(以上为 TIMS 和 SHRIMP U–pb 数据)。最新的同位素年龄数据汇总于表 1（略）。新的地质学和年代学资料表明"中央造山带"内确实存在强烈而广泛的早古生代泛华夏造山作用。

上述早古生代泛华夏造山作用与泛非和加里东造山作用一样，在全球从罗迪尼亚超大陆破裂到联合大陆形成的过程中，是具有同等重要意义的一次全球重大地质事件。

# 秦–祁–昆造山带中前寒武纪地块的类型及主要地质特征

陆松年，李怀坤，王惠初，陈志宏，相振群

天津地质矿产研究所

“秦–祁–昆造山带为一条巨型显生宙造山带，经历了从新元古代末期–古生代早期和古生代末至中生代早期复杂的洋–陆转换及陆陆碰撞过程。它的北部从西向东大致以库地断裂、北阿尔金断裂、北祁连北缘断裂、滦川断裂和大别–苏鲁北缘断裂为界，分别与塔里木和华北克拉通南缘相邻；南部则以康西瓦断裂、阿尼玛沁断裂、勉–略断裂和大别–苏鲁南缘断裂为界，与羌塘地块和扬子克拉通北缘相接。其间主要包括多条缝合带、多个由前寒武纪岩层组成的地块和变质地体，以及卷入造山带中的古陆块大陆边缘”。本文仅讨论康西瓦–阿尼玛沁–勉略断裂带以北早古生代造山带的组成及演化，重点阐述其中前寒武纪地块的类型及主要地质特征。

根据早古生代秦–祁–昆造山带内被卷入的前寒武纪地块、变质地体和同造山过程中所形成地质体（蛇绿岩套、洋弧、洋岛、大陆边缘岛弧和弧后盆地中的产物）的特点及空间配置型式判断，秦–祁–昆造山带内的基本地质特征是多条缝合带和多个地块、变质地体的共存。秦–祁–昆造山带不是两个大陆板块直接碰撞和其间大洋闭合的产物，因此在中央造山带内不存在纵贯整个造山带的“主缝合带”，总体特征与其北的“中亚造山带”十分相似，以地块之间或地块与陆台之间的碰撞及同造山过程中地质体向陆台或地块边缘的增生拼贴为主，但秦–祁–昆造山带显生宙的陆壳生长速率远不如中亚造山带，主要表现以古陆壳的活化再造为主，初生地壳的形成为辅。

秦–祁–昆造山带中地质构造单元主要划分为 3 种类型：第一类是同造山过程中形成的地质构造单元，如岛弧、洋盆、海山等，现已成为克拉通与地块之间，或地块与地块之间的缝合带(suture)，是板块边缘增生拼贴的标志；第二类是由前寒武纪岩层所组成的地块或微陆块，它们已不同程度受到显生宙造山作用的影响，卷入造山作用之中，地块的边界被缝合带所围限；第三类是被卷进显生宙造山作用中的陆台大陆边缘，在显生宙造山过程中受到強烈改造，成为造山带的组成部分，但仍可辨别与陆台之间的亲缘关系，且未完全被缝合带所围限。

“缝合带(Suture)”是指板块边界断裂带或剪切带，位于缝合带两侧的地质体在地理上可能曾经相距很远的距离。中央造山带中的缝合带是地块与地块之间，或与陆台之间汇聚过程的产物，由于它们之间通常存在规模不等的洋盆、海山、洋弧，因此，缝合带中

保存了这些洋盆、海山、洋弧的残留，形成以蛇绿岩或蛇绿混杂岩为主的缝合带。同时，由于汇聚过程中深俯冲及其后发生的折返作用，高压—超高压带的存在也是缝合带的标志。这些缝合带在构造上是薄弱带，在后期地质作用影响下，多以断裂带或剪切带的形式出现。秦–祁–昆造山带早古生代缝合带有库地、北阿尔金、北祁连、柴达木地块北缘、昆中、朱阳关–夏馆和商丹等 7 条缝合带，主要地质特征及对比列于表 1（略）。

"地块（Massif）"一词系指卷入造山带中的地质块体，其主体的形成时代早于造山作用形成的时代，但其整体或边缘受到造山作用的强烈改造。前者如北秦岭地块，其中"秦岭岩群"形成于中元古代，但在早古生代造山过程中整体受到强烈影响，产生变质、变形和深熔作用；后者如祁连–全吉地块，地块内部还保留了清晰的前南华纪变质基底和未变质的南华纪–震旦纪沉积盖层的双层结构特征，但其南缘出现了早古生代大陆边缘火山弧，北缘也出现俯冲带的标志，说明地块的边缘已卷入早古生代造山作用。"中央造山带"中的地块主要包括祁连–全吉地块、柴达木–中阿尔金地块和北秦岭地块等。文中将西昆仑划为"性质不明的变质地体"，原因是组成西昆仑的桑珠塔格岩群和布伦阔勒岩群的地层时代还不能很好确定，即目前还不能界定它们是前寒武纪或早古生代的产物，因此，将西昆仑划为性质不明的变质地体，以示与地块之间的差异。各地块的主要地质特征列于表 2（略）。

秦–祁–昆造山带中的前寒武纪地块可划分为三种类型：

第一种类型可简称为"全吉型"，以祁连–全吉地块为代表，其特点是(1)具有较老的古元古代变质基底；(2)具有与塔里木陆台相似的由前南华纪变质基底和南华纪–震旦纪未变质沉积盖层所组成的双层结构；(3)造成变质基底与沉积盖层之间不整合面的全吉运动与塔里木陆台上的塔里木运动的特点及时代具有可比性；(4)前寒武纪地质演化过程中的一些关键地质事件与塔里木陆台具有相似性，如古元古代初期双峰式岩浆活动、～820Ma 基性岩墙群、震旦纪末期与塔里木陆台库鲁克塔格群顶部汉戈尔乔克组相似的红铁沟组冰碛层等；(5)地块边缘发育早古生代岛弧(南缘)或被动陆缘(北缘)，而核部在早古生代造山过程中保持相对稳定。

第二种类型可简称为"柴达木型"，以柴达木–中阿尔金地块为代表，它具有与"全吉型"地块不同的特点，表现为：(1)迄今未发现大面积展布的古元古代岩层，组成地块的主体是中元古代金水口岩群及侵入其中的新元古代早期花岗片麻岩；(2)未保留前南华纪变质基底和南华纪–震旦纪沉积盖层所组成的双层结构及其间的不整合面；(3)前泥盆纪岩层全部受到早古生代造山作用的改造，早古生代变质、变形及深熔作用发育；(4)未发现前泥盆纪基性岩墙群，说明柴达木–中阿尔金地块比祁连–全吉地块的稳定化程度低。

北秦岭地块具有“柴达木型”地块的基本特征，主要由中元古代秦岭岩群及侵入其中的新元古代早期花岗片麻岩所组成，整体上受到早古生代造山作用的改造，早古生代变质、变形及深熔作用发育，因此，北秦岭地块向西难以和祁连–全吉地块相连，它的特点与柴达木–中阿尔金地块更相似。

第三种类型可简称为“西昆仑型”，以西昆仑地块或变质地体为代表，它的组成以较年青的(新元古代晚期)变质岩层为主、不仅受到早古生代造山作用的影响，而且也受到古生代末期至中生代早期热–构造运动的叠加。东昆仑地块的特点与西昆仑地块具有较多的相似性，它不仅受到早古生代造山作用的影响，而且也受到中生代早期热–构造运动的叠加，突出表现在两地块北缘分别为早古生代库地和昆中缝合带，而南缘则为古生代末期至早中生代的康西瓦和阿尼玛沁缝合带，因此，东、西昆仑地块受到两期造山作用的影响比其他类型地块更明显和更强烈。

秦–祁–昆造山带中的前寒武纪地块均不同程度地卷入了早古生代造山作用，并与塔里木和华北陆台拼合，形成一个统一的陆块群。这既是形成中国大陆雏形，亦是形成亚洲大陆雏形的早期增生作用，在全球从罗迪尼亚超大陆破裂到联合大陆形成的约 600Ma 的过程中，与泛非和加里东造山运动一样，具有同等重要意义的全球重大地质事件。

# Mantle Lithosphere beneath the Tibetan Plateau, Part I: Constraints from Shear-Wave Splitting with Special Reference to New Results from the Hi-CLIMB Seismic Array

Michael Martin[1], Wang-Ping Chen[1], Tai-Lin (Ellen) Tseng[1], Zhaohui Yang[1], Mei Jiang[2], Heping Su[2], Youxue Wang[2], John Nabelek[3], Bor-Shouh Huang[4], and the Hi-CLIMB Seismic Team[5]

[1] Department of Geology, University of Illinois at Urbana-Champaign Urbana, IL 61801 USA
[2] Chinese Academy of Geological Sciences, Beijing, People's Rep. of China
[3] College of Oceanography, Oregon State University, Corvallis, OR USA
[4] Institute of Earth Sciences, Academia Sinica, Taiwan, R. O. C.
[5] Other Principal Scientists: M. R. Pandey, S. Sapkota, and B. Kafle, Department of Mines and Geology, Kathmandu, Nepal, and John Chen, Institute of Geophysics, Peking University, People's Rep. of China

The centrepiece of Project Hi-CLIMB (An Integrated Study of the Himalayan-Tibetan Continental Lithosphere during Mountain Building) is a broadband seismic array of over 800 kilometers in length across the Himalayan-Tibetan collision zone. Along a north-south trending corridor between 84°E and 86°E meridians, the array extended from the southern edge of the Ganga foreland basin, over both Lesser and Higher Himalayas, crossing the Indus-Yarlung Suture (IYS) and the Bangong-Nujiang Suture (BNS), then reaching into the heartland of the Tibetan plateau. In three phases between 2002 and 2005, over 300 seismic stations were deployed at an average spacing of 3-8 km. In this study, we report new results of polarization anisotropy based on birefringence of *SKS* and *SKKS* phases recorded by the Hi-CLIMB array (Figure 1).

New results of Hi-CLIMB mainly come from high-quality, broadband seismic waveforms of 36 earthquakes between 2003 and 2005. After comparing results from different algorithms, we found that the method of *Wolfe & Silver* (1998) yields the most stable solutions. In this procedure, for each possible combination between the orientation of polarization for the fast-travelling component ($\phi$) and split-time ($\delta t$), one calculates a misfit function by summing the squares of the resulting transverse component's amplitude over the time window of interest for each station-event pair. Then, after normalization, misfit functions from all events recorded at a given station are stacked. Best-fitting values of $\phi$ and $\delta t$ are estimated from the minimum of the stacked misfit function. When compared with estimates from single event-station pairs where minima of the misfit functions are often indistinct, solutions from the stacked misfit function are usually stable and with significantly less uncertainty. More import, in the presence of noise, stacked solutions typically yield consistent results among closely spaced, neighbouring stations which is often not the case for un-stacked estimates.

Consistent with previous results elsewhere in Tibet, the Himalayas and the Indian shield (*Chen & Ozalaybey*, 1998 and references therein), null birefringence prevails south of the IYS ($\delta t \leq 0.3$ s). Significant splitting starts about 80 km north of the IYS. Further northward, $\phi$ gradually changes from NE-SW to E-W while $\delta t$ decreases from about 1.3 s to 0.6 s. Near the surface trace of the BNS, $\delta t$ increases rapidly to 1.5 s or so, suggesting a localized region of significant changes in anisotropic properties of the upper mantle. North of the BNS, $\delta t$ levels off to between 0.5 s and 1.0 s whereas $\phi$ remains approximately E-W.

In general our new results are consistent with those obtained along the Yadong-Gulmod profile except for the obvious difference that there is a ten-fold improvement in spatial resolution along the Hi-CLIMB profile. As such, any change associated with the BNS was not detected along the Yadong-Gulmod profile. Furthermore, we are now exploiting the dense spacing of the Hi-CLIMB array in order to constrain depths of seismic anisotropy.

An exceptionally abrupt jump in $\delta t$, from null to 2.2 s, was reported by *Huang et al.* (2000) about 40 km south of the BNS along the INDEPTH-III profile (Figure 1). Such a jump is too abrupt for mantle sources of anisotropy yet the magnitude of $\delta t$ is about ten times too large to result from crustal sources alone. We re-analyzed their data (available in the public domain) using stacked misfit functions and reduced the peak in $\delta t$ to about 1.8 s. Moreover, the increase in $\delta t$ now extends over a distance of at least 50 km, a reasonable value for mantle anisotropy.

Based on stacked misfit functions, Figure 1 shows a detailed comparison of shear-wave splitting between Hi-CLIMB and INDEPTH-III profiles. Two observations are worth noting. First, while the region of null splitting is consistent between Hi-CLIMB and Yadong-Gulmod profiles, null splitting extends farther north along the INDEPTH profile, suggesting a lateral change in the northern limit of intact Indian mantle lithosphere. Second, part of uncertainties in both $\phi$ and $\delta t$ result from discordant estimates from *SKS* and *SKKS* phases which are typically from distinct events with different back-azimuths. Preliminary analysis suggests that there seems to be a major change in mantle anisotropy near the BNS – a new direction of research that may have profound implications for the tectonic history of central Tibet.

**Acknowledgements.** This work is supported by the Continental Dynamics Program of the US National Science Foundation under Grant No. EAR9909362. Any opinions, findings and conclusions or recommendations expressed in this material are those of the authors and do not necessarily reflect those of the National Science Foundation. We also thank the IRIS PASSCAL Instrument Center for unwavering support throughout the long duration of Hi-CLIMB.

**References**

Chen, W.-P. & Özalaybey 1998. Correlation between seismic anisotropy and Bouguer gravity anomalies in Tibet and its implications for lithospheric structures, *Geophys J. Int.*, **135**, 93-101.

Huang, W.-C., Ni, J.F., Tilman, F., Nelson, D., Guo, J., Zhao, W., Mechie, J., Kind, R., Saul, J., Rapine, R. & Hearn, T.H. 2000. Seismic polarization anisotropy beneath the central Tibetan Plateau, *J. Geophys. Res.*, **105**, 27979-27989.

Wolfe, C.J. & Silver, P.G. 1998. Seismic anisotropy of oceanic upper mantle: Shear wave splitting methodologies and observations, *J. Geophys. Res.*, **103**, 749-771.

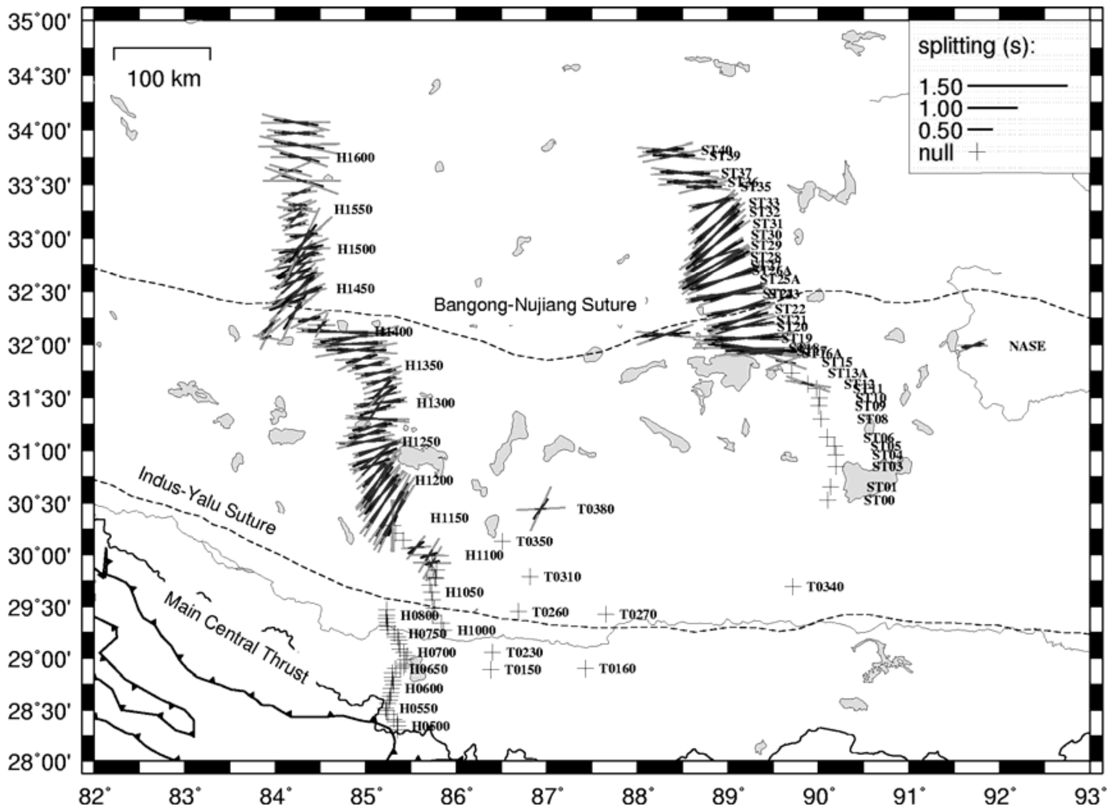


Figure 1: A map summarizing results of shear-wave birefringence across the Himalayan-Tibetan collision zone, including 1) new observations from the Hi-CLIMB seismic array and 2) those from a critical re-evaluation of data along the INDEPTH-III profile. Trends of thick lines indicate orientations of polarization for the fast-travelling component of *SKS* and *SKKS* phases, while lengths of lines are proportional to split-times. Straddling each thick line, crossed pairs of thin lines show uncertainties in orientation (at 95 % confidence-level of the misfit function). Crosses mark sites of null birefringence.

# 西藏南部林子宗火山岩系：印度—亚洲碰撞时限及大陆生长的记录

莫宣学[*]　董国臣　周　肃　赵志丹

中国地质大学（北京），北京 100083

广泛发育在西藏冈底斯岩浆岩带中的林子宗火山岩及其与下伏地层间的区域性不整合，提供了印度—亚洲大陆碰撞时限及陆壳生长的新证据(图 1)，它的地球动力学意义正日渐凸现。

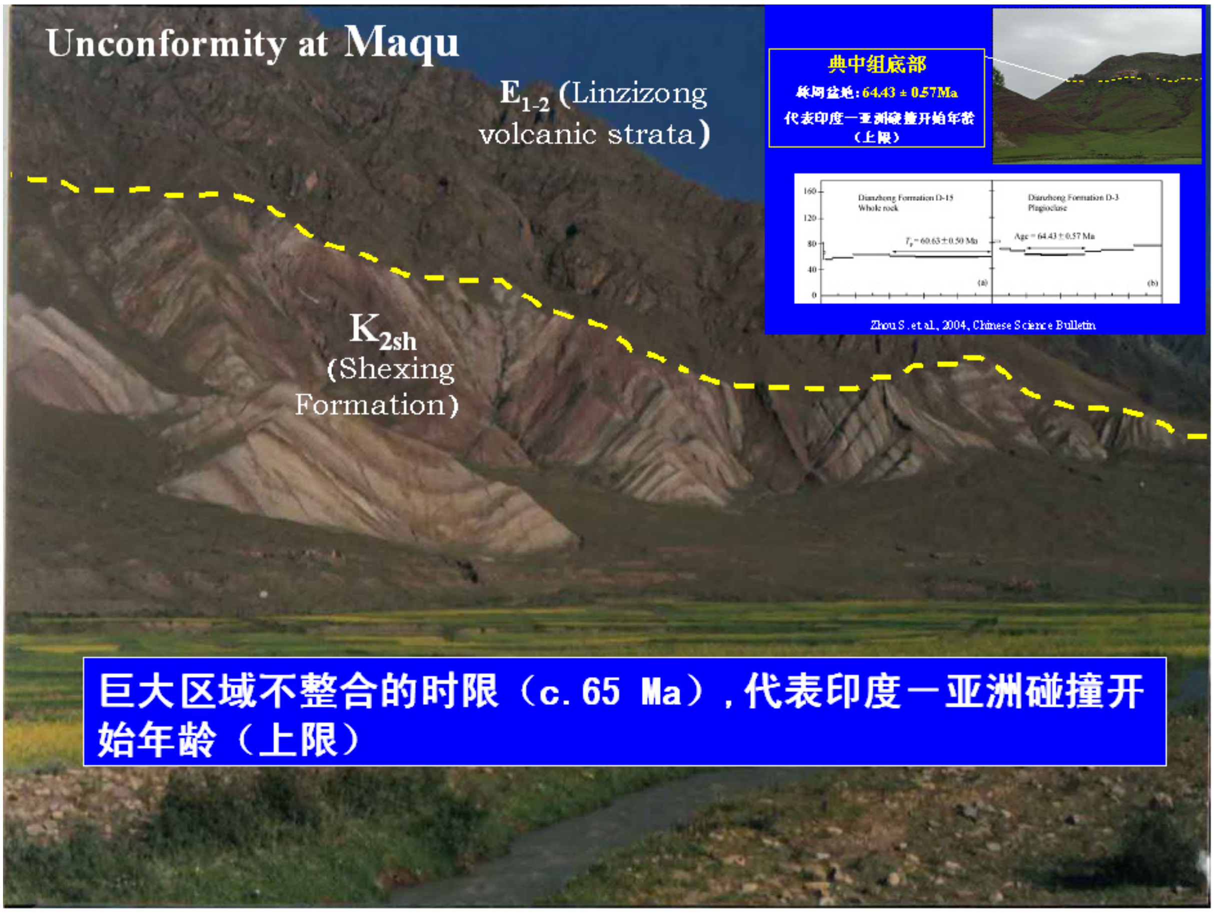


## 西藏林子宗火山岩系的组成与特征

### 林子宗火山岩系的岩石组成

林子宗火山岩系是指角度不整合于上白垩统或更老地层之上，其上又被渐新世红层不整合覆盖的一套火山—沉积岩系，最早由李璞先生（1950）在拉萨附近的林周盆

[*] 电子邮箱地址：moxx@cugb.edu.cn

地命名。该处火山岩系厚度超过 5000m，发育齐全，自下而上分为典中组、年波组和帕那组三个组。

下部典中组厚达 2400m, 呈角度不整合覆盖在上白垩统设兴组之上，底部为一层底砾岩。其上火山岩以安山质岩石为主体，爆发指数达 55%。$SiO_2$ 含量 55.21～72.41％，平均 60.50％； $K_2O$ 平均含量 1.89%。晚期有花岗细晶岩脉及辉绿玢岩脉侵入。在 $K_2O$–$SiO_2$ 图中主要落在钙碱性岩区，显示大陆边缘弧火山岩的特征。

中部年波组厚约 700m，其下与典中组的不同层位呈小角度不整合接触。该组中沉积岩占 70％左右。而火山岩为流纹质—英安质火山碎屑岩、钾玄岩及玄武粗安岩，晚期有钾玄质岩脉及钾质辉绿玢岩脉侵入。$SiO_2$ 含量 52.23%～85.47%, 平均含量 71.58%；$K_2O$ 平均含量 2.37%。在 $K_2O$—$SiO_2$ 图中, 落在钾玄岩区（SHO）及高钾钙碱性区（HKCA）岩石达 40%。强过铝质岩石达 50%，表明地壳物质对岩浆的影响已比较明显。

上部帕那组的厚度超过 2000m,下与年波组呈喷发不整合接触，顶部与二叠系呈断层接触。主要由巨厚的高钾流纹质熔接凝灰岩组成。 $SiO_2$ 含量 69.53%～80.55%, 平均 74.17%； $K_2O$ 平均含量 5.25%, 最高可达 7.94%。80%以上岩石成分点落在 SHO 区及 HKCA 区，A/CNK＞1.1 的强过铝岩石占 60%以上，更加清楚地显示出大陆碰撞及地壳加厚的构造环境。晚期也有钾玄岩脉及流纹斑岩的侵入。

区域上，林子宗火山岩系近东西向延伸达 1300km 以上，沿走向上述三个组均存在，但区域不整合面之下的地层却不尽相同。

**形成时代**

在地层学研究基础上，进行了系统的 $^{40}Ar/^{39}Ar$ 同位素测年 [1, 2]，确定林周盆地林子宗火山岩的喷发年龄为 64.43－43.93 Ma，其中典中组 64.4－ 60.6 Ma，年波组 60.6－50 Ma，帕那组 50－43.93 Ma。结合区域资料，可以确定林子宗火山岩形成于 65－40 Ma，喷发延续了 20 百万年以上。特别应当指出，林子宗火山岩的底部年龄限定了该火山岩系与下伏地层之间区域性不整合事件的最晚时限（65Ma 左右），提供了印度－亚洲大陆碰撞起始时间的约束，具有重要的意义。

**稀土元素与微量元素地球化学特征**

林子宗火山岩的稀土元素分配型式总体上表现为 LREE 富集的右斜曲线，$\sum REE=97.1-358.3\times10^{-6}$, $(La/Yb)_N=7.31-23.9$。典中组火山岩的稀土元素总量∑REE

$=106.6\times10^{-6}-148.6\times10^{-6}$，平均 $120.3\times10^{-6}$，(La/Yb)n 为 7.31－15.13，基本无 Eu 负异常。年波组火山岩∑REE 在 $97.1\times10^{-6}$—$227.4\times10^{-6}$ 之间，平均 $190.8\times10^{-6}$；(La/Yb)n 为 9.9－21.1，平均 14.8。帕那组火山岩∑REE＝$147.1\times10^{-6}$—$358.3\times10^{-6}$，平均 $207.7\times10^{-6}$，(La/Yb)n＝9.4－23.9，平均 18.6，具有中等－强烈的负 Eu 异常（δEu 值＝0.6－0.1），显示斜长石在岩浆中明显的分离结晶作用，或在地壳源区中呈难熔残余相存在。

林子宗火山岩微量元素分配型式，总体上富集强不相容元素 Rb, Th, U，而亏损 Nb, Ta, Ti, ( P, Sr )。晚期 Th，U 的富集程度越来越高，Nb，Ta，Ti，P，Sr 谷不断加深，曲线总体斜率及峰谷反差愈来愈大。帕那组蛛网图的形状，已与典型的碰撞后钾质火山岩极为相似。微量元素蛛网图中 Nb、Ta、Ti 谷通常被解释为与俯冲作用有关的，或源于大陆岩石圈的火成岩的特点。

**Nd–Sr–Pb 同位素组成**

从 εNd(t)－$^{87}$Sr/$^{86}$Sr 图解可以看到，林子宗火山岩的 εNd (t)＝＋3.24—－5.58，多数靠近 0 值，其中最基性岩石的 εNd(t)值达到＋3.24，说明其岩浆源区有地幔端员成分，陆壳中含有大量初生地壳成分。林子宗火山岩在 εNd—$^{87}$Sr/$^{86}$Sr 相关图上，与冈底斯东段和滇西后碰撞钾质火山岩分布区大致一致，靠近 PREMA 位于混合曲线的左上方，分布范围比较局限。

在 $^{207}$Pb/$^{204}$Pb－$^{206}$Pb/$^{204}$Pb 图及 $^{208}$Pb/$^{204}$Pb－$^{206}$Pb/$^{204}$Pb 图中，林子宗火山岩所有成分点均投在北半球参考线（NHRL）的左上方，以及地球等时线的右侧，源区具有类似印度洋 MORB 的富集特征。$^{206}$Pb/$^{204}$Pb 比值变化不大，而 $^{207}$Pb/$^{204}$Pb 和 $^{208}$Pb/$^{204}$Pb 比值变化范围较大（分别为 18.641-18.969, 15.491－15.764, 38.655－40.264），从靠近 PREMA，穿过下/上地壳交界区、EM2 区，向上地壳端员方向延伸，暗示幔源岩浆与地壳物质之间的相互作用。

**讨论**

**印度－亚洲大陆碰撞的起始时间**

关于印度－亚洲大陆碰撞的起始时间，一类意见认为，印度－亚洲大陆碰撞的起始时间晚于 50Ma；另一类意见认为其早于 50Ma。造成这些差异的原因，可能是由于各人的事实依据及所论的地点不同。我们对冈底斯带林子宗火山事件及区域不整合事件的研究，提供了西藏南部关于印度－亚洲大陆碰撞的起始时间的火成岩证据。

如前所述，东西延伸约 1300 km 的林子宗火山岩系与下伏地层的巨大区域不整合，

代表了白垩纪末以来最大的一次地质事件。该不整合下伏地层包括二叠系到上白垩统，均属海相，褶皱强烈；其上覆地层林子宗群属古新统－始新统，为陆相，地层近水平，与下伏地层在沉积相、变形样式与程度上截然不同。而且，不整合面以上的林子宗火山岩记录了由新特提斯俯冲结束过渡到印度—亚洲大陆碰撞的信息。因此，这一巨型不整合，应当是印度—亚洲大陆开始碰撞的结果，大陆碰撞（在西藏南部）开始时间应在 65Ma 左右。 尽管在林子宗火山岩系内部也有小型的角度不整合，但其规模和性质与前者完全不能相提并论。

地层、古生物及沉积学的研究也与此结论一致[3, 4]。

**大陆碰撞导致的青藏高原地壳生长与增厚**

林子宗火山岩系也包含着印度－亚洲碰撞导致的青藏地壳生长与增厚的丰富信息，也提出了许多科学问题。比如，为什么在通常认为不利于产生大量岩浆的同碰撞构造环境下，会相伴出现分布广泛、数量巨大的林子宗火山岩（65－40 Ma）及冈底斯带同碰撞期花岗岩类（峰期年龄 ~50 Ma）？又如，林子宗火山岩总体上类似大陆地壳的平均成分，林子宗早期火山岩及冈底斯同碰撞期花岗岩的 εNd(t) 多为正值，显示冈底斯南带的初生陆壳性质。根据林子宗火山岩中 $K_2O$ 含量估算，以及后碰撞期（25－12 Ma）埃达克质岩石[5, 6]的出现来判断，冈底斯南带的地壳厚度在 50 Ma 前基本仍为正常厚度，在~50 Ma 之后才开始有显著的地壳（特别是下地壳）的加厚。引起加厚的原因是什么？加厚是怎样的深部过程？地幔物质加入，及构造挤压缩短，对青藏南部地壳增厚的相对贡献各有多少？从对林子宗火山岩及冈底斯带其它与碰撞－后碰撞作用有关的火成岩的研究中，已经有了某些认识，今后还应进一步地加深。

**主要参考文献**

[1]董国臣，2002，博士学位论文，中国地质大学，北京，134pp.

[2] Zhou S., Mo X, Dong G.-C, Zhao Z.-D, Qiu R.-Z, Guo T.-Y & Wang L.-L, 2004, *Chinese Science Bulletin* 49 (18), 1970-1979.

[3] Wan X, Jansa, L F, Sarti, M., 2002, *Lethaia* 35(2): 131-146.

[4] Ding, L., Kapp, L., Wan, X., 2005, Tectonics (in press).

[5] Chung, S.-L., Liu, D.-Y., Ji, J.-Q., Chu, M.-F., Lee, H.-Y., Wen, D.-J., Lo, C.-H., Lee, T.-Y., Yian, Q., Zhang, Q., 2003. Geology 31, 1021-1024.

[6] Hou, Z.-Q., Gao, Y.-F., Qu, X.-M., Rui, Z.-Y., Mo, X.-X., 2004, Earth Planetary Science Letter 220, 139-155.

# 北山北部古生代两类花岗岩及有关矿床的钕同位素特征

聂凤军、胡朋、江思宏、刘妍

中国地质科学院矿产资源研究所，北京 10037

**摘要：**北山北部地处西伯利亚地台与哈萨克斯坦-北山板块汇聚带内，区内各种类型花岗岩体分布广泛，并且与金属矿床具密切空间分布关系。所有这些花岗岩可划分为两种成因类型，即深源型和浅源型，前者全岩样品 εNd(t)值均为正值，而后者的 εNd(t)值均为负值。研究结果表明，幔源岩浆活动导致了深源型花岗岩、铜、钼-金和铁矿床的形成，而壳源岩浆活动为浅源型花岗岩、钨和钨-锡-铋矿床的形成提供了物质和动力来源。两种成因类型花岗岩的厘定对于探讨本区地壳演化历史、揭示成矿作用本质和指导找矿勘查均具重要意义。

**关键词：**两类花岗岩、钕同位素、成因类型、金属矿床、北山北部

北山北部位于中国内蒙古、新疆和甘肃与蒙古国接壤地带，大地构造位置属西伯利亚地台与哈萨克斯坦-北山（以下简称哈-北板块）汇聚带上，东西长 500km，南北宽 50-80km，面积为 35000 km$^2$。受古亚洲洋壳与两大古板块长时期、多阶段俯冲、碰撞和对接作用影响，区内前寒武系变质岩块体分布广泛、古生界火山-沉积岩地层出露齐全、深大断裂纵横交错、花岗岩体十分发育，各类金属矿床星罗棋布。该研究区不仅是中亚巨型成矿带的重要组成部分，同时也是揭示古大陆地壳生长过程的理想窗口[1-4]。

通过半个多世纪的地质工作，人们先后在本区范围内完成 1/20 万和 1/5 万地质填图 35 幅，圈定花岗岩类岩体数百处。统计数据表明，北山北部花岗岩出露面积为 10000km$^2$，占整个岩（体）层面积的 48%，其中海西期花岗岩约占全部花岗岩体数量的 2/3[3]。在找矿勘查方面，人们先后在本区发现各类矿床百余处，代表性矿床有黑鹰山铁矿床、流沙山钼-金矿床、红尖兵山钨矿床、东七-山铷-钨-锡矿床、额勒根铜-钼矿床、马庄山金矿床和南金山金矿床。 尽管上述金属矿床可在各种类型和不同时代的围岩中产出，但是绝大多数矿床与海西期花岗岩体具密切时空分布关系，其中蚀变花岗岩是良好的找矿标志。认真总结海西晚期花岗岩及有关矿床地质特征，全面查明岩浆活动与金属成矿作用关系，进一步厘定成岩环境与物质来源，对于提高本区花岗岩及有关矿床研究水平和促进隐伏矿床找矿勘查均具重要意义[1-4]。

## 1 成岩（矿）地质环境

研究区地处西伯利亚地台与哈-北板块之间的中亚-蒙古造山带内，主要由一系列向南凸的弧形构造-岩浆岩带所构成。尽管地质学家在两大古板块运动机制的细节上仍存在有不同认识，但是他们均认为，该区的主体构造为古大陆边缘地体拼接带，单个地体形成环境既可以是前寒武纪古陆块，也可以是古生代岩浆弧、断陷盆地和古洋壳残片[1-6]。前寒武纪古陆块大多呈孤岛状或条带状为古生界火山-沉积岩地层所包裹，岩石类型主要有片麻岩、斜长角闪岩和大理岩。相比之下，古生界地层主要是一套海相碎屑沉积岩和中酸性火山岩，并且以分布范围广、出露厚度大和层序齐全为特点。中新生界为一套陆相沉积岩，主要分布在一些山间盆地中。区内各类侵入岩十分发育，除了少量镁铁质侵入岩外，主要出露有大面积海西期花岗岩。根据花岗岩体的产出环境，大体将其划分为两大类，即深源型和浅源型，前者大多在晚古生代构造-地层单元内产出，围岩为古生代碎屑沉积岩和中酸性火山岩，并且以富含镁铁质火成岩包体为特征，岩石类型有石英闪长岩、花岗闪长岩和二长花岗岩。全岩样品磁铁矿和碱质组份（$K_2O+Na_2O$）含量相对较高；后者大多在前寒武纪陆块及邻区产出，围岩为中新元古代变质岩，并且以富含硅铝质变质岩捕虏体为特点。岩石类型主要有花岗闪长岩、黑云母花岗岩和钾长花岗岩。全岩样品磁铁矿和碱质组份（$K_2O+Na_2O$）含量相对较低。需要提及的是，深源型花岗岩与铜、铁和钼-金矿床具密切时空分布关系，而浅源型花岗岩则伴生有钨和铷-钨-锡矿床[4-6]。

## 2 金属矿床地质特征

研究区金属矿床的产出特点可概述为分布广泛、类型繁多、成矿时代集中和容矿围岩复杂，其中大多数矿床与中酸性火成岩具密切时空分布关系。初步统计数据显示，在所调查的 48 处矿床中，与海西晚期花岗岩有关的矿床为 38 处，占总数的 79%，相比之下，与加里东期和燕山期花岗岩有关的矿床分别为 4 处和 6 处，分别占总数的 8%和13%。限于篇幅，这里着重对 4 处与海西期火成岩有关的矿床进行简要论述。

流沙山钼-金矿床和黑鹰山铁矿床均位于哈-北板块红石山-黑鹰山地体东段，容矿围岩分别为海西期花岗闪长岩和石炭系英安岩。 流沙山矿床由一组相互平行或大致平行的环状石英-钾长石脉或石英脉所构成，金属矿物有辉钼矿、白钨矿、自然金、辉铋矿和黄铁矿，脉石矿物有石英、长石和萤石，其中 6 件辉钼矿样品铼-锇同位素等时线年龄为 $260\pm10Ma(2\sigma)$[4]。相比之下，黑鹰山铁矿床由似层状、囊状和透镜状矿体所构成，金属矿物有磁铁矿和赤铁矿，脉石矿物为磷灰石、石英、绿泥石和碧玉， 其中 6 件磷

灰石样品钐-钕同位素等时线年龄为 322±4.3Ma(2σ)[6]，与其东南部花岗闪长斑岩辉钼矿铼-锇同位素等时线年龄相近（332±9Ma））[7]

东七-山铷-钨-锡矿床和红尖兵山钨矿床分别是西北地区最大的稀有多金属矿床和重要钨矿床之一[4-5]。前者位于哈-北板块马鬃山中间地块北侧，围岩为加里东期似斑状花岗岩株和新元古代大理岩，后者地处哈-北板块红石山-黑鹰山地体与公婆泉-月牙山地体汇聚处，围岩为石炭系流纹质凝灰岩和海西期二长花岗岩。东七-山矿床由一系列细脉浸染状块体、石英-萤石脉和石英脉所构成，金属矿物有黑钨矿、白钨矿、辉铋矿和锡石，脉石矿物有石英、长石、锂云母、萤石和条纹长石。5 件萤石样品钐-钕同位素等时线年龄为 511±5Ma（2σ）。相比这下，红尖兵山矿床由黄玉-石英脉和云英岩化条带所组成，金属矿物有黑钨矿、锡石、辉钼矿、辉铋矿和黄铁矿，脉石矿物有石英、黄玉、月光榴石、长石、云母和萤石，钨矿床成矿作用与海西晚期中酸性岩浆活动有关[4-5]。

## 3 钕同位素特征

**3.1 古生代深源型花岗岩及有关金属矿床：**对远离前寒武纪古陆块的花岗岩体及有关矿床的样品进行了钕同位素分析，在此基础上，结合野外地质证据，讨论了其物质来源和形成过程。前人同位素年代数据表明，无论是深源型花岗岩，还是与其相关的矿床，它们的形成时代集中分布在两个时间段，即 355-322Ma 和 299-255Ma[4-6]。考虑到辉钼矿呈浸染状分布在花岗岩体中，其铼-锇同位素年龄代表了岩体和矿体的形成时间，因此，采用两个年龄值（332Ma 和 260Ma）计算了花岗岩及有关矿床岩（矿）石样品的 εNd(t)值，并且绘制了 $T_{DM}$ 对 εNd(t)图（图 1a 和 1b）。当 t=332Ma 时，9 件花岗岩样品的 εNd(t)值变化范围为 0.79-7.86，平均值为 3.85；黑鹰山铁矿床 8 件磷灰石样品 εNd(t)值为 1.67-7.35，平均值为 3.50；流沙山钼-金矿床 6 件含矿花岗岩样品 εNd(t)值为 1.79-11.54，平均值为 6.88。在 $T_{DM}$ 对 εNd(t)图（图 1b）中，除少数几件样品外，大部分样品数据点投绘在兴蒙造山带花岗岩区内，其钕同位素组成特征与该区具有正 εNd(t)值的花岗岩相似[1、4]。采用同样方式，以 260Ma 为参照值，对上述样品 εNd(t)值进行了计算，所获结果与前述 εNd(332Ma)值基本相似。

**3.2 古生代浅源型花岗岩及有关金属矿床：**对前寒武纪古陆块内及邻区产出的花岗岩及有关矿床的岩（矿）石样品进行了钕同位素分析，并且以 332Ma 和 260Ma 为参照值，计算了样品的 εNd(t)值。当 t=332Ma 时，16 件花岗岩样品 εNd(t)值变化范围为 -0.03--14.48，平均值为-5.33，东七-山铷-钨-锡矿床 5 件萤石样品 εNd(t)值为-5.81--2.80，平均值为-4.06；红尖兵山钨矿床的黑钨矿样品可分为 2 类：（1）5 件样品 εNd(t)值为

-8.07--4.22，平均值为-6.91；（2）2 件样品 εNd(t)值为 4.11-5.77。无论是萤石，还是黑钨矿样品，其 εNd(t)和 $T_{DM}$ 值变化较大，很难用 $T_{DM}$ 对 εNd(t)图表示。在 $T_{DM}$ 对 εNd(t)图（图 1b）中，**浅源型**花岗岩样品全部投绘在微陆块的花岗岩区或旁侧，与兴蒙造山带具正 εNd(t)值的花岗岩存在有较明显的差别[1、4]。另外，采用同种方式，以 260Ma 为参照值，对上述样品的 εNd(t)值进行了计算，所获结果与前述 εNd(332Ma)值基本相似（图 1a）。

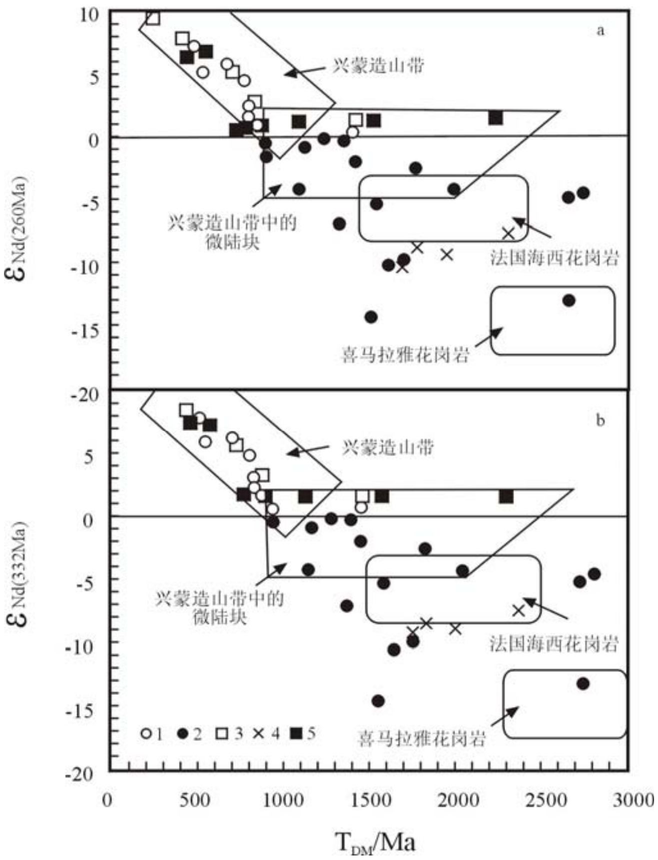


图 1 北山北部各类样品 εNd (t)对 $T_{DM}$ 关系图

1—深源型花岗岩；2—浅源型花岗岩；3—含钼-金花岗岩；4—前寒武纪变质岩；5—磷灰石

**3.3 前寒武纪古陆块变质岩**，如前所述，本区各个时代和不同规模前寒武纪古陆块和变质岩杂岩体星罗棋布，并且与古生代花岗岩和部分矿床具密切空间分布关系。交叉沟变质杂岩体中斜长角闪岩全岩钐-钕同位素等时线年龄为 1264±11Ma（2σ）[4]，这是迄今为止在本区发现的最古老岩石。在本次研究中，分别采用 1264Ma、332Ma 和 260Ma 计算了各类变质岩样品的 εNd(t)值。当 t=1264Ma 时，4 件变质岩样品 εNd(t)值为-1.5-1.18，平均值为 0.20；当 t=332Ma 和 t=260Ma 时，样品 εNd(t)值变化范围分别为-7.24--9.59，平均值-8.51 和-7.68--10.42，平均值-9.16。在 $T_{DM}$ 对 εNd(t)图（图 1a 和 1b）中，各变质岩样品数据点均落在兴蒙造山带微陆块区花岗岩区或旁侧，与华北陆台和塔里木地台前寒武纪变质岩钕同位素特征相似[1、4]。

**4 讨论与结论**

兴蒙造山带西段（新疆北部）和东段（内蒙古东部和辽-吉-黑地区）花岗岩的 εNd(t)值变化范围分别为-3.31～8.40 和-2.22～7.11[1、4]。与上述几个地区相比，研究区花岗岩样品具有更大的变化范围（7.86 - -14.48）和更明显的负 εNd(t)值，反映了更为复杂的成岩过程。通常情况下，具有正 εNd(t)值的岩（矿）体被认为是其物质来源与幔源岩浆活动或幔源组分占优的地壳重熔作用有关[1、4]，而具有明显负 εNd(t)的岩（矿）体则反映了其形成过程中有大量古陆壳物质的混入，由此来看，本区壳-幔物质相互作用的强度和复杂性要远高于新疆北部和东北地区。

众所周知，晚古生代时期，古亚洲洋壳对哈-北板块的多期次俯冲诱发了大规模构造-岩浆活动，进而形成大面积分布的海西期花岗岩及有关金属矿床。各类花岗岩和金属矿床很可能是通过下述 3 种途径形成的，其一、受洋壳与古大陆俯冲和碰撞作用影响，幔源岩浆的上涌或年轻地壳（含大量地幔物质）与部分古大陆岩（体）层的重熔，均可形成具有正 εNd(t)值的深源型花岗岩，同源热液流体形成具有正 εNd(t)值的铜、铁和钼-金矿体[1、4-6]；其二、强烈的构造作用同样可以导致前寒武纪古陆块发生重熔，进而形成具有负 εNd(t)值的浅源型花岗岩，同源热液流体形成了具明显负 εNd(t)值的钨和铷-钨-锡矿体[1、4-6]；其三，受构造应力驱动，以幔源组份为主的岩浆在上侵过程中遭受到古大陆岩（体）层的同化混染，进而形成具有正 εNd(t)值或负 εNd(t)值的花岗岩。同源热液流体形成的金属矿床 εNd(t)值变化范围较大[1、4-6]。尽管到目前为止，尚无确切地质证据来判定本区两类花岗岩究竟是通过哪种方式形成的，但是有两点是可以肯定的：（1）幔源组分为主导的岩浆或热液流体活动为深源型花岗岩及有关矿床的形成提供了动力和物质来源，相比之下，（2）壳源组份为主导的岩浆或热液流体活动在浅源型花岗岩及有关矿床的形成过程中发挥了重要作用。

通过前面的简要论述，得到以下几点结论：（1）与中亚造山带东段和西段花岗岩相比，本区花岗岩 εNd(t)值具有更大的变化范围和更明显的负 εNd(t)值，反映了较为复杂的成岩过程；（2）本区花岗岩及有关矿床大体可划分为两种成因类型，即具有正 εNd(t)值的深源型花岗岩以及铜、铁和钼-金矿床，具有负 εNd(t)值的浅源型花岗岩以及钨和铷-钨-锡矿床；（3）深源型花岗岩及有关矿床与幔源组份为主岩浆和热液活动有关，而浅源型花岗岩及有关矿床中则含有更多的古陆壳组份；（4）具有正 εNd(t)值的花岗岩是寻找铜、铁和钼-金矿床的良好找矿标志，而具有负 εNd(t)值的花岗岩则可成为寻找钨和铷-钨-锡矿床的重要线索。

**参考文献**


1. 洪大卫，王试光，谢锡林，等.2000. 兴蒙造山带正 ε(Nd, t)值花岗岩的成因和大陆地壳生长[J]. 地学前缘，7(2):441-456.

2. 刘雪亚,王荃.1995.中国西部北山造山带的大地构造及其演化[J]. 地学研究,(28)37－48.

3. 内蒙古自治区地质矿产局.1991.内蒙古自治区区域地质志[M].北京：地质出版社，1-725.

4. 聂凤军,江思宏,白大明, 等. 2002.北山地区金属矿床成矿规律及找矿方向[M]. 北京：地质出版社，1-499.

5. 聂凤军，江思宏，胡朋.等. 2004. 甘肃北山红尖兵山钨矿床地质特征及成矿物质来源. 矿床地质，23（1）：11-19.

6. 聂凤军，江思宏，刘妍，等. 2005. 内蒙古黑鹰山富铁矿床磷灰石钐－钕同位素年龄及其地质意义. 矿床地质，24（2）：134-140.

7. 聂凤军，屈文俊，刘妍，等.2005.内蒙古额勒根斑岩型钼（铜）矿化区辉钼矿铼-锇同位素年龄及地质意义. 矿床地质，24（4）（印刷中）.

# Spatial-Temporal Framework of the Gangdese Orogenic Belt and Its Evolution

PAN GuiTang[1], MO XuanXue[2], HOU ZengQian[3], ZHU DiCheng[1], WANG LiQuan[1], LI GuangMing[1], ZHAO ZhiDan[2], GENG QuanRu[1], LIAO ZhongLi[1]

1. Chengdu Institute of Geology and Mineral Resources, Ministry of Land and Resources, Chengdu, 610082, China
2. School of the Earth Sciences and Resources, China University of Geosciences, Beijing, 100083
3. Institute of Mineral and Resources, Chinese Academy of Geological Sciences, Beijing, 100037

The tectonic nature and subdivision of Gangdese Orogenic Belt is always one of the hottest scientific problems related to fundamental geology of Qinghai-Tibetan Plateau. The tectonic framework, subdivision and the Late Paleozoic – Mesozoic evolutional history of Gangdese Orogenic Belt have been studied based on regional geological survey (1:250, 000) and our data. Our study shows that the geological context of Gangdese can be well revealed by six major tectonic units and eighteen secondary units. Based on the analysis for spatial-temporal framework of different tectonic units and related magmatic records, we suggest that the Gangdese Orogenic Belt is not a simply block or continental segment, or terrane, but likely a complex orogenic belt experienced six arc-forming accretionary to a principal axis named Long'ge'er-Nyainqentanglha at Carboniferous-Permian, Early-Middle Triassic, Late Triassic, Early-Middle Jurassic, Late Jurassic-Early Cretaceous and Late Cretaceous-Eocene, as well as related arc-continent, continent- continent collision, and ultimately finalized its profile at the late Cenozoic. It is therefore evident that the evolutional history of Gangdese Orogenic Belt may have influenced from both the southward subduction of Bangong Co-Nujiang Tethyan Ocean crust and northward subduction of Yarlung Zangbo neo-Tethyan Ocean crust. It is emphasized that volcanic-magmatic arc formed at accretionary arc has the best potential for porphyry copper deposit in Gangdese, as revealed by Anglonggangri volcanic-magmatic arc, Dongqia Co accretionary arc and Sangri volcanic-magmatic arc, etc.

**Key words**: Evolutional history, Tectonic unit, Bi-directional subduction, arc-forming, Gangdese Orogenic Belt

# 新疆博格达地区早二叠世后碰撞期陆内裂谷和水下垮塌构造的几何学、地球化学与年代学制约

舒良树[1]　朱文斌[1]　王博[1]　Charvet J[2]　Faure M[2]

1,南京大学地球科学系，南京 210093;
2, Institut des Sciences de la Terre d'Orléans,Université d'Orléans, 45067 Orléans cedex 02, France

近年我们对博格达山南麓七角井-车轱辘泉一带和乌鲁木齐市白杨沟地区晚古生代后碰撞期陆内双峰式火山岩进行了较系统地几何学、岩石学、地球化学和定年学等研究。工作中，在乌鲁木齐东侧５０km 处的白杨沟发现一个后碰撞期水下滑塌构造。通过测制剖面、系统采样和分析测试，初步确定它和七角井-车轱辘泉一带的双峰式火山岩形成背景相似，均为早二叠世陆内裂谷环境的产物。研究表明，在博格达山南缘的七角井-车轱辘泉一带，玄武岩和流纹岩互层产出，构成厚度较大的后碰撞期双峰式火山岩系，呈近东西方向平行造山带展布，堆积在早二叠世红色磨拉石之上；在乌鲁木齐市白杨沟一带，后碰撞水下滑塌堆积岩与火山岩共存，构成一个厚 1565m 的滑塌构造剖面，由水下滑塌堆积岩夹双峰式火山岩带、枕状熔岩-气孔状玄武岩带和硅质、泥砂质岩带所组成。其底部以北东走向的拆离断层和晚石炭世灰岩、砂岩岩层接触。在岩石地球化学特征上，火山岩的 $SiO_2$ 含量在 53%-67%之间出现间断。其中，流纹岩 $SiO_2$ 平均 71.65%, CaO 2.15%, $Na_2O$ 与 $K_2O$ 含量相近(3.2-3.7%),含碱量>含钙量，ANKC 值<1.1；轻稀土富集、稀土总量高，铕亏损，具明显 Eu 负异常。与之共生的玄武岩则以富硅贫碱为特征，$SiO_2$ 平均 51.05%，$TiO_2$ 含量变化较大，轻稀土轻度富集，铕异常不明显，属拉斑系列玄武岩类。玄武岩属于不相容元素富集型，富集大离子亲石元素 Rb、Th、Ce,较贫难溶于水的高场强元素 Zr、Nb、Ta，适度亏损 Ba，配分样式呈上凸型。流纹岩普遍富集 Rb、Th、Zr、Hf,显著贫 Ti、Sr 和 P，适度亏损 Nb 和 Ba，可能是由于斜长石和磷灰石在花岗岩浆中不同程度分离结晶效应所致。其特征和东非阿法尔裂谷的双峰式火山岩相近，反映陆内裂谷环境。在 2*Nd-Zr/4-Y 和 Ti-Zr 微量元素构造背景判别图中，绝大多数样品分别落在板内拉斑玄武岩和板内玄武岩中，其成因机制可能与玄武岩浆底侵作用有关。对滑塌堆积岩带中的玄武岩和辉绿玢岩分别作锆石的 SHRIMP 和 U-Pb 法测年，获 298.7±3.6Ma（SHRIMP）和 289±5Ma（U-Pb）年龄值，相当于早二叠世。从晚二叠世开始，全区处于相对稳定的剥蚀-堆积环境中，形成了厚度较大的磨拉石，并逐渐演化为三叠纪的准平原化环境。研究提出，早二叠世陆内裂谷双峰式火山岩系和水下滑积岩、偏碱性水下玄武质熔岩喷发活动代表了该区后碰撞期的区域伸展作用，它和

区域规模的走滑韧性剪切作用、玄武岩浆底侵作用一道，共同导致了古生代天山造山带的解体。

本研究获国家973西部项目（2001CB409804）和国家自然科学基金项目（40573038）资助。

**关键词：**双峰式火山岩　水下滑积构造　后碰撞作用　二叠纪　博格达南缘

# Principal Geological Features of Nanling Tectonic Belt, South China

Shu Liangshu[1], Deng Ping[2], Zhou Xinmin[1], Sun Yan[1]

1, Department of Earth Sciences, Nanjing University, Nanjing 210093;
2, Institute of Geology, Chinese Academy of Geological Sciences, 100037 Beijing, China

The Nanling belt is distributed on a strong folded basement area and developed the largest scale Early Mesozoic granitoids and Middle Jurassic rifting basins in South China. The basement is composed of the metamorphosed and deformed Neoproterozoic-Ordovician flysch-volcanic series and the non- metamorphosed Late Devonian-Early Triassic sedimentary rocks. Five regional fault zones were recognized, which are closely related to tectonic evolution of the Nanling belt, including the Pingxiang-Guilin, the Longyan-Haifeng, the Ganjiang River, the Chaling-Guangchang and the Wuzhou-Sihui that affected the size, distribution and attitude of Meso-Cenozoic basins and granitic ranges. Both material source and geodynamical setting forming the Nanling belt were constrained by the Dabie orogenic belt to the north and the Indosinian orogenic belt to the southwest. Three sub-E-W trending granitic zones occupied this belt and were controlled by deep-seated structure and shallow-seated folding-faulting. The ages of bodies in the three granitic zones show a migrate trend from west to east and become younger toward Pacific direction. The sub-E-W trending Mesozoic granitoid zones were developed along the fault zones of paleo-Tethys tectonic regime; magmatic doming extensional tectonics and metamorphic core complex occurred generally in the intersection of two group faults. Mesozoic-Cenozoic basins were divided into three types, namely the T3-J1 para-foreland basin, the J2 rifting basin and the K1-Paleogene fault-depression basin including the K1 volcanic accumulation basin and the K2-Paleogene fault depression basin. The pre-Mesozoic basins were mainly affected by Tethys regime and Indosinian tectonic event, the basins since Cretaceous were co-constrained by both Pacific regime and intral-continental deep-seated tectonic-magmatism. Studied results suggest that the Wuyishan belt is a Late Mesozoic geographic and paleo-climate boundary, the Ganjiang River fault is a western boundary of the Late Mesozoic volcanic zone and the Western Fujian-Southern Jiangxi-East Guangdong area was a sub-E-W trending Middle Jurassic intra-continent rifting zone. The Mesozoic-Cenozoic basins and granitic ranges have an evident connection of space-time and origin, they co-built the South China basin and range tectonic system. The extensional tectonics is the most developed type coupling basin with range. Finally, pre-Mesozoic tectonism, Indosinian tectonic event and transposition of two tectonic regimes were discussed. Geological facts and studied data don't support the viewpoint that a Late Pasleozoic ocean existed in the eastern South China. The Isotopic ages of Mesozoic granitoid-volcanic rocks from 344 samples of SE-SCB show that there is a ~ 25 Ma magmatically inactive period during the Early Jurassic ($J_1$, 205Ma～180Ma). This tectonic quiescence in fact corresponds to the tectonic regime transposition from the influence of the *Indosinian* orogeny as part of the large scale Tethyan tectonics to the influence of the *Yanshanian* orogeny genetically associated with the western Pacific tectonics. The basins that were formed between $J_2$ and J3 display distinctly differences on the mechanical nature, rock assemblages and stress field, which is an important mark of tectonic regime transposition from the Paleo-Asian-Tethys regime to the Pacoific regime. This transposition was finished during J3. The eastern Nanling belt is one of the best candidates of tectonic transposition position.

The supports of the National Science Foundation of China (40572118, 40372092， 40132010) are thanked.

**Keywords:** E-W-direction tectonic regime, Basin and range system, Meso-Cenozoic, Tectonic transposition, Nanling belt

# Volcanism and Evolution of the north Luzon Arc

Sheng-Rong Song（宋聖榮）and Yu-Ming Lai（賴昱銘）

Department of Geosciences, National Taiwan University, Taiwan

The Neogene Coastal Range volcanics, more than 4000 m in thickness, are an igneous complex dominated by andesitic rocks and situated within the arc-continent collision zone of eastern Taiwan. They constitute the northern segment of the Luzon Arc and might have formed during the subduction of the South China Sea plate into the Philippine Sea plate, and finally adhered to the continental margin through arc-continent collision. Meanwhile, offshore islands, the Lutao, Lanhsu and Hsiaolanhsu of the east Taiwan are also a part of north Luzon Arc (Fig. 1).

The volcanics and their related rocks in the north Luzon arc mainly accumulated in the oceanic environment under the influence of a subducted tectonic region. They are composed of basaltic to andesitic pyroclastics, lava flows, shallow intrusives and volcaniclastics with limestones, which were regarded as reef deposits around the volcanic islands. Volcanic stratigraphies and features have been destroyed and became ambiguous due to the late arc-continent collision. Based on the field occurrences, volcanic lithofacies and geochemistry, the volcanic rocks in the Coastal Range can be distinguished into four volcanic bodies. They are the Yumei, Chimei, Chengkuanou and Tuluanshan volcanoes. The volcanic eruptions might commence on a deep ocean floor in early Miocene, pour out in a shallowing environment in middle to late Miocene and, finally, take place in a subaerial condition at the end of Miocene (Fig. 1). The subaqueous eruptions produced voluminous pillow lavas and breccias, hyaloclastites, massive lavas and thick volcaniclastic deposits. But, the subaerial eruptions only yielded limited amount of ignimbrites and basaltic lavas. After the cessation of volcanism due to the arc-continent collision, the volcanoes rapidly subsided and later overlaid with thick continent-derived sediments.

Geochemically, the north Luzon arc shows the LREE-enrichment increasing and $\varepsilon$Nd value decreasing from the north to the south and from the older to the younger volcanics (Fig. 2). Meanwhile, the end of volcanism in the northern Coastal Range was around 6.1 Ma, and then southwardly propagated to the south (3.0 Ma), Lutao (0.54 Ma) and Lanshu (0.02 Ma) due to the oblique arc-continent collision. It is characterized that the variations of geochemistry may be resulted from the subducted sediments involved into the genesis of magma during the north Luzon arc approaching to the Asian continent.

## References

Chen, C.H., Lee T., Shieh Y. N., Chen C. H. and Mertzman A., (1990) Nd-Sr-O isotopic evidence for source contamination and unusual mantle component under Luzon arc. Geochim. Cosmochim. Acta, 54, 2473-2483.

Song, S.R., and Lo, H.J. (1987) Volcanic rocks of the Coastal Range of Taiwan as the products of submarine eruption –the evidences from Loho area. Acta Geologica Taiwanica 25, 97-110.

Song, S.R. and Lo, H.J. (1988) Volcanic geology of Fengpin-Takankou area, Coastal Range of Taiwan. Acta Geologica Taiwanica 26, 223-235.

Song, S.R. and Lo, H.J. (2002) Lithofacies of volcanic rocks in the Coastal Range, eastern Taiwan: implications for island arc evolution. J. Asian Earth Sci. 21, 23-38.

Yang, T.F., Tien, J.L., Chen, C-H., Lee, T., Punongbayan, R.S., 1995. Fission-track dating of volcanics in the northern part of the Taiwan–Luzon Arc: eruption ages and evidence for crustal contamination. J. SE Asian Earth Sci. 11, 81–93.

Yang, T.F., Lee, T., Chen, C-H., Cheng, S.N., Knittel, U., Punongbayan, R.S., Rasdas, A.R., 1996. A double island arc between Taiwan and Luzon: consequence of ridge subduction. Tectonophysics 258, 85–101.

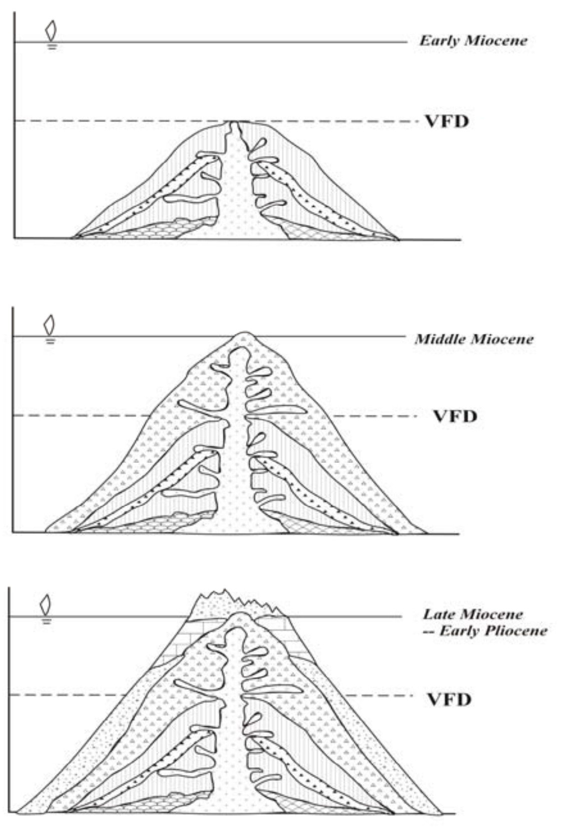


**Figure 1**: Model for the evolution of volcanism of the central Coastal Range, eastern Taiwan. Abbreviation of VFD means volatile fragmentation depth, which is generally shallower than 500 meters. The volcano commenced eruption in deep water wnvironment in early Miocene, then evolved to shallow marine in middle Miocene, finally erupted in subaerial condition in late Miocene to early Pliocene.

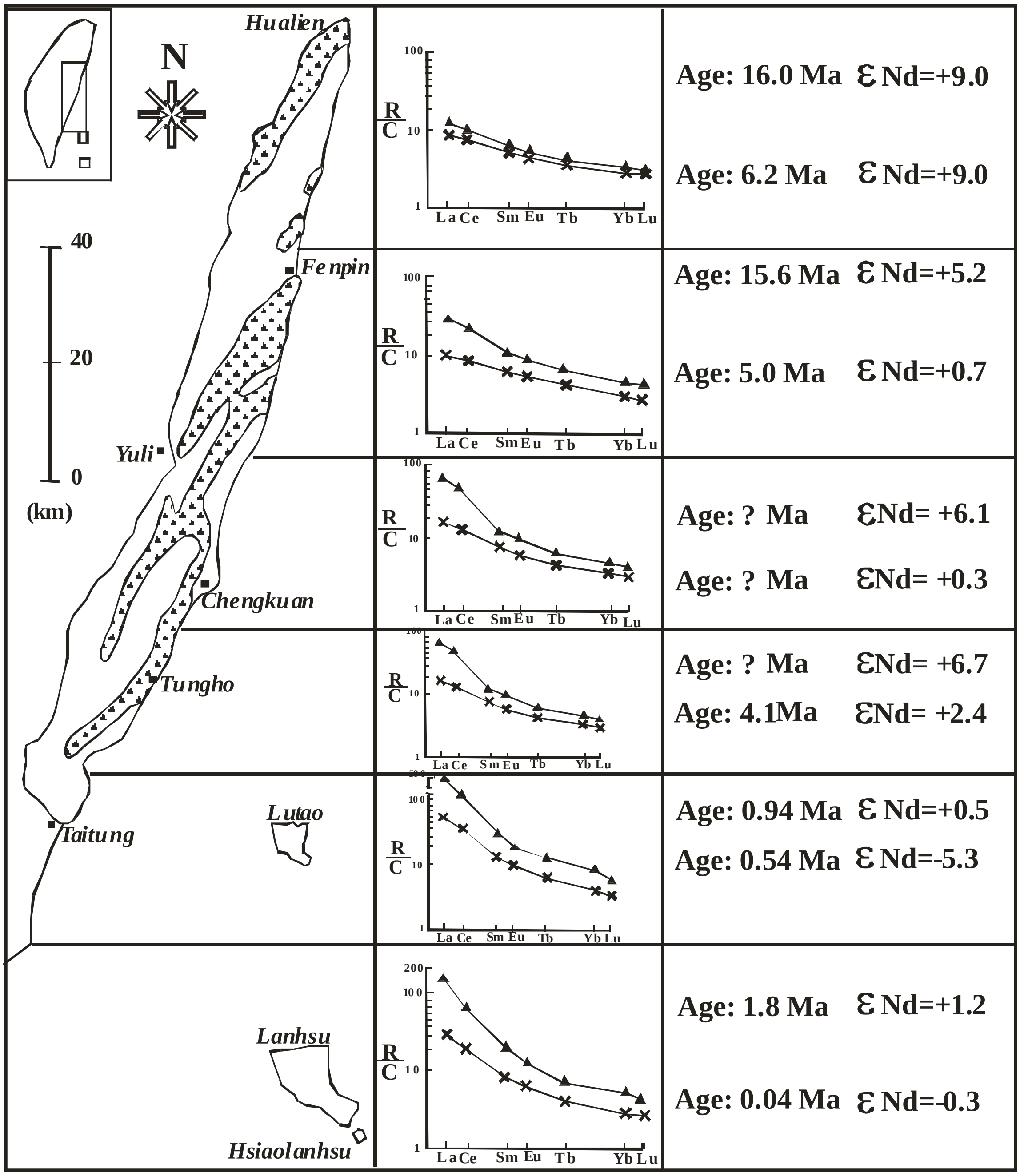


**Figure 2**: Spatial and temporal variations of geochemical characteristics along the north Luzon arc from the north to the south. (Data from Chen et al., 1990; Yang et al., 1995, 1996, Song, 1990).

# Zircon U-Pb ages of granitic gneisses and intrusions in the Central Terrane of the Chinese Altai Orogen and tectonic implications

Min Sun[1], Chao Yuan[2], Wenjiao Xiao[3], Xiaoping Long[2], Xiaoping Xia[1], Chunming Han[3], Shoufa Lin[4]

[1]Department of Earth Sciences, The University of Hong Kong, Hong Kong; [2]Guangzhou Institute of Geochemistry, Chinese Academy of Sciences, Guangzhou, China; [3]Institute of Geology and Geophysics, Chinese Academy of Sciences, Beijing, China; [4]Department of Earth Sciences, University of Waterloo, Waterloo, Ontario, N2L 3G1, Canada

The Central Terrane is the largest terrane in the Chinese Altai Orogen. It mainly consists of high-grade metamorphic rocks and granitic plutons (e.g. Windley et al., 2002). A Proterozoic basement is inferred based on zircon xenocrysts (Windley et al., 2002), Nd model ages (Hu et al., 2000; Chen and Jahn, 2002), and finding of Sinian fossils (He et al., 1990). Therefore this terrane may represent a micro-continent and play an important role in the tectonic evolution of the Altai collage of Central Asia.

Gneissic rocks were collected from the western part of the Central Terrane, north of Qiongkuer, and LA-ICP-MS was employed for this study. These rocks were mapped as Ordovician or Sinian-Cambrian strata, but our geochemical data show that they have granitic compositions. Zircons separated from five gneissic samples, from different locations, all yield ~500 Ma U-Pb zircon ages. Similar zircon evaporation ages (505 Ma) have been reported for the felsic metavolcanic rocks of this terrane, and the data were used to propose the existence of a continental magmatic arc along the western margin of the Central Terrane during the Ordovician time (Windley et al., 2002). Our data indicate that the Ordovician magmatic activity was much more extensive than previously considered, both volcanic and intrusive rocks were produced. The granitic gneisses occupy large areas in the Central Terrane and its tectonic significance was probably under-estimated in previous tectonic configurations. Zircon xenocrysts are present in these gneisses and mostly give 700 to 1040 Ma ages. One zircon xenocryst has 2550 Ma age, which is the oldest age dated so far for the region.

The gneisses were intruded by plutonic intrusions. We obtained ~ 410 Ma U-Pb ages for three samples from such intrusions. Similar ages were also obtained using zircon evaporation technology (Windley et al., 2002) and clearly record another important granitic activity in the region. Zircon xenocrysts are also present in these intrusions, but are mostly younger than the gneisses (440-500), excepting one giving Proterozoic age (1300 Ma).

The Central Terrane is bounded by a shear zone in the west with the Qiongkuer-Abagong Terrane that is made of low-grade rocks of island arc origin. Little deformed pegmatitic rocks intruding the shear zone give ~280 Ma U-Pb ages, which may imply that the Devonian island arc collided with the Central Terrane prior to the Permian.

**References**

Chen B and Jahn B-M, Geochemical and isotopic studies of the sedimentary and granitic rocks of the Altai orogen of NW China and their tectonic implications. Geol. Mag., 139: 1-13.

He G, Han B, Yue Y and Wang J, 1990. Tectonic division and crustal evolution of Altay orogenic belt in China. Geosci. Xinjiang 2:9-20.

Hu A, Jahn B-M, Zhang G, Chen Y and Zhang Q, 2000. Crustal evolution and Phanerozoic crustal growth in northern Xinjiang: Nd isotope evidence. 1. Isotopic characterization of basement rocks. Tectonophysics, 328, 15-51.

Windley B, Kroner A, Guo J, Qu G, Li Y and Zhang C, 2002. Neoproterozoic to Paleozoic geology of the Altai Orogen, NW China: new zircon age data and tectonic evolution. Journal of Geology, 110, 719-737.

This study is supported by Hong Kong RGC (HKU7040/04P).

# Late Cenozoic Orogeny of Taiwan

Louis S. Teng
Institute of Geosciences, National Taiwan University

As one of the youngest and most dynamic mountain belts in modern world, the Taiwan orogen formed by the collision between the Luzon Arc and the China continent in late Cenozoic time. Though small in size and short in lifetime, the Taiwan mountain belt provides an actualistic model that demonstrates how a collisional orogen can build up and collapse. The processes involved not only can be deciphered from the geologic records of Taiwan but are presently observable in the areas around.

The Taiwan orogen comprises two geologic provinces separated by the Longitudinal Valley Fault of eastern Taiwan. The Coastal Range to the east comprises volcanic and siliciclastic sequences of the accreted Luzon Arc system. The Central Range and the Western Foothills to the west consist of metamorphic and sedimentary rocks of the deformed China continental margin. The pre-Tertiary metamorphic complex of the Central Range represents the unroofed continental basement, and the Tertiary sequences of the slate terrain and the Western Foothills were the sedimentary cover. The coastal plain and the Taiwan Strait west of the mountain belt are the remnant China continental margin that has not been involved in the collision.

Before the collision started in Late Miocene time, the Taiwan area was part of the rifting China continental margin that had been subsiding and accumulating sediment since the Late Cretaceous. The Luzon Arc was situated more than 500 km to the southeast and was moving north-northwest with the underlying Philippine Sea plate. The northern tip of the Luzon Arc hit the outer continental margin in southern Ryukyu at around 10 Ma and began to shovel the continental strata into the accretionary wedge. At around 5 Ma, the accretionary wedge was pushed onto the outer continental shelf and emerged as a small island, which signaled the onset of the collision orogeny. Then the Luzon arc shifted its direction of motion to west-northwest and quickly overrode the continent. At about 3 Ma, drastic collision commenced and raised the accretionary wedge into high mountain ranges. As the oblique collision propagated from northeast to southwest, the mountain belt was incrementally pushed to the west and elongated to the south until it has finally accrued to its present form.

Following the southwest-propagating collision, the north-dipping Philippine Sea plate beneath the Ryukyu Arc also extended westward and caused flipping of subduction polarity in the northern part of the collisional orogen. The orogenic pile above the newly flipped subduction zone, thus, lost the compressive support by the colliding plates and became subjected to lithospheric stretching induced by trench suction. In consequence the defunct orogen collapsed and foundered, and its central part was torn apart by a widening rift basin. The process of flipping of subduction and ensuing orogenic collapse first commenced in southern Ryukyu at around 5 Ma and has since been propagating westward into northeastern Taiwan.

Currently the process of orogenic buildup and collapse is still going on in the contemporary Taiwan area. The Philippine Sea plate is actively moving northwestward, subducting beneath the Eurasian plate north of Taiwan while overriding the Eurasian plate to the south. The Luzon Arc is progressively overriding the outer continental margin south of Taiwan, where the submarine accretioanry wedge is fast growing. In central and southern Taiwan, the Luzon Arc is pressing the collisional orogen and raising the mountain ranges to their climax. In northeastern Taiwan, however, the subduction polarity has flipped and the collision ceased. The mountain ranges have been lowering under the influence of crustal extension, and two rift basins, Taipei and Ilan, developed atop the orogenic basement. Further northeast in the offshore area, the foundered orogen has been buried by Quaternary sediment, and its central rift basin opened as the Okinawa Trough.

**References**

Ho, C. S., 1986, A synthesis of the geologic evolution of Taiwan: Tectonophysics, v. 125, p. 1-16.

Teng, L. S., 1990, Geotectonic evolution of late Cenozoic arc-continent collision in Taiwan: Tectonophysics, v. 183, p. 57-76.

Teng, L. S., 1996, Extensional collapse of the northern Taiwan mountain belt: Geology, v. 24, p. 949-952.

Teng, L. S., Lee, C. T., Tsai, Y. B., and Hsiao, L. Y., 2000, Slab breakoff as a mechanism for flipping of subduction polarity in Taiwan: Geology, v. 28, p. 155-158.

# Two contrast geochemical and geochronological characters of adakitic rocks from the Laohushan area, North Qilian orogen, NW China

Chien-Yuan Tseng[1,*], Houng-Yi Yang[1], Huai-Jen Yang[1], Fancong Meng[2], Yusheng Wan[3], Dunyi Liu[3], Chiu-Kuang Cheng [4], Da-Jen Wen[4]

[1]Department of Earth Sciences, National Cheng Kung University, Tainan 701;
[2]Institute of Geology, Chinese Academy of Geological Sciences, Beijing 100037;
[3]Beijing SHRIMP Centre, Institute of Geology, Chinese Academy of Geological Sciences, Beijing
[4]Department of Geosciences, National Taiwan University, Taipei 106

The diorite- tonalite- quartz monzonite- granodiorite- granite stocks occur along the Leigonshan- Maomaoshan- Laohushan Mountain in the North Qilian orogen, NW China. Among them, the Leigonshan tonalitic and Shenmutou quartz monzonitic intrusions show adakitic geochemical signatures, such as low concentrations of HREE (4.43-8.48 ppm), Y (6.2-11.3 ppm), and Sc (7.3-8.5 ppm), with high Sr (613-766 ppm) and Ba (687-974 ppm) abundances, resulting in high Sr/Y (>70) and $(La/Yb)_N$ (>14) ratios (Figure 1). However, these two intrusions are geochronologically distinct. The $^{206}Pb/^{238}U$ ages for igneous zircon calculated from SHRIMP data are 453.4 ± 5.6 Ma for Leigonshan tonalitic intrusion and 429.9 ± 6.1Ma for Shenmutou quartz monzonitic intrusion. Four inherited zircons form the Shenmutou quartz monzonitic intrusion reveal scattered inheritance ages of Palaeoproterozoic to Archaean ($^{207}Pb/^{206}Pb$ age: 1528~3350 Ma), implying association with North China craton rather than South China craton. No inherited zircons were found from the Leigonshan tonalitic intrusion. The Leigonshan tonalitic and Shenmutou quartz monzonitic intrusions are also compositionally distinct. The former is lower in MgO (Mg#: ~40), Cr (9-20 ppm), and Ni (3-15 ppm) contents, implying limited interaction with mantle peridotite. It is inferred to derive from partial melting of the thickened lower continental crust, which might be compositionally similar to the Saraycık granodiorite. In contrast, the Shenmutou quartz monzonitic intrusion is more abundant in MgO (Mg#: ~58), Cr (58-99 ppm), and Ni (38~58 ppm). Higher MgO, Ni and Cr contents have been interpreted as results of interacting with mantle peridotite. These geochemical signatures together with the Palaeoproterozoic to Archaean ages of inherited zircons can be explained by derivation from the delaminated lower continental crust that was incorporated into the mantle regime. Melts generated from such source can interact with mantle materials during ascent to surface. The tectonic implications of two episodic adakitic plutons with different compositional characters intruded in early Paleozoic continental arc stratum of the North Qilian orogen remain uncertain and will be the focus of our future work.

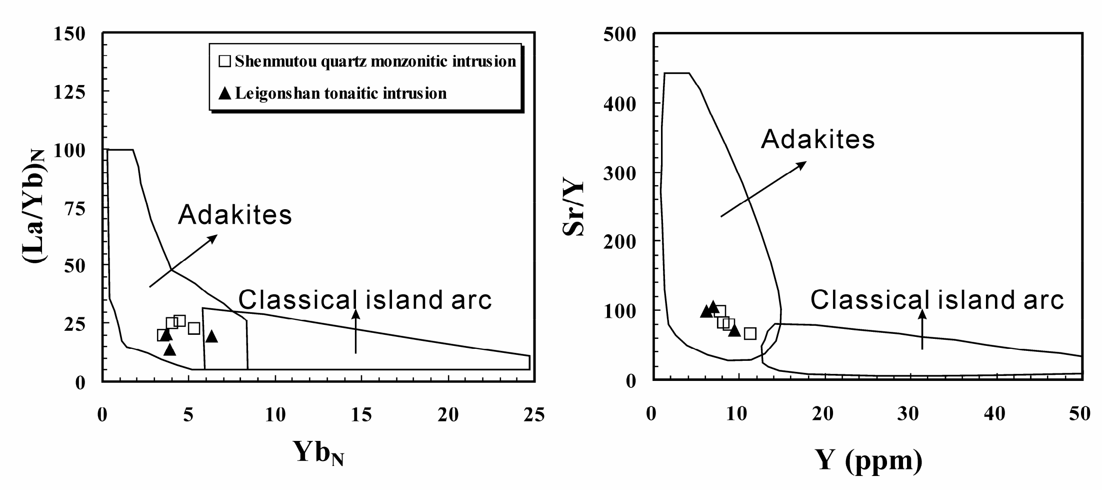


Figure 1: Chondrite-normalized $(La/Yb)_N$ vs. chondrite-normalized $Yb_N$ abundances and (Sr/Y) vs. Y in rocks from the Leigonshan tonalitic and Shenmutou quartz monzonitic intrusions.

# Small 660-km Seismic Discontinuity beneath Tibet Implies Resting Ground for Detached Lithosphere

Tai-Lin Tseng and Wang-Ping Chen

Department of Geology, University of Illinois at Urbana-Champaign, Urbana, IL 61801 USA

Using seismic profiles comprising high-resolution, triplicate waveforms across apertures of over 1,000 km, we show that due to high *P*-wave speed ($V_P$) near the bottom of the mantle transition zone, the contrast in $V_P$ across the 660-km discontinuity beneath central Tibet is small: only about three-fourth of that beneath the northern Indian shield and western China. This aseismic, sub-horizontal anomaly of high $V_P$ is most likely a remnant of detached mantle lithosphere that recently sank to depth, thus providing key evidence for a direct connection between spectacular deformation near the surface and deep-seated processes in the mantle during continental collision.

**Acknowledgements.** This work is supported by the US National Science Foundation under Grant No. EAR9909362 (Project Hi-CLIMB: An Integrated Study of the Himalayan-Tibetan Continental Lithosphere during Mountain Building). Any opinions, findings and conclusions or recommendations expressed in this material are those of the authors and do not necessarily reflect those of the National Science Foundation.

**References:**

Chen, W.-P., and S. Özalaybey, Correlation between seismic anisotropy and Bouguer gravity anomalies in Tibet and its implications for lithospheric structures, *Geophys. J. Int.*, *135*, 93–*101*, 1998.

Jin, Y., M. K. McNutt, and Y.-S. Zhu, Mapping the descent of Indian and Eurasian plates beneath the Tibetan Plateau from gravity anomalies, *J. Geophys. Res.*, *101*, 11275–11290, 1996.

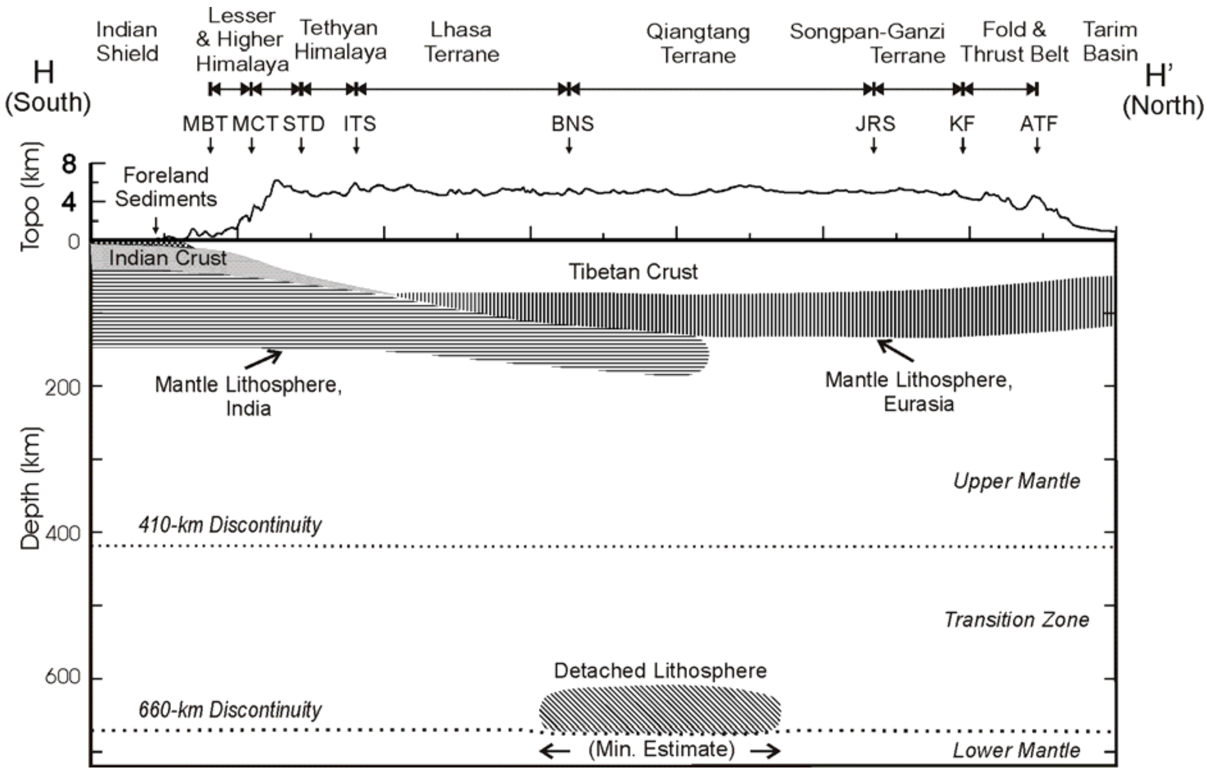


**Figure 1.** A schematic cross-section showing configuration of lithosphere beneath the Himalayan-Tibetan collision zone. For depths above 200 km, the configuration of lithosphere is from a joint interpretation of shear-wave birefringence and gravity data [*Chen and Ozalaybey*, 1998; *Jin et al*, 1996], while the detached piece of mantle lithosphere resting above the 660-km discontinuity is based on results of this study.

# Sr-Nd isotopic mapping for intrusions from the Altai orogen, NW China: Implications for magma origin, accretionary orogeny and continental growth

Tao Wang[1,2], V. P. Kovach[3], Ying Tong[1], Bor-Ming Jahn[4], Da-Wei Hong[1], Bao-Fu Han[5]

1. Institute of Geology, Chinese Academy of Geological Science, Beijing 100037
2. Beijing SHRIMP center, Chinese Academy of Geological Science, Beijing 100037, China
3 Institute of Precambrian Geology and Geochronology, Russian Academy of Sciences, Makarova emb., St-Petersburg 199034, Russian Federation
4. Institute of Earth Sciences, Academia Sinica, Taiwan;
5. Key Laboratory of Orogenic Belt and Crustal Evolution, Peking University, Beijing, 100871, China

Nd isotopic mapping has been successfully applied to tectonic analyses. However, there have been few examples of isotopic mapping for young accretionary orogens to describe their terrane compositions and to evaluate the amount of crustal growth. The Altaid Collage (Sengor et al. 1993) or Central Asian Orogenic Belt (CAOB; e.g., Jahn et al., 2000a) is the world's largest Phanerozoic accretionary orogenic belt and the most important site of crustal growth in the Phanerozoic (e.g., Sengor et al., 1993; Kovalenko et al., 1996; 2004; Wickham et al., 1996; Jahn et al., 2000a, b, c). Identifying the proportion of the old and juvenile crust and quantitatively evaluating the role of both have become an important new issue. The Altai orogen is compose of many terranes, and is a typical locality of the Altaid Collage. It is an ideal place for isotopic mapping, and the mapping of which will be very helpful in dealing with this issue.

Based on establishment of four Paleozoic plutonic events at ca.460 Ma, 410-400 Ma, 375 Ma and 270-290 by our new zircon age data, along with the available age information, we use 65 Sr-Nd data to make Nd isotopic maps of intrusions from various terranes in the Chinese Altai Mountains, a typical locality of the Altaid Collage which is the world's largest Phanerozoic accretionary orogen and the most important site of Phanerozoic crustal growth. The maps indicate that the εNd (T) values increase from -4 – +2 in the central Altai (Terranes 2 and 3) to +1.4 - + 6 in the southern Altai (Terranes 4 and 5), and the $T_{DM}$ values decrease from 1.6 – 1.1 Ga to 1.0 – 0.5 Ga, except for a continental fragments in Terrane 4. These results demonstrate that the central Altai contains widespread old continental basement, whereas the southern Altai predominately consists of juvenile compositions, confirming that the crust grew southward. In addition, our new data suggest that Terranes 2 and 3 belong to a single unit. In contrast, the southern Altai (Terrane 4), which was regarded as a young island arc system, should be subdivided into two parts: a younger arc system and an older continental fragment. This suggests that continental fragments were involved in the early accretion. We further estimated the amount of the juvenile materials added to the crust, and the crustal growth rates, respectively. These illustrate quantitatively synorogenic, horizontal and postorogenic, vertical continental growth in the Altai, although they are minimum estimation and much lower than average growth rate of Earth.

This paper presents a detailed case study on the mechanism and the amount of crustal growth of the Altaid Collage, and provides an example demonstrating that isotopic mapping is an effective approach to elucidate terrane compositions of accretionary orogens and continental growth. Supported by Major State Basic Research Program of China No. 2001CB409800, International cooperation project of NSFC (40211120647, 40472101), the China Geological Survey No.20011390001), and NSF-Taiwan No. 93-2116-M-001-025.

# 准噶尔初生陆壳省及其成矿作用

王京彬　王玉往　王丽娟

北京矿产地质研究院，北京：100012

新疆准噶尔地区由准噶尔盆地和周边造山带组成。其范围北以额尔齐斯断裂为界与西伯利亚板块（阿尔泰地体）相接，南与塔里木板块以艾比湖－康古尔断裂为分界，东、西至国境。

准噶尔周边造山带主要有以下特点：缺乏前寒武纪变质岩系。有化石依据的最老地层是奥陶－志留系，以含碳细碎屑岩为主，夹少量碳酸盐岩，在造山带中呈断块出露。至今无可靠的年龄数据表明该区发育一定规模的前寒武纪变质岩系；盆地周边造山带中蛇绿岩带发育。时代以晚前寒武纪－早古生代（626－447Ma）为主，为准噶尔地区时代老、分布较广的地质体，是该区存在洋壳基底的直接证据；早古生代花岗岩类不发育，广泛分布的晚古生代花岗岩类以正 εNd(t)值和年轻的 Nd 模式年龄、较低的 $^{87}Sr/^{86}Sr$ 初始比值为特征，反映了准噶尔基底的不成熟陆壳性质；盆地周边造山带总体上变形弱、变质程度低（以低绿片岩相为主），造山带中常见的区域混合岩化和大规模推覆构造不发育。

上述特点结合已有的地球物理资料推测，准噶尔地区总体上具有早古生代形成的年青（Immature）陆壳基底，即经加里东期弱造山作用拼贴在一起的、由洋壳－岛弧－盖层沉积岩±前寒武纪陆壳碎块组成的复合体。准噶尔早古生代年青陆壳省的形成，可能是中亚造山带面积性侧向增生造山的重要事件。

准噶尔地区早古生代形成的年青陆壳基底是该区晚古生代构造－岩浆－成矿作用发育的基础，并由此形成了独特的年青陆壳成矿省。其成矿特点是：（1）早古生代除与蛇绿岩有关的豆夹状铬铁矿外，其它矿床不发育，大规模成矿主要发生在晚古生代；（2）选择性富集了铬、铜、镍、金等亲铁亲硫元素的矿床，目前该区发现的大中型矿床均是此类矿床，而与成熟陆壳有关的铅锌矿床、铌钽铍钨等稀有金属矿床不发育。目前在东准噶尔发现的萨热什克等锡矿床也只有小型规模，且与 A－型花岗岩有关，其成矿特点明显不同于华南与 S－型花岗岩有关的大型－超大型锡矿床；（3）与成矿有关的岩体具有正 εNd（t）值、低的 $^{87}Sr/^{86}Sr$ 初始比值，矿床硫化物的 $\delta^{34}S$ 多在 0 值附近，呈塔式分布，铅同位素显示正常铅，放射性成因铅不发育，其成矿物质来源具有明显的幔源特征。从成矿的角度印证了准噶尔基底的初生陆壳特性。

邻近的阿尔泰成矿省的成矿特点与准噶尔成矿省明显不同。阿尔泰成矿省广泛发育

了中下元古代结晶基底，陆壳成熟度高，在阿巴宫－库尔提断裂以北地区，发育了大量的后碰撞 S－型花岗岩类，多具负的 εNd（t）值，与稀有金属成矿有关，是我国重要的 Li-Be-Nb-Ta 矿带，产有世界著名的可可托海超大型稀有金属矿床；在阿尔泰山南缘泥盆纪海相火山－沉积盆地中产有可可塔勒等大型铅锌矿床、蒙库大型铁矿床。总体上，阿尔泰成矿省是以锂铍铌钽等稀有金属和铅锌（铁）为优势矿种的富集区。

由此可见，新疆北部可分出两类不同的成矿省，一是以准噶尔成矿省为代表的、由洋壳－岛弧－盖层沉积岩±前寒武纪陆壳碎块复合体为基底的年青陆壳成矿省（Immature Crust－Related Metallogenic Province），是铬、铜、镍、金等的成矿集中区；另一是以阿尔泰为代表的具有前寒武纪结晶基底的成熟陆壳成矿省（Mature Crust－Related Metallogenic Province），以铅锌（铁）、稀有金属成矿为主。两类成矿省的确定，对深入理解中亚型成矿作用，明确找矿主攻方向具有重要的意义。

# Kyanite- and andalusite-type metamorphic zones from the Altai orogen, Xinjiang, China

CHUNJING WEI, WEI TIAN AND LIN QIU

School of Earth and Space Sciences, Peking University, Beijing 100871, China, cjwei@pku.edu.cn

The progressive metamorphic zones in the Chinese Altai orogen have long been grouped as the kyanite– and andalusite–types. The kyanite type involves a zonal sequence of biotite, garnet, staurolite, kyanite, sillimanite and, locally, garnet–cordierite zones. The zonal sequence in the andalusite type is the same as the kyanite type at the lower–*T* condition with the biotite, garnet and staurolite zones and at the higher–*T* condition with the sillimanite and garnet–cordierite zones. These two types are distinguished with the kyanite–type involving kyanite zone, and the andalusite–type having staurolite–andalusite and andalusite–sillimanite zones in the intermediate–*T* condition. Spatially, the andalusite–type metamorphic zones are more extensive than the kyanite–type, and kyanite–bearing assemblages often show relic character in the staurolite–andalusite, andalusite–sillimanite and sillimanite zones. Using pseudosection approach in the KMnFMASH and KFMASH systems and in a combination with the field distribution of the metamorphic zones and textural relations in metapelites, phase relations and *P–T* paths are delineated on the *P–T* pseudosections for each metamorphic zone. It is concluded that the metamorphic zones from the Chinese Altai orogen do not represent progrades along unique *P–T* arrays as simply divided into the kyanite and andalusite types, but represent *P–T* and mineral assemblage changes along different *P–T* arrays. It seems that all these metamorphic zones were originated from an earlier prograde zonal sequence of kyanite type. In the lower temperature sequence such as the (biotite), garnet, staurolite zones, are mostly preserved their peak mineral assemblages of the typical kyanite type which bear only trivial changes during decompression. In the higher temperature sequence including the sillimanite and garnet–cordierite zones, is also predominated by one stage of mineral assemblage but a transitional sillimanite type, which may be formed in the uplifting processes of earlier higher pressure rocks. The clear low–pressure metamorphism characteristic of andalusite overprinting on the existing kyanite– and sillimanite–types took place only in the intermediate–temperature condition, which could not result in the mineral assemblages reaching an equilibrium state at the andalusite–stable field.

It has been studied that the Altai orogen was developed from an arc-continent collision in Late Devonian, and the kyanite-type metamorphic zones were formed due to the collision. Related to the magmatic intrusions in late-post collision stage, the earlier kyanite-type rocks were uplifted and differently overprinted by andalusite-type metamorphism. Consequently, the metamorphism is mostly synchronous with emplacement of the granitic plutons which, according to some advanced age dating with zircon ($^{207}Pb/^{206}Pb$ age and SHRIMP), has been dated as 360–390 Ma.

# The Gangdese batholith, southern Tibet:
# Ages, geochemical characteristics and petrogenesis

Da-Jen Wen[1], Sun-Lin Chung[1], Jianqing Ji[2], Qing Qian[3],
Biao Song[4], Dunyi Liu[4], Ching-Hua Lo[1]

[1] Department of Geosciences, National Taiwan University, Taipei
[2] School of Earth and Space Sciences, Peking University, Beijing
[3] Institute of Geology and Geophysics, Chinese Academy of Sciences, Beijing
[4] Institute of Geology, Chinese Academy of Geological Sciences, Beijing

The Gangdese batholith is conventionally recognized as an Andean-type arc resulted from northward subduction of the Neo-Tethyan slab under Asia. However, the more detailed and comprehensive knowledge of the continental arc itself is previously lacking. Here we present the results of the systematic geochronologic, as well as elemental and isotopic studies on the eastern Gangdese batholith, within the narrow belt between 88˚E and 94˚E in southern Tibet. In compilation with the available age data in the literature, our new SHRIMP U-Pb zircon dates reveal that the Gangdese plutonism took place from 120 to 45 Ma, yet with a probable magmatic gap right after 80 Ma. According to the spatial distribution and the geochemical characteristics, the Gangdese plutonism can be grouped into at least four episodes: 103 to 85 Ma, ca. 80 Ma, 65 to 53 Ma and 51 to 45 Ma. Though the predominant ca. 100-85 Ma and the ca. 50-45 Ma episodes of magmas spread all over the eastern Gangdese belt, the former stage of plutons only distribute strictly along the trench-side edge of the batholith. With the new age data we confirm the 65-60 Ma plutons which emplaced near Zedong area.

In particular, the first recognized ca. 80 Ma peraluminous plutons in the eastern belt (between Langxian and Lilong), are distinct with adakitic geochemical features relative to the other calc-alkaline arc magmas originated in the mantle wedge. Marked by apparently higher Sr/Y and La/Yb, coupled with lower Y and HREE, these deep-seated (0.6 to 1.1 GPa) epidote-bearing granodiorites exhibit lower crust melting features in Late Cretaceous. Supported by the Sr, Nd isotopic data and the inherited zircon ages, the granodiorites are interpreted to have been the juvenile crust derived from the mid-Cretaceous basaltic underplating above the mantle wedge and, later thickened by tectonic contraction due to flattening of the Neo-Tethyan subduction.

Except the ca. 80 Ma lower crustal melts, the geochemical characteristics of different stages of Gangdese plutonism are generally similar. They are overall medium to high potassium calc-alkaline series arc magmas, showing widely ranged silica contents, metaluminous to weakly peraluminous characteristics (A/CNK = 0.75-1.15), altogether with significant large ion lithophile element (LILE) enrichment, high field strength element (HFSE) depletion, with or without Eu anomaly, as are the typical characteristics of common arc magmas. Although the derivation may have been through fractional crystallization or partial melting of basaltic parent magmas, the main mechanism of the arc formation is magma mixing involving variable degree of assimilation-fractional crystallization (AFC) processes. Most importantly, the juvenile mantle signatures are all observed within each episode of the arc magmatism. The earliest 103 to 85 Ma magmas exhibit most primitive compositions [$SiO_2$ mostly less than 60%; εNd = +3 to +5; (La/Yb)n = 2 to 10] than others. In contrast, the most pervasive episode of 51 to 45 Ma plutons display the most heterogeneous nature with $SiO_2$ contents ranging from 50 to 76%, and εNd from –1.2 to +5.2. These variations may reflect the tectonomagmatic evolution from initial slab subduction (103 to 85 Ma), shallowing (ca. 80 Ma), rollback to breakoff (51 to 45 Ma), respectively.

# Geochronological Framework of the Immense Granites in Northeastern China

Fu-Yuan Wu[1], De-You Sun[2], Wen-Chun Ge[2], Yan-Bin Zhang[1], Simon A. Wilde[3], Bor-Ming Jahn[4]

1: Institute of Geology and Geophysics, Chinese Academy of Sciences, P. O. Box 9825, Beijing 100029
2: College of Earth Sciences, Jilin University, Changchun 130061
2: Department of Geology, National Taiwan University, P.O. Box 13-318, Taipei, 10699
3: Department of Applied Geology, Curtin University of Technology, Perth, Western Australia, 6845
4: Institute of Earth Sciences, Academia Sinica, P. O. Box 1-55, Nankang, Taipei 115

Northeastern (NE) China is located within the eastern part of the Central Asian Orogenic Belt, and is called the Xingmeng (Xing'an-Mongolian) orogenic belt in the Chinese literature. This area is characterized by widespread Phanerozoic granitic rocks. According to the regional geological survey, the granites occupy at least 50% of the area in the mountainous regions, such as the Zhangguangcai Range in the east and Great Xing'an Range in the west and Lessor Xing'an Range in the north. Furthermore, underneath the flat-lying Songliao Basin, much of the basement is composed of granites.

Although it was traditionally thought that these granites were emplaced in several periods from the early Paleozoic to Mesozoic with majority in the late Paleozoic (Hercynian), few reliable geochronological data are provided. During last decade, about 300 zircon U-Pb ages have been obtained for these granites. It is shown that the Paleozoic granites are scarcely distributed in the area, the 100,000 $km^2$ granites in the Zhangguangcai Range were mostly emplaced in the Early-Middle Jurassic. Although the granites in the Great Xing'an Ranges show larger age variation from 495 to 120 Ma than other areas, most of them emplaced during the Late Jurassic-Early Cretaceous. Therefore, the available data suggest that most of these granites were not emplaced in the Paleozoic as previously thought, but in the Mesozoic with a younging trend westward.

The above spatial and temporal distribution of the granites indicates that the formation of the huge amount of Mesozoic granites in NE China was mainly controlled by subduction of the Paleo-Pacific plate, not by the Paleozoic tectonic processes during the evolution of the Paleo-Asian Ocean between the Siberia and the North China Craton.

# Is Himalaya Unique Among the Collision Mountain Ranges? Results of HIMNT experiment

Wu[1], F. T., Huang[1], G. C., Sheehan[2], A. F., Roecker[3], S., Liu[4], H. B., Gao[5], R.

[1]SUNY Binghamton, NY, USA, [2]U of Colorado, [3]RPI, [4]Chinese Acad of Sci., [5]Chinese Geol. Survey

Correspond to the giant superstructures of many mountains created by plate collisions are the mountain roots. Thus the roots under South Island, New Zealand, Tianshan in western China, Taiwan, are well-imaged. Himalaya is the grandest among the mountains where the collision is known to be strong and where the idea of mountain root originated (Pratt 1855; Airy 1855). But recent gravitational interpretation (Cattin and others, 2001) show that Himalaya overlies a transition from a relatively thin crust under the foothills to the 75 km or so thick crust under Tibet. A significant isostatic anomaly exists there. Although the gravity interpretation is known to be highly non-unique, this conclusion is bolstered by the receiver function analysis of Schulte-Pelkum et al. (2005).

The HIMNT broadband seismic deployment in 2001-2002, source of Schulte-Pelkum et al.'s data, was one of the first attempts to record both local earthquakes and teleseisms on both sides of the high Himalaya. While the receiver functions may image the zone of seismic wave conversion (mainly from P to S) it lacks velocity resolution. Using the arrival times of both local and teleseismic seismic waves recorded at the stations we can tomographically image the structures from the Himalaya foothills to the Tibetan plateau in the north. The arrival times of P and S waves from these earthquakes can be used jointly to image the crustal and upper mantle velocities directly. Instead of tracing crust/mantle transition along one profile in the receiver function analysis, with the HIMNT network covering an area of about 300 x 400 $km^2$, a three-dimensional view of the Central Himalaya crustal and upper mantle can be obtained. Another interesting seismological measure in the mountain ranges is the S-splitting. Judging by the time delays between and fast and slow S waves the source of the splitting is placed in the upper mantle. It is notable that for stations in many mountains show trend-parallel fast directions and relatively large delay times (> 1second) between the slow and fast S waves, leading to conclusions involving vertical coherent deformation of mountain range (Molnar et al., 1999). Fast directions in Himalaya and the delays in the

Central Himalaya are found to be quite different from those in the other mountains. Is Himalaya unique and why?

During 2001–02, we operated 29 broadband seismic stations in Tibet and Nepal (HIMNT experiment) for 14 months (Fig. 1). Harsh physical environment did impact on the instruments and the data retrieval is not ideal. Data from previous deployments with more limited spatial coverage are added to extend the area of coverage and improve the resolution of especially the upper mantle images. From the combined data sets we identified a total of 551 earthquakes at teleseismic distances in the PDE (USGS) list that produced adequate signals for inclusion. Events with at least two arrivals were used and a total of 7154 teleseismic P-phase were used. At the same time, local earthquakes recorded by HIMNT were first automatically picked and located. There readings were reviewed and arrival times redetermined when necessary. A total of 1003 local events, 8957 P and 7869 S wave readings were available. A minimum of 3 arrival times at the stations for each adopted event is required. The sampling rate of the broadband stations was 40 sps and thus the precision of the reading is less than 0.025 s.

Most of the local events are located to be in the upper crust or lower crust; only a few were in the lower crust and even fewer in the upper mantle, mainly below the higher ranges. Rays from these event sample the upper and lower crust well. To constrain the velocities at the bottom of the crust and in the mantle teleseismic rays are needed. It is logical to combine data from both sets of events to constrain the structures of the whole crust and upper mantle. The relatively new algorithm (Roecker et al., 2004) efficaciously performed the task.

Checkboard tests show that the available station-event geometry should allow us to resolve well structures down to 100 km and although resolution worsens at greater depth velocity anomalies should nevertheless be revealed. The main results indicate a transition from the relatively thin crust under the plains of southern Nepal to a 75 km thick crust under the Tethys Himalaya. No “root” is seen under the high Himalaya. An anomalously low velocity zone was found in mid-crust between the high peaks area and the Yalung Zangbo suture. A weak high velocity anomaly appears to dip northward under the Himalayas, suggesting the possible existence of a fossil subduction zone.

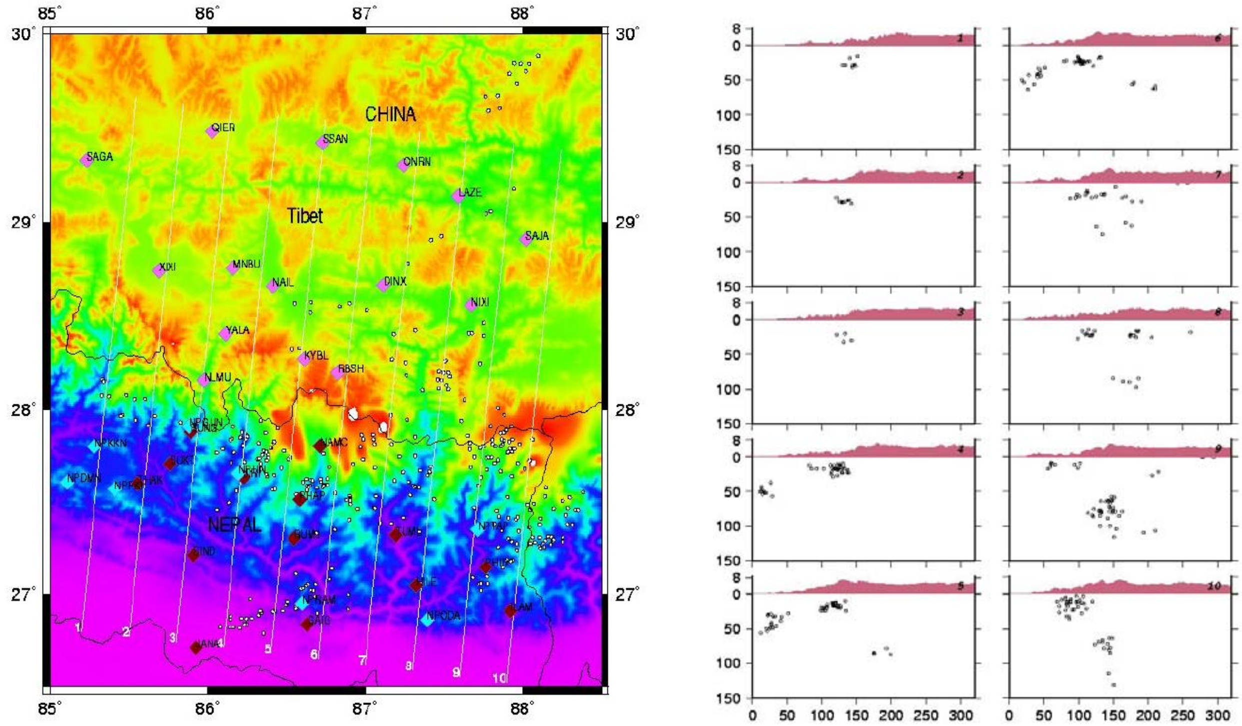


The HIMNT stations (pink diamonds in Tibet and red diamonds in Nepal) and the relocated hypocenters of events in map view on the left and in cross-sections on the right. The locations of the profiles are shown on the right. In addition to shallow seismicity there are events below the crust under the high Himalyas. These events, together with teleseismic arrivals recorded on the HIMNT as well as INDEPTH II stations, are used to image the crust and upper mantle across the Himalaya.

# The Tianshan Carboniferous-Permian rift-related volcanism and mantle plume

Lin-Qi Xia† Zu-Chun Xia Xue-Yi Xu Xiang-Min Li Zhong-Pin Ma Li-She Wang

Xi'an Institute of Geology and Mineral Resources, Ministry of Land and Resources,
Xi'an, Shaanxi 710054, China

## INTRODUCTION

The Tianshan Carboniferous-Permian rift-related volcanim in northwestern China (Xia et al., 2003,2004) represents an important recently discovered large igneous province (LIP). This study focuses on the basalts, which dominate (>80 vol.%). We use the isotopic data as well as a detailed suite of major and trace element analyses (Xia et al., 2003,2004) to evaluate the role of asthenospheric and continental lithospheric sources in the generation of the Tianshan Carboniferous-Permian LIP basalts.

## REGIONAL GEOLOGICAL EVOLUTION

The Tianshan orogenic belt is part of a large-scale, composite orogenic belt located in northwestern China (central Asia). It was the product of accretion, subduction, and collision of various continental blocks during the formation, evolution, and disappearance of the Paleo-Asian ocean between the northern Siberia plate and the southern Tarim and North China plates (Fig. 1). By the Early Mississippian (i.e. early part of the early Carboniferous), the Paleozoic ocean basin had already closed. The consequent suture zone became an area of thickened crust characterized by complex tectonic and magmatic activity and uplift. A major regional upwelling and partial melting event led to the development of the Tianshan Carboniferous-Permian rift system and its associated large igneous province (Xia et al., 2002, 2004). The rift system comprises five parts: the Keping rift situated in the northwestern margin of the Tarim plate; and the western Tianshan Yili rift; the Central Tianshan rift; the eastern Tianshan Bogda rift; and the eastern Tianshan Jueluotage rift (Fig. 1).

A typical cross section is as follows: In the Luotuogou area north of Baluntay, the Mississippian Maanqiao Formation volcanic-sedimentary formation consists of (from bottom to top) thick-bedded boulderstone, conglomerate (of which the gravels consist of basement rocks), gritstone, sandstone, sandstone and siltstone interbedded with shale and intercalated with limestone, basalts, and a few rhyolites. It has an angular unconformity or faulted contact with the Proterozoic granite-gneiss in the Baluntay micro-continental block of the central Tianshan. The aforementioned Mississippian volcanic-sedimentary formation (in the central Tianshan) is characterized by a progradational sequence of transition from continental to marine facies and reflects a progressive rift extension.

† E-mail: geologyx@pub.xaonline.com

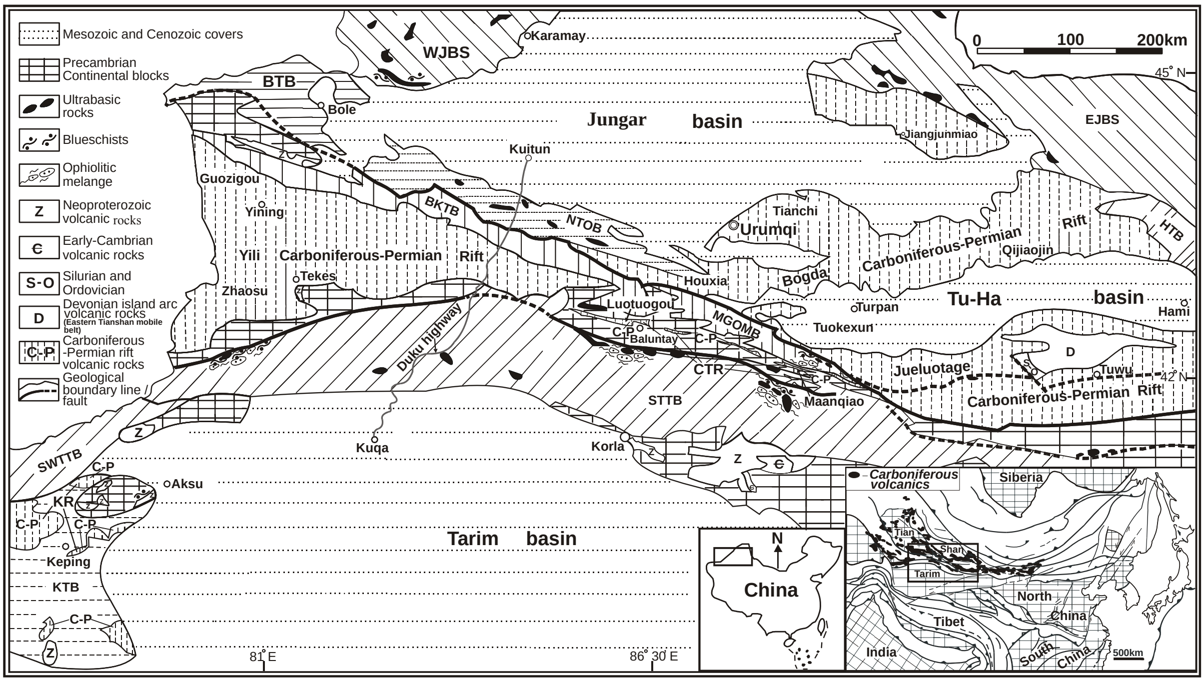

Figure 1. Sketch map of geologic tectonic units of the Tianshan orogenic belt showing the distribution of Carboniferous volcanic rocks (modified after Xia et al., 2004). WJBS—West Jungar trench-arc-basin system (Paleozoic); EJBS—East Jungar arc-basin system (Paleozoic); BTB—Bole tectonomagmatic belt (late Paleozoic); NTOB—North Tianshan ophiolite belt (late Paleozoic); HTB—Harlike tectonomagmatic belt (late Paleozoic); BKTB—Boluokenu tectonomagmatic belt (early Paleozoic); MGOMB—Mishigou-Gangou ophiolitic mélange belt (early Paleozoic); SWTB—Southwestern Tianshan tectonomagmatic belt (late Paleozoic); STTB—South Tianshan tectonomagmatic belt (Silurian-late Paleozoic); KTB—Keping tectonomagmatic belt (Neoproterozoic-Paleozoic); CTR—Central Tianshan Carboniferous-Permian rift situated in the Baluntay micro-continental block; KR—Keping Carboniferous-Permian rift.

The entire region of Carboniferous-Permian rift-related volcanic rocks are mainly exposed in a dumbbell-shaped province of ~210,000 km$^2$ within the Tianshan orogenic belt (Fig. 1). This area represents a minimum estimate because the volcanic rocks extend west and east from China and also have a widespread distribution in Kazakstan, Kirgizstan and Mongolia, respectively. They cover approximately 343,000 km$^2$ (Fig. 1). The thickness of the entire volcanic sequence varies from over 13,000 m in the eastern Tianshan, to several hundred meters in the central Tianshan, to over 7000 m in the western Tianshan. The magmatic province consists mainly of basaltic lavas and subordinate amounts of intermediate and silicic lavas, and pyroclastic rocks. The average lava thickness of the Tianshan LIP is estimated to be about 2000 m, thus the entire volume of the Tianshan basalts is ~ $0.7 \times 10^6$ km$^3$. The earliest eruptions began some time after the late Tournaisian (350–345 Ma) (calibration of stage boundaries after Gradstein et al. 2004). After the Carboniferous peak of activity, subsequent Permian volcanism was sporadic.

## GEOCHEMISTRY OF TIANSHAN BASALTS

Based on petrogeochemical data, the Tianshan basalts can be classified into two major magma types: high-Ti/Y (HT, Ti/Y > 500, Nb/Zr < 0.12, in the western Tianshan) and low-Ti/Y (LT, Ti/Y < 500) basalts (Fig. 2A). The LT lavas can be further divided into two subtypes. LT1 lavas in the central and eastern Tianshan exhibit lower Nb/Zr (< 0.12); the LT2 lavas in the northwestern Tarim have higher Nb/Zr (> 0.16) (Fig. 2A). Most of HT lavas belong to the alkaline series; the LT2 lavas also belong to alkaline series; most of the LT1 lavas belong to tholeiitic series (Xia et al., 2004). Most of the Tianshan basalts plot in the Within-Plate Basalts (WPB) field (Fig. 2B). This is consistent with the geological evidence for an intracontinental rift setting. In the primordial-mantle-normalized spider diagrams, the central Tianshan basalts display noticeable negative Th anomalies that are associated with slightly positive Nb anomalies. A conspicuous negative Sr anomaly is also noted in samples of this area (Fig. 3B). The western and eastern Tianshan basalts are characterized by significant depletion of Nb and Ta relative to Th and by marked negative P and Y anomalies (Fig. 3F). The basalts of the Keping area (in the northwestern Tarim) and a sample (Bb-263-4) of Luotuogou area (in the central Tianshan) are characterized by slight depletion of Nb and Ta relative to Th and by prominent negative Sr and Zr anomalies (Fig. 3D).

Nd and Sr isotopic data are illustrated in Fig. 4A. The samples from the eastern Tianshan have a relatively limited range of compositions: $\varepsilon_{Nd(t)}$=+5.4 to +9.6; $^{87}Sr/^{86}Sr_{(t)}$=0.703354–0.704411. Samples from the central Tianshan are displaced to higher $^{87}Sr/^{86}Sr_{(t)}$ (0.703645–0.706726) and lower $\varepsilon_{Nd(t)}$ (+3.1 to +6.2). One sample from the western Tianshan (Zhaosu area) has lower $\varepsilon_{Nd(t)}$ (–1.1) , that distinguishes it from all other samples from the Tianshan LIP, but its $^{87}Sr/^{86}Sr_{(t)}$ ratio (0.704399) is similar. Samples from the northwestern Tarim (Keping area) have highest $^{87}Sr/^{86}Sr_{(t)}$ (0.706821–0.708080) and lowest $\varepsilon_{Nd(t)}$ (–0.98 to –2.91).

Lead isotopic compositions vary more widely (Fig. 4B). The eastern Tianshan basalts have relatively low $^{206}Pb/^{204}Pb_{(t)}$ ratios, from 17.593 to 17.966, and low $^{207}Pb/^{204}Pb_{(t)}$ (15.384–15.473). The central Tianshan basalts have relatively high $^{206}Pb/^{204}Pb_{(t)}$, from 17.773 to 18.142, and, with the exception of one sample (BT-4, 17.590), high $^{207}Pb/^{204}Pb_{(t)}$ (15.478–15.619). The basalt from the western Tianshan has intermediate $^{207}Pb/^{204}Pb_{(t)}$ (15.490) ratio and still higher $^{206}Pb/^{204}Pb_{(t)}$ (18.134).

Each region or volcanic sequence in the Tianshan LIP has, therefore, a distinct trace element and Pb-Sr-Nd isotopic composition.

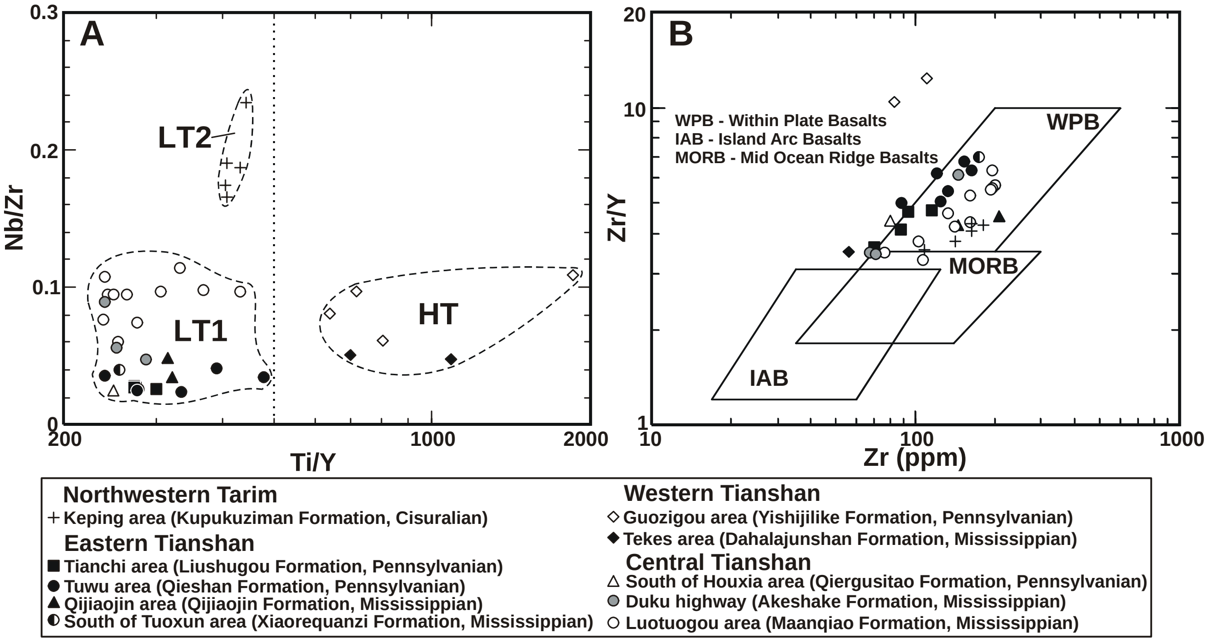


Figure 2. Diagrams showing variation of (A) Nb/Zr vs. Ti/Y and (B) Zr/Y vs. Zr (after Pearce, 1982) for the Carboniferous and Permian basalts from the Tianshan orogenic belt. Data source: Xia et al. (2004).

## DISCUSSION

### Evidence for plume involvement

Saunders et al. (1992) suggested that plume or asthenospheric components are characterized by low $^{87}Sr/^{86}Sr$ ratios, high εNd values and oceanic Pb isotopes such as those that have been reported in the Ambenali Formation of the Deccan (Fig. 4B and C), tholeiites from the East Coast of Madagascar, and the youngest parts of the Lower Lavas and the successions along the Blosseville Coast in eastern Greenland. These same units also have Th/Nb ratios of less than one (Saunders et al., 1992; Fig. 3A). In mantle-normalized plots (Fig. 3B), the majority of central (Luotuogou, Duku highway) Tianshan basalts have patterns that are broadly similar to CFBs with plume affinity (Fig. 3A). These samples from central Tianshan exhibit trace element ratios that overlap with the field of oceanic island basalts (OIB) (Fig. 4D). They are characterized by mantle-normalized Th/Nb ratios of less than one (Saunders et al., 1992; Fig. 3A and B). The pronounced negative Sr anomaly in these lavas suggests that they have been affected by extensive fractionation of plagioclase. One sample (BT-4, Duku Highway) with low trace element abundance also shows high $\varepsilon_{Nd(t)}$ (3.1) and low $^{87}Sr/^{86}Sr_{(t)}$ (0.703719) and $^{206}Pb/^{204}Pb_{(t)}$ (17.59) values, thus likely reflecting the isotopic signature of the least-contaminated Tianshan plume head component. The enrichment of Rb and Ba relative to Th observed in several samples may be due to alteration. The samples from Luotuogou area are pillow tholeiites (Xia et al., 2004) that show a trend of increasing $^{87}Sr/^{86}Sr_{(t)}$ ratios with relatively constant $\varepsilon_{Nd(t)}$ values (Fig. 4A). This may suggest interaction with seawater or contamination with carbonate crust during subaqueous eruption (Yogodzinski et al., 1996).

We conclude that a plume or asthenospheric component was involved in the generation of the Tianshan lavas.

**Evidence for lithosphere involvement**

Many Tianshan lavas show negative Nb and Ta anomalies suggesting that components other than a plume must have been involved in the generation and evolution of the Tianshan basalts. The most likely components are from lithosphere.

It is concluded that Tianshan basalts also recorded significant lithospheric input from crustal and subcrustal sources. Thus, in addition to the plume component discussed above, two other important components can be identified. The first component, CLM, is seen in basalts of the Kupukuziman Formation of the Keping area from the northwestern Tarim, and in one sample (Bb-263-4) of the Maanqiao Formation of the Luotuogou area from the central Tianshan. In terms of trace elements, these basalts have a mantle-normalized Th/Nb ratio slightly greater than 1, which distinguishes them from the plume-related group, but this value is much lower than the Th/Nb ratio in crustally-contaminated basalts (Saunders et al., 1992; Fig. 3). These patterns are rather similar to those of CFBs with lithosphere affinity of the Mahabaleshwar Formation of the Deccan, the Urubici (high titanium) basalts from the Paraná Province, and a suite of low $^{206}Pb/^{204}Pb$-ratio basalts from Madagascar (Fig. 3C). Isotopically, these Tianshan basalts are highly variable, but are characterized by low to intermediate $\varepsilon_{Nd(t)}$ (-2.91 to + 4.38), moderate to high $^{87}Sr/^{86}Sr_{(t)}$ (0.705793 to 0.708743), and intermediate $^{206}Pb/^{204}Pb_{(t)}$ (17.92). These patterns suggest an interaction between the plume- or asthenosphere-derived magmas and the lithosphere mantle.

The second component, a crustal component, shown by the high La/Nb, high Th/Nb, and highly variable isotopic compositions is seen in basalts of the Tekes and Gouzigou areas from the western Tianshan Yili rift, and the South of Tuokexun (Jueluotage rift) and Tianchi (Bogda rift) basalts from the eastern Tianshan (Figs 3 and 4). Note in particular, the distinctive trace element patterns of these basalts that are characterized by very high mantle-normalized Th/Nb ratios much greater than 1 or a pronounced negative Nb-Ta anomaly. These patterns are analogous to those of the crustally contaminated basalts of the Bushe Formation from the Deccan, a group of low-Ti basalts from the East Coast of Madagascar, and the Gramado (low-Ti) basalts from the Paraná province (Saunders et al., 1992; Fig. 3E and F). Although a high La/Nb ratio is a reliable trace element index of crustal contamination, Keppler (1996) and You et al. (1996) suggested that subduction-related fluids carry La in preference to Nb. Thus, arc rocks tend to have higher La/Nb than OIB. In Figure 5D, the majority of eastern Tianshan (Bogda rift and Jueluotage rift) basalts have higher

La/Nb ratios indicative of the influence of a subduction component. This may be related to the contamination of upper crust containing Devonian island-arc volcanic rocks and/or to a pre-Carboniferous subduction enrichment of the lithospheric mantle source region.

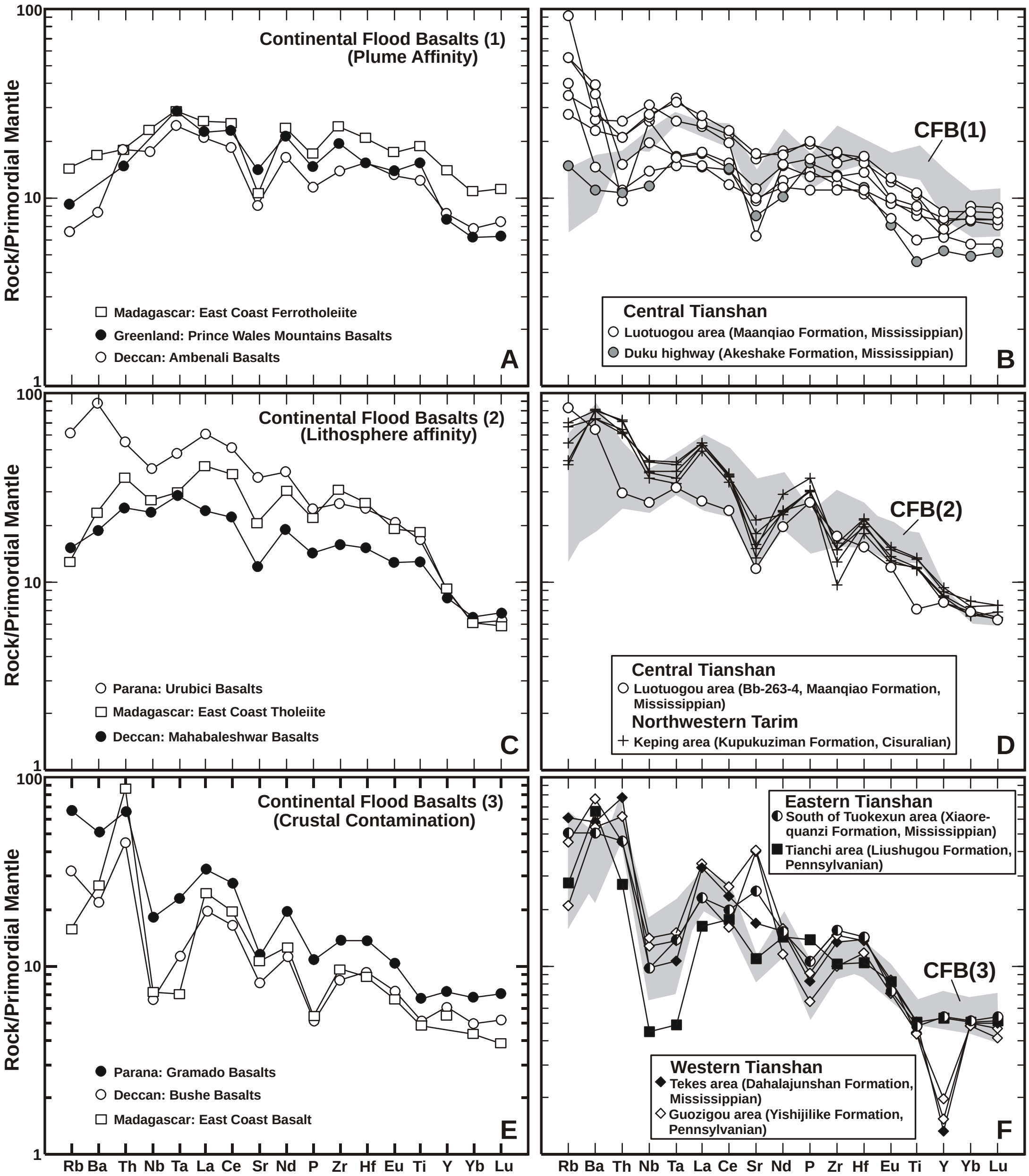


Figure 3. Primordial-mantle-normalized multi-element plots for basalts from various continental flood basalts (continental Large Igneous Provinces, LIPs) shown for reference (A, C, and E) and the Tianshan LIP (B, D, and F). Normalizing values from Sun and McDonough (1989). Note the variation of Th/Ta, Rb/Ta and Ba/Ta ratios (the enrichment of Rb and Ba relative to Th in the Tianshan basalts may be due to secondary alteration). Data sources: Tianshan basalts: Xia et al. (2004); Deccan (averages values for Ambenali, Madabaleshwar and Bushe): Lightfoot and Hawkesworth (1988); Greenland (Prince of Wales Mountains): Hogg et al. (1989); Madagascar: East Coast samples MAN 90-43 (plume-related), MAN 90-8 (mantle lithosphere affinity) and MAN 90-35 (crustally contaminated) from Saunders et al. (1992); Paraná Urubici ('high-Ti') and Gramado ('low-Ti') basalts are averages from Peate (1989).

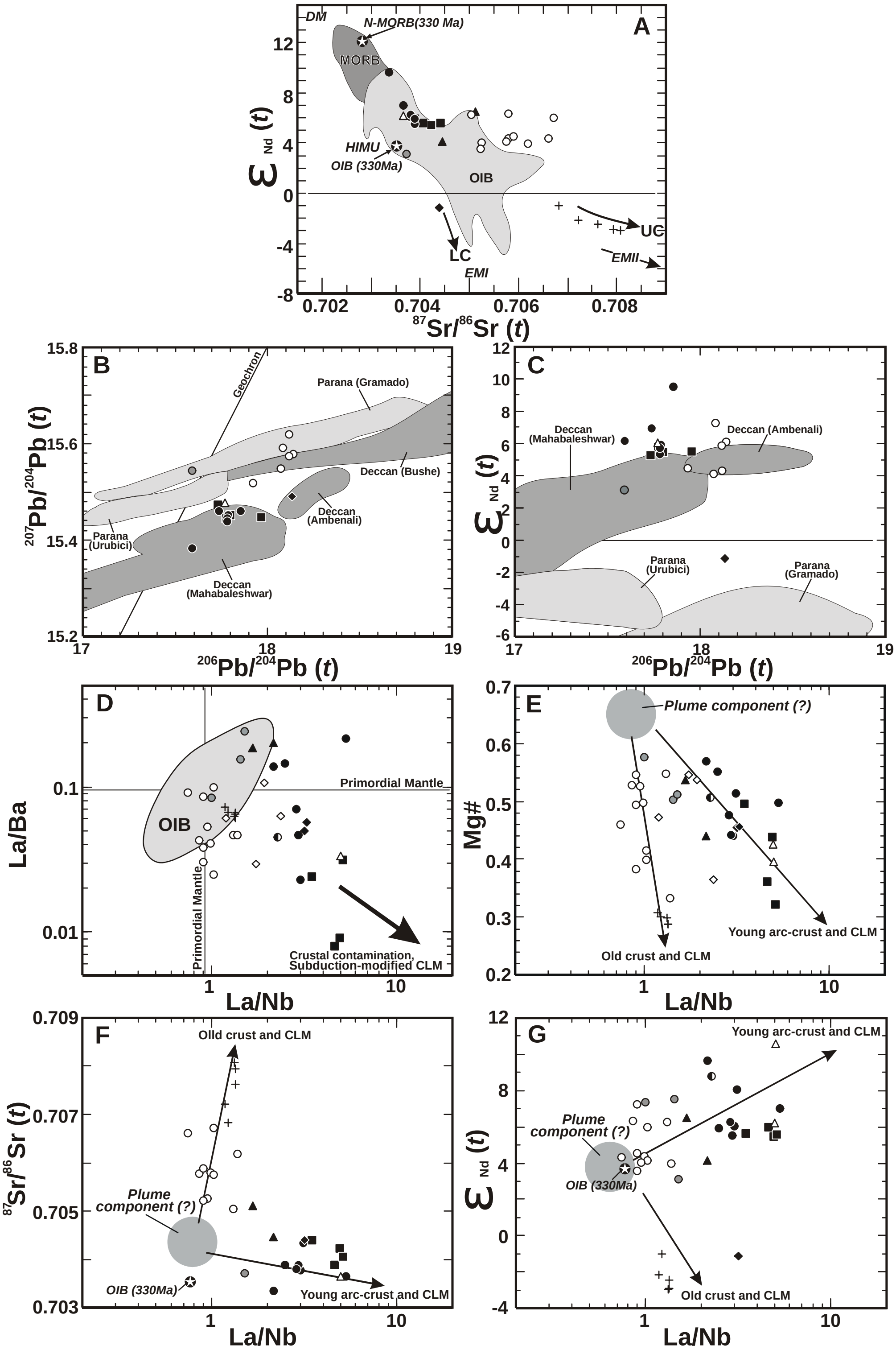


Figure 4. Plots of (A) $\varepsilon_{Nd\,(t)}$ vs. $^{87}Sr/^{86}Sr_{(t)}$ (after DePaolo, 1979; Zindler and Hart, 1986), (B) $^{207}Pb/^{204}Pb$ vs. $^{206}Pb/^{204}Pb_{\ (t)}$, (C) $\varepsilon_{Nd\,(t)}$ vs. $^{206}Pb/^{204}Pb_{\ (t)}$ (corrected to $t$ = 345 Ma and 325 Ma for Mississippian lavas, to 320 Ma for Pennsylvanian lavas and to 280 Ma for Permian (Cisuralian) lavas), (D) La/Ba vs. La/Nb, (E) Mg# vs. La/Nb, (F) $^{87}Sr/^{86}Sr_{(t)}$ vs. La/Nb and $\varepsilon_{Nd\,(t)}$ vs. La/Nb for the Carboniferous and Permian basalts of the Tianshan. A: UC–upper crust; LC–lower crust; EMI and EMII–enriched mantle I and II sources; HIMU–high-μ mantle source; DM–depleted mantle source. Comparative mean MORB and OIB (Sun and McDonough, 1989) compositions (corrected to 330 Ma) are shown. B and C: data sources as for Figure 4. D: Field for ocean island basalts (OIB) is from Fitton et al. (1991). F and G: Comparative mean OIB composition (Sun and McDonough, 1989) corrected to 330 Ma is shown. All other symbols and data sources as for Figs. 2 and 3.

In summary, the geochemical variation of the Tianshan Carboniferous (—Permian) Basalts can be accounted for by interaction between the plume-derived magmas and the continental lithosphere. We suggested that a large mantle melting anomaly or a plume existed beneath the Tianshan (central Asia) LIP during Carboniferous (–Permian) period (Xia et al., 2004).

**Composition of plume component**

Negative correlation between Mg# and La/Nb for Tianshan basalts indicates that the magmas forming the lavas with lower Mg# have undergone stronger contamination of continental lithosphere (Fig. 4E). Figure 4E also shows that the Tianshan basalts form two different trend lines: one is for the basalts from the central–western Tianshan and the northwestern Tarim that have Precambrian basement, and the other is for the samples from the eastern Tianshan mobile belt with younger (Devonian) arc-crust basement. Similarly, in $^{87}Sr/^{86}Sr_{(t)}$ versus La/Nb (Fig. 4F) and $\varepsilon_{Nd(t)}$ versus La/Nb (Fig. 4G) diagrams the plots of basalts from a relatively stable micro-continental block (or microcraton) and those from a mobile belt also distribute along two different trend lines. The place at which the trend lines intersect might locate the plume head component ($^{87}Sr/^{86}Sr_{(t)} \approx 0.7045$, $\varepsilon_{Nd(t)} \approx +4$) for the Tianshan Carboniferous (–Permian) LIP.

**CONCLUSION**

The Tianshan Carboniferous (—Permian) rift-related volcanic rocks comprise a newly-recognized large igneous province. The isotopic and principal chemical variations within the Tianshan basalts can be accounted for by contamination of a plume component (87Sr/86Sr(t) ≈ 0.7045, εNd(t) ≈ + 4) by upper crust or CLM (continental lithospheric mantle).

# 新疆北部古生代复式增生造山作用与中亚大陆侧向生长*

肖文交[1)]，韩春明[1)]，秦克章[1)]，袁超[2)]，孙敏[3)]，陈汉林[4)]，李继亮[1)]，孙枢[1)]

1) 中国科学院地质与地球物理研究所岩石圈演化国家重点实验室，北京, 100029
2) 中国科学院广州地球化学研究所，广州，510640
3) 香港大学地球科学系
4) 浙江大学理学院，杭州，310027

新疆北部地区位于古亚洲洋构造域南部，其大地构造演化历史研究涉及大陆造山作用类型以及大陆生长等基础理论前沿，但关于其大地构造演化历史的认识仍存在重大分歧。本文解剖该地区不同大地构造单元及其配置，讨论其时空演化历史。本研究表明自早古生代以来发育阿尔泰－东准-东天山、西准与伊犁－西天山等俯冲增生体系。泥盆纪时期，这些俯冲增生体系进一步发展，其中阿尔泰－东准俯冲增生体系发生近走向堆叠作用，西准与天山俯冲增生体系分别演化成类似现今西南太平洋的多岛海格局。早中石炭世各俯冲增生体系逐渐接近并发生增生－拼贴作用，主体呈现一幅复杂的安加拉地块南缘增生图式。早二叠世发生大规模走滑。相对位于南面（现今体系）的塔里木陆块在二叠纪晚期拼贴到该增生体系上，最终结束了古亚洲洋的演化历史，形成了宽阔的中亚复式增生造山带。这种复式造山作用是中亚大陆侧向增生主要机制之一，在演化过程中动态地发育弧前增生、弧后扩张与增生弧－增生楔等复杂造山作用，洋盆消减具有多重构造极性。这对研究增生型造山带复杂的构造演化过程与探索其成矿作用规律均具有重要意义。

**关键词**　新疆北部　古生代　中亚复式造山　大陆侧向生长

---

* 国家重点基础研究发展规划项目(2001CB409801)、国家重点攻关项目(96-915-07)、国家自然科学基金项目(40172080)与香港研究基金项目(HKU7040/04P)联合资助

第一作者简介：　肖文交，男，1967年生，研究员，博士生导师，从事造山带构造地质学与大地构造学研究，E-mail：wj-xiao@mail.igcas.ac.cn

# 青藏高原新生代下地壳岩浆活动及其成因：年代学和地球化学证据

许继峰，王强，董彦辉，陈建林，王宝弟

中国科学院广州地球化学研究所，同位素年代学和地球化学重点实验室,五山，广州，510640，中国

在青藏高原的拉萨、羌塘和松潘—甘孜三个地块上，广泛分布有新生代岩浆活动(Turner et al., 1996; Miller et al., 1999; Chung et al., 2005)，所产生的火山岩和侵入岩通常可以划分成超钾质、钾质和钙碱性（埃达克质）三类火成岩（Miller et al., 1999; Chung et al., 2005）。前人曾认为在青藏高原上的新生代超钾质、钾质火山岩甚至钙碱性岩石都来自一个富集的岩石圈地幔源区，或者是一个幔源玄武质（或钾玄武质）岩浆的演化产物(Turner et al., 1996; Miller et al., 1999)。然而，近年来一些研究已经识别出一些钾质火山岩和钙碱性火成岩等可以来自一个下地壳源区（Chung et al., 2003; Hou et al., 2004; Lai, 2004；Wang et al., 2005；等等）。我们新的研究结果显示下地壳岩浆活动的产物广泛出现在拉萨、羌塘和松潘—甘孜三个地块上，它们包括曾被认为来自地幔源区的钾质火山岩和钙碱性埃达克质火成岩。本研究拟依据这些火山岩的年代学和地球化学新数据，试图了解下地壳产生这些火成岩的过程，示踪触发下地壳熔融的构造事件，探询火山岩的形成与高原隆升之间的可能联系。

在藏北松潘—甘孜地块上的可可西里地区，下地壳来源的火山岩主要形成在 15—18 百万年之间（Wang et al., 2005），主要为一套高钾钙碱性和钾玄质的粗面岩和粗安岩等，它们具有典型的埃达克质成分特征，也就是高的 Sr/Y 比值和低的 Y、Yb 但高 Sr 含量，其锶和钕同位素组成明显不同于前人报道的新生代钾玄武质中基性火山岩（Turner et al., 1996），而与青藏高原发现的一些基性麻粒岩下地壳包体的同位素组成相似。值得注意的是在可可西里地区还未发现与下地壳来源的火山岩时代相同或相近的玄武质岩浆活动，暗示前者可能不是一个玄武质母岩浆的演化产物。

羌塘地块上的下地壳来源的火山岩明显形成要早，尽管前人报道该地块上的这些火山岩形成在 9—15 百万年(Turner et al., 1996)，但我们新的同位素年代学研究表明它们更可能喷发在 35—40 百万年之间。羌塘地区的这些火山岩主要为一套高钾钙碱性的安山岩、英安岩和粗面岩，它们都具有典型的埃达克质岩石的地球化学组成，根据富镁的程度可进一步将它们分成高镁的和正常的火山岩两组。羌塘地区的高镁火山岩组与中国东部下地壳拆沉成因的埃达克质岩石（Xu et al., 2002）组成相似，而羌塘正常的埃达克质火山岩与下地壳直接部分熔融形成的岩石的成分相当。

在拉萨地块上，新生代下地壳岩浆作用也相当广泛且更为复杂，其产物火山岩和侵入岩明显可以分为两类，一类是近年已被前人广泛研究、并且与成矿密切相关的钙碱性埃达克质斑岩，其主要形成在 13－26 百万年期间，被认为是该时期区域伸展事件导致的下地壳直接部分熔融的产物（Chung et al., 2003; Hou et al., 2004），；第二类为分布在拉萨地块西部的钾质（或称为钾玄质）的中酸性火山岩（英安岩、粗面岩和粗安岩等），我们新的同位素年龄数据显示其主要形成在 12－21 百万年之间。这些钾质中酸性火山岩的成因相对复杂，其中部分与超钾质火山岩共生者可能是前者母岩浆的演化产物，而那些分布更为广泛且不与超钾质岩共生的钾质中酸性火山岩可能是下地壳部分熔融的产物。由于这部分钾质火山岩的岩浆源区很可能不同于拉萨地块上的埃达克质斑岩，现在还不清楚钾质火山岩起源于那些下地壳部位和何种构造事件导致了它们的形成。

综上所述，目前的资料显示青藏高原上的下地壳岩浆活动主要有两期，一期在 35－40 百万年，另外一期在 12－21（26？）百万年。下地壳岩浆活动产生了青藏高原上的钾质中酸性火山岩和钙碱性的埃达克质火成岩。目前看来，这些下地壳来源的中酸性火山岩和侵入岩可能至少有以下三种成因：(1) 拆沉下地壳的部分熔融并且与上覆地幔的反应，如羌塘地区的高镁安山岩；(2) 区域伸展作用导致下地壳部分熔融，如拉萨地块上的钙碱性埃达克质斑岩；(3) 陆内俯冲和陆块叠置的脱水诱发上覆下地壳的部分熔融，如可可西里的富钾埃达克质火山岩。值得重视的是，两期下地壳岩浆活动可能暗示青藏高原上两次重要的构造事件，但是导致下地壳发生部分熔融的原因和其蕴藏的地质意义仍然是十分不清楚的，值得深入研究和进一步思考。我们初步认为与下地壳岩浆活动相关的两次构造事件可能对应着青藏高原所发生的两次快速隆升。

本研究得到中国 973 项目（2002CB412602）、中科院知识创新工程重要方向性项目（KZCX3-SW-122，KZCX3-SW -143）和中国国家杰出青年基金项目（40425003）资助

**主要参考文献**

Chung, S.L., Liu, D.Y., Ji, J.Q., Chu, M.F., Lee, H.Y., Wen, D.J., Lo, C.H., Lee, T.Y., Qian, Q., and Zhang, Q., 2003, Adakites from continental collision zones: Melting of thickened lower crust beneath southern Tibet: Geology, v. 31, p. 1021-1024.

Chung S L, Chu M F, Zhang Y Q, Xie Y W, Lo C H, Lee T Y, Lan C Y, Li X H, Zhang Q, Wang Y Z. 2005. Tibetan tectonic evolution inferred from spatial and temporal variations in post-collisional magmatism. Earth-Science Reviews 68:173-196

Hou Z Q, Gao Y F, Qu X M, Rui Z Y, Mo X X.2004.Origin of adakitic intrusives generated during mid-Miocene east-west extension in southern Tibet. Earth and Planetary Science Letters,220:139-155

Miller, C., Schuster, R., Klötzli, U., Frank, W., and Purtscheller, F., 1999, Postcollisional potassic and ultrapotassic magmatism in southwest Tibet: Geochemical and Sr-Nd-Pb-O isotopic constraints for mantle source characteristics and petrogenesis: Journal of Petrology, v. 40, p. 1399–1424.

Turner, S., Arnaud, N., Liu, J., Rogers, N., Hawkesworth, C., Harris, N., Kelley, S., van Calsteren, P., and Deng, W., 1996, Postcollision, shoshonitic volcanism on the Tibetan plateau: Implications for convective thinning of the lithosphere and the source of ocean island basalts: Journal of Petrology, v. 37, p. 45–71.

Wang Qiang, McDcermott Frank, Xu Ji-feng, Bellon Herve, Zhu Ying-tang. 2005. Cenozoic K-rich adakitic volcanic rocks in the Hohxil area northern Tibet: Lower-crustal melting in an intracontinental setting. Geology, 33: 465-468.

Xu J F, Shinjio R, Defant M J, Wang Q, and Rapp R P. 2002. Origin of Mesozoic adakitic intrusive rocks in the Ningzhen area of east China: Partial melting of delaminated lower continental crust? Geology, 32: 1111–1114.

# 准噶尔盆地西北缘古生代
# 陆壳侧向与垂向增生事件的SHRIMP年龄信息

徐 新[1] 何国琦[2] 李华芹[3]

1.新疆资源环境中心，乌鲁木齐市北京南路40号， 380011
2.北京大学造山带与地壳演化教育部重点实验室，北京，100871
3.宜昌地质矿产研究所

紧贴准噶尔盆地边缘的克拉玛依蛇绿岩带及其与上覆地层之间的不整合面的发现为探索古亚洲洋消亡事件的演变过程的研究提供了理想场所；大量发育的中基性脉岩、上覆地层中火山岩及广泛发育的碱性花岗岩岩基提供了丰富的陆壳垂向增生的深部岩浆作用信息。在中新生代覆盖区钻孔岩心中也识别出配套齐全的蛇绿岩套及后碰撞期的各类岩石组合，不仅为后碰撞造山和陆内盆山耦合造山研究提供重要信息，也为探索准噶尔盆地基底性质提供比较可靠的科学依据。

2005年野外调研中发现的克拉玛依蛇绿岩和增生杂岩带，沿准噶尔盆地西部盆山结合部位延伸，在山区边缘出露，断续延伸长达80km，可分为三段，即白碱滩段、百口泉段、红浅段，其中，以白碱滩段发育最全，宽度最大、组分最齐全，由盆边向山区方向依次排列着变质橄榄岩为基质的混杂岩片、以枕状玄武岩和辉绿岩为主体的混杂岩片、以深海硅泥质为基质的混杂岩片，分别相当于古洋壳的下、中、上部，其中，变质橄榄岩为基质的超镁铁混杂岩片长约7km，宽0.5～2km，发生了强烈的蛇纹石化、滑石化和碳酸盐化；以枕状玄武岩和辉绿岩为主体的混杂岩片规模不大，与超镁铁岩紧密相伴；以深海硅泥质为基质的增生混杂岩片分布面积较大，长16km以上，宽1～2km，红色、绿色的深海相硅质泥质岩与蚀变碎裂玄武岩杂乱无序的堆积在一起，在露头上组成红绿相杂的鲜艳图画，产放射虫和铁碧玉。

从蛇绿混杂岩和硅泥质增生岩片向西，为以细火山灰凝灰岩为主的复理石沉积，两者之间断层接触。复理石沉积褶皱强烈，地层产状多数近于直立，部分倒转。在蛇绿混杂岩和硅泥质增生岩和复理石沉积中均有大量以闪长岩为主的缓倾角的脉岩穿插，这些脉岩随着远离蛇绿岩带而逐步减少。蛇绿岩的上覆地层为一套陆缘碎屑砂砾岩、酸性和中基性火山岩，底部普遍有底砾岩层，砾石成分复杂，但以下伏蛇绿岩组分为主，基本无花岗质砾石和石英砾石，见到清楚的不整合现象

目前，我们已经取得了一批同位素年代学测定数据，测定的对象有白碱滩蛇绿岩中的辉长岩、达尔布特蛇绿岩中的闪长岩、上覆地层中的辉石闪长岩、侵入玄武岩中

的闪长岩脉、斜长花岗斑岩株、碱长花岗岩基等。

白碱滩蛇绿混杂岩中辉长岩属强蚀变辉长岩，其中，斜长石葡萄石化强烈，辉石多数变为绿泥石，保留变余辉长结构，SHRIMP 法测定集中在两组年龄 412±8Ma 和 313Ma±11Ma；闪长岩脉也已强烈蚀变，SHRIMP 法测定集中在 423±46Ma 和 325Ma±6Ma 两组年龄；不整合与蛇绿岩之上地层中的辉石安山岩， SHRIMP 法测定集中在 409±9Ma 和 336Ma±5Ma 两组年龄；对红山碱长花岗岩体作 SHRIMP 法测定得出 305±4Ma。另外在对达尔布特蛇绿岩带中闪长岩测定时得出 550(个别信息) 418、304、三组数据。从以上已经分析出的数据来看，突出显示出西准噶尔地壳 3 次主要增生事件，即 550（尽管数据量很少）、423～409、336～305。其中，最后一期增生事件内容十分丰富，结合 Sm-Nd 等时线、Rb-Sr 等时线、Ar-Ar 坪年龄测试结果，以及稀土、微量元素的分析研究，可以为探讨陆壳侧向增生向垂向增生转换过程提供大量的深部作用的信息。

# Multiple sources and magma mixing for the origin of Early Cretaceous I- and A-type granites in the eastern North China Craton

Jin-Hui Yang [a], Fu-Yuan Wu [a], Simon A. Wilde [b]

[a] State Key Laboratory of Lithospheric Evolution, Institute of Geology and Geophysics, Chinese Academy of Sciences, P.O. Box 9825, Beijing 100029, China

[b] Department of Applied Geology, Curtin University of Technology, P.O. Box U1987, Perth, Western Australia

Whole rock geochemistry and Sr-Nd isotopic data and *in situ* U-Pb and Hf isotopic measurements in zircons, obtained from mafic microgranular enclaves and their host I- and A-type granites from the Early Cretaceous Gudaoling batholith and Qianshan pluton in NE China identifies that multiple sources and magma mixing were involved in I- and A-type granite genesis.

In the Gudaoling I-type granitic batholith, the zircon U-Pb age of the enclaves (120 ± 1 Ma) is identical to that of the host monzogranite (120 ± 1 Ma), establishing that the mafic and felsic magmas were coeval. Monzogranites have relatively high $^{87}Rb/^{86}Sr$ ratios (0.672-0.853), low initial $^{87}Sr/^{86}Sr$ ratios (0.7052-0.7086) and $\varepsilon_{Nd}(t)$ values (-18.5 to -20.9) indicating that they were mainly derived from a newly underplated crustal source with a short crustal residence time. The enclaves have igneous textures and abundant acicular apatites. They have low $Al_2O_3$ (13.5-16.4 wt.%) and high MgO (Mg# = ~72.3) concentrations, low initial $^{87}Sr/^{86}Sr$ ratios (0.7058-0.7073) and negative $\varepsilon_{Nd}(t)$ values (~-7.2), and are enriched in LILEs and LREEs and depleted in HFSEs, suggesting they were derived from a mantle source. The Hf isotopic composition of the enclaves ($\varepsilon_{Hf}(T)$ = +4.5 to -6.2) is distinct from the host monzogranite ($\varepsilon_{Hf}(T)$ = -15.1 to -25.4), indicating that both depleted mantle and crustal sources contributed to their origin. Some wall-rock contamination is indicated by inherited zircons with considerably older U-Pb ages and low initial Hf isotopic compositions.

The Qianshan A-type pluton includes hornblende alkali-feldspar granite, graphic biotite granite and mafic microgranular enclaves. The hornblende alkali-feldspar granites have high $SiO_2$, $Fe_2O_{3T}/MgO$, $K_2O+Na_2O$, Rb, Zr and LREE contents and low Ba and Sr concentrations with strongly negative Eu anomalies. Their high Rb/Sr ($^{87}Rb/^{86}Sr$ = 16.76-24.15) and initial $^{87}Sr/^{86}Sr$ ratios (0.7215 to 0.7283), negative $\varepsilon_{Nd}(t)$ values (-14.1 to -16.5) and zircon $\varepsilon_{Hf}(t)$ values (-18.9 to -11.5) indicate they were mainly derived from a crustal source, but with involvement of high $\varepsilon_{Nd}(t)$ and $\varepsilon_{Hf}(t)$ materials. Graphic biotite granites have similar

geochemical features and Sr-Nd-Hf isotopic compositions to enclaves, indicating they were the result of crystal fractionation of evolved mafic magmas, but with involvement of low $\varepsilon_{Nd}(t)$ and $\varepsilon_{Hf}(t)$ materials. The mafic enclaves have an igneous texture and contain acicular apatite, suggesting quenching of mafic magmas that have co-mingled with the host granites. They have low initial $^{87}Sr/^{86}Sr$ ratios (0.7097-0.7148), negative $\varepsilon_{Nd}(t)$ (-14.5 to -11.9) and zircon $\varepsilon_{Hf}(t)$ (-17.1 to -6.9) values, and are enriched in LILEs and LREEs and depleted in HFSEs. When coupled with the high MgO (Mg# up to 54), this indicates derivation from an enriched lithospheric mantle source, but contaminated by crustal materials.

Whole rock geochemical and Sr- and Nd-isotopic compositions and zircon U-Pb data and Hf isotopes rule-out simple crystal-liquid fractionation or restite unmixing as the major genetic link between enclaves and host rocks. Instead, magma mixing of mafic mantle-derived and juvenile crustal-derived magmas, coupled with crystal fractionation and assimilation of ancient lower crust, is compatible with the data. This example shows that the I- and A-type granitoids in the eastern North China Craton are not produced by pure intracrustal melting, but formed through a complex, multi-stage hybridization process, involving mantle- and crustal-derived magmas and several concomitant magmatic processes (crystal fractionation, crustal assimilation and crustal anatexis).

# The significance of near-orthogonal overprinting matrix foliations in shear zone: an example from the Red River Shear Zone

Meng-Wan Yeh[a]*, Tung-Yi Lee[a], Pao-Chu She[a] , Ching-Hua Lo[b], Sun-Lin Chung[b], Tran Tuan Anh[c]

[a]Department of Earth Sciences, National Taiwan Normal University, Taipei, Taiwan
[b]Department of Geology, National Taiwan University, Taipei, Taiwan
[c] Institute of Geology, National Centre for Natural Science and Technology, Vietnam

The Red River Shear Zone is characterized by the development of dextral transcurrent shear sense indicators and shallowly plunging NW-SE trending stretching lineations consistent with a sinistral transverse deformational regime. The RRSZ was considered to be a steep shear zone that penetrated the entire lithosphere and which played a significant role in East Asia tectonism since the collision of India and Eurasia. 3-D microstructural analysis of 19 oriented samples from the DNCV metamorphic complex in northern Vietnam has revealed 4 generations of matrix foliations ($S_{0/1}$, $S_1$, $S_2$ and $S_3$), that are near- orthogonal in orientation instead of simple S-C fabrics as other studies had indicated. Near-orthogonal overprinting matrix foliations are commonly recognized and documented from orogenic belts around the world. However, this pattern was rarely observed in shear zones. We suggested that the orthogonal overprinting pattern recorded in the Red River Shear zone reflects horizontal compression and gravitational loading at the macroscopic scale during Indian Eurasia collision and crustal thickening of Tibet. With sub-vertical shortening (India-Eurasia collision) or collapse occurring when a build up of gravitational potential energy (crustal thickening of Tibet), induces collapse and lateral extrusion along the Red River Shear Zone.

# 新疆西南天山超高压变质带中榴辉岩的 SHRIMP 定年和 Sm/Nd 同位素不平衡

张立飞 艾永亮 李强 李旭平 宋述光 魏春景

造山带与地壳演化教育部重点实验室，北京大学地球与空间科学学院，北京 100871

新疆西南天山超高压变质带是目前极少保留的由洋壳岩石经历了超高压变质地区。地球化学研究显示新疆西南天山超高压变质榴辉岩的原岩相当于源于富集地幔的（εNd=-1.4~-0.4）具有 OIB 特点的变碱性玄武岩、.源于亏损地幔的（εNd=+6.7~+7.4）具有 NMORB 特点的洋中脊玄武岩和源于较富集地幔的（εNd=-2.5~+3.2）具有 EMORB 特点的洋中脊玄武岩，它们形成于海山环境下的洋壳。西天山榴辉岩的变质时代一直存有争议，以往的定年工作主要有前寒武纪变质 729－634Ma（Rb/Sr 等时线）和晚古生代年龄（如 Sm/Nd 等时线年龄为 343 ±44～346 ±3 Ma； Ar/Ar 年龄为 334±2 Ma ～347±2 Ma)。近来我们进行了榴辉岩中锆石 SHRIMP 定年结果表明榴辉岩的原岩形成于石炭纪（>310Ma）之前，高压-超高压变质发生在三叠纪(220-230Ma)；而 5 个 Sm/Nd 全岩和内部单矿物（石榴石、绿辉石等）分析的结果没有一个能构成等时线而产生有意义的年龄的，表明西南天山榴辉岩形成过程中的 Sm/Nd 没有达到同位素的平衡。结合岩石学的研究，西南天山榴辉岩 Sm/Nd 同位素不平衡的主要原因是峰期变质温度低于石榴石的 Sm/Nd 同位素的封闭温度（650~850$^{o}$C） (Burton et al., 1995; Thoni et al., 2002)，再有就是西南天山榴辉岩中变斑晶石榴石含有大量的富轻稀土的包裹体矿物如帘石类矿物等，也造成了 Sm/Nd 同位素的不平衡。Sm/Nd 等时线测年方法不适合于对低温榴辉岩的测年。

# The Central Mongolian Microcontinent: Its Yangtze affinity and tectonic implications

Zhao Y.[1), Song B. [2), Zhang S.H. [1)

1) Institute of Geomechanics, CAGS, 100081, Beijing, P.R. China
2) Beijing SHRIMP Center, Institute of Geology, CAGS, 100037, Beijing, P.R. China

The Central Mongolian Microcontinent, located at Govi-Altay, Mongolia, is one of Precambrian terranes, which are distributed in the Paleo-Asian Orogens (Badarch et al., 2002; Li, 2006). So far it is still poorly understood its early history of high-grade basement rocks of the Central Mongolian Microcontinent. They are generally of the Pre-Vendian age by potassium-Argon age results (cf. Tomurtogoo, 2004). But some of which were regarded as old as Archean. In the microcontinent a Post-metamorphic Vendian-Lower Cambrian cover sequence can be observed, including late Neoproterozoic significant diamictite and phosphorite horizons.

To understand the evolution of the Central Mongolian Microcontinent we analyzed zircon samples from the high-grade basement and acid vulcanite. The first sample was directly from a potash-leucosome veinlet of migmatitic gneisses of Early Precambrian Havchig structural-metamorphic complex near Altay town. SHRIMP U-Pb dating of the zircon sample yield an age at 840±9Ma. We consider it as a migmatitization age, which was closely associated with the final amalgamation of the high-grade basement of the Central Mongolian Microcontinent because NW trending potash-leucosome foliation is the predominant one, resulting from the regional migmatitization, high-grade metamorphism and main deformation. Inherited zircon ages of the sample arrange from 2445Ma to 1440Ma. No Archean inherited zircon was detected. Their Hf model ages of the zircon grains analyzed by SHRIMP support the view that the Central Mongolian Microcontinent is a Proterozoic basement terrane, rather than an Archean basement terrane. Further SHRIMP U-Pb analyses of a zircon sample from acid vulcanite of the top of the late Riphean Zavhan formation give an age at 777±6Ma. Similar basement amalgamation ages, post-orogenic volcanic rocks, horizons of diamictite and one horizon of phosphorite of late Neoproterozoic demonstrate that the Central Mongolian Microcontinent, Yangtze Craton and Tarim Craton, even North American Craton and Australian Craton, have a close tectonic and paleogeographic relationship during late Neoproterozoic, probably connecting each other. The breakup of the Central Mongolian Microcontinent postdates middle Cambrian, which suggests the Paleo-Asian Ocean, located between the Siberian Craton, North China Craton and Tarim Craton, and probably the largest one during that time, is mainly formed in Phanerozoic. Therefore the crustal growth in the Paleo-Asian Orogens during Paleozoic is probably achieved by a lateral accretion of most Phanerozoic oceanic components of the Paleo-Asian Ocean.

We are grateful to DSc. Tomurtogoo O., who guided the field excursion and Mineral Resources Authority of Mongolia (MRAM) and Institute of Geology & Mineral Resources (IGMR), which organized the field excursion.

**References**

Badarch, G., Cunningham, W.D., Windley, B.F., 2002. A new terrane subdivision for Mongolia: implications for the Phanerozoic crustal growth of Central Asia. Journal of Asian Earth Sciences 21: 87–110.

Li, 2006. Permian geodynamic setting of Northeast China and adjacent regions: closure of the Paleo-Asian ocean and subduction of the Paleo-pacific plate. Journal of Asian Earth Sciences, 18pp, in press.

Tomurtogoo O., 2004. Terrane Tectonics of Mongolia, Field Excursion Guidebook, MRAM and IGMR, International Project: Compilation of the Atlas of Geological Maps for the Central Asia and Adjacent areas, 29May-6June, 2004, Govi-Altay Province, Mongolia, 54pp.

Xu B., Jian P., Zheng H.F., Zou H.B., Zhang L.F., Liu D.Y., 2005. U-Pb zircon geochronology and geochemistry of Neoproterozoic volcanic rocks in the Tarim Block of northwest China: implications for the breakup of Rodinia supercontinent and Neoperozoic glaciations. Precambrian Research 136:107-123.

# Timing of Major Mesozoic Deformational Episodes of the Yanshan Fold and Thrust Belt, northern North China: Their Tectonic Implications

Yue ZHAO.[1)], Gang XU.[1)], Shuanhong ZHANG.[1)], Biao SONG[2)],, Zhenyu YANG.[1)], Jianmin HU.[1)], Yinsheng MA.[1)]

1) Institute of Geomechanics, CAGS, 100081, Beijing, P.R. China

2) Beijing SHRIMP Center, Institute of Geology, CAGS, 100037, Beijing, P.R. China

The North China Block (NCB), assembled or cratonized in the late Paleoproterozoic, had become tectonically stable since early Mesoproterozoic (Zhao et al, 2000). Deformation of its cover sequence from the Mesoproterozoic to the early Paleozoic and the basement rocks of NCB commenced probably in late Paleozoic (Davis et al., 2001; Cui et al., 2002; Zhang et al., 2004), when the northern NCB developed into an Andean-style continental margin (Zhang et al., 2006 in press). Tectonic inheritance at the continental margin of NCB was triggered by the subduction of the Paleo-Asian oceanic crust beneath NCB. But what led to the formation of the Yanshan fold and thrust belt in Mesozoic, which was far from the plate boundaries at that time, has been debated for decades. The key issue is ages of the major Mesozoic tectonic events in the Yanshan fold and thrust belt, which are helpful to understand the cause and the geodynamic background of the deformational episodes. In this paper we present our new data on the geological investigation of the typical areas and SHRIMP U-Pb zircon dates, combined with previously published age results and data to demonstrate when the major Mesozoic deformational episodes of the Yanshan fold and thrust belt occurred.

It can be recognized that up to late Triassic regional deformation had been intense. The typical area of late Triassic deformation is the NEN trending Niuyingzi basin, western Liaoning, where the lower-middle Ordovician carbonate thrust upon the Laohugou formation, which contains late Triassic index fossils, on the western margin of the basin. The thrust duplex is well developed in the Taiyanggou, north of Laohugou. Thrusting on the both side of the basin controlled the deposition of the late Triassic Dengzhangzi Formation, a series of landslides and debris flows. The thrust is unconformably overlain by the Guojiadian formation, which contains early Middle Jurassic fossils and the latest Middle Jurassic volcanics of the Lanqi formation, from the base of which crystal zircon measured by SHRIMP U-Pb dating gives the ages at 158±1 Ma. Therefore regional thrusting and folding occurred in late Triassic, which postdates the deposition of the Laohugou formation, predates the deposition of the Middle Jurassic Guojiadian formation, synchronizes with the deposition of the late Triassic Dengzhangzi formation. To constrain exactly when regional deformation took place, we investigated the Panshan area, east of Beijing, where the ENE Jixian fault thrusts over the Fujunshan and Zhuangguoyu synclines and then the Panshan pluton intrudes into the Jixian fault. Furthermore the Mesoproterozoic strata is folded circularly around the Panshan Pluton. We analyzed the zircon samples from the Panshan pluton, and the Hongshikan sill, which yielded SHRIMP U-Pb ages at 210±4Ma and 214±3Ma respectively, which shows that regional folding and thrusting occurred during 214±3Ma and 210±4Ma, the same age of the late amphibolite facies retrogressive event in the ultrahigh-pressure Sulu terrane, eastern China (Liu et al., 2004).

The major tectonic events occurred in Jurassic is what is called "Yanshanian Movement", first recognized and proposed by Wong (1929) ca. 80 years ago. The E-W trending Yanshan fold and thrust belt was finally achieved in Jurassic. By the study of the typical areas of western Beijing, northeastern Hebei and western Liaoning (Davis et al., 2001; Zhao et al., 2002, 2004; Xu et al., 2003, 2006; Hu et al., 2004,2005), the deformational episode of Yanshanian A marked by the unconformity beneath the Tiaojishan volcanics occurred in middle Jurassic, predating 160±5 Ma and the deformational episode of Yanshanian B marked by the unconformity beneath the Zhangjiakou volcanics happened in late Jurassic, prior to 135±1 Ma. The extensional tectonics prevailed gradually in Cretaceous in the Yanshan belt and eastern China.

The background of the Yanshan deformational episodes is conversion of tectonic regimes in East Asia, which is essentially the transformation of its geodynamic system, that is, the transformation from one collision process to one subduction process. The core issue is that when inception of Paleo-Pacific subduction along the eastern Eurasian continental margin occurred. The earliest accretionary complexes resulted from the inception subduction, continental volcanic arc and the related surface deformation successively took place during this unique tectonic process. This paper emphasizes the natural, notable and recognizable marker, that is, the emergence of the Yanshanian volcanic eruptions on a large scale on the East Asia continental margin, which represents inception of Paleo-Pacific subduction, that is, the conversion of the geodynamic system.

**References**


1. Cui S. Q., Li J. R., Wu Z. H., et al., 2002. Mesozoic and Cenozoic intracontinental orogenesis of the Yanshan area, China. Beijing: Geological Publishing House, 385 p (崔盛芹,李锦蓉,吴珍汉,等. 2002. 燕山地区中新生代陆内造山作用. 北京: 地质出版社. 385 p)

2. Davis G. A., Zheng Y. D, Wang C., et al. 2001, Mesozoic tectonic evolution of the Yanshan fold and thrust belt, with emphasis on Hebei and Liaoning Provinces, Northern China. GSA Memoir. 194, 171-197.

3. Hu J. M., Liu X. W., Xu G., et al., 2005. The sliding-slump-mud flow sedimentation during the late Late Triassic to Middle Jurassic in western Liaoning Province, China. Acta Geologica Sinica. 70(4), 453-464 (胡健民,刘晓文,徐刚,等. 2005, 辽西晚三叠世末—中侏罗世崩塌-滑坡-泥石流沉积及其构造意义. 地质学报. 70(4), 453-464)

4. Hu J. M., Liu X. W., Zhao Y., et al., 2004, On Yanshan intraplate orogene: An example from Taiyanggou area, Lingyuan, western Liaoning Province, Northeast China. Earth Science Frontiers. 11(3), 255-271 (胡健民,刘晓文,赵越,等. 2004, 燕山板内造山带早期构造变形演化：以辽西凌源太阳沟地区为例. 地学前缘. 11(3), 255-271)

5. Liu F. L., Xu Z. Q., Liou J. G., et al., 2004, SHRIMP U–Pb ages of ultrahigh-pressure and retrograde metamorphism of gneisses, south-western Sulu terrane, eastern China，Journal of Metamorphic Geology. 22(4), 315-326)

6. Wong W. H.. The Mesozoic orogenic movement in eastern China. Bulletin of Geological Society of China. 1929,8:33-44

7. Xu G, Zhao Y., Hu J. M., et al., 2003, The Late Triassic thrusting in the Niuyingzi region, western Liaoning, China. Acta Geologica Sinica. 77(1), 1-11 (徐刚,赵越,胡健民,等. 2003, 辽西牛营子地区晚三叠世逆冲构造. 地质学报. 77(1), 1-11)

8. Xu G, Zhao Y., Liu X. W., et al., 2006, Intraplate deformation of the Jurassic sedimentary basins in the Yanshan fold and thrust belt: Examples from the Xiabancheng, Chengde-Shangbancheng and Beitai sedimentary basins. Acta Geoscientia Sinica, in press (徐刚,赵越,刘晓文,等. 2006, 燕山褶断带中生代盆地变形－板内变形过程的记录—以下板城、承德-上板城、北台盆地为例. 地球学报. 27(1) 出版中)

9. Zhang S H, Zhao Y, Song B, et al., 2004, The late Paleozoic gneissic granodiorite pluton in early Precambrian high-grade metamorphic terrains near Longhua County in northern Hebei Province, North China: result from zircon SHRIMP U-Pb dating and its tectonic implications. Acta Petrologica Sinica. 20(3), 621-626 (张拴宏,赵越,宋彪,等. 2004, 冀北隆化早前寒武纪高级变质区内的晚古生代片麻状闪长岩—锆石 SHRIMP U-Pb 年龄及其构造意义. 岩石学报, 20(3), 621-626)

10. Zhang S. H., Zhao Y., Song B., 2006, Hornblende therobarometry of the Carboniferous granitoids from the Inner Mongolian Paleo-uplift: Implications for the geotectonic evolution of the northern margin of North China block. Mineralogy and Petrology, 86, DOI 10.1007/s00710-005-0116-2

11. Zhao Y., Cui S. Q., Guo T., et al., 2002. The Evolution of the Jurassic Basin of the Western Hills, Beijing, North China: Implications for Jurassic Tectonics of East Asia. Geological Bulletin of China, 21(4-5), 211-217 (赵越,崔盛芹,郭涛,等. 2002, 北京西山侏罗纪盆地演化及其构造意义, 地质通报, 21(4-5), 211-217)

12. Zhao Y., Xu G., Zhang S. H., et al., 2004b, Yanshanian movement and conversion of tectonic regimes in East Asia. Earth Science Frontiers. 11(3), 319-328 (赵越,徐刚,张拴宏,等. 2004b, 燕山运动与东亚构造体制的转变. 地学前缘. 11(3), 319-328)

13. Zhao Y., Zhang S. H., Xu G., et al., 2004a, The Jurassic major tectonic events of the Yanshan intraplate deformational belt, North China. Geological Bulletin of China. 23(9-10), 22-31 (赵越,张拴宏,徐刚,等. 2004a, 燕山陆内变形带侏罗纪主要构造事件. 地质通报. 23(9-10), 22-31)

14. Zhao, G. C., Cawood, P. A., Wilde, S. A.,et al., 2000. Metamorphism of basement rocks in the Central Zone of the North China Craton: implications for Paleoproterozoic tectonic evolution. Precambrian Res. 103, 55-88.

# 新疆北部晚古生代地壳增生方式的多样性

# -来自埃达克岩及富碱火成岩的证据

赵振华 王强 熊小林 张海祥 牛贺才 许继峰 白正华 乔玉楼

中国科学院广州地球化学研究所，广州

自本文作者首次发表了阿尔泰地区晚古生代花岗岩类具有高 $^{143}Nd/^{144}Nd$ 比值，$\varepsilon_{Nd}(t)$ 为正值，并提出其源区物质为新生、不成熟地壳以来（赵振华等，1991,1993，1996），在东中亚地区显生宙的陆壳增生受到了越来越广泛关注，1998 年，江博明教授领导的 IGCP-420 项目将北疆乃至中东亚显生宙陆壳增生研究推向了一个新阶段（Jahn et al ,1998,2000; Han et al ,1997; 洪大卫等，2000，Wu et al.,）。在新疆北部，相继发现了大量富碱花岗岩与富碱火山岩，如橄榄玄粗岩系（shoshonitic series）火山岩、碱性火山岩，这些富碱火成岩从阿尔泰山向天山呈多条带状展布，组成了乌伦古、卡拉麦里、达拉布特、伊什基里克-阿吾拉勒、那拉提及塔里木克拉通北缘等六条富碱火成岩带，构成了新疆北部富碱火成岩省（Zhao et al.,2000）。此外，在新疆北部相继发现了埃达克岩、富 Nb 玄武岩和富 Mg 安山岩（熊小林等，2001a,b,2005;许继峰等，2001；王强等，2003；张海祥等，2004；赵振华等，2004；Zhao et al.，2004，Wang et al., 2005）。本文将其划分为两种类型，一是洋壳俯冲型，简称俯冲型，形成于泥盆纪-早石炭世晚期（≥320Ma）；另一类型为玄武质岩浆底侵型，简称底侵型，形成于中晚二叠世（≤280Ma）。

上述碱性花岗岩、橄榄玄粗岩系火山岩、碱性火山岩和两类埃达克岩的岩石学、地球化学均显示了新疆北部晚古生代陆壳增生方式具有明显的多样性特点。

## 1 碱性花岗岩、橄榄玄粗岩系火山岩

**1.1 岩石学特征**：碱性花岗岩主要包括含碱性暗色矿物钠（铁）闪石或霓（辉）石花岗岩及与之密切组合的钾长花岗岩。碱含量高，$K_2O+Na_2O$>8%。$SiO_2$ 含量高，标准矿物石英含量大于 25%；$Al_2O_3$ 含量低，多低于 13%；$Al_2O_3/CaO+K_2O+Na_2O\le1.0$,属铝不饱和或准铝质。

橄榄玄粗岩系火山岩包括橄榄玄粗岩（shoshonite）、橄榄粒玄岩(absorokite)、橄云安粗岩（banakite），共同特点是在基质中均含有大量微晶钾长石，标准矿物中出现霞石。碱含量高，$K_2O+Na_2O$ 5-14%, $K_2O$ 含量高达 8.4%， $K_2O>Na_2O$，当 $SiO_2$ 含量较低时（50%±），$K_2O<Na_2O$。Ti、Fe 含量低，$Al_2O_3$ 含量高，变化大。

**1.2 稀土与微量元素地球化学：**碱性花岗岩 REE 总量变化大，$100\times10^{-6}$-$600\times10^{-6}$，Eu 强烈亏损，$Eu/Eu^*$一般为 0.20，HREE 相对富集，$(La/Yb)_N$~5，有时小于 1，呈近水平的球粒陨石标准化分布型式。富碱火山岩 REE 总量较低，变化范围大，$40\times10^{-6}$-$260\times10^{-6}$，多为 $100\times10^{-6}$ 左右，Eu 亏损不明显，$Eu/Eu^*$多在 1.0 左右，HREE 无明显富集，$(La/Yb)_N$2.15-11.97，多在 5 左右。

碱性花岗岩富 LIL,如 Rb,K,LREE 及 HFSE,如 Zr,Nb；Ba、Sr、P、Ti 含量低。在原始地幔标准化图解中，多呈 Nb 亏损，部分亏损弱或无亏损。富碱火山岩富含 K、Rb、Sr、Ba、Th，Ce，Nb、Ta、Zr、Hf、Ti 也相当富集。在原始地幔标准化图解中，与 K、La 相比，Nb、Ta、Ti 呈明显亏损。

**1.3 同位素年龄与 Sr、Nd、O 同位素地球化学：**碱性花岗岩的 Rb-Sr、Ar/Ar 及锆石 U-Pb 年龄可划分为两组：240-290 Ma,290-320Ma,分别相当于二叠纪和晚石炭世。$^{87}Sr/^{86}Sr)_I$ 值一般低于 0.710，范围 0.7017-0.7096。$^{143}Nd/^{144}Nd$，一般为 0.51250 左右，$\varepsilon_{Nd}(t)$+0.67-+8.4，大部分为+5-+6。Nd 模式年龄 $T_{2DM}$较低，小于 1.0Ga。在 $\varepsilon_{Nd}(t)$-$^{87}Sr/^{86}Sr)_I$ 图解中主要位于第一象限。$\delta O^{18}$ 值一般低于花岗岩下限值，范围 2.6-9.0‰。橄榄玄粗岩系火山岩同位素年龄 280-250Ma,属中晚二叠世。富碱火山岩 $^{87}Sr/^{86}Sr)_I$ 值一般低于 0.710，集中分布于 0.7050；$^{143}Nd/^{144}Nd$ 比值较高，范围为 0.51250-0.51290，$\varepsilon_{Nd}(t)$ 为+1-+6.在 $\varepsilon_{Nd}(t)$-$^{87}Sr/^{86}Sr)_I$ 图解中分布于第一象限。Nd 模式年龄 $T_{2DM}$较低，小于 1.0Ga。

**2，埃达克岩**

俯冲型埃达克岩及其家族岩石有埃达克岩、富 Nb 玄武岩（NEB）、高（富）Mg 安山岩 MA, 它们主要分布在阿拉套山、科古琴-博罗科努山（达巴特、果子沟、阿希）、中天山（骆驼沟和巴仑台）、东天山土屋-延东、阿尔泰陆缘富蕴-青河南、准噶尔西缘克拉玛依及腹地陆梁等地区。底侵型埃达克岩主要分布于西天山阿吾拉勒山和东天山的哈密南三岔口。

**2.1 两类埃达克岩的岩石学特征:**俯冲型埃达克岩包括埃达克岩及富 Nb 玄武岩和高（富）Mg 安山岩，主要包括玄武安山岩和石英闪长斑岩、花岗闪长斑岩、斜长花岗斑岩、英云闪长岩、花岗闪长岩，闪长岩及英安岩和安山岩等。既有低 Si 型 LSA($SiO_2$<60%), 也有高 Si 型 HSA($SiO_2$>60%);$Al_2O_3$ 含量高，范围 14.28-18.25%,普遍高于 15%,A/NKC 1.05-1.66，属过铝质; $Na_2O$ 含量较高，普遍高于 $K_2O$, $Na_2O/K_2O$1.85-7.83，属中钾钙碱性系列（个别岩体属橄榄玄粗岩系列）; Mg#中等 31-71，一般<50。富 Nb 玄武岩属低 Si 型，$Al_2O_3$ 含量低于埃达克岩， A/NKC 0.90-1.94, 属准铝质-过铝质；$Na_2O$>.$K_2O$，索尔

库都克和准噶尔陆梁的富 Nb 玄武岩 Na、K 含量高，属碱性系列;Mg#略低于埃达克岩 25-66。高（富）Mg 安山岩（闪长岩）的显著特点是 MgO 含量高，Mg#值 54-74;$Al_2O_3$ 含量较低 9.59-16.32%, A/NKC 0.68-1.88，从准铝质到过铝质；$K_2O$ 含量一般高于 $Na_2O$。

底侵型埃达克岩未发现与富 Nb 玄武岩和高（富）Mg 安山岩组合，而与橄榄玄粗岩系火山岩密切组合。其岩石类型主要为浅侵位或侵入相，石英钠长斑岩、英云闪长岩、斜长花岗斑岩、英云闪长斑岩，部分为喷出相，如英安岩。$SiO_2$ 含量 62-71%，均属高 Si 型埃达克岩 HSA，$Al_2O_3$ 含量 13.03%-16.32%， A/NKC0.85-1.16,个别达 1.22，属准铝-弱过铝质。阿吾拉勒地区埃达克岩明显富碱，特别是富 $K_2O$，含量 2.06-4.62%，属高钾钙碱性系列，$K_2O+Na_2O$ 范围 6.46-11.11%。MgO 含量较低，<3.0%，Mg#范围 35-56 平均 45,略低于俯冲型埃达克岩。

**2.2 稀土与微量元素地球化学**：俯冲型埃达克岩明显富轻稀土，$(La/Yb)_N$ 4.1-13(个别样品为 2.9),Yb 含量低,0.59μg/g-2.54μg/g, 均低于 1.9μg/g（Defant et al., 1990）。Eu/Eu*0.81-1.41。富 Nb 玄武岩为轻稀土弱富集型，$(La/Yb)_N$ 1.56-6.34;Yb 含量 2.2μg/g-5.17μg/g，明显高于埃达克岩；Eu/Eu*0.76-1.11。富 Mg 安山岩（闪长岩）明显富集轻稀土，$(La/Yb)_N$ 0.98-6.37;Yb 含量较低， 1.01μg/g-2.37μg/g，Eu/Eu*为 0.82-1.10，主要呈无异常-弱负异常。

底侵型埃达克岩强烈富轻稀土，三岔口的 $(La/Yb)_N$ 4.9-5.1，阿吾拉勒地区高达 13.35-33.46,Yb 含量很低,为 0.3.2μg/g-1.67μg/g，低于 1.9μg/g,也明显低于区内俯冲型埃达克岩；Eu 富集, Eu/Eu*1.02-1.27。球粒陨石标准化分布型式呈右陡倾斜型。

俯冲型埃达克岩富 Sr, 含量 329μg/g-1812μg/g,集中于 500μg/g。Y 含量较低，为 7.0μg/g -18μg/g，普遍低于 18μg/g；Sr/Y 比值高，为 18-100，普遍高于 20-40（Defant et al.,1990）。在 Sr/Y-Y 图解中均分布于埃达克岩区。富 Nb 玄武岩 Sr 含量低于埃达克岩，含量 260μg/g -826μg/g。Y 含量较高，为 16μg/g -64μg/g ，Sr/Y 比值低，为 8.0-20.8。在 Sr/Y-Y 图解中落入普通岛弧火山岩区。富 Mg 安山岩（闪长岩）与埃达克岩相似，Sr 含量较高，含量 225μg/g -1007μg/g， Y 含量低，含量为 8.0μg/g -23.2μg/g 。 Sr/Y 比值较高，范围 5.45-125.9, 在 Sr-Y 图解中主要落入埃达克岩区。在原始地幔（PM）标准化的微量元素蛛网图中，埃达克岩、富 Mg 安山岩的 Sr 含量呈明显正异常，大离子亲石元素 K、Rb、Ba 明显富集，Nb、Ta、Ti 呈明显负异常。富 Nb 玄武岩与之不同，Sr 正异常不明显，Nb 含量较高，范围 4.81μg/g-24.0μg/g, La/Nb 值较低 0..56-2.42,多数低于 1.40, Ti 与 Nb 类似。在 PM 标准化蛛网图上 Nb、Ti 呈弱负异常-正异常。

底侵型埃达克岩 Sr 含量高、Y 含量低。Sr 含量 303μg/g-1633μg/g，集中于 800μg/g；

Y 含量 4μg/g-15μg/g，均低于 18μg/g ；Sr/Y 比值高，51-327，在 Sr/Y-Y 图解中落入埃达克岩区；在原始地幔标准化微量元素蛛网图上，Sr 呈正异常程度低于俯冲型埃达克岩。La/Nb2.9-8.6，Nb、Ta、Ti 负异常程度高于俯冲型埃达克岩。

**2.3 同位素年龄 与 Sr、Nd 同位素地球化学**

俯冲型埃达克岩的同位素年龄明显分为两组，一组为≥320Ma,属早石炭世。底侵型埃达克岩≤280Ma（250-280Ma），属二叠纪。

俯冲型埃达克岩的 $^{143}Nd/^{144}Nd$ 初始值范围 0.512310-0.512819，$\varepsilon_{Nd}(t)$均为正值，范围+1.59~+9.11，集中于+5~+8， $^{87}Sr/^{86}Sr$ 初始值低，范围 0.7032~0.7049。在 $\varepsilon_{Nd}(t)$-（$^{87}Sr/^{86}Sr$）$_i$ 图解中集中分布于第二象限，沿地幔排列分布，与世界范围新生代洋壳板片熔融形成的埃达克岩一致。富 Nb 玄武岩 $^{143}Nd/^{144}Nd$ 初始值较高，变化范围小，$\varepsilon_{Nd}(t)$ +3.80~+10.0；$^{87}Sr/^{86}Sr$ 初始值变化较大，0.7007~0.7067,在图解中分布于 1-2 象限上部,呈近水平分布。高（富）Mg 安山岩(闪长岩)$\varepsilon_{Nd}(t)$均为低正值, ,+1.59~+3.78,（$^{87}Sr/^{86}Sr$）$_i$ 变化范围较大,0.7029~0.7061。

底侵型埃达克岩（$^{143}Nd/^{144}Nd$）$_i$ 值较低，0.512384-0.512572, $\varepsilon_{Nd}(t)$+1.57~+5.69,（$^{87}Sr/^{86}Sr$）$_i$ 初始值高于俯冲型，为 0.7039-0.7054,在 $\varepsilon_{Nd}(t)$-（$^{87}Sr/^{86}Sr$）$_i$ 图解中主要位于第一象限,在地幔排列线右侧。

**3.碱性花岗岩、橄榄玄粗岩及埃达克岩成岩机理及其动力学意义**

**3.1 碱性花岗岩、橄榄玄粗岩及埃达克岩是陆壳增生物质的产物**

上述碱性花岗岩、橄榄玄粗岩 REE 及微量元素、Sr、Nd 同位素组成特点表明它们的源区物质具有深源特征。碱性花岗岩的源区为年轻不成熟地壳，橄榄玄粗岩系火山岩较高的+$\varepsilon_{Nd}(t)$值暗示其源区物质来自地幔。俯冲型埃达克岩的 Sr、Nd 同位素组成与洋中脊玄武岩及新生代俯冲洋壳形成的埃达克岩很相似(Defant et al ,1992;Kay,et al,1993; Stern et al ,1996;Petfond et al ,1995)，表明其源区物质为洋壳板片。富 Nb 玄武岩的 $\varepsilon_{Nd}(t)$ 值高，（$^{87}Sr/^{86}Sr$）$_I$ 值变化范围大，Mg#较高，Nb、Ta、Ti 含量较高，轻稀土及 Eu 富集程度较低，表明其源区具有俯冲洋壳及上覆地幔楔的共同特点，是受到斜向俯冲洋壳板片形成的埃达克质熔体上升过程中交代（熔体-固体反应）的地幔楔橄榄岩发生部分熔融所形成（Sajona et al ,1993,1996;Kepezinskas,et al ,1996）。高 (富)Mg 安山岩（闪长岩）与同一地区俯冲埃达克岩相比，其 Mg 含量高（Mg#高达 70），Cr、Ni，Y、Yb 含量高，Sr/Y 比值低，Eu 亏损增加；（$^{87}Sr/^{86}Sr$）$_i$ 值较高（0.7029-0.7061），$\varepsilon_{Nd}(t)$值较低（+1.57-+3.78）。这些特点表明成岩过程中较多弧前增生物质的参与，是弧前增生棱柱

物质受俯冲剥蚀作用（subduction erosion,,Kay et al. 2004）和洋壳共同熔融形成的埃达克质岩浆，并在上升过程中受地幔楔橄榄岩混染作用 (Yogodzinski et al.,1995;Keleman et al.,1995;Sen et al.,1994)。

**3.2 碱性花岗岩、橄榄玄粗岩及埃达克岩形成的构造环境**

碱性花岗岩的微量元素构造环境判别图解表明其形成于后碰撞期，部分为后造山期，有 $A_1$ 型，也有 $A_2$ 型。橄榄玄粗岩系火山岩主要为后碰撞弧（PAP）和大陆弧(CAP)。结合它们的同位素年龄和野外产状，它们应与二叠纪区内较广泛的底侵作用有关。

埃达克岩强烈亏损 Nb、Ta、Ti，同位素年龄（≤320Ma）及产出在早、中泥盆统或石炭系火山岩中，表明它们形成于岛弧环境，是本区晚古生代多岛洋体系中洋壳分别向西伯利亚板块-哈萨克斯坦板块和塔里木板块俯冲期。轻稀土的强烈富集、Eu 富集及高场强元素 Nb、Ta、Ti 的亏损表明，在洋壳部分熔融过程中残留相含石榴子石、金红石，不含斜长石。埃达克岩浆形成是在角闪岩向榴辉岩相过渡，即 1.0-1.5Gpa 以上的压力（33km-50km 以下）（Defant et al.,1990;Rapp et al.,1991,1995; Sen et al.,1994;Proutean et al.,2001,熊小林等，2005）。

底侵型埃达克岩低正 $\varepsilon_{Nd}(t)$ 值和略高的（$^{87}Sr/^{86}Sr$）$_i$ 值，显示其源区为源自地幔的、新生的玄武质物质底侵于壳幔边界。与俯冲型埃达克岩明显不同的是，在同一地区未发现与底侵埃达克岩同时的富 Nb 玄武岩或高（富）Mg 安山岩（闪长岩），表明其源区没有地幔楔参与。其成岩时代属中、晚二叠世（≤280Ma），新疆北部在该时期已进入造山过程的后碰撞-后造成山阶段，该阶段埃达克岩浆的形成与俯冲无关。最可能的机制是玄武质岩浆底侵至壳幔界面，引起地壳加厚而发生熔融作用。新疆北部在晚古生代（二叠纪）发生了底侵作用的地质、地球物理和地球化学证据主要有：强烈增厚的地壳，西天山地壳厚 52-62km，准噶尔盆地 44-56km（李秋生等 2001）；复杂的壳幔界面，天山地区该界面厚 20km（由 7-8 层薄互层组成，赵俊猛等 2001）；高热流值（天山 $100mw \cdot m^{-2}$），为塔里木的两倍；基性麻粒岩（279±5Ma, 陈汉林等 2005）的产出等。碱性花岗岩、橄榄玄粗岩系火山岩、基性脉岩及埃达克岩是底侵作用的重要标志之一。

富蕴-青河南产出的埃达克岩、富 Nb 玄武岩和富（高）Mg 安山岩，与该区的中泥盆世苦橄岩(陈毓川等，2004)，喀拉通克的苏长岩、橄榄苏长岩，共同构成了晚古生代较完整的富 Mg 火成岩组合，区内乔夏哈拉 Cu、Fe、Au 矿床的 Sr、Nd、Pb 同位素组成显示了较典型的“塞浦路斯型”特征（万博等，2005）。这种特殊的岩石组合及矿床特点，表明了本区在晚古生代地热梯度高，暗示本区发生了软流圈物质通过板片窗（slab window）上涌, 其产生的机制可能是俯冲板片发生撕裂、断离、随之软流圈上涌；或洋

（盆）脊俯冲至地幔楔下形成软流圈窗（Yogodzinski et al.,2001,　Kay et al.,1993）。

**3.3 新疆北部晚古生代陆壳增生方式的多样性-复式增生**

本区碱性花岗岩、橄榄玄粗岩系火山岩及两类埃达克岩、富 Nb 玄武岩、 高(富)Mg 安山岩（闪长岩）的厘定，揭示了本区陆壳增生方式具有明显的多样性：在增生的构造过程上，有泥盆纪-早石炭世晚期洋壳板片的斜向俯冲；俯冲洋壳板片的撕裂、板片窗；俯冲剥蚀作用及二叠纪时期玄武质物质的底侵；在增生的物质上，有地幔楔，也有洋壳板片、洋壳板片熔体交代地幔楔形成的熔体、受俯冲剥蚀作用的弧前增生棱柱物质、受地幔楔混染的洋壳板片熔体、底侵的幔源玄武质物质、年轻的不成熟地壳；在增生的方向上，有洋壳板片的侧向俯冲，也有玄武质物质垂向上底侵于壳-幔边界。这种复式增生应是中亚型造山过程的重要特征。

# 云南怒江走滑挤压剪切带

郑亚东 季建清 魏春景 宋述光

北京大学地球与空间科学学院

云南怒江走滑挤压剪切带位于印度板块与欧亚板块碰撞带的东侧，夹持在东侧的崇山和西侧的高黎贡山南北向韧性剪切带之间，由古生界变质砂岩、变质泥岩、大理岩和侵入其间的花岗岩类组成,宽约 20 公里(图 1)。岩石变形按构造层次和变形机制分为早期韧性变形和晚期脆性断裂两类构造。

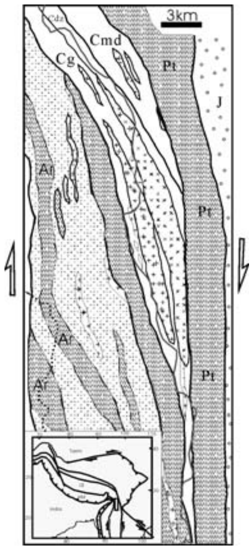


图 1 怒江走滑挤压构造带的构造背景及组成:
Ar-太古界片麻岩; Pt-元古界片麻岩;C –石炭系变质沉积岩; J –侏罗系沉积岩; γ-花岗岩类

**一、 韧性变形构造** 韧性变形表现为早期形成平卧褶皱，进而叠加北北西向近直立的紧闭褶皱，形成北北西向共轴叠加褶皱。伴随近直立的紧闭褶皱形成透入性的轴面片理和近水平的拉伸线理。层理绝大部分被平行褶皱的轴面面理置换，导致层理一般与片理平行，仅在褶皱转折端处见有残余层理与面理相交。根据近百次的野外测定，面理总体走向 335-340°，主要倾向北东东，部分倾向南西西，倾角 72°。线理近水平，倾伏角一般小于 20°(图 2A)。

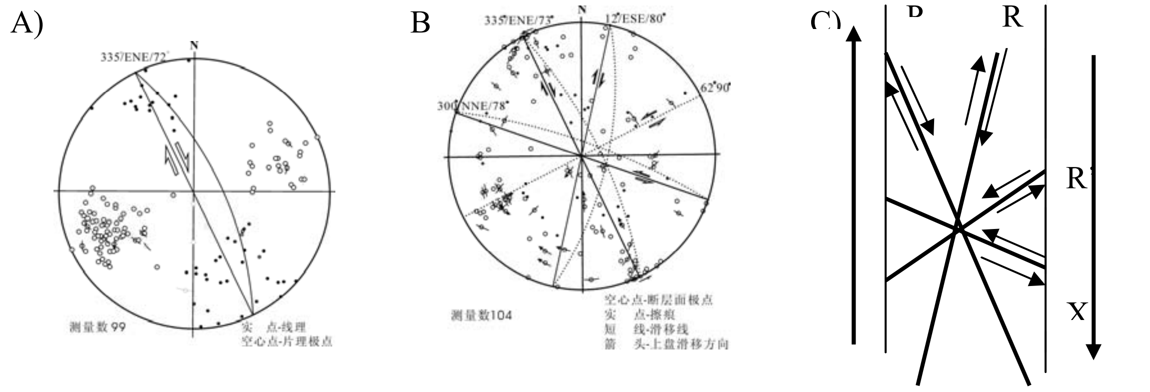


图 2 怒江走滑挤压构造带中的面理、线理（A ）、断层滑移系（B ）及解释（C ）

片理由片状矿物和条带状矿物集合体的定向排列构成，与近直立的褶皱轴面平行。沿片理常发育石香肠构造。露头规模和显微尺度的共轭伸展劈理，其共轭锐角等分面与片理平行。表明片理为平行有限应变椭球的 X Y 面的 S 面理。然而，沿片理常显示顺片理的右行剪切的标志, 特别是沿片理发育的韧性剪切带。这些剪切标志包括：岩石中 S/C 组构、条带状石英中的斜向面理、不对称σ-型和δ-型长石碎斑、“云母鱼”、不对称褶皱、标志体的剪切错断。指示顺片理的右行走滑剪切。东西侧剪切带的条带变粒岩的片理 350°，东倾 80°，线理近水平。顺片理的长英质脉体构成的σ、δ-碎斑和不对称褶皱都指示顺片理的右行剪切。填图规模上，东西两侧韧性剪切带的糜棱面理总体走向近南北，拉伸线理近水平与怒江河谷古生界变质沉积岩的片理与东侧元古界崇山岩群构成的南北向大型剪切带呈 10°左右的小角度相交, 构成大型的 S/C 组构。这一宏观组构表明全区经历了大规模右行走滑挤压韧性剪切带。

**二、脆性断裂构造** 叠置在韧性变形的岩石之上，发育不连续的脆性断层。除沿东部崇山剪切带西部边界有明显位移、构成不连续边界外，断层总体规模不大，不影响早期韧性变形构成的总体构造格局。根据野外百余断层产状的测量，按断层走向分成北北西，北北东、北东东、南东东四组(图 2B): 北北西向断层为工程区最主要一组断层，沿早期韧性变形片理的薄弱面发育，形成顺片理的断层。沿主断面发育早期水平擦痕和晚期倾向擦痕。断裂带中发育左阶式雁列张性石英脉。脉列走向 306°，脉尾走向北北东，指示断层早期的右行滑动。沿断层的滑动面发育断层泥膜，发育倾向擦痕，表明晚期的正断活动。北东东向断层发育最密集的一组断层。根据地面观察，大致呈等间距分布，

间距一般为 10 米左右。但规模不大，断层带宽度一般为几厘米, 延伸几百米。野外观察表明，北北东向一组断层切断早期面理。根据断层擦痕、阶步、旁侧伴生构造和标志层的错断等标志判断，早期为左行剪切，晚期为正断滑动。北北东向断层发育程度远不如上述两组。断层相关构造指示沿断层的右行剪切滑动，而断层两侧的构造层次差异，则表明东盘具有相当规模的相对向下滑动。判断断层的右行正断滑动代表北北东向断层的运动方式。 北西西向断层 与北东东向断层相似，断层规模不大，但发育程度差，一般显示左行滑动。

**三. 怒江走滑挤压构造带的运动学与动力学分析**

怒江区的岩石角闪岩相变质作用，北东部的岩石出现绿片岩相岩石。古生界岩层内普遍发育的北北西向平卧褶皱和叠加的近直立褶皱，表明该区经历了北东东-南西西的大规模的地壳缩短和垂向的地壳增厚。这一地壳增厚可解释古生界表壳岩进入中下地壳并经历角闪岩-绿片岩变质-变形作用。

根据现代韧性剪切带的研究成果(Blenkinsop and Treloar, 1995; Passchier and Trouw, 1996)，岩石在一般剪切作用下(Simpson De Paor, 1993)，发育三组面理：S-面理, C –面理和 C’-面理。S-和 C-面理为透入性面理。S-面理平行有限应变椭球体的 XY 面，垂直最大有限缩短方向，C –面理平行剪切方向，两者间的锐夹角指示剪切指向， C ’-面理为间隔性面理，出现在剪切带宽度减小的一般剪切带中(Zheng et al., 2004 及待刊) ，其剪切指向与剪切带的总体剪切指向一致。 区内普遍发育的片理与近直立的紧闭褶皱轴面平行，代表有限应变椭球的 XY 面的 S 面理。填图规模上，怒江河谷古生界变质沉积岩的片理与东西两侧南北向韧性剪切带构成大型的 S/C 组构。指示区域大规模右行走滑作用。

均质体瑞德尔力学实验和地震断裂的野外观察表明，水平剪切作用下形成 的断裂主要有 4 组：瑞德尔剪切断裂（R）, 共轭瑞德尔剪切断裂（R’）, 张断裂（T）和 p 剪切断裂(Tchalenko,1968)。Logan 等（1997，1992）的力学实验还揭示平行剪切带的 Y 剪切断裂和 R’对称、剪切指向与之相同的 X 剪切断裂(图 2C)。区内所观察到的 4 组断裂统计上具有共同的交点，表明其间具有密切的成因关系，构成一相当完整的走滑断层系(图 2C )。根据钾长石、角闪石和黑云母 Ar /Ar 年龄的测定和磷灰石裂变迳迹分析，变形-变质主期为 20-24Ma, 大约在 10-2Ma 隆升进入脆性变形域，3-4Ma 区域整体抬升并延续至今。

根据上述韧性变形的运动学分析和脆性断层的力学分析可以得出结论：怒江区的韧

性变形与脆性断裂同是近南北向右行剪切作用的产物，韧性变形在先，脆性断裂在后，运动学和动力学上具有继承性。沿北东东向和北西西向断层的正断滑动伴随断层泥的形成，表明是断层近地表活动的产物，可能与近期区域的隆升有关。近期区域的隆升体现怒江地区的深切河谷和沿江高阶地的形成。怒江区构造从中下地壳韧性变形，经上地壳的走滑脆性断层到近地表脆性正断活动，代表该区地壳因走滑挤压导致的地壳增后，表壳沉积岩进入下地壳，经历角闪岩相的变质并伴随岩石部分熔融。地壳增厚和岩石的部分熔融导致怒江区浅色花岗岩类的形成和区域的晚期隆升。Tapponnier & Molnar (1977) 和 Tapponnier (1982)提出由于印度板块与欧亚板块俯冲碰撞导致亚洲东部新生代的挤出动力学模式可解释怒江区构造的运动学和动力学特征。

**参考文献**

Blenkinsop, T.G. and Treloar, P.J., 1995, Geometry, classification and kinematics of S-C and S-C' fabrics in the Mushandike areas, Zimbabwe. *Journal of Structural Geology* 17, 397-408.

Logan,J.M. et al., 1992, Fabrics of experimental fault zones: their development and relationship to mechanical behavior. In Fault Mechanics and Transport Properties of rocks. 33-67.Academic Press Ltd.

Passchier, C. W. and Trouw, R.A., 1996, Microtectonics. Spinger-Verlag Berlin Heidelberg.

Simpson, C., and De Paor, D.G., 1993. Strain and kinematic analysis in general shear zones. *Journal of Structural Geology,* 15: 1-20.

Tchalenko, J.S.,1968, The evolution of kink bands and the development of compression textures in shear clay. Tectonophysics 6: 159-174.

Zheng, Y., Wang, T., Ma, M., Davis, G. A., 2004. Maximum effective moment criterion and the origin of low-angle normal faults. *Journal of Structural Geology* 26: 271-285.

Zheng, Y.D., Wang, T. and Wang, X.S., (In press) Maximum effective moment criterion (MEMC) and its implications in structural geology. *Acta Geologica Sinica*

# Late Jurassic – Early Cretaceous geodynamic setting in middle – northern Gangdese: new insights from volcanic rocks

ZHU DiCheng[1], PAN GuiTang[1], MO XuanXue[2], WANG LiQuan[1], LIAO ZhongLi[1], ZHAO ZhiDan[2], DONG GuoChen[2], ZHOU ChangYong[1]

1. Chengdu Institute of Geology and Mineral Resources, Chengdu, 610082, China

2. China University of Geosciences, Beijing, 100083

Distribution, volcanism-age constrained by stratigraphy, paleontology and isotopic dating for the Late Jurassic – Early Cretaceous volcanic rocks on Gangdese, and their tectonic setting, petrogenesis and subducted polarity have been preliminarily studied based on regional geological survey (1:250, 000) and our data. Our study shows that the Late Jurassic – Early Cretaceous volcanic rocks are not only distributed on southern Gangdese, but also widely exposed on middle, northern Gangdese and southern margin of Bangong Co – Nujiang suture zone. They started to erupt at about 120-130 Ma and likely lasted to the Late Cretaceous. However, the maximum volcanic activity occurred in middle - northern rather than southern Gangdese. Present geochemical data indicate that the Zenong Group volcanic rocks on middle Gangdese, which are mainly composed of partly intermediate-basic rocks of medium-K calc-alkaline series and dominant intermediate-acid rocks of high-K calc-alkaline series, are not consistent with traditional island-arc volcanic rocks but similar to volcanic rocks erupted in a thick crust from Central Andes, whereas the Duoni Formation volcanic rocks on northern Gangdese consist of mainly medium-K calc-alkaline series, resembling traditional island-arc volcanic rocks. It should be noted that all of these volcanic rocks have affinities with island-arc volcanic rocks. The Zenong Group intermediate-basic volcanic rocks on middle Gangdese are most likely derived from the partial melting of mantle wedge materials induced by fluid from subducted sediments and/or subducted basaltic crust and then experienced assimilation-fractional crystallization (AFC process) during ascending. The Zenong Group felsic rocks are dominantly related to crustal remelting, however, fractional crystallization of mafic magma cannot be entirely ruled out. The compositional variation, crustal thickness, distance relative to subducted zone revealed by present geochemical data of the Late Jurassic – Early Cretaceous volcanic rocks on middle-northern Gangdese, together with the distributions of contemporaneous volcanic rocks on Gangdese, indicating that the Late Jurassic – Early Cretaceous volcanic rocks on middle-northern Gangdese are most likely related to southward subduction of Bangong Co – Nujiang oceanic crust.

**Key words**: Subducted polarity, Island-arc volcanic rocks, Late Jurassic – Early Cretaceous, Middle-northern Gangdese, Tibet

邀請講者

| 姓名 | 單位 | 電話 | E-mail |
|---|---|---|---|
| 鄭亞東 | 北京大學 | 010－62754155 | ydzheng@pku.edu.cn |
| 陳斌 | 北京大學 | 010－62765798 | binchen@pku.edu.cn |
| 魏春景 | 北京大學 | 010－62754157 | cjwei@pku.edu.cn |
| 吳福元 | 中科院地質地物所 | 010－62007392 | wufuyuan@mail.iggcas.ac.cn |
| 高俊 | 中科院地質地物所 | 010－62007825 | gaojun@mail.igcas.ac.cn |
| 肖文交 | 中科院地質地物所 | 010－62008134 | wj-xiao@mail.igcas.ac.cn |
| 楊進輝 | 中科院地質地物所 | 010－62007900 | jinhui@mail.igcas.ac.cn |
| 王濤 | 地科院地質所 | 010－68999732 | taowang@pku.edu.cn |
| 李錦軼 | 地科院地質所 | 010－68999673 | jyli@cags.net.cn |
| 劉敦一 | 地科院地質所 | 010－68311545 | liudunyi@bjshrimp.cn |
| 高銳 | 地科院地質所 | 010－68999730 | gaorui@cags.net.cn |
| 姜枚 | 地科院礦床地質所 | 010－68999738 | meij@public3.bta.net.cn |
| 聶鳳軍 | 地科院礦床所 | 010－68999033 | nfjj@mx.cei.gov.cn |
| 趙 越 | 地科院地質力學所 | 010－68412307 | Yue_zhao@cags.cn.net |
| 舒良樹 | 南京大學地球科學系 | 025－83592921 | lsshu2003@yahoo.com.cn |
| 王京彬 | 北京地礦所 | 010－84931994 | wjb@bigm.com.cn |
| 趙振華 | 中科院廣州地化所 | 020－85290024 | zhzhao@gig.ac.cn |
| 胡靄琴 | 中科院廣州地化所 | 020－85290031 | huaq@gig.ac.cn |
| 許繼峰 | 中科院廣州地化所 | 020－85290282 | jifengxu@gig.ac.cn |
| 李獻華 | 中科院廣州地化所 | 886-2-83691242 | lixh@gig.ac.cn |
| 姚玉鵬 | 國家自然科學基金 | 010－62327166 | yaoyp@nsfc.gov.cn |
| 馬映軍 | 新疆烏魯木齊市中國科學院新疆生態與地理所，國家 305 辦公室 | 0991－7885383 | yjma@mail.wl.xj.cn |
| 王寶林 | 新疆烏魯木齊市克拉瑪依西路 2 號，國家 305 項目辦公室 | 0991-4845307 | xjwbl@vip.sina.com |
| 徐新 | 新疆烏魯木齊市克拉瑪依西路 2 號，國家 305 項目辦公室 | 0991－4844603 | xjwbl@vip.sina.com |
| 王煜 | 新疆烏魯木齊市克拉瑪依西路 2 號，國家 305 項目辦公室 | 0991－7885383 | xjwbl@vip.sina.com |
| 潘桂棠 | 成都地礦所 | 028－83220628 | cdzdc@cgs.gov.cn |
| 朱弟成 | 成都地礦所 | 886-2-83691242 | cdzdc@cgs.gov.cn |
| 陸松年 | 天津地質礦產研究所 | 022－24023530 | tjlsongnian@cgs.gov.cn |

| | | | |
|---|---|---|---|
| 夏林圻 | 西安地質礦產研究所 | 029－87821934 | geologyx@pub.xaonline.com |
| 莫宣學 | 中國地質大學（北京） | 010－82322712 | moxx@cugb.edu.cn |
| 李正祥 | University of Western Australia | 886-2-83691242 | zli@tsrc.uwa.edu.au |
| 孫　敏 | 香港大學地球科學系 | 2859-2194 | minsun@hkucc.hku.hk |
| 陳望平 | Prof., Dept. Geology, Univ. Illinois | 217-3332744 | wpchen@uiuc.edu |
| 吳大銘 | Prof., Dept. Geological Sci., State Univ. of New York, Binghamton | 607-7772512 | francis@binghamton.edu |
| 鄧屬予 | 台灣大學地質系教授 | 886-2-33662937 | tengls@ntu.edu.tw |
| 盧佳遇 | 台灣大學地質系教授 | 886-2-33662926 | chia@ntu.edu.tw |
| 宋聖榮 | 台灣大學地質系副教授 | 886-2-33662938 | srsong@ntu.edu.tw |
| 李昭興 | 海洋大學應用地球科學所教授 | 886-2-24631811 | leecs@mail.ntou.edu.tw |

其他參與人員

| 姓名 | 單位 | 電話 | E-mail |
|---|---|---|---|
| 江博明 | 中研院地球科學研究所 | 886-2-27839910*619 | jahn@earth.sinica.edu.tw |
| 俞震甫 | 中研院地球所研究員 | 886-2-27839910*621 | tfyui@earth.sinica.edu.tw |
| 黃柏壽 | 中研院地球所研究員 | 886-2-27839910*323 | hwbs@earth.sinica.edu.tw |
| 劉玲根 | 中研院地球所特聘研究員 | 886-2-27839910*503 | lliu@earth.sinica.edu.tw |
| 葉義雄 | 中研院地球所研究員 | 886-2-27839910*519 | yehyh@earth.sinica.edu.tw |
| 李太楓 | 中研院地球所研究員 | 886-2-27839910*613 | typhoon@earth.sinica.edu.tw |
| 王錦華 | 中研院地球所研究員 | 886-2-27839910*326 | jhwang@earth.sinica.edu.tw |
| 余水倍 | 中研院地球所研究員 | 886-2-27839910*416 | yusb@earth.sinica.edu.tw |
| 汪中和 | 中研院地球所研究員 | 886-2-27839910*513 | chwang@earth.sinica.edu.tw |
| 藍晶瑩 | 中研院地球所研究員 | 886-2-27839910*614 | kyanite@earth.sinica.edu.tw |
| 扈治安 | 中研院地球所研究員 | 886-2-27839910*607 | huh@earth.sinica.edu.tw |
| 李德貴 | 中研院地球所研究員 | 886-2-27839910*426 | tqlee@earth.sinica.edu.tw |
| 邱宏智 | 中研院地球所研究員 | 886-2-27839910*315 | chiu@earth.sinica.edu.tw |
| 郭本垣 | 中研院地球所研究員 | 886-2-27839910*507 | byk@earth.sinica.edu.tw |
| 陳中華 | 中研院地球所研究員 | 886-2-27839910*615 | china@earth.sinica.edu.tw |
| 林正洪 | 中研院地球所研究員 | 886-2-27839910*521 | lin@earth.sinica.edu.tw |
| 劉啟清 | 中研院地球所副研究員 | 886-2-27839910*517 | liucc@earth.sinica.edu.tw |
| 沈君山 | 中研院地球所副研究員 | 886-2-27839910*616 | mountain@earth.sinica.edu.tw |
| 蔡主權 | 中研院地球所副研究員 | 886-2-27839910*316 | ctsai@earth.sinica.edu.tw |
| 林忠成 | 中研院地球所副研究員 | 886-2-27839910*504 | cclin@earth.sinica.edu.tw |
| 李德春 | 中研院地球所副研究員 | 886-2-27839910*617 | dclee@earth.sinica.edu.tw |

| | | | |
|---|---|---|---|
| 李建成 | 中研院地球所副研究員 | 886-2-27839910*413 | jclee@earth.sinica.edu.tw |
| 洪崇勝 | 中研院地球所副研究員 | 886-2-27839910*424 | cshorng@earth.sinica.edu.tw |
| 陳國誠 | 中研院地球所副研究員 | 886-2-27839910*324 | chenkc@earth.sinica.edu.tw |
| 詹瑜璋 | 中研院地球所助研究員 | 886-2-27839910*411 | yuchang@earth.sinica.edu.tw |
| 戚務正 | 中研院地球所助研究員 | 886-2-27839910*510 | chi@earth.sinica.edu.tw |
| 王國龍 | 中研院地球所助研究員 | 886-2-27839910*603 | kwang@earth.sinica.edu.tw |
| Georg Zellmer | 中研院地球所助研究員 | 886-2-27839910*602 | gzellmer@earth.sinica.edu.tw |
| 劉忠智 | 中研院地球所研究技師 | 886-2-27839910*208 | ccliu@earth.sinica.edu.tw |
| 黃文紀 | 中研院地球所研究助技師 | 886-2-27839910*323 | wgee@earth.sinica.edu.tw |
| 郭隆晨 | 中研院地球所研究助技師 | 886-2-27839910*405 | kuo@earth.sinica.edu.tw |
| 陳宏宇 | 中研院地球所研究助技師 | 886-2-27839910*417 | chenhy@earth.sinica.edu.tw |
| 飯塚義之 | 中研院地球所研究助技師 | 886-2-27839910*217 | yiizuka@earth.sinica.edu.tw |
| 陳春燕 | 中研院地球所研究助技師 | 886-2-27839910*609 | chunyen@earth.sinica.edu.tw |
| 梁文宗 | 中研院地球所研究助技師 | 886-2-27839910*522 | wtl@earth.sinica.edu.tw |
| 趙里 | 中研院地球所客座助研究員 | 886-2-27839910*320 | zhaol@earth.sinica.edu.tw |
| 仝來喜 | 中研院地球所博士後研究 | 886-2-27839910*605 | tong@earth.sinica.edu.tw |
| 王正誠 | 中研院地球所博士後研究 | 886-2-27839910*523 | jcwang@earth.sinica.edu.tw |
| 李健平 | 中研院地球所博士後研究 | 886-2-27839910*311 | cplee@earth.sinica.edu.tw |
| 李憲宗 | 中研院地球所博士後研究 | 886-2-27839910*311 | sjlee@earth.sinica.edu.tw |
| 鍾孫霖 | 台灣大學地質系教授 | 886-2-33662934 | sunlin@ntu.edu.tw |
| 陳正宏 | 台灣大學地質系教授 | 886-2-33665872 | chench@ntu.edu.tw |
| 羅清華 | 台灣大學地質科學系教授 | 886-2-33662915 | loch@ntu.edu.tw |
| 陳宏宇 | 台灣大學地質系教授 | 886-2-33662946 | hchen@ntu.edu.tw |
| 陳文山 | 台灣大學地質系教授 | 886-2-33662913 | wenshan@ntu.edu.tw |
| 陳于高 | 台灣大學地質系教授 | 886-2-33665877 | ygchen@ntu.edu.tw |
| 楊燦堯 | 台灣大學地質系副教授 | 886-2-33665874 | tyyang@ntu.edu.tw |
| 洪淑蕙 | 台灣大學地質系助理教授 | 886-2-33662925 | shung@ntu.edu.tw |
| 胡植慶 | 台灣大學地質系助理教授 | 886-2-33662943 | jchu@ntu.edu.tw |
| 吳逸民 | 台灣大學地質系助理教授 | 886-2-33662942 | drymwu@ntu.edu.tw |
| 龔源成 | 台灣大學地質系助理教授 | 886-2-33662923 | ycgung@ntu.edu.tw |
| 林立虹 | 台灣大學地質系助理教授 | 886-2-33661694 | lhlin@ntu.edu.tw |
| 陳汝勤 | 台灣大學海洋系教授 | 886-2-23660991 | jcchen@oc.ntu.edu.tw |
| 劉德慶 | 台灣師範大學地質系教授 | 886-2-29309544 | liutc@ntnu.edu.tw |
| 李通藝 | 台灣師範大學地質系教授 | 886-2-29347120*21 | T44001@ntnu.edu.tw |
| 李錫堤 | 中央大學應地所副教授 | 886-3-4227837*65856 | ct@gis.geo.ncu.edu.tw |
| 張中白 | 中央大學太空遙測中心助 | 886-3-4257232*57627 | cpchang@csrsr.ncu.edu.tw |

| | | | |
|---|---|---|---|
| | 理教授 | | |
| 王維豪 | 中正大學地震研究所教授 | 886-5-2720411*66206 | seiwhwg@eq.ccu.edu.tw |
| 李元希 | 中正大學地震研究所助理教授 | 886-5-2720411*66212 | seilee@eq.ccu.edu.tw |
| 呂學諭 | 中正大學地震研究所助理教授 | 886-5-2720411*66211 | seishei@eq.ccu.edu.tw |
| 黃奇瑜 | 成功大學地球科學系教授 | 886-6-276-692 | huangcy@mail.ncku.edu.tw |
| 楊懷仁 | 成功大學地球科學系助理教授 | 886-6-2757575*65429 | hjyang@mail.ncku.edu.tw |
| 劉瑩三 | 花蓮教育大學地球科學所副教授 | 886-3-8227106*2413 | yingsan@mail.nhlue.edu.tw |
| 蔡金河 | 花蓮教育大學地球科學所助理教授 | 886-3-8227106*2172 | tsai@mail.nhlue.edu.tw |
| 林朝宗 | 中央地質調查所所長 | 886-2-29462793*203 | lincc@moeacgs.gov.tw |
| 朱傚祖 | 中央地質調查所 | 886-2-29462793*253 | chuht@moeacgs.gov.tw |
| 鄧大量 | Prof., Dept. Geological Sciences, Univ. of Southern Calif. | 213-7405838 | lteng@usc.edu |
| 葉孟宛 | 師大地科系博士後研究 | 886-2-29347120*41 | marywyeh@pchome.com.tw |
| 劉政 | 大漢技術學院土木系講師 | 886-3-8263936 | cliu@ms01.dahan.edu.tw |
| Shoufa Lin | Dept. Earth Sciences, Univ. Waterloo, Canada | +1 (519) 888-4567 ext. 6557 | shoufa@uwaterloo.ca |